

# **Regulation and desensitisation studies on the nicotinic acid receptors**

**A thesis presented for the degree of  
Doctor of Philosophy**

**Sanam Mustafa**

**Division of Biochemistry and Molecular Biology**

**Faculty of Biomedical and Life Sciences  
University of Glasgow  
July 2008**



**University  
of Glasgow**

## **Abstract**

The lipid-modifying qualities of nicotinic acid, a B3 vitamin, have been exploited for many years to prevent cardiovascular disease and its associated mortality. Despite its widespread availability and clinical use, the clinical target and precise molecular mechanism by which nicotinic acid acts remains elusive. In order to maximise nicotinic acid's full potential as a lipid-modulating drug, overcome its related side effects and further develop novel and more potent drugs it is vital to understand its molecular mechanism of action. Fifty years on from its arrival on the market, receptors which this drug acts upon have recently been identified as the G protein-coupled 'nicotinic acid receptors'.

A family of three highly homologous receptors, HM74, HM74A and GPR81 are characterised by their differing affinities for nicotinic acid. Comparison of these homologues revealed a high degree of similarity between them, with the greatest similarity between HM74 and HM74A. The main structural difference between these receptors is the longer C-terminal tail of HM74. As the C-terminal tail of GPCRs is often implicated in receptor regulation it was hypothesised that the differences in this region may result in differential regulation of HM74 and HM74A. This hypothesis was tested by examining the regulation and desensitisation characteristics of each receptor in a heterologous expression system. Both HM74 and HM74A failed to interact with  $\beta$ -arrestin 2 or internalise in response to nicotinic acid. However, both receptors were phosphorylated in an agonist-dependent manner. HM74 but not HM74A was demonstrated to desensitise as result of prolonged nicotinic acid exposure. The importance of the C-terminal region was further analysed by the use of chimeric nicotinic acid receptors, in which the C-terminal tail of HM74 and HM74A were exchanged. It was shown that the C-terminal tail of HM74 may be implicated in the desensitisation characteristics of this receptor. Furthermore, it was shown that HM74 and HM74A display differential characteristics with respect to ERK1/2 phosphorylation.

## Contents

1.	Introduction.....	21
1.1.	Early studies.....	22
1.2.	Introduction to nicotinic acid therapy.....	23
1.3.	Nicotinic acid: Molecular mechanism of action?.....	24
1.4.	Introduction to G protein-coupled receptors.....	29
1.4.1.	Brief history.....	29
1.4.2.	GPCR classification.....	30
1.4.3.	GPCR structure.....	31
1.4.4.	GPCR oligomerisation.....	33
1.4.5.	Introduction to G proteins and classical signal transduction.....	35
1.4.6.	Regulation of GPCR signalling.....	36
1.4.7.	Novel mechanisms of GPCR signalling: signal specificity.....	46
1.5.	Nicotinic acid mediates its response via G protein-coupled receptors.....	64
1.5.1.	Introduction to nicotinic acid receptors.....	65
1.5.2.	Ligands for nicotinic acid receptors.....	66
1.5.3.	Homology modelling and structural determinants of ligand binding.....	68
1.6.	Clinical targets for nicotinic acid.....	69
1.7.	Mechanism of 'niacin flush'.....	70
1.8.	Other effects?.....	71
1.9.	Project aims.....	82
2.	Materials and Methods.....	83
2.1.	Materials.....	83
2.1.1.	General reagents, enzymes and kits.....	83
2.1.2.	Tissue culture plastic ware and reagents.....	86
2.1.3.	Radiochemicals.....	87
2.1.4.	Antisera.....	87
2.1.5.	Molecular Probes, Eugene, Oregon, USA.....	88
2.2.	Buffers.....	88
2.2.1.	General buffers.....	88
2.2.2.	Molecular biology solutions.....	89
2.3.	Molecular biology protocols.....	91
2.3.1.	Preparation of LB agar plates.....	91
2.3.2.	Preparation of competent bacterial cells.....	91
2.3.3.	Transformation of competent bacterial cells.....	91

2.3.4.	Preparation of plasmid DNA .....	92
2.3.5.	Quantification of DNA .....	92
2.3.6.	Digestion of DNA with restriction endonuclease.....	93
2.3.7.	DNA gel electrophoresis .....	93
2.3.8.	DNA purification from agarose gels .....	93
2.3.9.	Alkaline phosphatase treatment of plasmid vectors .....	93
2.3.10.	Ligation of DNA .....	94
2.3.11.	Polymerase chain reaction .....	94
2.3.12.	DNA sequencing .....	96
2.4.	Cell Culture .....	96
2.4.1.	Cell recovery .....	96
2.4.2.	Cell maintenance .....	97
2.4.3.	Passage of cells.....	98
2.4.4.	Liquid nitrogen storage .....	98
2.4.5.	Differentiation of 3T3 L1 .....	98
2.4.6.	Pertussis toxin treatment .....	99
2.4.7.	Transient transfection .....	99
2.4.8.	Stable transfection .....	99
2.4.9.	Generation of stable Flp-In CHO-K1 cell line .....	100
2.4.10.	siRNAi .....	100
2.4.11.	Cell harvesting .....	100
2.5.	Biochemical assays and other methods of analysis.....	101
2.5.1.	Preparation of cell membranes .....	101
2.5.2.	Preparation of cell lysates.....	102
2.5.3.	BCA protein quantification .....	102
2.5.4.	Sodium dodecyl sulphate polyacrylamide gel electrophoresis.....	103
2.5.5.	Western blotting .....	103
2.5.6.	Endoglycosidase treatment.....	104
2.5.7.	Nicotinic acid preparation .....	104
2.5.8.	ERK1/2 activation .....	104
2.5.9.	Biotinylation.....	105
2.5.10.	[ <sup>32</sup> P] Orthophosphate.....	106
2.5.11.	Cell surface receptor measurement and Enzyme-linked Immunosorbent assay (ELISA).....	107
2.6.	Immunocytochemistry .....	108
2.6.1.	Immunostaining.....	108
2.6.2.	Confocal microscopy: Fixed cells .....	109

2.6.3.	Epifluorescence microscopy: Live cells.....	110
2.7.	Pharmacological assays.....	110
2.7.1.	[ <sup>35</sup> S] GTPγS Binding Assay: Filtration.....	110
2.7.2.	[ <sup>35</sup> S] GTPγS Binding Assay: Scintillation proximity assay.....	111
2.7.3.	Pre-treatment .....	111
3.	Generation of tools to study regulation and desensitisation mechanisms of the nicotinic acid receptors.....	112
3.1.	Introduction.....	112
3.1.1.	Detection and visualisation of GPCRs .....	112
3.1.2.	[ <sup>35</sup> S] GTPγS binding assay .....	113
3.2.	Optimisation of [ <sup>35</sup> S] GTPγS binding .....	114
3.3.	Generation of tagged receptor constructs.....	115
3.4.	Characterisation of receptor constructs.....	116
3.4.1.	Detection of recombinant receptor constructs.....	117
3.4.2.	Localisation studies .....	118
3.5.	Generation and characterisation of CHO-K1 cell lines stably expressing recombinant nicotinic acid receptors .....	119
3.5.1.	Screening and localisation studies.....	119
3.5.2.	Detection of recombinant receptor constructs.....	120
3.5.3.	Functional analysis.....	120
3.6.	Generation of Flp-In CHO-K1 cell lines stably expressing the recombinant nicotinic acid receptors .....	121
3.6.1.	Localisation, detection and functional analysis.....	121
3.7.	Receptor expression .....	122
3.8.	Generation of Flp-In TReX CHO-K1 .....	123
3.8.1.	Strategy A.....	124
3.8.2.	Strategy B.....	124
3.9.	Discussion .....	125
4.	Regulation and desensitisation studies on the nicotinic acid receptors .....	157
4.1.	Introduction.....	157
4.2.	Basic pharmacology .....	158
4.3.	Nicotinic acid stimulates ERK1/2 phosphorylation.....	159
4.4.	Desensitisation studies on the nicotinic acid receptors .....	160
4.5.	Regulation studies on the nicotinic acid receptors .....	160
4.5.1.	Study of Gα <sub>i</sub> expression level.....	161
4.5.2.	Internalisation studies on the nicotinic acid receptor .....	161

4.5.3.	Nicotinic acid-induced phosphorylation of the nicotinic acid receptors .....	164
4.5.4.	Kinase inhibitor study .....	164
4.6.	Discussion .....	165
5.	Nicotinic acid receptor chimeras as tools to study desensitisation .....	197
5.1.	Introduction .....	197
5.2.	Generation of nicotinic acid receptor chimera constructs .....	198
5.3.	Generation of Flp-In CHO-K1 cell lines stably expressing the chimeric nicotinic acid receptors .....	198
5.3.1.	Localisation, detection and functional analysis .....	199
5.3.2.	Internalisation studies .....	200
5.4.	Desensitisation studies .....	200
5.4.1.	VSV-G HM74/HM74A eYFP .....	200
5.4.2.	VSV-G HM74A/HM74 eYFP .....	201
5.5.	Discussion .....	201
6.	Discussion .....	216
7.	Reference List .....	232

## List of Figures

Figure 1.1 Proposed mechanism of nicotinic acid action .....	28
Figure 1.2 Schematic diagram illustrating the main structural features of a GPCR.....	51
Figure 1.3 Organisation of rhodopsin in native mouse membranes .....	52
Figure 1.4 Summary of G protein subunits and intracellular effectors .....	53
Figure 1.5 The G protein activation cycle .....	54
Figure 1.6 Schematic representation of the domain structure for GRK .....	55
Figure 1.7 Structure of arrestins .....	56
Figure 1.8 Schematic illustration of GRK- and $\beta$ -arrestin-dependent desensitisation and internalisation .....	57
Figure 1.9 Diagram illustrating fates of internalised class A and class B receptors.....	58
Figure 1.10 Schematic diagram summarising the three $\beta$ -arrestin mediated regulatory mechanisms .....	59
Figure 1.11 MAPK cascades .....	60
Figure 1.12 Updated domain structure of $\beta$ -arrestin annotated for binding sites .....	61
Figure 1.13 A model for $\beta$ -arrestin-mediated regulation of transcription .....	62
Figure 1.14 Summary: Diversity of GPCR signalling.....	63
Figure 1.15 Schematic diagram of the possible lipid-modifying mechanism of action of nicotinic acid via a $G_i$ coupled GPCR .....	73
Figure 1.16 Molecular structures: Highlighting role of carboxyl group .....	74
Figure 1.17 Physiological role of the nicotinic acid receptors: Negative feedback mechanism during starvation? .....	75
Figure 1.18 Molecular structures of ligands at HM74A.....	76
Figure 1.19 Predicted structure of the human nicotinic acid receptor HM74A.....	78
Figure 1.20 Interaction model of nicotinic acid at the binding site of HM74A .....	80
Figure 1.21 Activation of HM74A .....	81
Figure 3.1 Schematic diagram illustrating the principle of the [ $^{35}$ S] GTP $\gamma$ S assay .....	129
Figure 3.2 Optimisation of [ $^{35}$ S] GTP $\gamma$ S assay: Incubation time.....	130
Figure 3.3 Optimisation of [ $^{35}$ S] GTP $\gamma$ S assay: GDP concentration .....	132
Figure 3.4 Optimisation of [ $^{35}$ S] GTP $\gamma$ S assay: Nicotinic acid concentration response curve utilising optimised GDP concentration.....	133
Figure 3.5 Optimisation of [ $^{35}$ S] GTP $\gamma$ S assay: Protein amount .....	135
Figure 3.6 Nicotinic acid concentration response curve: HM74 .....	136

Figure 3.7 Schematic map of pcDNA3 vector and schematic diagram of the HM74 and HM74A receptor constructs generated.....	138
Figure 3.8 Immunoblot detecting VSV-G epitope and eYFP-tagged forms of the nicotinic acid receptors .....	140
Figure 3.9 Cell surface receptor measurement by ELISA.....	141
Figure 3.10 Localisation of VSV-G HM74A eYFP receptors .....	142
Figure 3.11 Identification of CHO-K1 cell lines stably expressing the VSV-G HM74A eYFP receptor .....	143
Figure 3.12 Identification of a CHO-K1 cell line stably expressing the VSV-G HM74 eYFP receptor .....	144
Figure 3.13 Detection of VSV-G and eYFP tagged forms of the HM74A receptor stably expressed in CHO-K1 cells .....	145
Figure 3.14 Detection of VSV-G and eYFP tagged forms of the HM74 receptor stably expressed in CHO-K1 cells .....	146
Figure 3.15 Functional analysis of CHO-K1 cell lines stably expressing modified versions of the nicotinic acid receptors.....	148
Figure 3.16 Localisation and detection of modified nicotinic acid receptors stably expressed in Flp-In CHO-K1 cells .....	149
Figure 3.17 Functional analysis of Flp-In CHO-K1 cell lines stably expressing recombinant nicotinic acid receptors.....	151
Figure 3.18 VSV-G HM74A eYFP expression compared to VSV-G HM74 eYFP.....	152
Figure 3.19 Biotin labelling of cell surface expressed nicotinic acid receptors .....	153
Figure 3.20 Flp-In TREx system .....	154
Figure 3.21 Flp-In TREx CHO-K1 cell line stably expressing VSV-G HM74A eYFP.....	155
Figure 3.22 Flp-In TREx CHO-K1 cell line not expressing VSV-G HM74 eYFP .....	156
Figure 4.1 Nicotinic acid stimulated [ <sup>35</sup> S] GTPγS binding is abolished by pertussis toxin treatment.....	171
Figure 4.2 Nicotinic acid stimulates ERK1/2 phosphorylation. ERK1/2 phosphorylation was abolished by pertussis toxin treatment .....	174
Figure 4.3 Nicotinic acid induced ERK1/2 activation via HM74A was rapid and sustained. Nicotinic acid induced ERK1/2 activation via HM74 was slower and more transient .....	175
Figure 4.4 Nicotinic acid pre-treatment causes desensitisation of HM74 mediated activation of Gα <sub>i</sub> .....	176
Figure 4.5 Nicotinic acid pre-treatment does not cause desensitisation of HM74A mediated activation of Gα <sub>i</sub> .....	177

Figure 4.6 No change in $G\alpha_{i1}$ and $2$ G protein expression level in control and nicotinic acid pre-treated HM74 samples.....	178
Figure 4.7 Lack of detectable internalisation of the nicotinic acid receptors transiently expressed in mouse embryonic fibroblasts when challenged with nicotinic acid .....	180
Figure 4.8 Lack of detectable internalisation of the nicotinic acid receptors stably expressed in CHO-K1 cells when challenged with nicotinic acid .....	181
Figure 4.9 Nicotinic acid does not internalise VSV-G HM74A eYFP.....	183
Figure 4.10 Lack of internalisation of the nicotinic acid receptors .....	185
Figure 4.11 Nicotinic acid does not internalise either VSV-G HM74 eYFP or VSV-G HM74A eYFP .....	187
Figure 4.12 No change in $\beta$ -arrestin 2 GFP distribution in CHO-K1 cells stably expressing either HM74 or HM74A following nicotinic acid treatment.....	188
Figure 4.13 VSV-G HM74A eYFP was phosphorylated in an agonist-dependent manner ..	189
Figure 4.14 Schematic diagram illustrating predicted phosphorylation sites on the C-terminus of HM74 .....	190
Figure 4.15 VSV-G HM74 eYFP was phosphorylated in an agonist-dependent manner. PKC and PKA inhibitors did not abolish nicotinic acid induced phosphorylation .....	192
Figure 4.16 RO318220 inhibits ERK1/2 phosphorylation. H89 inhibits CREB phosphorylation .....	194
Figure 4.17 Alignment of human and bovine $\beta$ -arrestin 2 amino acid sequences.....	195
Figure 4.18 Knockdown of GRK2 in CHO-K1 cells .....	196
Figure 5.1 Schematic diagram of C-terminal tail nicotinic acid receptor chimeras generated .....	204
Figure 5.2 Localisation and detection of chimeric nicotinic acid receptors stably expressed in Flp-In CHO-K1 cells.....	206
Figure 5.3 Functional analysis of FlpIn CHO-K1 cell lines stably expressing chimeric nicotinic acid receptors.....	208
Figure 5.4 Nicotinic acid does not internalise the chimeric receptors.....	209
Figure 5.5 Nicotinic acid pre-treatment does not cause desensitisation of VSV-G HM74/HM74A eYFP mediated activity of $G\alpha_i$ .....	212
Figure 5.6 Nicotinic acid pre-treatment does not cause desensitisation of VSV-G HM74/HM74A eYFP mediated activity of $G\alpha_i$ .....	214
Figure 5.7 No significant reduction in the maximum binding of [ $^{35}$ S] GTP $\gamma$ S observed in nicotinic acid pre-treated samples .....	215
Figure 6.1 Diagram illustrating principles of RET based techniques.....	227
Figure 6.2 GSK 3: A novel and potent HM74A agonist that does not induce flushing .....	228

Figure 6.3 GSK 3 stimulated ERK1/2 phosphorylation. ERK1/2 phosphorylation was abolished by pertussis toxin treatment .....	230
Figure 6.4 GSK 3-induced phosphorylation of VSV-G HM74A eYFP .....	231

## List of Tables

Table 1.1 Summary of the biological effects of nicotinic acid .....	26
Table 1.2 Effects of nicotinic acid on plasma concentrations of lipids and lipoproteins .....	27
Table 1.3 Pharmacological profile of ligands that act on the nicotinic acid receptors	77
Table 2.1 Covaris acoustic cell disrupter settings.....	102
Table 2.2 Primary and secondary antibody dilutions for immunoblotting .....	104
Table 2.3 Primary and secondary antibody dilutions for immunocytochemistry .....	109
Table 3.1 Primer sequences .....	139
Table 4.1 HM74 basic pharmacology .....	172
Table 4.2 HM74A basic pharmacology .....	173

## **Acknowledgements**

**“My success depends completely on God; I trust in Him, and I submit to Him”**

**Sura 11, verse 88, Quran**

It would not have been possible to achieve this PhD without the advice, influence and support of many people in my life. I would like to thank everyone from teachers at school who laid the foundation and sparked my enthusiasm for knowledge and science; my lecturers, during my undergraduate years, for providing me with an insight into real science in both academic and industrial settings; and most importantly my family; my dad, my brothers and especially my mum who has always been a source of inspiration. Without all these people I would not have been in a position to take on a PhD.

I would like to thank Prof. Graeme Milligan, not only for his guidance throughout my PhD and support during my write up, but for offering me this project despite knowing I did not have a background in pharmacology. I really appreciate the opportunity and challenge you gave me. I am grateful also to Dr. Alan Wise for the encouragement and motivation he provided especially when I needed it the most. Your constant support and constructive feedback was greatly appreciated.

Thank you to all the past and current members of the Molecular Pharmacology group – your support helped to keep me sane when “experiments were not working”. Special thanks to Dr. Joris Robben. Dr. Tim Palmer has been a great support and I would like to thank him for the useful discussions and his invaluable time. I would also like to acknowledge the help and patience of James Rowedder and Dr. Namir Hassan for taking time out from their busy schedules to help me in whatever way that they could while I was at GlaxoSmithKline. And of course my best friends and fellow PhD students, Nadia and Fozia; we started this together and we will finish it together!

Last but not least, I would like to thank Ati, for his constant encouragement and support during the past 4 years. Thank you for listening to me when I was down and thank you for supporting me when things got tough. Without your support I may not have survived this project.

## **Author's declaration**

The work presented in this thesis was conducted by the author and has not previously been submitted for a degree or diploma at this University or any other institution.

## Abbreviations

[<sup>35</sup>S] GTP $\gamma$ S [<sup>35</sup>S] guanosine-5'-O-(3-thio) triphosphate

AA arachidonic acid

ABCA1 ATP-binding cassette A1

AC adenylyl cyclase

AcAc acetoacetate

Amp ampicillin

AP-2 adapter protein 2

ASK1 apoptosis signal-regulating kinase 1

ATP adenosine triphosphate

BRET bioluminescence resonance energy transfer

BSA bovine serum albumin

bp base pair

BGH pA bovine growth hormone and polyadenylation signal

Ca<sup>2+</sup> calcium ion

cAMP cyclic adenosine monophosphate

cDNA complementary DNA

CETP cholesteryl ester transfer protein

CHO	Chinese hamster ovary
CCK	cholecystokinin
CMV	cytomegalovirus
CREB	cAMP response element binding protein
DNA	deoxyribonucleic acid
dNTP	deoxynucleotide triphosphate
eCFP	enhanced cyan fluorescent protein
ELISA	Enzyme-linked Immunosorbent assay
ER	endoplasmic reticulum
ERK	extracellular signal regulated kinase
ET	endothelin receptor
eYFP	enhanced yellow fluorescent protein
FBS	foetal bovine serum
FFA	free fatty acid
FRET	fluorescence resonance energy transfer
FRT	Flp recombinase target
G $\alpha$	G protein $\alpha$
G protein	guanine nucleotide binding protein

GABA	$\gamma$ -aminobutyric acid
GDP	guanosine diphosphate
GFP	green fluorescent protein
GnRH	gonadotrophin-releasing hormone
GTP	guanosine triphosphate
GTP $\gamma$ S	guanosine-5'-O-(3-thio) triphosphate
GOI	gene of interest
GPCR	G protein-coupled receptor
GRK	G protein-coupled receptor kinase
GSK	GlaxoSmithKline
H4	histone 4
HEK	human embryonic kidney
HDL	high density lipoprotein
HSL	hormone sensitive lipase
I $\kappa$ B $\alpha$	Inhibitor of kappa light chain gene enhancer in B cells, alpha
IP	inositol phosphate
IP <sub>6</sub>	inositol hexakisphosphate
JNK	c-Jun N-terminal kinase

K <sup>+</sup>	potassium ion
KAc	potassium acetate
kbp	kilobase pair
LB medium	Luria-Bertani medium
LDL	low density lipoprotein
MAPK	mitogen-activated protein kinase
MDM2	murine double minute
MEF	mouse embryo fibroblasts
MEK	MAPK/ERK kinase
MEKK	MEK kinase
MKK	MAPK-kinase
MLK	mixed-lineage protein kinase
MOPS	morpholinopropane sulfonic acid
MPCA	5-methyl pyrazole-3-carboxylic acid
NAD	nicotinamide adenine dinucleotide
NADP	nicotinamide adenine dinucleotide phosphate
NEFA	non-esterified fatty acid
NES	nuclear export signal

NSF	<i>N</i> -ethylmaleimide-sensitive fusion protein
PAR	protease-activated receptors
PBS	phosphate buffered saline
PCR	polymerase chain reaction
PDE-3B	phosphodiesterase 3B
PGI <sub>2</sub>	prostaglandin I <sub>2</sub>
PGE <sub>2</sub>	prostaglandin E <sub>2</sub>
PGD <sub>2</sub>	prostaglandin D <sub>2</sub>
PKA	cAMP-dependent protein kinase A
PKC	protein kinase C
PLA <sub>2</sub>	phospholipase A <sub>2</sub>
PLC $\beta$	phospholipase C $\beta$
PLC	phospholipase C
PMA	phorbol 12-myristate 13-acetate
PPAR $\gamma$	peroxisome proliferator activated receptor $\gamma$
PUMA-G	protein upregulated in macrophages
RET	resonance energy transfer
RGS	regulators of G protein signalling

RhoGEFs	Rho guanine nucleotide exchange factor
RIPA	radioimmune precipitation assay buffer
RLuc	<i>Renilla</i> luciferase
RNA	ribonucleic acid
SPA	scintillation proximity assay
SDS	sodium dodecyl sulphate
SDS-PAGE	sodium dodecyl sulphate polyacrylamide gel electrophoresis
siRNA	small interfering RNA
T.A.E.	tris acetate EDTA
T.E.	tris EDTA
TetR	Tet repressor
TG	triglyceride
TM	transmembrane region
T <sub>m</sub>	melting temperature
TNF	tumor necrosis factor
TRAF6	TNF receptor associated factor 6
VIP 1	vasoactive intestinal peptide type 1 receptor
VLDL	very low density lipoprotein

Sanam Mustafa, 2008

VSV-G      vesicular stomatitis virus glycoprotein

## 1. Introduction

With obesity now accepted as a global issue, the occurrence of obesity related diseases, such as cardiovascular diseases, have become a major concern and strain on health services around the world. A constant race exists amongst pharmaceutical companies to develop 'miracle' drugs to treat affected individuals, recently of all ages. However, in order to aid drug discovery there is an imminent need to identify the mechanisms of action of existing 'successful' drugs on the market.

Many risk factors for cardiovascular disease have been identified, dislipidaemia, for example, is a condition where the plasma levels of one or more lipoproteins is abnormally high or low. A dislipidaemic patient most at risk from cardiovascular disease would likely exhibit raised levels of low density lipoprotein (LDL) cholesterol and triglycerides while at the same time also displaying low levels of high density lipoproteins (HDL). A dislipidaemic patient is also at high risk of suffering from atherosclerosis. Atherosclerosis is characterised by accumulation of cholesterol, other lipids, extracellular matrix and various inflammatory cells which results in the narrowing of the vessel lumen. If the atherosclerotic lesion becomes unstable it can lead to arterial thrombosis. High levels of LDL cholesterol are therefore a risk factor. However, HDL cholesterol is thought to have anti-atherogenic properties due to its role in reverse cholesterol transport (Lewis & Rader, 2005).

Nicotinic acid, also known as niacin, is a B3 vitamin abundant in red meat, fish, poultry and green leafy vegetables. Its vitamin effects, including promoting the health of the nervous system, skin, hair and eyes, were demonstrated in the early 20<sup>th</sup> century. As little as 20 mg/day is sufficient to benefit from its vitamin properties. In 1955 the lipid-lowering qualities of nicotinic acid were published by Altschul and colleagues (Altschul et al., 1955). Since its arrival on the market as the first lipid-based intervention proven to prevent cardiovascular disease and associated mortality, it has been available both over the counter and by prescription in various formulations. When given in gram doses nicotinic acid produces many desirable effects in patients, such as lowering of total plasma levels of cholesterol, LDL cholesterol and total triglycerides and it is the only available drug that also decreases

lipoprotein involved in cholesterol transport (Parsons, Jr. & Flinn, 1959; Altschul et al., 1955; Malik & Kashyap, 2003). Nicotinic acid is also known to selectively increase HDL cholesterol and apolipoprotein AI-only containing HDL particles (Lp AI) – which are believed to be implicated in reverse cholesterol transport (Shepherd et al., 1979; Sakai et al., 2001). Nicotinamide, also a B-complex vitamin, however does not display any of these lipid-modifying qualities. These observations led to much more interest in the beneficial effects of nicotinic acid in humans and on going research into the mechanism by which this vitamin successfully modifies lipid levels to more favourable concentrations. The biological effects of nicotinic acid as a vitamin and lipid-modifying drug have been summarised in Tables 1.1 and 1.2.

## 1.1. Early studies

Not long after the lipid-modifying effects of nicotinic acid were reported, Carlson and co-workers demonstrated that nicotinic acid was able to inhibit a noradrenaline-stimulated increase in plasma levels of free fatty acid (FFA) (Carlson & Oro, 1962). In later studies it was shown that nicotinic acid was able to reduce FFA levels by inhibiting lipolysis in adipose tissue (Carlson, 1963). The uptake of nicotinic acid by adipose tissue was very neatly established with the use of [<sup>3</sup>H]-labelled nicotinic acid (Carlson & Hanngren, 1964). The mechanism by which nicotinic acid is thought to act has been illustrated in Figure 1.1.

With respect to clinical studies, the Coronary Drug Project was the first study to show that nicotinic acid monotherapy of 3 g/day prevented cardiovascular disease and its associated mortality (Canner et al., 1986; Coronary Drug Project Research Group, 1975). This study also demonstrated the long lasting effects of nicotinic acid therapy. Patients who had stopped taking nicotinic acid for 9 years still experienced an 11 % decrease in total mortality compared to those on placebo (Canner et al., 1986).

Around this time, in the late 1980s, cholesterol synthesis inhibitors (statins) were introduced. Although they have been shown to effectively reduce elevated levels of LDL cholesterol they have only little or no effects on HDL cholesterol and triglyceride levels. To take advantage of nicotinic acid's ability to increase HDL cholesterol levels, studies were then conducted to examine the combined use of

nicotinic acid with a statin called simvastatin (Brown et al., 2001). The HDL Atherosclerosis Treatment Study (HATS) demonstrated that combined treatment was more beneficial than monotherapy with statin alone. Compared to placebo, a reduction of around 60 % in clinical cardiovascular events was recorded.

## **1.2. Introduction to nicotinic acid therapy**

As is the case with many drugs, the use of nicotinic acid is associated with side effects which are relatively harmless but often limit patient compliance. The so called 'niacin flush', being the prime culprit, is the flushing of the skin due to a prostaglandin D2-mediated vaso-cutaneous reaction (Morrow et al., 1989). Flushing of the face and upper body can be induced within minutes of administering as little as 50 mg of nicotinic acid. Higher doses of 1 g of nicotinic acid can result in pronounced cutaneous vasodilation over the whole body lasting around half an hour. Starting in the upper body around the face and neck region, the patient experiences intense feelings of warmth and itching. It can then spread to the arms and chest and occasionally the legs and feet. Although this nicotinic acid-induced flushing can be substantially reduced by continuous treatment and/or the administration of cyclooxygenase inhibitors, for example aspirin, many patients discontinue their treatment due to severe discomfort (Kaijser et al., 1979). During the time of absence, the patient loses the tolerance developed to the flushing response and if treatment is commenced again the flushing will also develop. Although tolerance to the nicotinic acid-induced flushing is observed, patients do not develop tolerance to its lipid-modifying effects. Hepatotoxicity, ranging from minor elevation in liver enzymes to hepatic necrosis and death, is another complication associated with nicotinic acid treatment. Other reported side effects include gastrointestinal upset (such as heartburn, indigestion, nausea, diarrhoea and stomach pain) and hyperuricemia (McKenney, 2004).

Early studies indicated that nicotinic acid treatment was not safe for diabetic patients. It had been reported that diabetic patients were at risk of developing insulin resistance as a result of long-term treatment (Kahn et al., 1989; Garg & Grundy, 1990). An initial increase in FFA levels following nicotinic acid treatment was blamed for the insulin resistance. However, recent studies are now concluding that when given in

moderate doses under strict monitoring, nicotinic acid is not only safe but also effective in diabetic patients (Elam et al., 2000; Grundy et al., 2002).

The severity of these niacin-induced side effects depends greatly on the specific formulation given to patients. These formulations fall under three categories outlined below (McKenney, 2004; Mills et al., 2003).

### **Unmodified/Immediate Release**

Available over-the-counter, immediate release nicotinic acid has been used therapeutically for 50 years in doses as high as 12 g a day. For optimum effects this formulation needs to be taken three times a day. Unmodified niacin is often associated with higher occurrences of skin flushing, gastrointestinal symptoms and elevated blood glucose levels.

### **Modified/Sustained Release**

Originally designed to reduce flushing in patients, this formulation is metabolised slowly. It has been associated with liver toxicity and hence abandoned in clinical trials.

### **Extended Release**

Available by prescription for a single daily dose, the absorption rate of this formulation is an intermediate of the two previously described forms. It is associated with fewer episodes of flushing, gastrointestinal symptoms and hepatotoxicity.

## **1.3. Nicotinic acid: Molecular mechanism of action?**

As statins do not display the side effects associated with nicotinic acid, statins were widely welcomed by medical practitioners and nicotinic acid therapy was largely 'neglected'. However, unlike nicotinic acid, statins have no effect on elevated levels of Lipoprotein (a) (Lpa) or low levels of HDL. With increasing awareness of the importance of the levels of different lipids in plasma as risk factors for cardiovascular disease, the past few years has witnessed a new interest in this vitamin.

Despite the widespread availability and clinical use of nicotinic acid, the exact mechanism by which it acts is not fully understood. In order to maximise the full potential of nicotinic acid as a lipid-modulating drug, overcome niacin-related side effects and further develop novel and more potent drugs to treat cardiovascular disease, it is vital to elucidate the molecular mechanism of action of nicotinic acid. This has only become possible with the recent identification of the G protein-coupled nicotinic acid receptors as the molecular target for nicotinic acid (Soga et al., 2003; Tunaru et al., 2003; Wise et al., 2003).

<b>Nicotinic acid</b>		
<b>Use</b>	<b>Vitamin</b> <b>Physiological role</b> precursor for NAD <sup>+</sup> , NADP <sup>+</sup>	<b>Anti-dislipidaemic drug</b> <b>Pharmacological use</b>
<b>Required dose</b>	<b>&gt; 15 – 20 mg/day in the diet</b>	<b>500 – 2000 mg/day</b>
<b>Required plasma level</b>	<b>100 – 400 nM</b>	<b>4 -16 µM</b> <b>Peak concentration: 50 – 300 µM</b>
<b>Nicotinamide</b>	<b>Equivalent to nicotinic acid as a vitamin</b>	<b>No anti-dislipidaemic effects</b>

**Table 1.1 Summary of the biological effects of nicotinic acid**

Abbreviations: NAD, nicotinamide adenine dinucleotide (major electron acceptor in the oxidation of fuel metabolites; NADP, nicotinamide adenine dinucleotide phosphate. Table adapted from (Offermanns, 2006).

<b>Lipid/Lipoprotein</b>	<b>Effects on plasma concentrations</b>
<b>VLDL</b>	↓ 25 – 40 %
<b>LDL cholesterol</b>	↓ 6 – 22 %
<b>HDL cholesterol</b>	↑ 18 -35 %
<b>Total cholesterol</b>	↓ 4 – 16 %
<b>Triglyceride</b>	↓ 21 – 44 %
<b>Lipoprotein Lp(a)</b>	↓ 16 – 36 %

**Table 1.2 Effects of nicotinic acid on plasma concentrations of lipids and lipoproteins**

The above effects are summarised for nicotinic acid treatment in excess of 1.5 g/day. VLDL, very low density lipoprotein. Table adapted from (Gille et al., 2008).

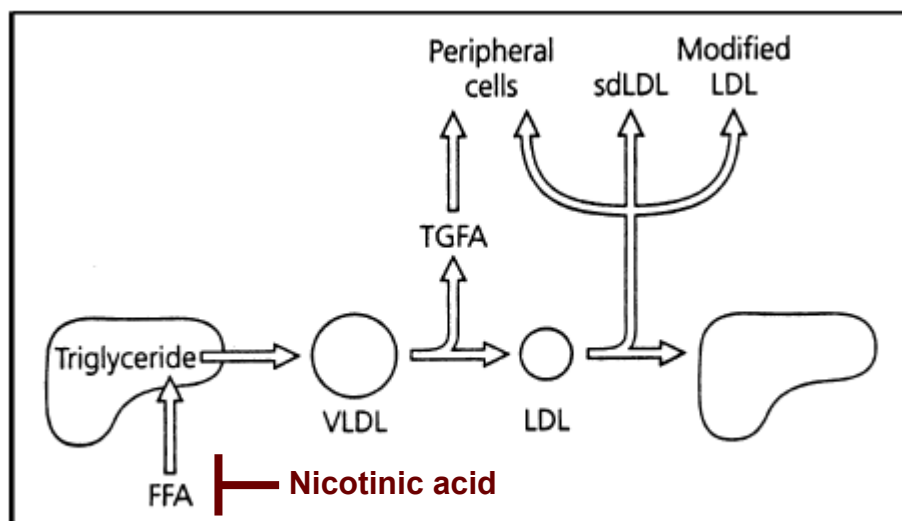


**Figure 1.1 Proposed mechanism of nicotinic acid action**

Plasma FFA act as precursors of liver triglycerides which in turn are precursors for VLDL and so forth as illustrated above. By inhibiting FFA mobilisation in adipocytes, nicotinic acid is thought to reduce the flow of FFA into the liver. This reduces the synthesis of VLDL and therefore also LDL. Figure adapted from (Carlson, 2005).

## 1.4. Introduction to G protein-coupled receptors

G protein-coupled receptors (GPCRs) make up the largest family of cell-surface receptors. By responding to a vast array of stimuli, known as ligands, such as sensory messages (photons and odours) and messenger molecules (lipids, nucleotides, and peptides), GPCRs allow cells to communicate with each other and their surroundings (Kristiansen, 2004). As their name suggests, these receptors transduce extracellular signals via guanine nucleotide binding proteins (G proteins) to intracellular effectors. Widely expressed in the human body, GPCRs are implicated in a wide range of disease pathways including pain, arthritis, cancer and schizophrenia (Lundstrom, 2006). It is estimated that 50 % of all drugs on the market regulate GPCR function, of which 30 % directly target GPCRs (Jacoby et al., 2006). Despite this, however, out of the 800 or so receptors that make up this superfamily, drugs directed at these receptors act on approximately only 30 receptors (Wise et al., 2004). This knowledge, taken together with their diverse physiological and pathological roles, highlights the potential for drug discovery in this field.

### 1.4.1. *Brief history*

Although physiological techniques had been used to study the effects of drugs on receptors since the early 20<sup>th</sup> century, the understanding of receptors as discrete molecular entities did not exist until the development of radioligand binding studies in the late 1960s. The first such pioneering studies demonstrated the binding of [<sup>3</sup>H] atropine to endogenously expressed muscarinic receptors in guinea-pig ileum smooth muscle (Paton & Rang, 1965). Despite this, the existence of molecular receptors was only widely accepted when purified and reconstituted  $\beta_2$ -adrenergic receptor was demonstrated to respond to catecholamines in systems not normally responsive to  $\beta$ -adrenergic agonists (Cerione et al., 1983). The eventual cloning of hamster  $\beta_2$ -adrenergic receptor revealed sequence and structural homology to rhodopsin, a seven transmembrane spanning light receptor protein that resides inside cell membranes of retinal rod cells (Dixon et al., 1986). Homology approaches were then adopted to clone several members of the GPCR family. For example, low stringency Southern blotting utilising  $\beta_2$ -adrenergic receptor cDNA as a probe identified the first orphan

receptor (a receptor with an unknown function and/or ligand) (Kobilka et al., 1987). This receptor was later recognised as 5-HT<sub>1A</sub>, the first serotonin receptor to be cloned (Fargin et al., 1988). In an independent attempt, again employing the  $\beta_2$ -adrenergic receptor as a probe in low stringency hybridization experiments, rat dopamine D<sub>2</sub> receptor was isolated (Bunzow et al., 1988). Thereafter, rapid progress in the search for new GPCRs was the result of the exploitation of the relatively new PCR technology. DNA probes were designed to conserved sequences in the third and sixth transmembrane domains of cloned GPCRs (Libert et al., 1989). In a similar approach the use of degenerate primers, based on the dozen or so receptors cloned by then, allowed the cloning of a large family of olfactory receptors (Buck & Axel, 1991).

### **1.4.2. GPCR classification**

Members of the GPCR superfamily can be divided into five major subfamilies, which show considerable sequence conservation within members of one family but not between families. The major differences between the GPCR subfamilies are the variability in the length and function of the N-terminus and the location of the ligand-binding domain. The GPCR superfamily can be divided into the following five groups/families (Lagerstrom & Schioth, 2008).

#### **1.4.2.1. Rhodopsin family/class A**

The Rhodopsin family is the largest of the GPCR superfamily. Although members of this family contain residues that are highly conserved, the primary structure is diverse. Conserved motifs, E/DRY (Glu/Asp-Arg-Tyr) motif in TM III and the D/NPXXY (Asp/Asn-Pro-X-X-Tyr) motif in TM VII, are hallmarks of receptors belonging to this family. Class A receptors also often contain cysteine residues which form a disulphide bond connecting the first and second extracellular loops.

These receptors characteristically have short extracellular N-terminal tails and for this reason are primarily activated by interactions between the ligand and the TM regions and the extracellular loops. Based on their ligand binding properties, class A receptors can be further sub-divided into four groups. Group A $\alpha$  is composed of GPCRs with small ligands, such as rhodopsin and the  $\beta$ -adrenergic receptors, which have binding sites within the seven transmembrane region. Peptide-binding receptors form group

A $\beta$ . Ligands bind to these receptors at the N-terminal tail or the extracellular loops. Receptors in group A $\gamma$  bind to peptides and lipid-like compounds and include opioid, angiotensin and chemokine receptors. The final group, A $\delta$ , contain nucleotide- and glycoprotein-binding receptors and are characterised by large extracellular domains containing the ligand binding sites.

#### **1.4.2.2. Secretin receptor family/class B**

A family of around 15 receptors, they share a similar morphology to class A receptors but generally have a larger extracellular N-terminal tail which is involved in ligand binding. The N-terminal region of these receptors contains several cysteine residues which form a network of disulphide bridges. These receptors are activated by high molecular weight peptide hormones such as glucagon and secretin.

#### **1.4.2.3. Adhesion receptor family/class B**

The second largest GPCR family with 33 members is characterised by long N-terminus regions. The endogenous ligands for many receptors from this family are not known. However, the few orphanised receptors bind extracellular matrix molecules.

#### **1.4.2.4. Glutamate receptor family/class C**

The smallest family of GPCRs contains metabotropic glutamate receptors, GABA-B receptors, calcium sensing receptors and the sweet and umami taste receptors. These receptors are characterised by a long N-terminus tail, which folds to incorporate a separate ligand-binding domain.

#### **1.4.2.5. Frizzled/Taste2 receptors**

This group includes the frizzled/smoothed receptors that are known to be involved in embryonic development. The 25 bitter taste receptors also belong to this family of receptors and can be further divided due to the sequence diversity between the receptors.

### **1.4.3. GPCR structure**

Insight into the structure of GPCRs can aid understanding of the mechanisms of ligand binding and receptor activation. This knowledge can then be exploited to

design novel ligands but also to predict novel receptor binding sites. However, due to the inherent flexibility of GPCRs, especially in the third intracellular loop, these receptors are difficult to crystallise. Until recently the only high resolution crystal structure, at 2.8 Å, available was for bovine rhodopsin in its inactive state (Palczewski et al., 2000). In 2007, published reports presented two crystal structures of the human  $\beta_2$ -adrenergic receptor (Cherezov et al., 2007; Rasmussen et al., 2007; Rosenbaum et al., 2007). The third intracellular loop was stabilised by either binding to an antibody fragment, Fab5, (Rasmussen et al., 2007) or by replacing it with T4 lysozyme, a small soluble protein (Cherezov et al., 2007; Rosenbaum et al., 2007). In both cases, carazolol, an inverse agonist was also present. As carazolol only suppresses around 50 % of basal activity of  $\beta_2$ -adrenergic receptor, the crystal structures therefore do not represent a fully active or inactive receptor.

Crystal structures confirmed data generated from hydrophobicity analysis and electron microscopy that GPCRs share a heptahelical structure where a single polypeptide chain spans the membrane seven times, resulting in an extracellular N-terminus and an intracellular C-terminus. The seven transmembrane helices (TM I – TM VII) vary in length and are linked by three alternating intracellular (ICL) and extracellular loops (ECL), as shown in Figure 1.2. From sequence homology of members of the GPCR family, it is clear that TM domains are the most highly conserved regions amongst GPCRs. Unsurprisingly, the extra- and intracellular regions are more divergent as these domains allow the receptors to interact with a myriad of structurally different ligands and couple to different intracellular effectors respectively.

When viewed from the extracellular surface, the seven helices are arranged in an anticlockwise manner and although TM IV and VI are roughly perpendicular to the membrane, due to the presence of certain amino acids such as prolines, the remaining helices are slightly tilted and kinked. This results in the receptor being split into three functional domains; an extracellular region for ligand binding, an intracellular region for intracellular interactions and a linking region in between the two allowing signal transduction (Madabushi et al., 2004). Within the transmembrane region, the C-terminal end of TM III contains a highly conserved DRY motif which has been implicated in the stabilisation of the inactive state by allowing the formation of an

'ionic lock' between R135 (R in DRY motif) and E247 in TM VI (Ballesteros et al., 2001). The constitutive activity of  $\beta_2$ -adrenergic receptor may be partly due to the absence of the 'ionic lock' observed in the rhodopsin crystal structure. The NPXXY motif which is highly conserved in TM VII has also been shown to be important in stabilising the inactive state of the receptor by allowing TM VII to interact with TM VI.

From the rhodopsin crystal structure, the extracellular domain forms a compact structure, often referred to as a 'lid'. It is thought this plays a role in preventing rapid dissociation of rhodopsin's ligand (Sakmar, 2002; Palczewski, 2006). However, with respect to the  $\beta_2$ -adrenergic receptor, the crystal structure obtained suggests a more open conformation allowing it to interact with diffusible ligands. The extracellular loops of rhodopsin also contain two conserved cysteine residues which form a disulphide bond stabilising the receptor structure. Virtually all GPCRs possess one or more N-linked glycosylation sites (Asn-X-Ser/Thr) in the extracellular region, where X can be any amino acid except proline or asparagine (Kristiansen, 2004). For several GPCRs, prevention of glycosylation results in reduced cell surface expression of the receptor but has a limited effect on ligand binding or the function of the receptors that are successfully delivered to the cell surface (Davidson et al., 1995; Ray et al., 1998).

The intracellular domains of GPCRs display flexibility allowing these regions to undergo conformational changes following receptor activation and interact with various intracellular effectors. Due to this high degree of flexibility this region is poorly defined in the crystal structures. However, studies have shown that the serines and threonines in this region can form recognition sites for protein kinases and therefore play a role in receptor regulation.

#### **1.4.4. GPCR oligomerisation**

In the past few years a new phenomenon of GPCR dimerisation/oligomerisation has been described. Challenging traditional models of GPCRs as monomeric signalling units, initial evidence supporting oligomerisation was obtained over twenty-five years ago but largely ignored (Salahpour et al., 2000). These experiments typically reported the identification of molecular species with molecular mass consistent with the

presence of dimers not monomers. These results were overlooked until 1993 when Maggio and co-workers explored this idea further. Complementation experiments were set up using two chimeric  $\alpha_2$ -adrenergic- $m_3$ -muscarinic receptors which when expressed alone failed to induce any signals. However, when expressed together agonist-dependent activation of phospholipase C was detected (Maggio et al., 1993). This observation was explained by intermolecular interactions between the two mutant receptors.

The discovery by different groups that the GABA<sub>B</sub> receptor was in fact a heterodimer of two distinct subunits, GABA<sub>B</sub>R1 and GABA<sub>B</sub>R2, further strengthened the faith of followers of the dimerisation theory (Jones et al., 1998; Kaupmann et al., 1998; White et al., 1998). It was shown that the GABA<sub>B</sub>R1 subunit was unable to bind ligand or traffic to the cell surface when expressed in a heterologous system due to the presence of an endoplasmic reticulum retention motif identified within the C-terminal tail of the GABA<sub>B</sub>R1. The interaction of GABA<sub>B</sub>R1 with the C-terminal tail of the GABA<sub>B</sub>R2 subunit masks the retention signal, allowing the heterodimer to be exported and trafficked to the cell surface (Margeta-Mitrovic et al., 2000; Pagano et al., 2001). The importance of heterodimerisation for receptor function was demonstrated in studies with mutant GABA<sub>B</sub>R1 subunits that displayed cell surface expression (Margeta-Mitrovic et al., 2000). These subunits were not functional despite expression at the plasma membrane.

Despite the generation of experimental evidence supporting dimerisation, there are many sceptics among the scientific community who dismiss the results as artefacts. Concerns are mainly due to the shortcomings of the experimental techniques used to detect dimerisation. For example, co-immunoprecipitation is a biochemical technique commonly used to detect protein-protein interactions between two differentially tagged receptors. Both tagged receptors are expressed in a single heterologous expression system and cell lysates are prepared. Using an antibody specific to one tag, one receptor is immunoprecipitated and the resulting samples are analysed by immunoblotting with a primary antibody to detect the second tag. Immunoreactivity suggests the presence of both receptors, possibly as a dimer. This detection method has been criticised as the high levels of receptors expressed and also the hydrophobic nature of GPCRs may cause artificial aggregation. For example, Salim and colleagues

reported that the 5-HT<sub>1A</sub> receptor interacted with any GPCR it was co-expressed with (Salim et al., 2002). Although negative controls have been developed, where lysates prepared from cells separately expressing each tagged receptor are mixed prior to immunoprecipitation, critics argue over the use of recombinant systems with high levels of expressed receptors and not native tissues.

Addressing the issue of using heterologous systems, atomic force microscopy was used to investigate the organisation of rhodopsin in native mouse disc membranes (Fotiadis et al., 2003; Liang et al., 2003). These studies showed the rhodopsin receptors arranged in an oligomeric array of closely packed dimers, as shown in Figure 1.3. However, these results have also been challenged. Firstly, it was argued that the tissue chosen for this study naturally expresses the rhodopsin receptor at very high densities, so therefore it can be argued that close proximity does not necessarily mean there are any physical interactions between the receptors. Also, Chabre and co-workers have argued that the oligomer-like arrangements seen by Fotiadis' and Liang's research groups are due to the segregation of proteins and lipids at low temperatures (Chabre et al., 2003). They strongly dismiss the results as rows of proteins packed in partially ordered microcrystalline arrays and refer back to the original X-ray crystal structure determined by Palczewski and colleagues, which gave no indication of rhodopsin existing as a dimer (Palczewski et al., 2000).

GPCR dimerisation with other GPCRs or unrelated receptors has the potential to make a significant contribution to the diversity and specificity of GPCR signalling. As there is a divide in the scientific community with regards to the existence of higher-order oligomeric complexes, much more research is needed in this field before any firm conclusions can be made firstly about their authenticity and then their functional significance.

#### **1.4.5. Introduction to G proteins and classical signal transduction**

Upon ligand binding, the cytoplasmic domain of the receptor undergoes a conformational change; rotation of TM VI uncovers the G protein binding sites causing it to acquire a high affinity for G proteins (Javitch et al., 1997). Consisting of

three separate polypeptides, these heterotrimeric G proteins are made up of highly conserved  $\alpha$ ,  $\beta$  and  $\gamma$  subunits. Based on sequence homology of the  $G\alpha$  subunit, G proteins are typically divided into four main classes;  $G_{i/o}$ ,  $G_s$ ,  $G_{q/11}$ ,  $G_{12/13}$ . In the inactive state, the guanine diphosphate (GDP) bound  $\alpha$  subunit is tightly associated with the  $\beta\gamma$  complex. The GPCR acts as a guanine nucleotide exchange factor and promotes the release of GDP from the  $\alpha$  subunit, which is then replaced with guanine triphosphate (GTP). Historically the exchange of GDP for GTP was thought to result in the dissociation of the  $\alpha$  subunit from the  $\beta$  and  $\gamma$  subunits. However, fluorescence resonance energy transfer (FRET)-based studies have suggested that a conformational re-arrangement, not a separation, of the  $\alpha$  and  $\beta\gamma$  subunits may occur (Bunemann et al., 2003). These subunits are then able to associate with various effectors, such as adenylyl cyclase, phospholipase C, calcium ( $Ca^{2+}$ ) and potassium ( $K^+$ ) channels, to transduce the signal from the receptor. G protein subunits and their effectors have been summarised in Figure 1.4. The intrinsic GTPase activity of the  $\alpha$  subunit terminates this signalling cascade by hydrolysing GTP back to GDP and re-uniting the  $\alpha$  subunit with the  $\beta\gamma$  complex, thus completing the cycle, as shown in Figure 1.5 (Brink et al., 2004). This GTP-GDP exchange is accelerated by proteins known as regulators of G protein signalling (RGS). RGS proteins are defined by a so called RGS domain which binds directly to activated  $G\alpha$  subunits to enhance their intrinsic GTPase activity (Berman et al., 1996; Hollinger & Hepler, 2002). More than 30 RGS and RGS-like proteins have been identified and, based on amino acid sequence and protein structure, can be divided into six distinct families.

#### **1.4.6. Regulation of GPCR signalling**

Many mechanisms have evolved for regulating receptor signalling. These mechanisms can operate at the level of the GPCR, G protein or further down the signalling cascade. For example, as mentioned previously, the RGS proteins involved in halting signals that have already been generated, provide a negative regulatory mechanism.

##### **1.4.6.1. Desensitisation of GPCR signalling**

At the receptor level, one of the most studied regulatory mechanisms is desensitisation. As a result of prolonged or repeated exposure to an agonist, signal

transduction can be either completely or partially abolished. This prevents the receptor from over-stimulating and is important in both physiological and pharmacological settings. Desensitisation can be classed as either homologous or heterologous. Homologous desensitisation refers to the situation where only the activated GPCR is desensitised, whereas in heterologous desensitisation, activation of one GPCR can lead to the desensitisation of other unrelated and often inactivated GPCRs. Many mechanisms of desensitisation exist, however GPCR phosphorylation plays a crucial role in the classical model of desensitisation (Krupnick & Benovic, 1998).

GPCR phosphorylation by second messenger-dependent protein kinases such as cAMP-dependent protein kinase A (PKA) and protein kinase C (PKC) were regarded as the principal mechanisms of receptor desensitisation (Benovic et al., 1985). It was only when the  $\beta_2$ -adrenergic receptor was shown to be phosphorylated in cells lacking functional PKA that the existence of other relevant kinases was acknowledged (Strasser et al., 1986). This led to the identification of  $\beta$ -adrenergic receptor kinase ( $\beta$ -ARK), which was later renamed G protein-coupled receptor kinase (GRK) 2 (Benovic et al., 1986).

GRKs are a family of serine/threonine protein kinases which preferentially phosphorylate residues of the third intracellular loop or C-terminal domain of agonist-occupied receptors. It is thought agonist binding causes the receptor to undergo a conformational change, unmasking the substrates for phosphorylation (Pitcher et al., 1998). The seven members of this family can be grouped into subfamilies based on sequence and functional similarities (Pitcher et al., 1998). The first group, comprising of GRK 1 and 7, are found exclusively in retinal rods and cones, respectively. They regulate rhodopsin and the colour opsins. The second group consists of GRK 2 and 3. These GRKs are distributed throughout the body and are responsible for phosphorylating a variety of receptors. Finally, GRK4, 5 and 6 make up the last subfamily. GRK4 is expressed at significantly high levels in testes and is the only GRK known to date that undergoes alternative splicing (Sallese et al., 1994). GRK5 is expressed at high levels in the heart, lung and retina. GRK6 is widely expressed throughout the body. Generally GRKs are considered to be cytosolic proteins, however both GRK5 and 6 are constitutively associated with membranes through

various mechanisms. For example, electrostatic interactions are thought to play a role in membrane association of GRK5, but in the case of GRK6, palmitoylation of the kinase is necessary (Stoffel et al., 1994; Kunapuli et al., 1994; Premont et al., 1994). GRKs are made up of three domains, where the catalytic domain is flanked by two regulatory domains (Figure 1.6). The N-terminal region is thought to be important for recognition and binding of the activated receptor and the C-terminal domain is responsible for interacting with inositol phospholipids and the G $\beta\gamma$  subunit of G proteins (Inglese et al., 1993). It is thought that the cytosolic proteins are recruited to the plasma membrane, at least partly, by the disassociated G $\beta\gamma$  subunits (Daaka et al., 1997b).

In the classical model of desensitisation, phosphorylation by GRK marks the receptor for further desensitisation by arrestin proteins. However, recently GRK2 and 3 have been reported to mediate phosphorylation-independent desensitisation of G $_q$  coupled GPCRs. By binding to both the GPCR and G $_q$  protein it prevents the receptor and G protein from interacting (Ferguson, 2007). It is also worth mentioning that arrestins can associate in an agonist-dependent manner with receptors that are not phosphorylated. This was first demonstrated in a study where phosphorylation deficient leukotriene B4 receptors were able to interact with  $\beta$ -arrestin and hence were desensitised and internalised (Jala et al., 2005).

Arrestins are a class of soluble proteins, which also play an important role in regulating receptor signaling. The evolutionary conservation of the arrestins in all mammals highlights their importance as 'housekeeping' proteins (Miller & Lefkowitz, 2001). The members of the arrestin family can be divided into two groups based on their sequence, function and tissue distribution. The visual arrestins make up the first group. Visual arrestin, also known as arrestin 1, was the first arrestin identified. It is the major protein constituent of the rod outer segments, localised primarily in the retina, where it was demonstrated to bind rhodopsin (Pfister et al., 1985; Smith et al., 1994). Subsequently, cone arrestin which shared a high degree of homology (around 50 %) with visual arrestin was identified and therefore was also placed into this group (Murakami et al., 1993; Craft et al., 1994). Cone arrestin is highly enriched in both the retina and the pineal gland but is mainly localised within

the cone photoreceptors of the retina (Craft et al., 1994). Both arrestins are implicated in the regulation of photoreceptor function.

The  $\beta$ -arrestins are expressed outside the retina, and are highly expressed in neuronal tissue and in the spleen (Attramadal et al., 1992). Their ubiquitous expression suggests they have relatively broad receptor specificity.  $\beta$ -arrestin 1 was originally identified as a co-factor required for GRK-mediated  $\beta_2$ -adrenergic receptor desensitisation *in vitro* and shares 59 % sequence homology with visual arrestin (Benovic et al., 1987; Lohse et al., 1990).  $\beta$ -arrestin 2 was cloned from bovine and rat brain (Sterne-Marr et al., 1993; Attramadal et al., 1992). Recent evidence indicates that  $\beta$ -arrestins can form both homo- and heterodimers (Storez et al., 2005). Evidence suggests that monomeric  $\beta$ -arrestin 1 displays nuclear localisation whereas oligomeric  $\beta$ -arrestin 1 is cytoplasmic (Milano et al., 2006). However,  $\beta$ -arrestin 2 does not display nuclear localisation and co-expression with  $\beta$ -arrestin 1 also prevents  $\beta$ -arrestin 1 accumulation in the nucleus.

The arrestin proteins are present in all mammals and share a highly conserved structure. With respect to receptor binding, mutagenesis studies on visual arrestin allowed it to be divided into two main domains; the N and C domains. These can be further subdivided into three functional and two regulatory domains (Gurevich et al., 1995). The functional domains are comprised of a receptor activation recognition domain (residues 24 -180), a secondary receptor binding domain (residues 180 – 330), and phosphate sensor domain (residues 163 – 182). The regulatory domains are at the N- and C-terminus, (residues 1 -24 and 330 – 404 respectively). The structure of arrestins has been summarised in Figure 1.7 (Ferguson, 2001). Crystal structure analysis of visual arrestin suggest the domains are composed largely of anti-parallel  $\beta$ -sheets (Hirsch et al., 1999). The N and C domains are connected by a hinge region and the C domain is also connected to the C-terminal tail by a flexible linker. The C-terminus also forms various interactions with parts of the N and C domains which results in a rigid structure. Splice variants of visual,  $\beta$ -arrestin 1 and  $\beta$ -arrestin 2 exist. However, these are not reported to possess any differences in their functional activity.

Following agonist stimulation of the receptor, arrestin proteins undergo a substantial conformational change into a high affinity receptor-binding state and translocate rapidly to the plasma membrane where they selectively bind GRK phosphorylated agonist-bound GPCRs (Lohse et al., 1990; Gurevich & Benovic, 1993). It has been proposed that the intramolecular interactions which stabilise the inactive arrestin are broken by an active phospho-receptor, thus allowing the transition of the inactive arrestin into a high affinity receptor binding state (Hirsch et al., 1999; Schleicher et al., 1989). By binding to the receptor the arrestin protein prevents G protein coupling by steric hindrance (Kuhn & Wilden, 1987; Krupnick et al., 1997). This in turn prevents the signalling cascade from initiating. The arrestin protein can then interact with various other proteins of the endocytotic machinery and internalise the GPCR (Goodman, Jr. et al., 1996).

#### **1.4.6.2. GPCR internalisation**

In addition to their classical role in GPCR desensitisation,  $\beta$ -arrestins have additional roles differentiating them from the visual arrestins. In 1996, Ferguson and colleagues reported that the rapid recruitment of  $\beta$ -arrestins to the phosphorylated  $\beta_2$ -adrenergic receptor was vital for the receptor to internalise into intracellular vesicles (Ferguson et al., 1996). Internalisation, or sequestration, is the physical process by which the receptor moves from the plasma membrane into the intracellular membrane compartments of the cell upon agonist activation – this is essential for down regulation of the signal and receptor resensitisation (the process by which internalised receptors are dephosphorylated and recycled back to the cell surface). Although GPCR internalisation is generally considered to be a result of agonist-stimulation, a number of published studies suggest some GPCRs are constitutively internalised in the absence of agonist binding. This constitutive internalisation was first reported for the  $\delta$  opioid receptors (Costa & Herz, 1989). Our understanding of the role of  $\beta$ -arrestins in internalisation and the fate of internalised GPCRs has been greatly advanced by the use of fluorescently tagged  $\beta$ -arrestins, which allow the visualisation of  $\beta$ -arrestin and receptor trafficking in live cells (Barak et al., 1997).

Studies by von Zastrow and Kobilka in 1994 proposed that the internalisation of the  $\beta_2$ -adrenergic receptor was mediated via the clathrin-coated vesicle pathway (von

Zastrow & Kobilka, 1994). In 1996, it was determined that  $\beta$ -arrestin is able to bind to clathrin with high affinity, which reinforced the idea that the  $\beta$ -arrestins were acting as adapter proteins by targeting GRK phosphorylated ligand-activated GPCRs to clathrin coated-pits for endocytosis (Goodman, Jr. et al., 1996).

$\beta$ -arrestins 1 and 2 have two recognition sites which allow them to link GPCRs with at least two components of the endocytic machinery; clathrin (the major structural component of the clathrin-based endocytic machinery) and the  $\beta$ 2-adaptin subunit of the clathrin adapter protein 2 (AP-2) complex (Goodman, Jr. et al., 1996; Laporte et al., 1999). The AP-2 complex is responsible for linking many receptors to the clathrin endocytic machinery by binding to clathrin and dynamin (Kirchhausen, 1999). The heterotetrameric AP-2 complex is composed of two large  $\alpha$ - and  $\beta$ 2-adaptin subunits of 100 kDa,  $\mu$ 2 subunit (50 kDa) and a small 17 kDa subunit named  $\sigma$ 2 (Kirchhausen, 1999). Dynamin, a GTPase that forms the neck of clathrin-coated pits, is essential for pinching off the vesicles from the plasma membrane (Urrutia et al., 1997). Its importance was demonstrated in studies where the presence of a dominant-negative mutant of dynamin impaired the endocytosis of  $\beta$ 2-adrenergic receptor (Zhang et al., 1996). Figure 1.8 is a schematic illustration showing the molecular mechanisms involved in GRK and  $\beta$ -arrestin-dependent desensitisation and internalisation. Internalised receptors bound to  $\beta$ -arrestin are either retained in large endosomes for recycling back to the membrane (resensitisation) or targeted for degradation by lysosomes (downregulation).

The functions of both  $\beta$ -arrestin 1 and 2 are regulated by post-translational modifications. The endocytic function of  $\beta$ -arrestin is regulated by phosphorylation. Despite sharing around 80 % amino acid identity each arrestin is phosphorylated by a different kinase.  $\beta$ -arrestin 1 is phosphorylated by extracellular signal regulated kinase (ERK) enzymes whereas  $\beta$ -arrestin 2 is phosphorylated by casein kinase II (Attramadal et al., 1992; Lin et al., 1999; Lin et al., 2002). Cytosolic  $\beta$ -arrestin 1 is phosphorylated at S412 and upon translocation to the membrane the arrestin protein is rapidly dephosphorylated where it can then bind with high affinity to both the receptor and clathrin ( Lin et al., 1999). The importance of this post-translational modification was demonstrated in a study where a S412  $\beta$ -arrestin 1 mutant,

mimicking the phosphorylated state of the protein, was introduced into cells expressing the  $\beta_2$ -adrenergic receptor. Although the mutant protein was able to mediate desensitisation it was only able to bind poorly to clathrin and therefore inhibited receptor sequestration. Hence it can be concluded that dephosphorylation is only required for its function in receptor- $\beta$ -arrestin-mediated endocytosis but not for receptor binding and desensitisation (Lin et al., 1997).

#### **1.4.6.3. GPCR downregulation and resensitisation**

Downregulation of GPCRs is caused by long term exposure of the receptor to an agonist and is characterised by a persistent loss of receptors from cells. This results in the attenuation of signal transduction. In contrast to receptor desensitisation or internalisation, agonist removal only slowly or incompletely reverses this process. Downregulation is the least understood mechanism involved in receptor regulation. However, one thing is certain, the control of cell surface receptor density not only occurs at the transcriptional level but also by ‘sorting’ of sequestered GPCRs to either degradation or recycling pathways (Whistler et al., 2002).

The physiological importance of receptor resensitisation is logical, as irreversible desensitisation would result in cells becoming unable to respond to extracellular stimuli – key to its survival. However, an example where reversible desensitisation is detrimental to the cell is also known. The protease-activated receptors (PAR) are ‘self-activated’ receptors, such that once cleaved by thrombin, the N-terminal tail folds over to act as a ligand. In this case, resensitisation would mean that the receptor would be delivered back to the cell surface in its activated form. To prevent this from occurring, in the case of the PAR receptors, all activated receptors are degraded and new receptors are synthesized (Hein et al., 1994). It is becoming clear that  $\beta$ -arrestins are highly involved in many aspects of receptor trafficking – resensitisation is no exception. A study by Zhang and colleagues, reported that unless  $\beta$ -arrestins were overexpressed in COS7 cells (which naturally only produce low levels of these proteins), no resensitisation of  $\beta_2$ -adrenergic receptors was observed (Zhang et al., 1997). It can therefore be presumed that  $\beta$ -arrestins maybe responsible for delivering receptors back to the plasma membrane in their inactivated and dephosphorylated state. Generally, dephosphorylation of the GPCRs is known to occur in an acidified

endosomal vesicle compartment (Krueger et al., 1997). However, an example where receptor internalisation is not necessary for dephosphorylation or resensitisation is the thyrotropin-releasing hormone receptor, which can undergo dephosphorylation at the cell membrane (Jones & Hinkle, 2005).

The rate at which GPCRs traffic from the plasma membrane to the endosomal compartment and back again to the cell surface varies depending on the subtype of the receptor. Depending on their interactions with  $\beta$ -arrestins, GPCRs are classed as either A or B receptors (Oakley et al., 1999; Oakley et al., 2000). Class A, including the  $\beta_2$  adrenergic receptor, bind preferentially to  $\beta$ -arrestin 2 in a transient manner, such that the receptor- $\beta$ -arrestin complex dissociates rapidly when the receptor is internalised (Pierce & Lefkowitz, 2001; Luttrell & Lefkowitz, 2002). This allows the receptor to be rapidly dephosphorylated and recycled back to the plasma membrane. Receptors designated as class B, such as vasopressin 2, bind equally to  $\beta$ -arrestin 1 and 2 to form more stable receptor- $\beta$ -arrestin complexes, thus allowing the targeting of the whole complex to the endosomes (Luttrell & Lefkowitz, 2002). As a result of this, class B receptors, therefore, recycle back to the plasma membrane slowly suggesting the stable receptor- $\beta$ -arrestin complexes may favour receptor degradation. The fates of both classes of receptors is illustrated in Figure 1.9 (Pierce & Lefkowitz, 2001). It is worth mentioning, however, that evidence exists for a class B receptor (the mutant S363A-V2R vasopressin receptor) to efficiently recycle back to the cell surface despite its stable interaction with  $\beta$ -arrestin (Innamorati et al., 2001). It is has therefore been proposed that other 'receptor intrinsic' or protein determinants must also exist.

The covalent attachment of ubiquitin, known as ubiquitination, was originally discovered in the context of cellular protein degradation. Now ubiquitination of  $\beta$ -arrestin has also been shown to play an important role in regulating GPCR internalisation and resensitisation. This was demonstrated in a study where internalisation of  $\beta_2$ -adrenergic receptor was inhibited in the absence of  $\beta$ -arrestin ubiquitination (Shenoy et al., 2001). Protein ubiquitination is mediated by the action of three enzymes, E1, E2 and E3. The first two enzymes are responsible for activating and escorting the activated ubiquitin. The third enzyme is then able to recognise and

modify the protein of interest. It is thought that the transient ubiquitination of arrestins results in an unstable GPCR-arrestin complex. In this case, the GPCR exhibits fast recycling to the plasma membrane. Conversely, prolonged arrestin ubiquitination equates to a stable GPCR-arrestin complex and therefore slow recycling of the GPCR to the membrane. Although GPCR ubiquitination is not thought to play a role in receptor endocytosis it is, however, implicated in lysosomal sorting and degradation of the activated receptor. An example of this is where a mutant  $\beta_2$ -adrenergic receptor unable to be ubiquitinated, was demonstrated to internalise but unable to be efficiently degraded (Shenoy et al., 2001).

The persistent degradation of cell surface receptors, due to long-term exposure to an agonist, is one of the most poorly understood regulatory mechanisms. This course of action can occur in a period of hours to days. What is certain, however, is that the role of  $\beta$ -arrestins is of paramount importance during this process. In 2001, Kohout and co-workers observed that downregulation of the  $\beta_2$  adrenergic receptors failed to take place in mouse embryo fibroblasts (MEF) cells lacking both  $\beta$ -arrestin 1 and 2 (Kohout et al., 2001). To summarise, the three  $\beta$ -arrestin-mediated regulatory mechanisms discussed in this chapter are illustrated in Figure 1.10 taken from (McDonald & Lefkowitz, 2001).

#### **1.4.6.4. Arrestin-independent desensitisation and internalisation pathways**

The exact consensus sequence dictating phosphorylation by a GRK or second messenger-dependent protein kinase is not known. It has recently been suggested that the negative charge introduced by phosphorylation is important for arrestin binding rather than the precise position (Gurevich & Gurevich, 2006). However, an increasing amount of evidence suggests that all phosphorylation events are not equal. For example, published studies suggest PKC or PKA phosphorylated receptors are not good substrates for arrestin binding (Pitcher et al., 1992). This has been demonstrated with the  $\beta_2$ -adrenergic receptor where phosphorylation by both PKA and GRK has been shown to result in desensitisation (Roth et al., 1991). However, only GRK-mediated phosphorylation results in arrestin binding (Lohse et al., 1992). In another independent study utilising FRET, the rapid disassociation of arrestin from  $\beta_2$ -

adrenergic receptor was observed when the agonist was removed but the receptor remained phosphorylated (Krasel et al., 2005). This is likely to be the case as evidence suggests both agonist occupancy and phosphorylation of a GPCR is necessary for arrestin recruitment. Unlike GRK phosphorylation, agonist occupancy of receptors is not a prerequisite for PKA or PKC phosphorylation. Taken together, these observations would go some way to explaining the lack of arrestin recruitment.

Nevertheless, both PKA and PKC phosphorylated receptors can undergo desensitisation and internalisation. Desensitisation of the D<sub>3</sub> dopamine receptor, for example, is mediated almost exclusively by the second messenger-dependent protein kinase, PKC (Cho et al., 2007). Earlier evidence suggesting phosphorylation by PKA is sufficient to impair receptor-stimulated GTPase activity has been published for the  $\beta_2$ -adrenergic receptor (Benovic et al., 1985). It is thought that receptor phosphorylation in a G protein coupling region by a second messenger-dependent protein kinase, but not a GRK, can sterically inhibit receptor/G protein interactions (Benovic et al., 1985). With respect to receptor internalisation,  $\beta$ -arrestin independent pathways have been identified.

This was first observed when the overexpression of dominant-negative  $\beta$ -arrestin proteins did not affect the internalisation of the vasoactive intestinal peptide type 1 (VIP 1) receptor or the endothelin type B (ET<sub>B</sub>) receptor (Claing et al., 2000). These studies suggested that the VIP 1 and ET<sub>B</sub> receptors internalised by a  $\beta$ -arrestin-independent mechanism. Evidence suggests that in the case of the ET<sub>B</sub> receptor internalisation is via the caveolar pathway (Teixeira et al., 1999).

Caveolae are small flask-shaped invaginations of the plasma membrane, rich in proteins and lipids. The shape and structural organisation of caveolae are due to the presence of caveolin proteins 1, 2 and 3. These proteins self-assemble in high mass oligomers to form a cytoplasmic coat on the membrane invaginations. Recent evidence associates caveolae with GPCR endocytosis and signalling. Initial evidence supporting the role of caveolae in receptor internalisation came from studies of the GPI-anchored folate receptor by Anderson and colleagues (Anderson et al., 1992). Since this initial discovery many receptors are now known to be present in caveolae, including the M<sub>2</sub> muscarinic receptor, the  $\beta_2$  adrenergic receptor and the endothelin

ET<sub>A</sub> receptor (Feron et al., 1997; Dupree et al., 1993; Chun et al., 1994). Evidence supporting their role in signal transduction comes from the observation that G proteins and other signalling molecules are also present (and enriched) in caveolae (Anderson, 1993; Lisanti et al., 1994). Not much is known about the precise mechanism by which caveolae-mediated pathways operate besides the knowledge that there is a requirement for cholesterol. Studies have shown treatment with inhibitors of cholesterol such as cholesterol-binding drugs inhibit endocytosis by caveolae (Anderson et al., 1996; Kiss & Geuze, 1997; Schnitzer et al., 1994). As caveolae are rich in lipids, presumably removal of cholesterol would affect the caveolar structure and hence function. In 1995, Roettger and co-workers looked at the internalisation of the cholecystokinin (CCK) receptors and their preferred internalisation pathways. It is known that approximately 80 % of these receptors internalise via the clathrin-coated pit pathway, whilst the remaining 20 % or so prefer internalising via caveolae following receptor stimulation (Claing et al., 2002). Roettger and co-workers demonstrated that when the clathrin-coated pit pathway was inhibited, surprisingly, nearly all the CCK receptors internalised (Roettger et al., 1995). These results not only confirmed that the caveolar pathway is another means for receptor internalisation but also suggested that CCK receptors (and possibly other GPCRs) can internalise via both pathways if the need ever arises.

The GTPase dynamin has also been implicated in the caveolae pathway as well as in clathrin-mediated endocytosis – it has been shown to be present at the neck of caveolar structures (Claing et al., 2002). Claing and colleagues have shown that overexpression of a dynamin dominant negative mutant reduces internalisation of the endothelin ET<sub>B</sub> and VIP 1 receptors (Claing et al., 2000). Internalisation pathways independent of both  $\beta$ -arrestin and dynamin have also been suggested (Claing et al., 2000; Gilbert et al., 2001; Lamb et al., 2001).

#### **1.4.7. *Novel mechanisms of GPCR signalling: signal specificity***

The vast number of receptors that make up the GPCR superfamily respond to a diverse array of stimuli, however, they rely on a limited number of intracellular effectors, second and third messengers to convey highly specific physiological

responses. In recent years it has become clear that signal transduction is not a simple linear pathway transferring information from the cell membrane to the nucleus, but a more intricate network of signalling dependent on a multitude of factors such as biased agonism, receptor oligomerisation, receptor density and cell type. This introduces novel aspects of GPCR signalling and regulation. The classical model of GPCR regulation has been described in section 1.4.6. Although a few examples which differed from the classical model were introduced, below is a somewhat limited summary of the current understanding of GPCR regulation and its complexities.

#### **1.4.7.1. Biased agonism**

It is now generally acknowledged that the 'two state' model where a receptor adopts either an active or inactive conformation is not entirely accurate. Instead it is thought the receptor can undergo a variety of conformational changes that can lead to different downstream signalling pathways. Biased agonism or agonist-directed trafficking describes the phenomenon where different ligands can act on the same receptor but induce different conformations and therefore different physiological responses (Kenakin, 1995). An example of differential signalling by different agonists via the same receptor is the serotonin 5-HT<sub>2C</sub> receptor (Berg et al., 1998; Backstrom et al., 1999). In the study by Berg and co-workers, it was demonstrated that some agonists preferentially activate the phospholipase C (PLC) pathway to mediate inositol phosphate (IP) accumulation or the phospholipase A<sub>2</sub> (PLA<sub>2</sub>) pathway resulting in arachidonic acid (AA) release (Berg et al., 1998). In a separate study it was demonstrated that, unlike serotonin, LSD was unable to promote calcium release (Backstrom et al., 1999).

#### **1.4.7.2. G protein-coupling**

Although little is known about the selectivity of this process as no consensus motif to predict G protein-coupling has been identified, in general, intracellular sequences closest to the plasma membrane appear to be crucially involved in G protein specificity (Ostrowski et al., 1992). It is now widely accepted that GPCRs can couple to more than one class of G proteins and therefore specificity of a cellular response can be achieved due to the existence of molecular variability within the G proteins (Hermans, 2003). The  $\beta_2$ -adrenergic receptor, for example, which is well documented to couple to G $\alpha_s$  can also couple to G $\alpha_i$  following receptor phosphorylation by PKA

(Daaka et al., 1997a). It has been suggested that PKA phosphorylation is mainly important at low agonist concentrations (Tobin, 1997). This provides an interesting example of where an agonist can control G protein specificity in a dose-dependent manner. Other examples of G protein promiscuity are the M<sub>2</sub> muscarinic and S1P<sub>2</sub> and S1P<sub>3</sub> sphingosine-1-phosphate receptors, which have been shown to couple to three different classes of G proteins (Michal et al., 2007; Siehler & Manning, 2002).

#### **1.4.7.3. $\beta$ -arrestin-mediated signalling**

Increasing evidence suggests that  $\beta$ -arrestins play a more prominent role in cellular signalling than initially envisaged. They have been shown to play a critical role in the signalling complexes that ultimately lead to activation of members of the mitogen-activated protein kinase family (MAPK).

The best characterised members of the MAPK family are extracellular signal regulated kinases (ERK) 1 and 2, c-Jun N-terminal kinase (JNK) and p38 MAPK. These proteins have key roles in the regulation of many biological processes, including cell growth, proliferation, differentiation and apoptosis. MAPKs represent a key step in the signalling cascades that relay signals from the plasma membrane to the nucleus. The core unit of a MAPK signalling complex is made up of a three-tiered protein kinase family – activation of each MAPK requires the phosphorylation of tyrosine and threonine by an upstream protein kinase as illustrated in Figure 1.11 (Miller & Lefkowitz, 2001; Pierce & Lefkowitz, 2001). ERKs are primarily cytoplasmic but their activation leads to their dissociation from cytoplasmic anchoring proteins, such as MEK. They can then translocate to the nucleus where they can phosphorylate substrates such as transcription factors. Initial evidence suggesting  $\beta$ -arrestins can function as transducers of GPCR signals came from a study where  $\beta_2$ -adrenergic receptor activation of MAPK was inhibited by the expression of a dominant-negative  $\beta$ -arrestin mutant (Daaka et al., 1998). Then the discovery that  $\beta$ -arrestins can interact with Src, a non-receptor tyrosine kinase involved in the Ras-dependent activation of MAPK, in an agonist-dependent manner lead to the conclusion that  $\beta$ -arrestins can act as scaffolds, linking receptors to downstream signalling pathways (Luttrell et al., 1999). This activation of signalling pathways by  $\beta$ -arrestin is often referred to as a ‘second wave of signal transduction’.  $\beta$ -arrestin

appears to directly interact with Src via the Src homology 3 (SH3) and the catalytic domains of Src (Luttrell et al., 1999; Miller et al., 2000). Recently,  $\beta$ -arrestins have been shown to regulate two MAPK family members; ERK 1/2 and JNK3 (DeFea et al., 2000; McDonald et al., 2000). By binding to JNK3,  $\beta$ -arrestin can recruit upstream kinases such as apoptosis signal-regulating kinase 1 and form scaffolding complexes to transduce signals from the cell membrane. It has been suggested that the recruitment of Src to GPCRs is essential for both the activation of the ERK cascade and for receptor internalisation – possibly Src may be involved in the phosphorylation of a key component involved in both pathways (Miller & Lefkowitz, 2001).

The angiotensin receptor system has provided a good model for studying  $\beta$ -arrestin-mediated signalling. A mutated angiotensin octapeptide, SII angiotensin, which is unable to stimulate G protein-mediated effects such as calcium mobilisation but retained the ability to recruit  $\beta$ -arrestin to the receptor and thereby induce receptor internalisation, was utilised to study  $\beta$ -arrestin-dependent ERK1/2 activation. It was demonstrated that angiotensin II type 1A receptor was able to activate ERK1/2 via G protein- and  $\beta$ -arrestin 1-dependent pathways in an independent manner (Ahn et al., 2004). The kinetics of ERK activation were also deduced, where G protein-mediated activation was rapid and transient. However,  $\beta$ -arrestin-mediated activation was slower but more prolonged. In general, G protein-mediated ERK activation results in the translocation of ERK to the nucleus.  $\beta$ -arrestin-mediated ERK activation is usually restricted to the cytoplasm (DeFea et al., 2000). In this case, ERK can phosphorylate cytosolic substrates, including transcription factors, which then translocate to the nucleus (Ebisuya et al., 2005).

Recent evidence suggests both  $\beta$ -arrestins can translocate to the nucleus and induce transcription of various genes by recruiting co-factors such as p300 and increasing histone acetylation (Kang et al., 2005). One such example is the translocation of  $\beta$ -arrestin 1 to the nucleus in response to the activation of the  $\delta$ -opioid receptor. By translocating to the nucleus it increased the transcription of p77 and *FOS* genes and thereby regulated the cell cycle. In a similar manner, activation of an odorant receptor can translocate  $\beta$ -arrestin 2 to the nucleus (Neuhaus et al., 2006). With respect to the 'new' roles of arrestin, Figure 1.12 is an updated diagram of the  $\beta$ -arrestin domain

structure illustrating binding sites, nuclear localisation and nuclear export (NES) (Ma & Pei, 2007). Also, a model for  $\beta$ -arrestin-mediated regulation of transcription has been illustrated in Figure 1.13 (Ma & Pei, 2007).

#### **1.4.7.4. Signalling by intracellular GPCRs**

Increasing amounts of evidence exist which strongly suggests the existence of functional intracellular GPCRs. Recently an example of a receptor, GPR30, which is exclusively targeted to the endoplasmic reticulum has been reported (Revankar et al., 2005). This fully functional estrogen receptor demonstrated intracellular calcium mobilisation upon agonist activation.

Challenging textbook understanding, published studies suggest that GPCRs and G proteins may be pre-assembled and then targeted to the plasma membrane (Dupre et al., 2006). This has further supported the idea of intracellular GPCR signalling, as intracellular receptor/G protein complexes have been shown to be sensitive to agonist (Rebois et al., 2006). It has been proposed that these intracellular receptors may activate signalling pathways that are distinct from those activated by cell surface receptors. One such example comes from receptors that signal from compartmentalised lipid rafts. Lipid rafts are planar domains of cell membranes and, like caveolae, are enriched in lipids and proteins, in particular cholesterol. G proteins and many GPCRs have been shown to localise in lipid rafts (Oh & Schnitzer, 2001). Via the  $G_q$  coupled-oxytocin receptor, oxytocin inhibits cell growth. However, fusion of this receptor with caveolin-2 localised this receptor to lipid rafts where it was then able to activate distinct pathways which resulted in the opposite response and promotion of cell proliferation (Guzzi et al., 2002). As oxytocin can stimulate and inhibit cell growth via a single receptor, this finding goes a long way to demonstrate how the differential localisation of a receptor can achieve signal specificity.

Clearly GPCR signalling is not as simple as first envisioned. In order to appreciate the complexities of this signalling cascade, it is becoming increasingly important to study these receptors in their native systems. The willingness of researchers to think 'outside the box' and the development of more sensitive experimental techniques are likely to uncover more surprises. To summarise, Figure 1.14 is an updated version of Figure 1.4 incorporating G protein-independent signalling pathways.

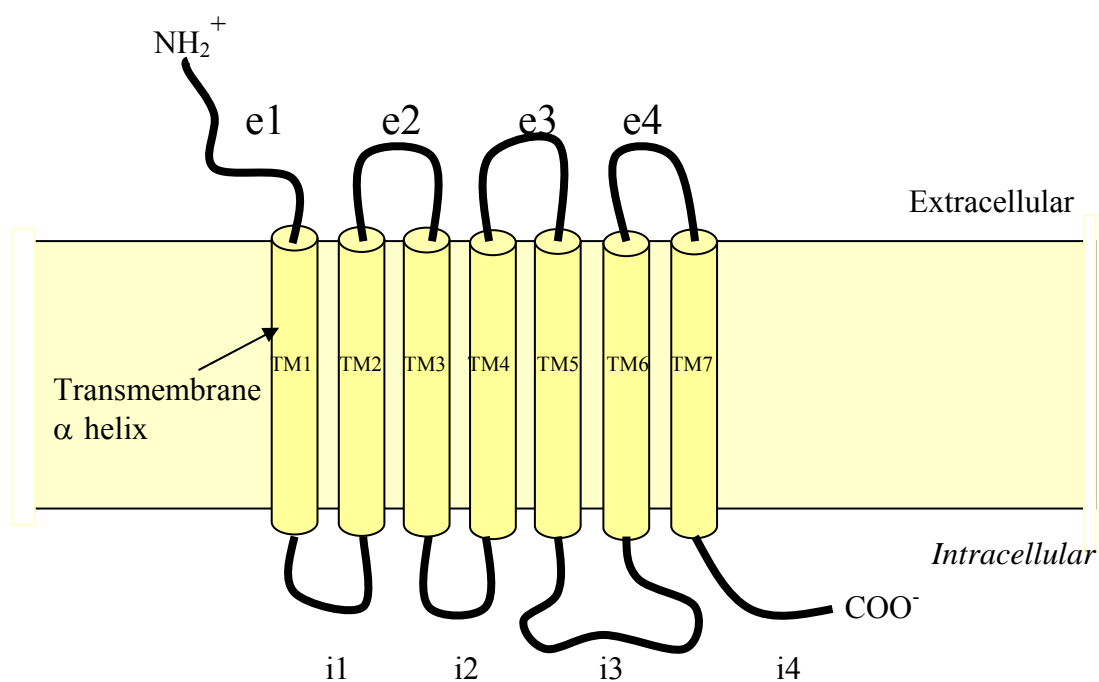


**Figure 1.2 Schematic diagram illustrating the main structural features of a GPCR**

The seven transmembrane (TM) helices are linked by three extracellular (e) loops and three intracellular (i) loops. GPCRs have an extracellular N-terminus tail and an intracellular C-terminus tail.

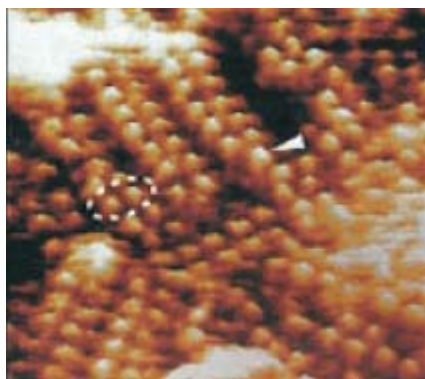


**Figure 1.3 Organisation of rhodopsin in native mouse membranes**

The atomic force microscopy image is presented to support the conclusion that the rhodopsin receptor is arranged in an oligomeric array of closely packed dimers in native mouse rod-outer segment disc membranes. A single rhodopsin dimer is indicated by a broken ellipse and the white arrowheads indicate a rhodopsin monomer. Image from (Liang et al., 2003).

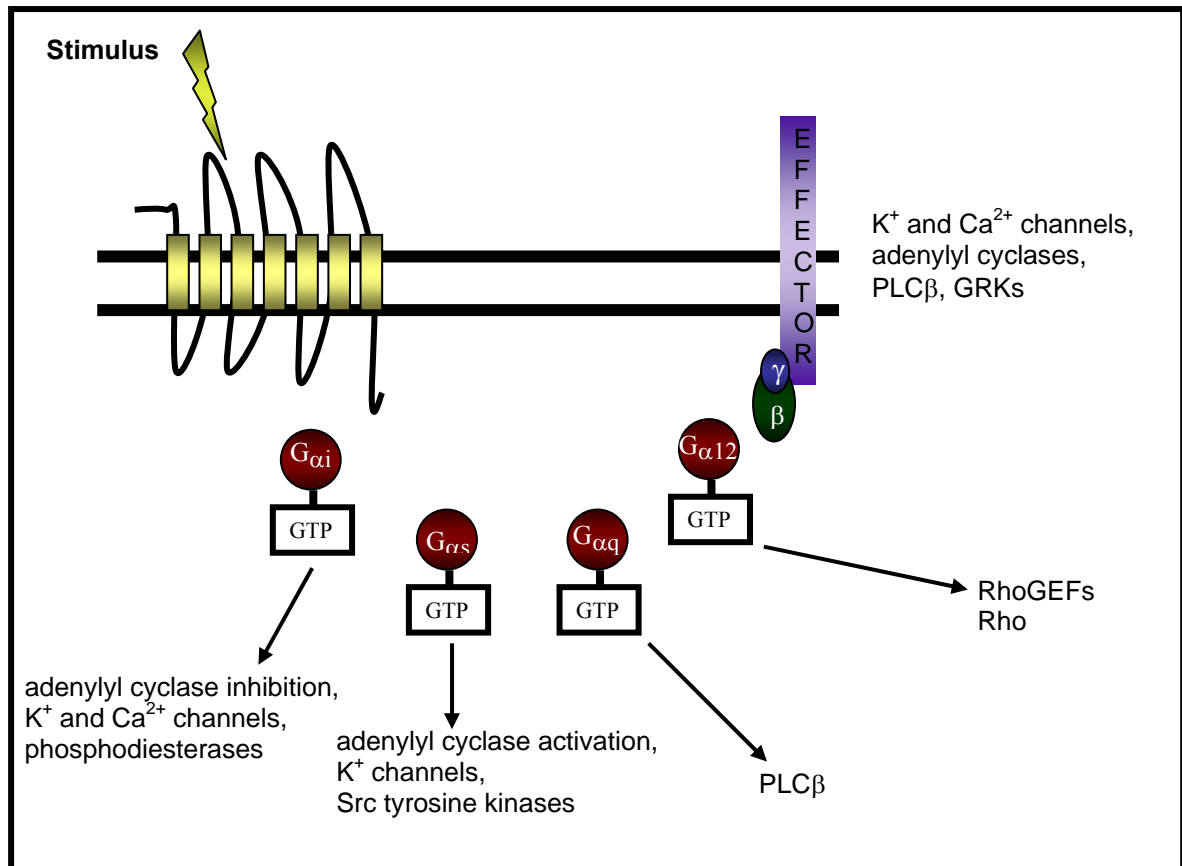


**Figure 1.4 Summary of G protein subunits and intracellular effectors**

Activation of GPCRs can mediate a variety of cellular responses via various intracellular effectors. PLCβ, phospholipase Cβ

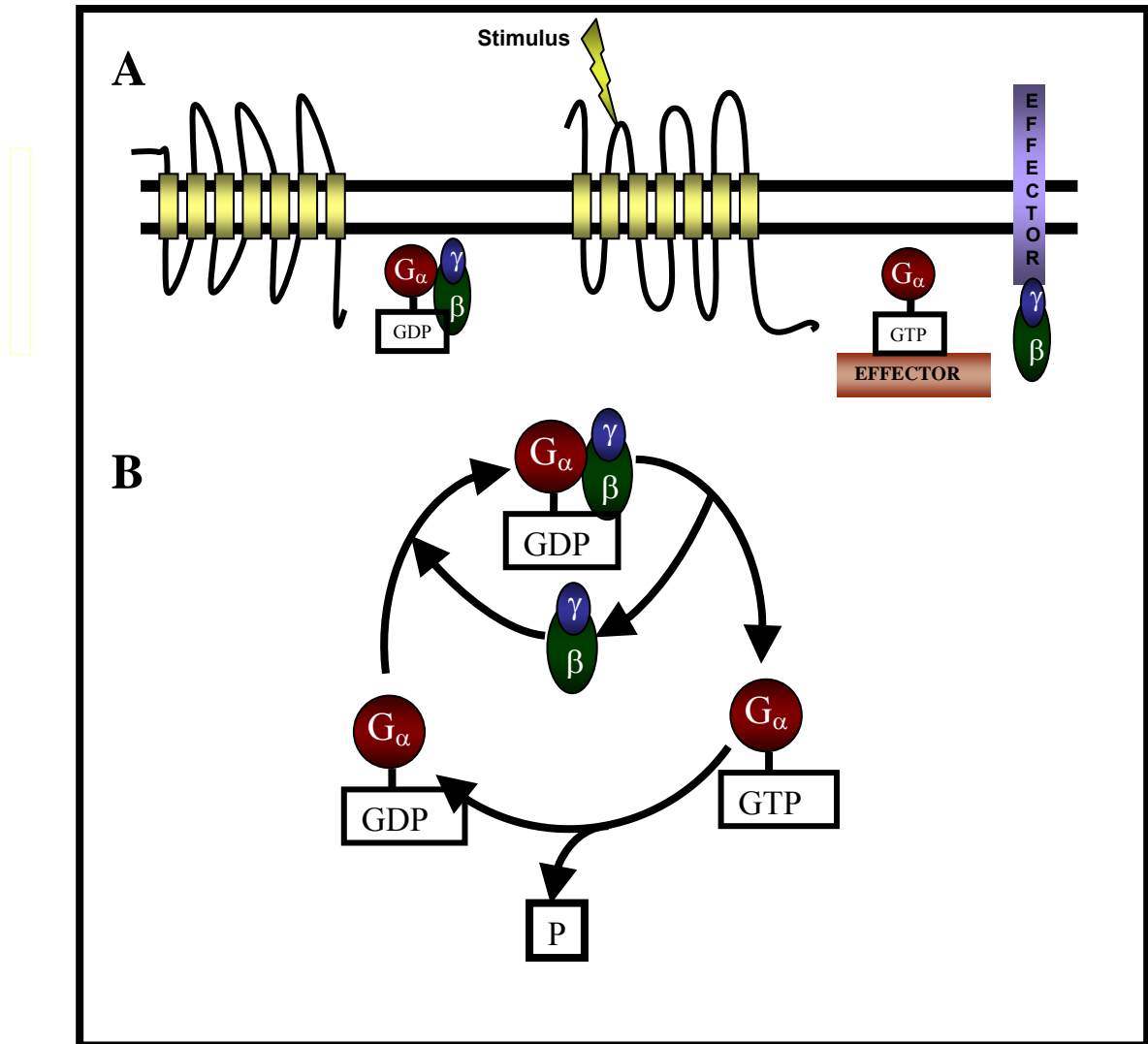


**Figure 1.5 The G protein activation cycle**

**A:** In the inactive state the GDP bound G protein  $\alpha$  ( $G_{\alpha}$ ) subunit associates with the  $\beta/\gamma$  complex to form an inactive heterotrimeric G protein. Upon ligand activation the GPCR undergoes a conformational change resulting in increased affinity for the G protein; this results in the exchange of GDP for GTP on the  $G_{\alpha}$  subunit, which reduces the affinity of the  $G_{\alpha}$  subunit for the  $\beta/\gamma$  complex and therefore leads to dissociation of the heterotrimeric G protein. Both the  $G_{\alpha}$  subunit and the  $\beta/\gamma$  complex can then interact with effectors, transducing the signal. **B:** The activated state lasts until the GTP is hydrolysed to GDP by the intrinsic GTPase activity of the  $G_{\alpha}$  subunit.

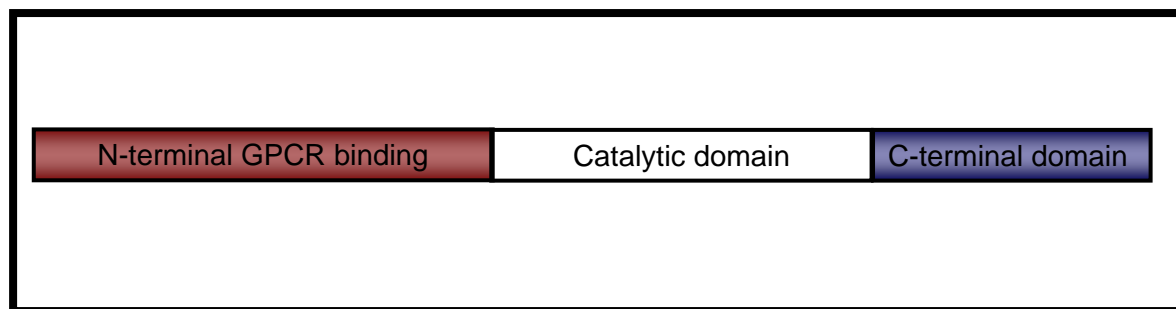


**Figure 1.6 Schematic representation of the domain structure for GRK**

The catalytic domain is flanked by two regulatory domains. The N-terminal domain plays a role in the recognition and binding of activated receptors. The C-terminal domain is responsible for interacting with intracellular effectors and G $\beta\gamma$  subunit of G proteins.

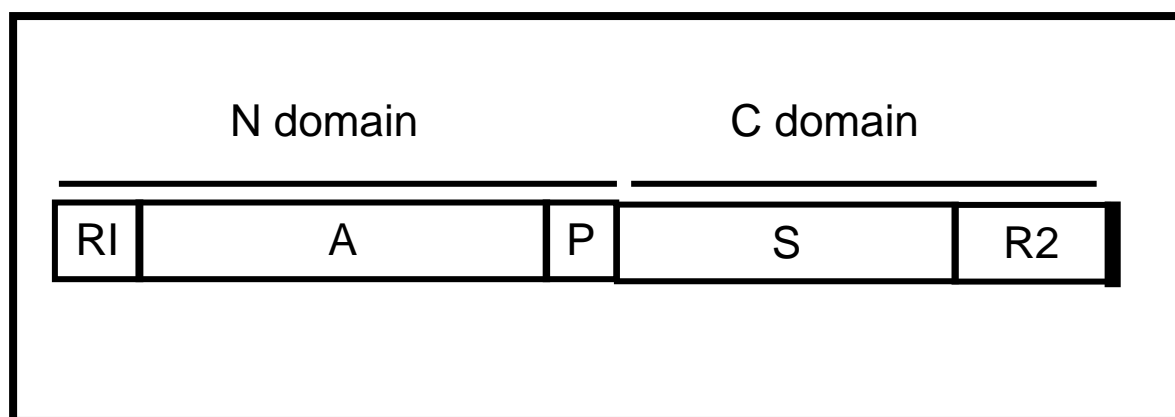


**Figure 1.7 Structure of arrestins**

The functional domains are comprised of a receptor activation recognition domain (A), a secondary receptor binding domain (S) and phosphate sensor domain (P). The regulatory domains (R1 and R2) are at the N- and C-terminus. The clathrin- and  $\beta$ -adapting-binding domains are represented by the black box at the extreme C-terminus. Figure from (Ferguson, 2001).

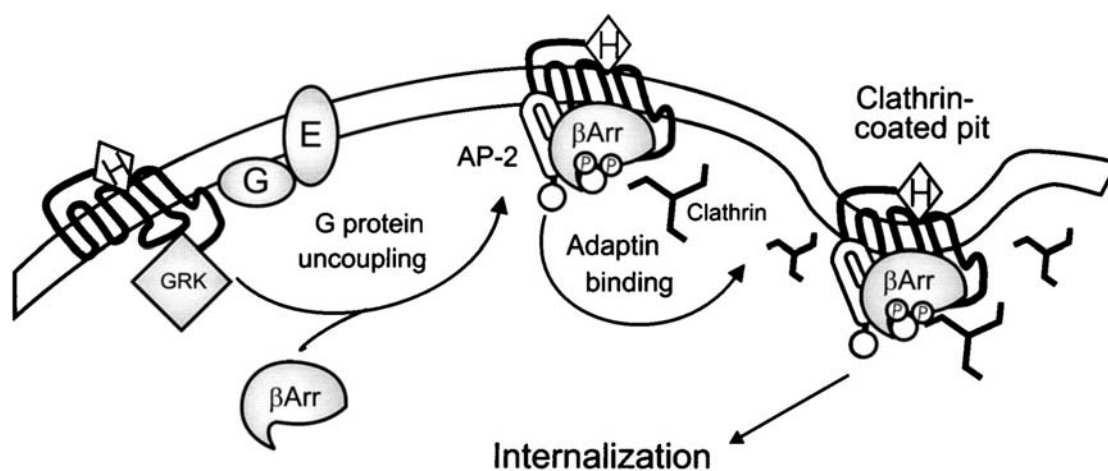


**Figure 1.8 Schematic illustration of GRK- and  $\beta$ -arrestin-dependent desensitisation and internalisation**

$\beta$ -arrestin proteins translocate to the cell surface and bind to the GRK phosphorylated receptor.  $\beta$ -arrestins then associate with clathrin and the AP-2 complex and target the bound GPCR to clathrin-coated pits, where the GPCR is internalised. (Ferguson, 2001). H, hormone; G, G protein; E, effector;  $\beta$ Arr,  $\beta$  arrestin.

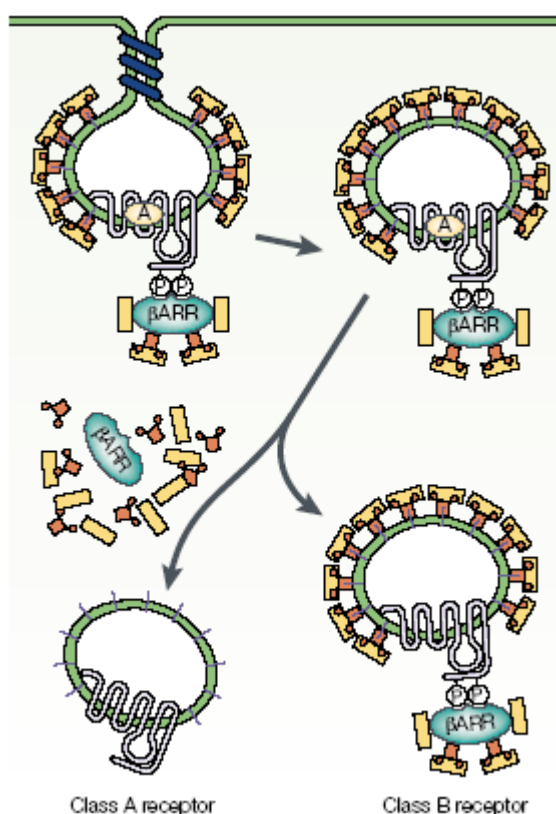


**Figure 1.9 Diagram illustrating fates of internalised class A and class B receptors**

Class A GPCRs preferentially internalise via  $\beta$ -arrestin 2 in a transient manner, where the interaction between the GPCR and the  $\beta$ -arrestin is not stable. It has been suggested that the transient ubiquitination of arrestin results in an unstable GPCR-arrestin complex. In this case  $\beta$ -arrestin does not localise with the GPCR in endosomes and the GPCRs are rapidly dephosphorylated and recycled back to the cell surface. GPCRs belonging to class B have been shown to internalise with either  $\beta$ -arrestin 1 or 2 via a more stable interaction. In this case ubiquitination of arrestin is more prolonged. The whole GPCR- $\beta$ -arrestin complex is targeted to endosomes. Class B receptors are more likely to be recycled slowly if not degraded. (Pierce & Lefkowitz, 2001). A, agonist;  $\beta$ ARR,  $\beta$  arrestin.

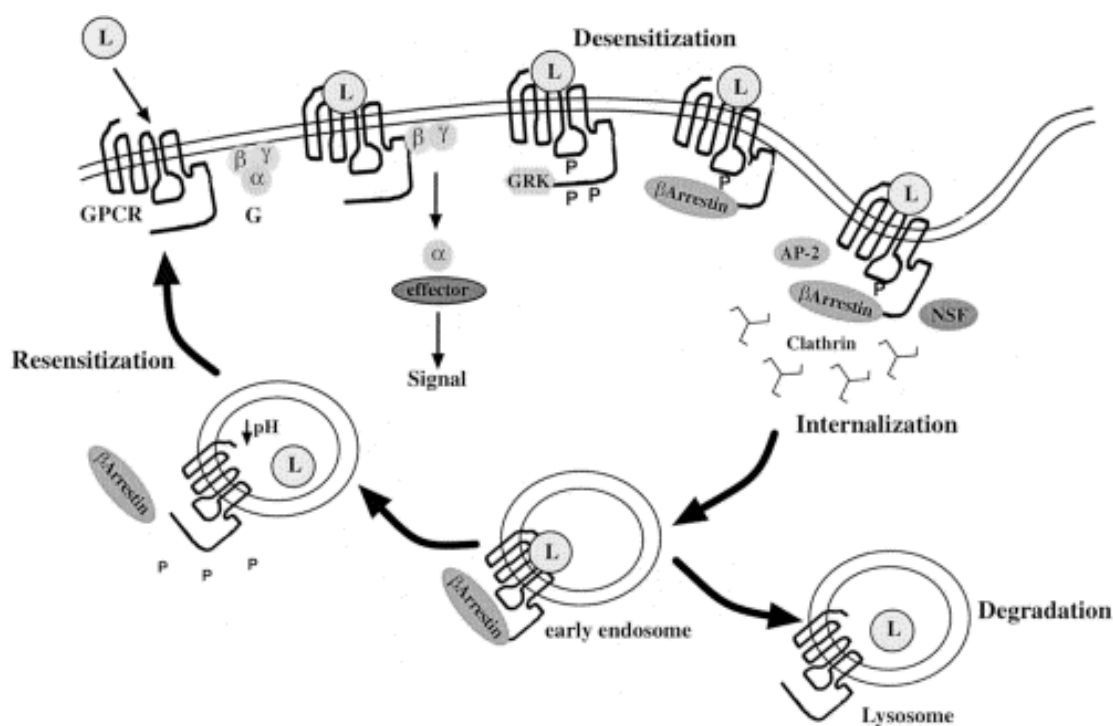


**Figure 1.10 Schematic diagram summarising the three  $\beta$ -arrestin-mediated regulatory mechanisms**

As discussed in the main text desensitisation of the GPCR by GRK phosphorylation and binding of  $\beta$ -arrestin is followed by  $\beta$ -arrestin-mediated internalisation via clathrin-coated vesicles. Receptors are then either targeted for degradation or resensitisation, where the whole process starts again upon ligand (L) activation. (McDonald & Lefkowitz, 2001). NSF, *N*-ethylmaleimide-sensitive fusion protein.

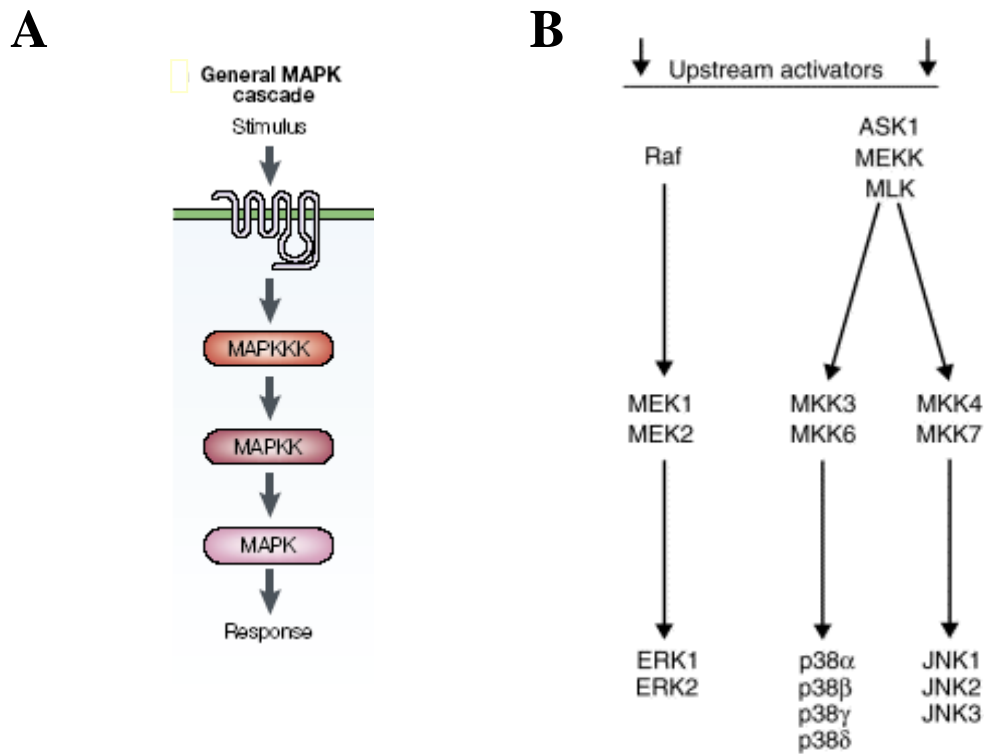


**Figure 1.11 MAPK cascades**

**A:** GPCR activation of MAPK cascades proceeds by the sequential activation of a MAPK kinase kinase (MAPKKK), a MAPK kinase (MAPKK) and a MAPK. (Pierce & Lefkowitz, 2001). **B:** Examples of members involved in each specific pathway (Miller & Lefkowitz, 2001).

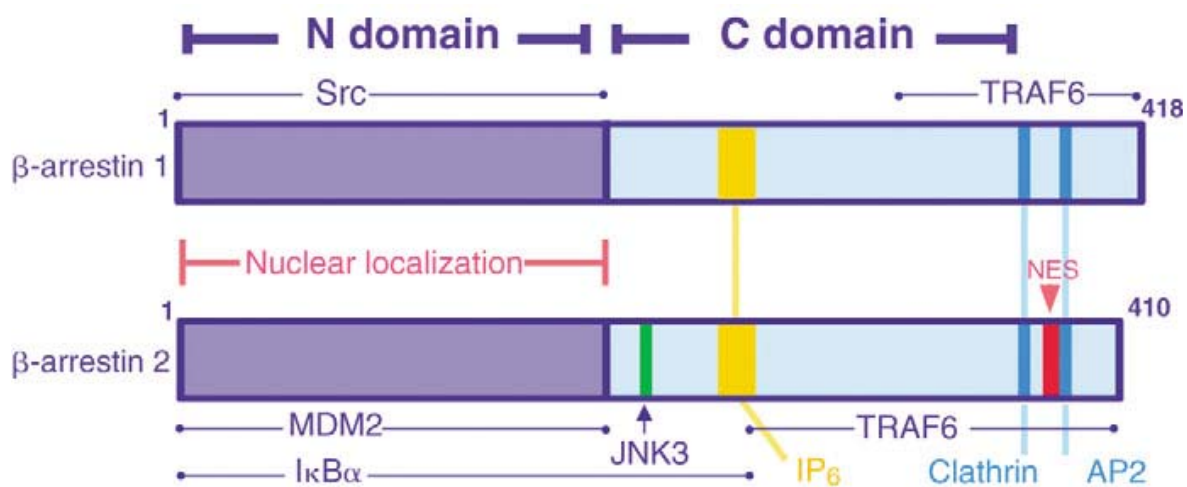


**Figure 1.12 Updated domain structure of  $\beta$ -arrestin annotated for binding sites**

Domain structure of  $\beta$ -arrestin 1 and 2 incorporating binding sites, nuclear localisation and nuclear export (NES) signals (Ma & Pei, 2007).

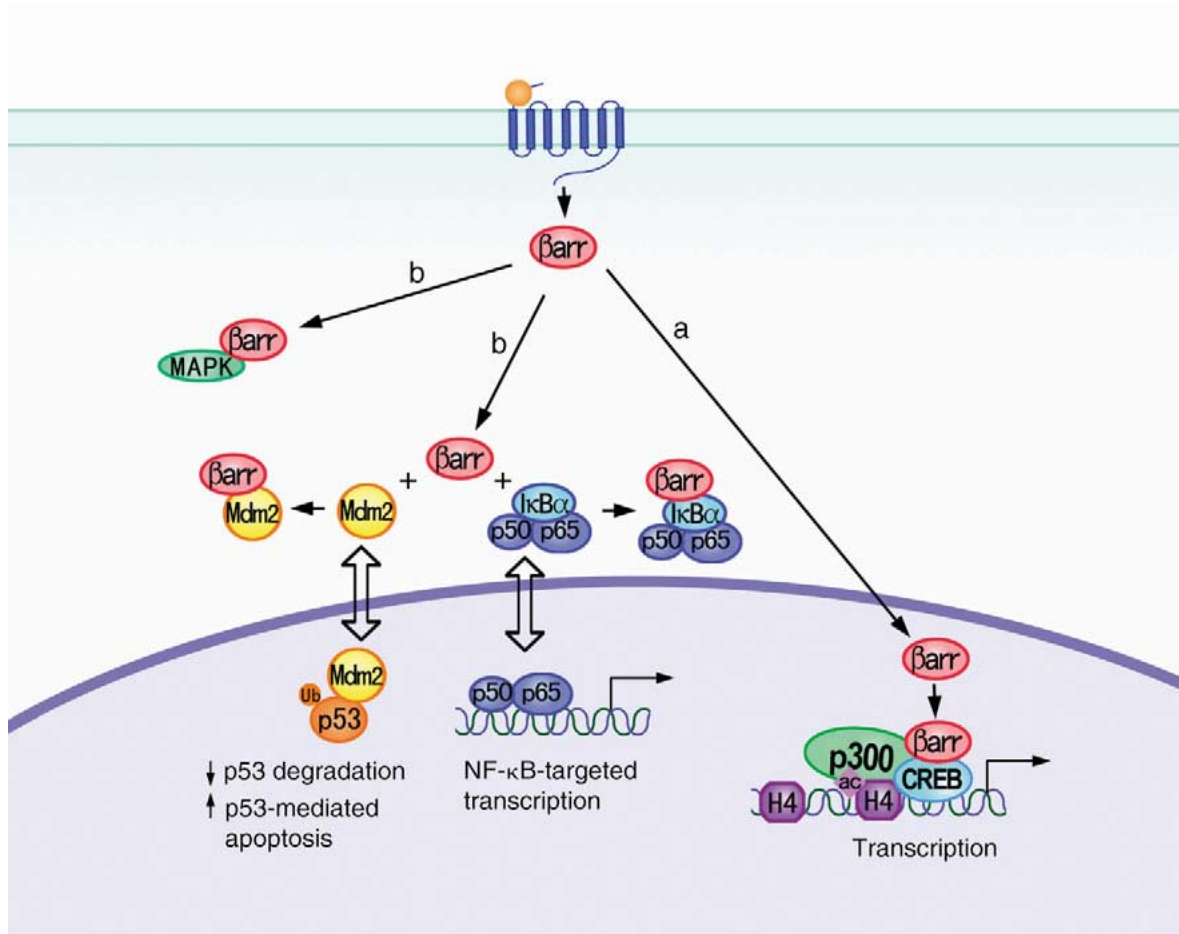


**Figure 1.13 A model for  $\beta$ -arrestin-mediated regulation of transcription**

**a)** Direct pathway: In response to receptor activation,  $\beta$ -arrestins ( $\beta$ arr) translocate from the cytoplasm to the nucleus and associate with transcription cofactors such as p300 and CREB at the promoters of target genes to promote transcription directly. **b)** Indirect pathway:  $\beta$ -arrestins interact with regulators of transcription factors such as I $\kappa$ B $\alpha$  and MDM2 in the cytoplasm, which results in changes in activity and the subcellular distribution of these binding partners, and thus exert regulatory effects on the activation of transcription factors indirectly. Ub, ubiquitylation. From (Ma & Pei, 2007).

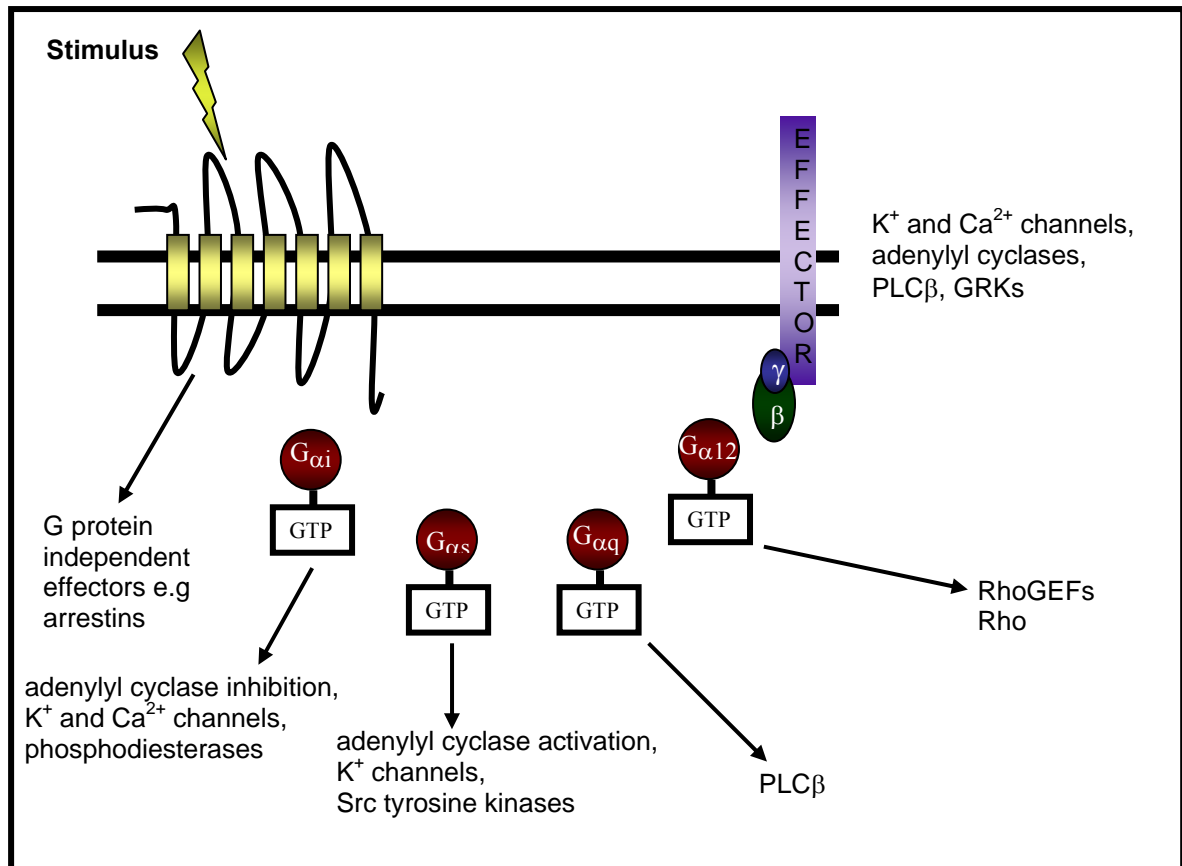


**Figure 1.14 Summary: Diversity of GPCR signalling**

Activation of GPCRs can mediate a variety of cellular responses via various intracellular effectors in a G protein-dependent or -independent manner.

## **1.5. Nicotinic acid mediates its response via G protein-coupled receptors**

It is believed that nicotinic acid lowers the high levels of lipids in blood by inhibiting lipolysis, the process of mobilisation of stored fat from adipocytes. This would involve the regulation of the rate-limiting enzyme, hormone-sensitive lipase. In general, anti-lipolytic agents act by inhibiting adipocyte adenylyl cyclase and thus lowering the cellular levels of cAMP, which in turn hinders the normal processes that lead to the release of non-esterified fatty acids (NEFA) into the circulation. In 1983, Aktories and colleagues presented the first evidence that the inhibition of adenylyl cyclase occurred via a functional  $G_i$  G protein (Aktories et al., 1983a). Further studies by Aktories' and Green's research groups supported the role of an inhibitory GPCR (Aktories et al., 1983b; Green et al., 1992). Based on these findings a schematic diagram of the possible metabolic mechanism is shown in Figure 1.15 (Pike & Wise, 2004).

In 2001, Lorenzen and co-workers confirmed specific binding of nicotinic acid to adipose tissue and spleen and reported that nicotinic acid acts on a specific membrane-bound receptor (Lorenzen et al., 2001). Interestingly, this data nicely corresponded to that obtained by Carlson and colleagues where nicotinic acid uptake was greatest by adipose tissue (Carlson & Hanngren, 1964). Based on the tissue expression profiles generated by Lorenzen and co-workers and the responses to nicotinic acid, in 2003 various groups published reports identifying the nicotinic acid receptor as protein upregulated in macrophages by  $IFN\gamma$  (PUMA-G) or HM74 (Soga et al., 2003; Tunaru et al., 2003; Wise et al., 2003). Nomura and colleagues had originally cloned this HM74 receptor from a cDNA library derived from human monocytes for a separate study (Nomura et al., 1993). Both Soga's and Wise's research groups further went on to report the existence of a high affinity receptor, (HM74A or HM74b) identified by a bioinformatics approach exploiting their highly homologous amino acid sequence. It is interesting to note that out of these three groups two have a commercial interest, highlighting the potential therapeutic significance of this discovery.

### **1.5.1. Introduction to nicotinic acid receptors**

Nearly fifty years on from its arrival on the market, the receptors on which nicotinic acid acts have recently been identified as the 'nicotinic acid receptors'. A family of three receptors, HM74 (GPR109B) and HM74A (GPR109A) are co-located with another orphan GPCR, GPR81, on chromosome 12q24.31 (Wise et al., 2003). Comparison of these homologues revealed a high degree of similarity between them. HM74 and HM74A are both single exon genes that differ by only 15 base changes at the DNA sequence level (Zellner et al., 2005). HM74A also has a 5 base-pair insertion at the 3' end of the gene changing the 3' coding sequence and ultimately resulting in HM74A possessing a shorter C-terminal tail (Wise et al., 2003). With 96 % identity at the protein level, these receptors differ by only 17 amino acids out of a total of around 400 amino acids (Zellner et al., 2005). As HM74 is present in humans but not in rodents it is thought that it is the result of a recent gene duplication event. GPR81 has 57 and 58% amino acid sequence identity with HM74 and HM74A respectively. Recently, hamster and guinea pig HM74A receptors were cloned and characterised, however there was no evidence of a HM74 homologue (Torhan et al., 2007). They have around 80 % sequence identity with human HM74A. HM74A is primarily expressed in adipose tissue, spleen and the lung in humans (Pike & Wise, 2004). Hamster and guinea pig HM74A have a similar expression pattern (Torhan et al., 2007). Both HM74A and HM74 are expressed in lymphocytes, but HM74 is more highly expressed.

To confirm that the receptors were indeed  $G_i$  coupled, receptor-expressing cell lines were pre-treated with pertussis toxin. This abolished signalling via the receptors and therefore it was concluded that the signal was transduced via  $G_i$  (Wise et al., 2003). When these receptors were individually expressed in a mammalian cell line, measurement of a functional response by [ $^{35}$ S] guanosine 5'-( $\gamma$ -thio) triphosphate (GTP $\gamma$ S) binding following nicotinic acid treatment found it to be an agonist for all three GPCRs. However, nicotinic acid was more potent at HM74A ( $\mu$ M range), followed by HM74 (mM range) and then GPR81 ( $>$  mM) (Wise et al., 2003). Wise and co-workers were also able to reproduce [ $^3$ H] nicotinic acid binding studies conducted by Lorenzen and colleagues to determine the affinity of HM74A for nicotinic acid (Lorenzen et al., 2001; Wise et al., 2003). [ $^3$ H] nicotinic acid binding

was around 30 % higher in membranes prepared from adipocytes than those generated from spleen (Lorenzen et al., 2001). Due to the low affinity of HM74 and GPR81 radioligand binding studies were not conducted and expression levels of these receptors have not been determined.

A patent application detailing the molecular identification of a novel nicotinic acid receptor has been published by Arena Pharmaceuticals (Arena Pharmaceuticals, Inc., 2008; Soudijn et al., 2007). Named RUP25, it is reported to be 99 % identical to HM74A. RUP25 has one amino acid difference where phenylalanine replaces glycine at position 65. It has been reported to possess similar affinities for nicotinic acid and its analogs as HM74A. Whether this is a novel receptor or a polymorphism of HM74A is questionable.

### **1.5.2. Ligands for nicotinic acid receptors**

Lorenzen and co-workers were the first to publish the pharmacological profile of a number of compounds that were structurally related to nicotinic acid (Lorenzen et al., 2001). These were tested in various assays including [<sup>35</sup>S] GTPγS and [<sup>3</sup>H] nicotinic acid binding studies on rat adipocytes or spleen. In hindsight, activity of the compounds tested represents activity at HM74A, as we now know HM74 does not have a rodent orthologue. Out of the compounds described in this report, only acifran activated both HM74A and HM74 (Wise et al., 2003). In [<sup>35</sup>S] GTPγS binding assays nicotinamide has been shown to be inactive at HM74A (Wise et al., 2003; Lorenzen et al., 2001). Nicotinic acid and nicotinamide are nutritionally equivalent and structurally similar; in nicotinamide, an amine group replaces the carboxyl group in nicotinic acid, as shown in Figure 1.16. This suggests that the carboxyl group is important for receptor activation and therefore lipid-modifying qualities. Acifran, which displays similar anti-lipolytic characteristics as nicotinic acid, also contains a carboxyl group (Figure 1.16). Not only is the presence of the carboxylic acid group essential but its position in the heterocyclic structure dictates activity levels (Soudijn et al., 2007). Synthetic analogs of acifran have been developed and demonstrated to be at least as active as acifran, if not more so, at both receptors (Jung et al., 2007; Mahboubi et al., 2006). Although a series of selective agonists at HM74A and HM74 have been identified, to date no antagonists have been reported.

### **1.5.2.1. HM74A**

The doses of nicotinic acid required to produce a pharmacological response are in excess of those achieved naturally. Therefore, it is unlikely that nicotinic acid is the endogenous ligand for either HM74 or HM74A. In 2006,  $\beta$ -hydroxybutyrate, a ketone body, was reported to selectively activate HM74A at relatively high concentrations ( $EC_{50} = 750 \mu\text{M}$ ) (Taggart et al., 2005). The ability of the ketone body to inhibit lipolysis in mouse adipocytes demonstrated its role in a more physiological context. Although under normal conditions  $\beta$ -hydroxybutyrate levels in plasma range from 50 – 400  $\mu\text{M}$ , in conditions of starvation these levels can increase to 6 – 8 mM. Therefore,  $\beta$ -hydroxybutyrate may be the endogenous ligand for HM74A, allowing a negative feedback mechanism during starvation to achieve metabolic homeostasis, as illustrated in Figure 1.17 (Gille et al., 2008).

Many selective agonists have been described for HM74A, some of which are not structurally related to nicotinic acid have been developed by pharmaceutical companies and are patented (Skinner et al., 2007c; Bodor & Offermanns, 2008; Soudijn et al., 2007). Interestingly, many of these ligands lack the carboxylic acid group which was thought to be important for receptor activation (Bodor & Offermanns, 2008). Partial agonists for this receptor have also been described (van Herk et al., 2003). Recently, a cAMP-based high throughput assay was described for identifying agonists at HM74A (Gharbaoui et al., 2007). The interest in identifying more potent and physiologically relevant ligands has clearly not declined.

### **1.5.2.2. HM74**

The endogenous ligand for HM74 has not been identified. Based on the high sequence homology between HM74 and HM74A, it is a possibility that a ketone body may be the natural ligand for this receptor. In the meantime selective HM74 agonists have been identified (Semple et al., 2006; Skinner et al., 2007a). In the case of 1-Alkyl-benzotriazole-5-carboxylic acids, they are some 20-fold less potent than nicotinic acid but nevertheless inhibit isoprenaline-stimulated glycerol production in human adipocytes (Semple et al., 2006).

To date no ligands have been described for GPR81. There is potential, therefore, to identify the natural ligand by screening against tissue extracts and bioactive

molecules. The molecular structures and the pharmacological profiles of compounds that act on the nicotinic acid receptors have been summarised in Figure 1.18 and Table 1.3 (Offermanns, 2006; Gille et al., 2008).

### **1.5.2.3. Biased agonism?**

Many studies have reported ERK1/2 activation by nicotinic acid and related compounds via HM74A (Richman et al., 2007; Tunaru et al., 2003; Mahboubi et al., 2006). Published reports by Richman and co-workers also suggest these compounds cause internalisation of HM74A (Richman et al., 2007). In these studies Richman and colleagues presented evidence to support their hypothesis that compounds that cause flushing also induce receptor internalisation and ERK1/2 activation. A number of HM74A pyrazole-based agonists have been reported as ‘non-flushing’ agonists which do not cause receptor internalisation or ERK1/2 activation (Richman et al., 2007). These compounds were also demonstrated to inhibit isoproterenol-stimulated lipolysis in adipocytes.

### **1.5.3. Homology modelling and structural determinants of ligand binding**

The nicotinic acid receptors contain conserved cysteine residues, at positions 100 and 177, which form a disulphide bridge between extracellular loops I and II. They also contain a DRY motif at the interface between TM III and the second intracellular loop. These are characteristics of receptors belonging to the class A family of GPCRs. Based on shared characteristics with the rhodopsin receptor, Tunaru and colleagues generated a structural model for the nicotinic acid receptors (Figure 1.19).

As mentioned earlier, in addition to a shorter C-terminal tail, HM74A differs from HM74 by 17 amino acids which cluster around the extracellular loops 1 and 2. Of these amino acids, 14 are conserved across different species and are thought to be implicated in ligand binding. Tunaru and co-workers determined the ligand binding site by systematically mutating each of the 14 amino acids (Tunaru et al., 2005). They also took advantage of the high degree of homology shared by HM74 and HM74A to generate receptor chimeras. Pharmacological profiling of these recombinant receptors was achieved by the use of nicotinic acid, which is nearly 1000 fold more potent at

HM74A than HM74 and acifran, a synthetic compound, which displays similar potency at both receptors and lipid-modifying effects. From these studies, TM helices II, III and VII, extracellular loop II and the junction of TM II/ECL I of HM74A were demonstrated to be directly involved in nicotinic acid binding. This differs from traditional binding sites of class A receptors which is formed by TM helices III, V and VI. With respect to key amino acid players in nicotinic acid binding, Asn86/Trp91 at the junction of TM II/ECL I and Ser178 in ECL II are essential (Tunaru et al., 2005). Also, Arg111, which is conserved in both HM74 and HM74A, is thought to be implicated in forming a salt bridge with the carboxylic acid group found in many agonists for the nicotinic acid receptors. Key amino acids in ligand binding have been highlighted in Figure 1.19 and an interaction model of nicotinic acid at the binding site of HM74A is shown in Figure 1.20.

## **1.6. Clinical targets for nicotinic acid**

With the identification of the nicotinic acid receptors there was much speculation with regards to the clinical target for nicotinic acid. In mice it was clearly demonstrated that nicotinic acid-mediated its effects through HM74A (PUMA-G) (Tunaru et al., 2003). Mice lacking HM74A were unable to decrease FFA and triglyceride plasma levels when administered with nicotinic acid (Tunaru et al., 2003).  $\beta$ -hydroxybutyrate was also unable to inhibit lipolysis in adipocytes from HM74A knock-out mice (Taggart et al., 2005). However, in humans due to the presence of both HM74A and HM74, deduction of the clinical target is more complicated. Taking into consideration the high doses of nicotinic acid required to produce a pharmacological response, HM74 seemed like a reasonable target to mediate the anti-lipolytic effects. However, studies in which human HM74 or HM74A cDNA was transfected and expressed in 3T3 L1 cells, nicotinic acid was only able to inhibit lipolysis in cells expressing human HM74A (Zhang et al., 2005). To address the gram doses required to generate therapeutic effects of nicotinic acid, it has been reported that 90 % of nicotinic acid administered is eliminated from the body as unchanged nicotinic acid or nicotinuric acid (Gille et al., 2008). The half-life of nicotinic acid in the plasma ranges from 20 – 45 minutes, so there is a possibility that the vitamin may not be able to maintain the concentrations required to activate HM74.

Although the above supports the role of HM74A as the clinical target for nicotinic acid, only studies conducted in native cell lines in a physiologically relevant context can be conclusive. For example, Zellner and co-workers have reported non-synonymous nucleotide changes that are predicted to fall within the transmembrane domains of HM74 (Zellner et al., 2005). Non-synonymous changes result in amino acid replacements and therefore can potentially impact receptor function. Therefore, there is the possibility that an individual's response to nicotinic acid may be dependent on which HM74 and HM74A haplotype they carry. Studies examining receptors in isolation do not allow for these types of issues to be addressed.

## **1.7. Mechanism of 'niacin flush'**

It has been known for many years that cyclooxygenase inhibitors can reduce the flushing experienced in patients taking nicotinic acid. This was the first indication that prostanoids are involved in nicotinic acid-induced flushing (Kaijser et al., 1979). The increase in levels of vasodilatory prostanoids (prostaglandin I<sub>2</sub> (PGI<sub>2</sub>), prostaglandin E<sub>2</sub> (PGE<sub>2</sub>) and prostaglandin D<sub>2</sub> (PGD<sub>2</sub>)) and their metabolites after nicotinic acid administration provided further evidence of their involvement (Eklund et al., 1979; Morrow et al., 1989). Decrease in levels of PGI<sub>2</sub> and PGD<sub>2</sub> after continuous treatment with nicotinic acid corresponding with the development of tolerance to the nicotinic acid-induced flushing was also reported (Stern et al., 1991). It was not then a surprise when Benyo and co-workers reported that receptors for both PGI<sub>2</sub> and PGD<sub>2</sub> were important for nicotinic acid-induced flushing (Benyo et al., 2005). In mice lacking these receptors reduced flushing was observed. Supporting this murine data, Cheng and colleagues demonstrated with the use of selective agonists and antagonists that the PGD<sub>2</sub> receptor was important in the nicotinic acid-induced flushing response in humans (Cheng et al., 2006). Further progress in deciphering the mechanism of the flushing response was made when HM74A was identified as the mediator of the nicotinic acid-induced flush (Benyo et al., 2005). It was nicely demonstrated that mice deficient in HM74A did not display flushing in response to nicotinic acid. As mentioned earlier, there is no rodent HM74 homologue. So there is a possibility that although HM74A may be the mediator of this nicotinic acid-induced flush in mice, it may not be the sole mediator in humans.

In the study conducted by Benyo and co-workers, mice deficient in HM74A were able to display the flushing response after transplantation of bone marrow from wild type mice (Benyo et al., 2005). This, taken together with the observation of HM74A expression on immune cells, suggested their involvement in the flushing response. It was hypothesised that arachidonic acid in immune cells was mobilised by nicotinic acid and converted to prostaglandins and thus caused the flushing response. With the recent report of HM74A signalling enhancing the arachidonic acid signalling pathway the arguments supporting this hypothesis were strengthened (Tang et al., 2006). Around the same time two independent groups reported epidermal Langerhans cells were crucial for the cutaneous flushing response induced by nicotinic acid (Maciejewski-Lenoir et al., 2006; Benyo et al., 2006). Benyo and co-workers demonstrated the flushing response can be abrogated by depleting mice of these cells (Benyo et al., 2006). The approach adopted by Maciejewski-Lenoir and co-workers, involved assaying PGD<sub>2</sub> release in various cells in response to nicotinic acid. Langerhans cells were the only cells to respond in this manner (Maciejewski-Lenoir et al., 2006).

## **1.8. Other effects?**

It has been suggested that nicotinic acid receptors expressed in macrophages may play a role in increasing HDL cholesterol and therefore a role in preventing atherosclerosis (Schaub et al., 2001). Recently, nicotinic acid has been reported to induce peroxisome proliferator-activated receptor  $\gamma$  (PPAR $\gamma$ ), CD36 and ATP-binding cassette A1 (ABCA1) expression and transcriptional activity in macrophages (Knowles et al., 2006; Rubic et al., 2004). These are key players in the reverse cholesterol transport pathway and therefore any increase in expression would result in an enhancement of cholesterol removal. The mechanism by which the nicotinic acid receptors regulate PPAR $\gamma$  is currently not known. However, it provides an interesting link to understanding how the nicotinic acid receptors are involved in reverse cholesterol transport.

The nicotinic acid-induced flushing response and expression of PPAR $\gamma$  are examples demonstrating how cell type specific expression of receptors can achieve signal

specificity and diverse physiological responses. The differential responses mediated by the nicotinic acid receptors have been summarised in Figure 1.21 (Pike, 2005).

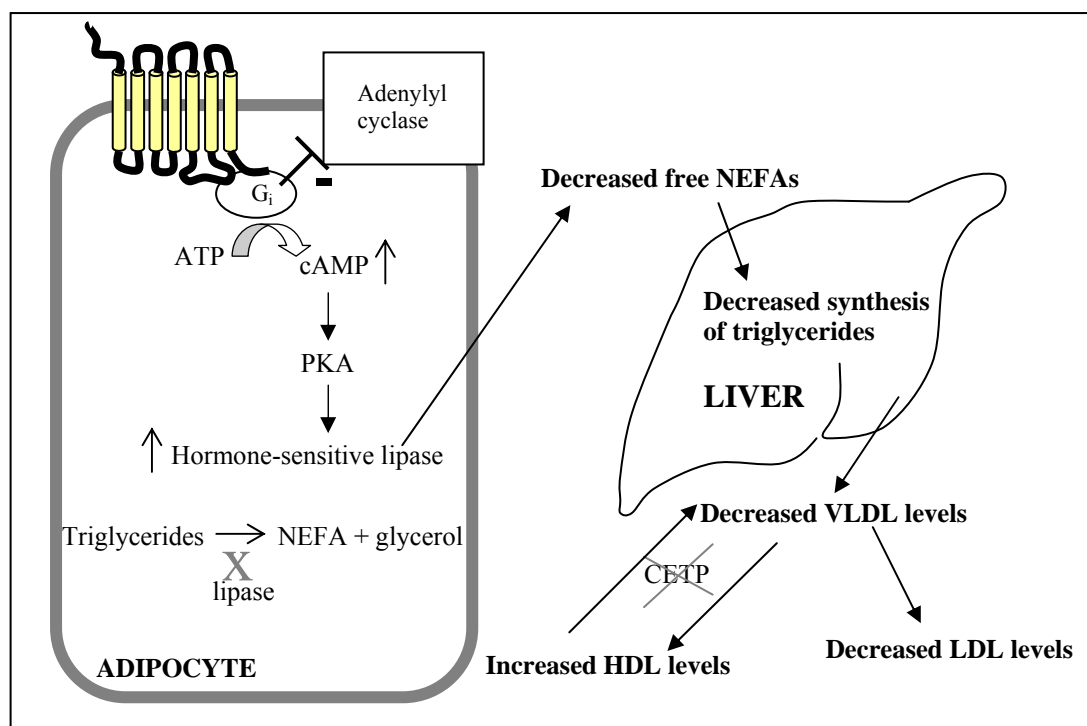


**Figure 1.15 Schematic diagram of the possible lipid-modifying mechanism of action of nicotinic acid via a G<sub>i</sub> coupled GPCR**

Abbreviations: CETP: cholesteryl ester transfer protein, G<sub>i</sub>: inhibitory G protein, NEFA: non-esterified fatty acids. Figure adapted from (Pike & Wise, 2004).

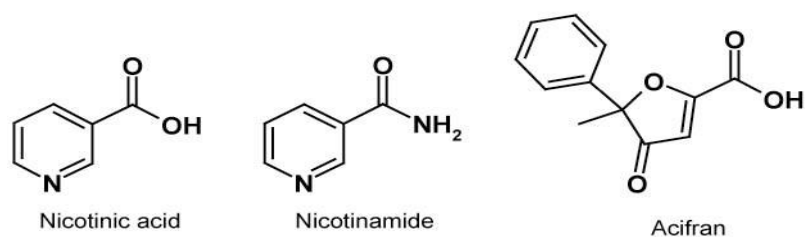


**Figure 1.16 Molecular structures: Highlighting role of carboxyl group**

The carboxyl group conserved in nicotinic acid and acifran is thought to be important for receptor activation. Nicotinamide, which does not display anti-lipolysis characteristics, does not share this structural feature. From (Gille et al., 2008).

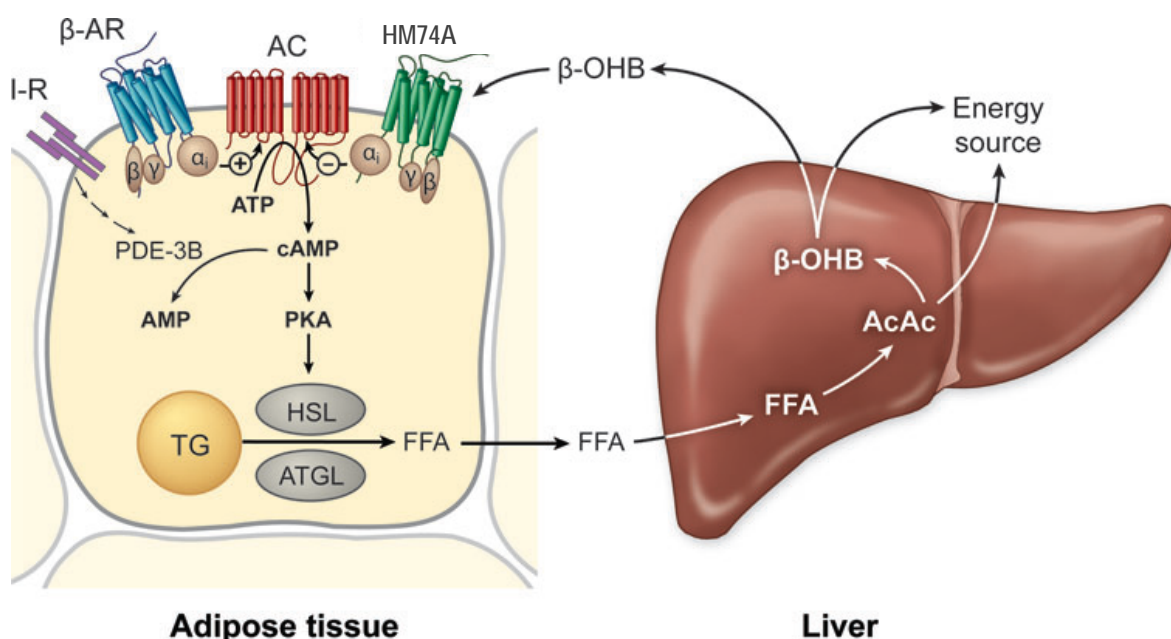


**Figure 1.17 Physiological role of the nicotinic acid receptors: Negative feedback mechanism during starvation?**

Under conditions of starvation,  $\beta$ -adrenergic receptor ( $\beta$ -AR) can mediate an increase in intracellular cAMP levels that stimulate lipolysis. FFAs that are released from fat cells are then metabolised in the liver to ketone bodies, including  $\beta$ -hydroxybutyrate ( $\beta$ -OHB).  $\beta$ -OHB can inhibit lipolysis via activation of HM74A. HM74A-mediated inhibition of adenylyl cyclase (AC) activity and therefore the decrease in cAMP synthesis would counteract the increased  $\beta$ -AR-mediated cAMP formation and the decreased cAMP degradation by phosphodiesterase 3B (PDE-3B) under starvation conditions. I-R, insulin-receptor (Gille et al., 2008).

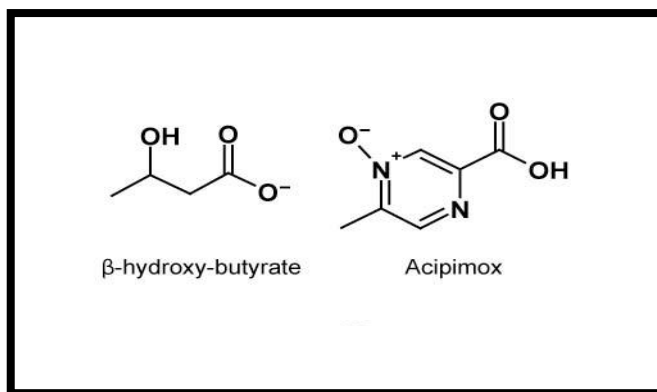


**Figure 1.18 Molecular structures of ligands at HM74A**

Examples of molecular structures of ligands that act on HM74A (Gille et al., 2008).

<b>Compound</b>	<b>HM74A EC<sub>50</sub> (μM)</b>	<b>HM74 EC<sub>50</sub> (μM)</b>
<b>Nicotinic acid</b>	<b>0.1</b>	<b>&gt; 100</b>
<b>Acifran</b>	<b>1.2</b>	<b>7</b>
<b>Acipimox</b>	<b>5.1</b>	<b>&gt; 100</b>
<b>β-hydroxybutyrate</b>	<b>750</b>	<b>25,000</b>

**Table 1.3 Pharmacological profile of ligands that act on the nicotinic acid receptors**

Summary of the potencies of the best described ligands of the nicotinic acid receptors. Acifran has similar potency at both HM74A and HM74. Other compounds described here are more potent at HM74A than HM74. Table adapted from (Offermanns, 2006).

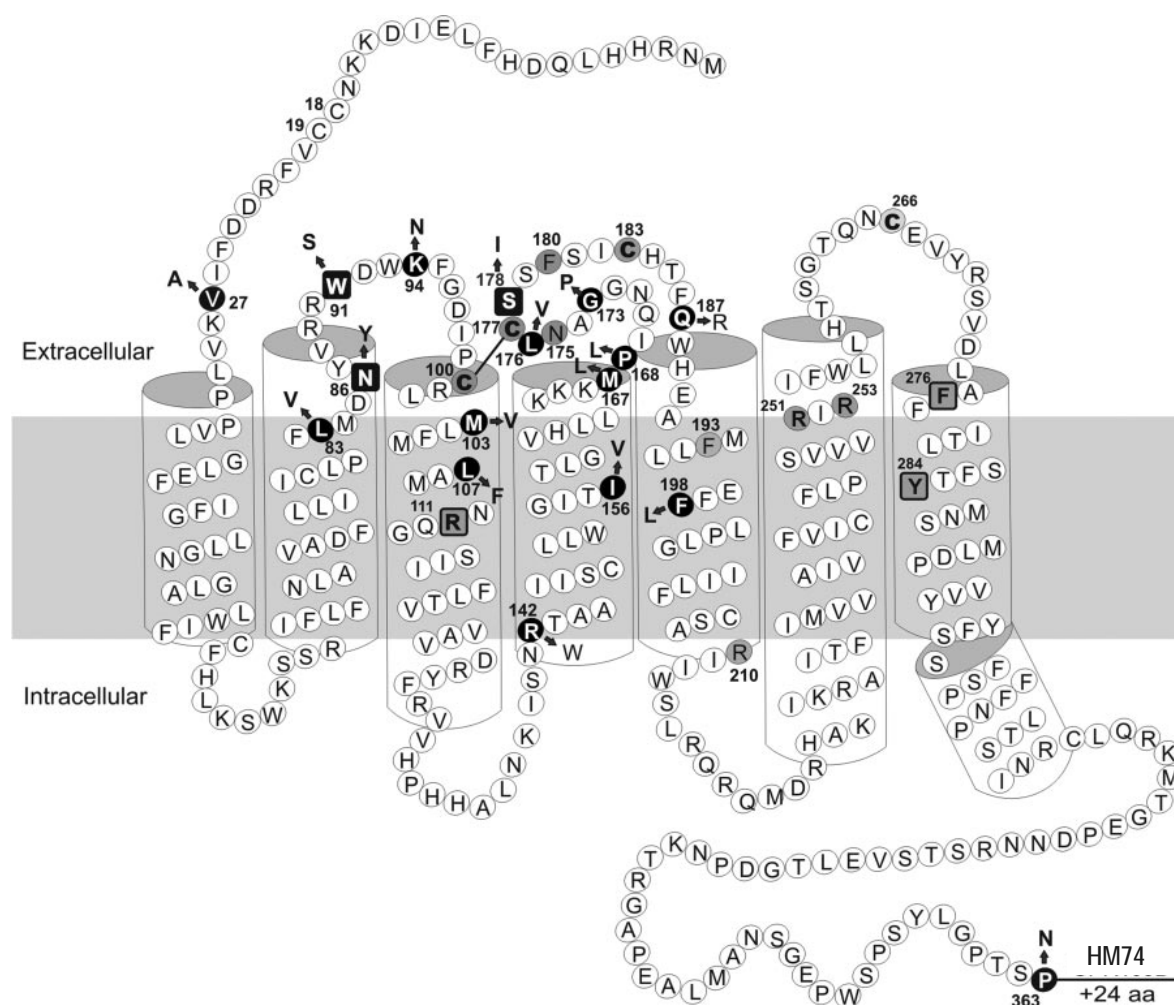
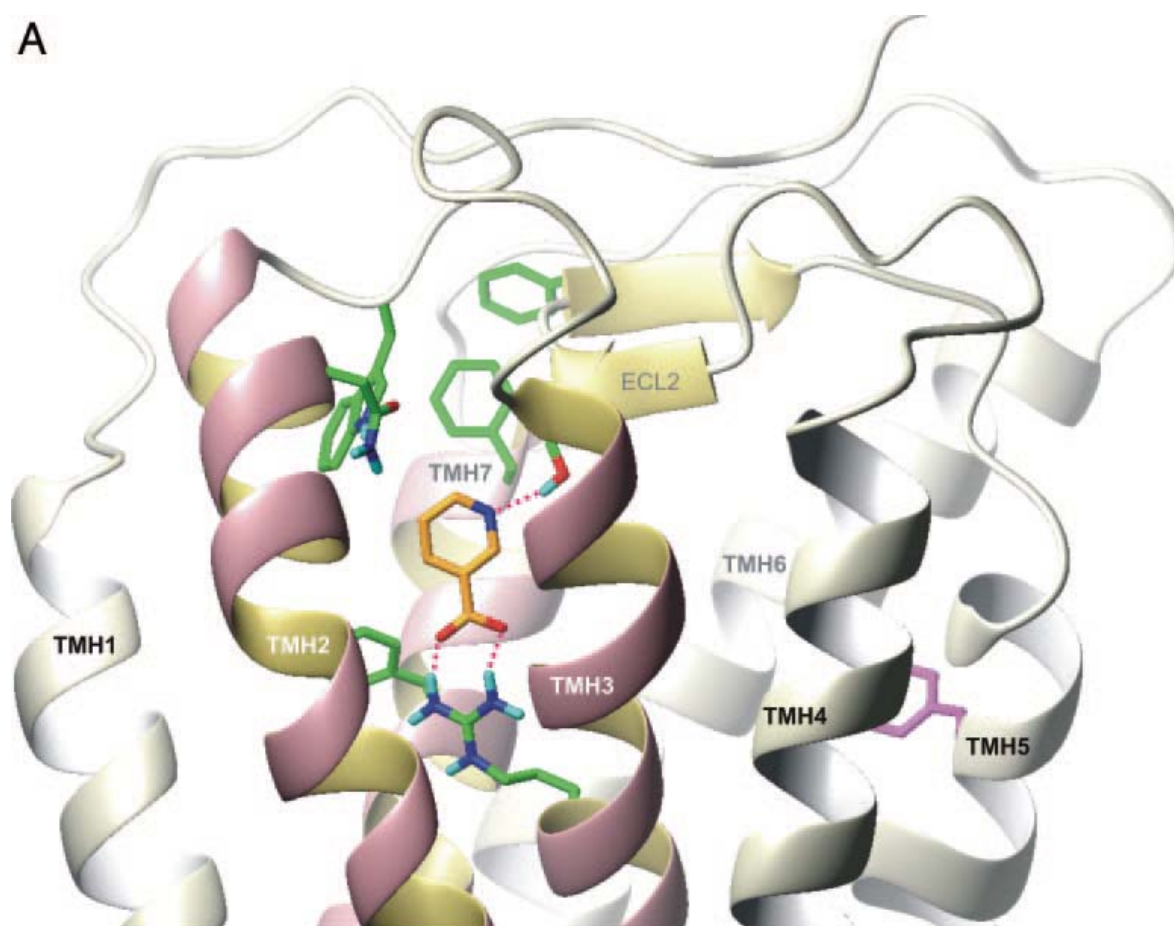


**Figure 1.19 Predicted structure of the human nicotinic acid receptor HM74A**

Extracellular, transmembrane, and cytoplasmic regions are based on the structure of rhodopsin. Straight line indicates the disulphide bond found in the extracellular part of the receptor. HM74 has a C-terminus that is extended by 24 amino acids. White amino acid symbols on black circles and squares indicate residues in HM74A that differ from HM74. The arrows point to the corresponding amino acid in HM74. Squares represent residues that showed a significant difference in nicotinic acid binding when mutated in HM74A (Tunaru et al., 2005).

A



B

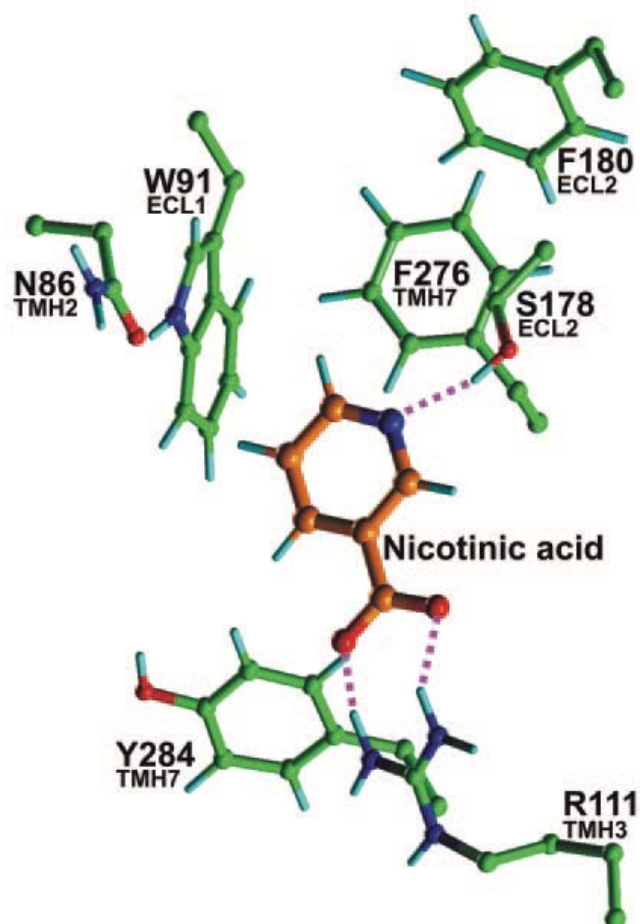


**Figure 1.20 Interaction model of nicotinic acid at the binding site of HM74A**

**A:** The binding site of nicotinic acid is located between TM II, III, and VII (pink/yellow ribbon). **B:** Close-up view of the binding site. Acidic group of nicotinic acid (orange) interacts with the basic anchor point Arg111 at TM III, whereas the pyridine ring is embedded between Trp91 at the junction TM II/ECL1, Phe276, and Tyr284 at TM VII. The pyridine nitrogen is also bound to Ser178 in ECL2 via an H bond. Asn86 (TM II) restrains the orientation of Trp91 by hydrogen bond, and Phe180 (ECL2) restrains the orientation of Phe276 by aromatic interactions leading to a suitable and rigid binding cleft. Figure from (Tunaru et al., 2005).

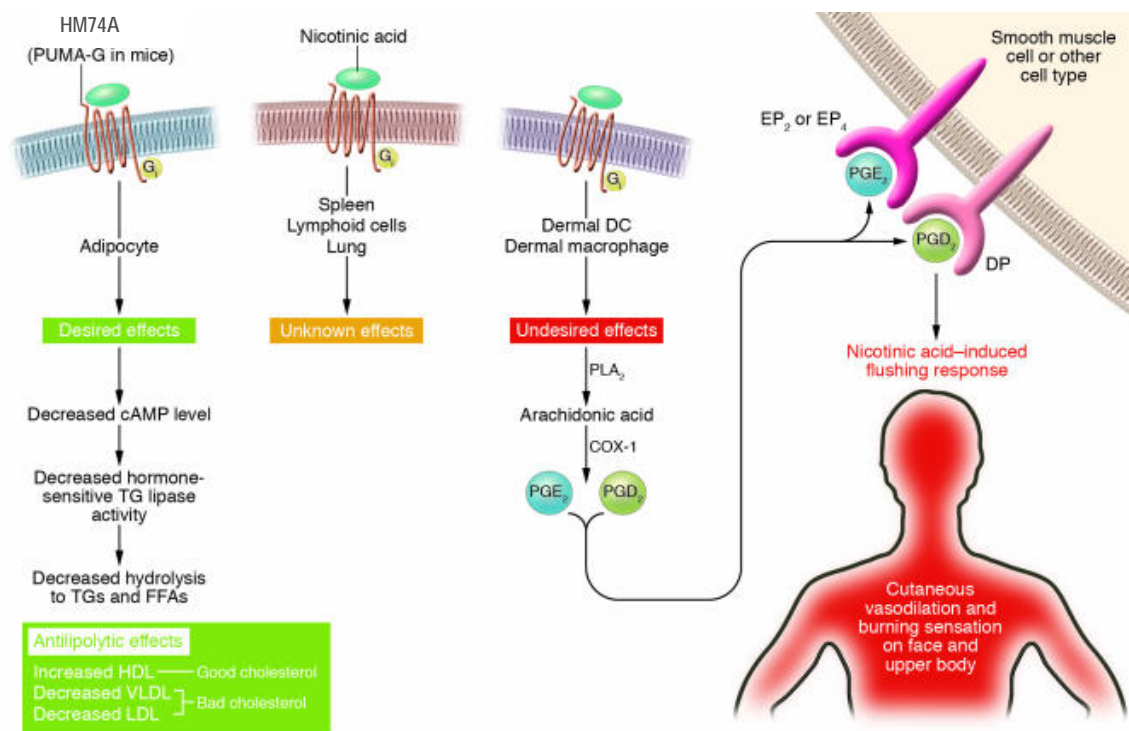


**Figure 1.21 Activation of HM74A**

Activation of HM74A can produce differential responses depending on the location of the receptor. TG, triglyceride. From (Pike, 2005).

## 1.9. Project aims

It has been a long journey since the lipid-modulating benefits of nicotinic acid were first described in the late 1950s. In the past 50 years, small but definitive steps have led to a greater understanding of the mechanism by which this vitamin acts. There are, however, many unanswered questions. The recent identification of the nicotinic acid receptors has now further intensified research in this field and in the past few years many informative reports describing the action of these receptors have been published. Despite this, the exact molecular mechanism by which nicotinic acid regulates lipid levels via the nicotinic acid receptors is still not fully understood. Little is known about the regulation of these receptors with respect to desensitisation or resensitisation.

As mentioned previously, HM74 and HM74A are highly homologous except in the C-terminal region. HM74 has a 24 amino acid longer C-terminal tail than HM74A. As the C-terminal region of GPCRs often plays an important role in the regulation of receptor signalling, it was hypothesised that these receptors may be regulated differentially. The aim of the study was to study the regulation of these receptors and identify any potential differences.

First, the tools required for this project were generated and the [<sup>35</sup>S] GTP $\gamma$ S binding assay was optimised to study these receptors. The tools included generation of epitope and fluorescent-tagged receptors to allow visualisation of the receptors in live and fixed cells. These recombinant receptors were then characterised first in transient then stable cell expression systems to confirm native pharmacology. The effects of agonist treatment on receptor internalisation,  $\beta$ -arrestin interaction and receptor phosphorylation were examined in stable cell lines expressing either the native or recombinant receptors. The kinetics of ERK1/2 activation were also studied to identify any potential differences between the two receptors. Nicotinic acid pre-treatment studies to examine the desensitisation characteristics of HM74 and HM74A were also conducted. To further examine the role of the C-terminal tail in the regulation of the nicotinic acid receptors, C-terminal tail chimeras were generated and the pre-treatment studies were repeated.

## **2. Materials and Methods**

### **2.1. Materials**

#### **2.1.1. *General reagents, enzymes and kits***

##### **Amersham Pharmacia Biotech UK Ltd., Little Chalfont, Buckinghamshire, UK**

Full range Rainbow™ molecular weight markers, 1st strand DNA synthesis kit, protein G Sepharose, wheatgerm agglutinin coupled polystyrene imaging beads

##### **BDH, Lutterworth, Leicestershire, UK**

22 mm coverslips, microscope slides, sodium di-hydrogen orthophosphate ( $\text{Na}_2\text{HPO}_4$ ), potassium hydroxide (KOH), potassium chloride (KCl), methanol, isopropanol

##### **Chemicon Europe Ltd., Chandlers Ford, UK**

ReBlot Plus solution

##### **Duchefa, Haarlem, The Netherlands**

Bactotryptone, yeast extract, bactoagar

##### **Fisher Scientific UK Ltd, Loughborough, Leicestershire, UK**

Sodium chloride ( $\text{NaCl}$ ), sodium hydroxide ( $\text{NaOH}$ ), potassium di-hydrogen orthophosphate ( $\text{KH}_2\text{PO}_4$ ), Tris base, HEPES, EDTA, SDS, calcium chloride ( $\text{CaCl}_2$ ), D-glucose, DTT, urea, glacial acetic acid, sucrose, potassium acetate ( $\text{C}_2\text{H}_3\text{O}_2\text{K}$ ), manganese chloride ( $\text{MnCl}_2$ ), glycerol, glycine, MOPS, ethylene glycol, ethanol, scintillation vials (7 ml)

**Flowgen Bioscience Ltd., Nottingham, UK**

Agarose

**Invitrogen Ltd., Paisley, UK**

NuPage Novex pre-cast 4-12 % Bis-Tris gels, NuPage MOPS SDS running buffer, deoxyribonuclease, Gel-Dry Drying solution

**Konica Europe, Hohenbrunn, Germany**

X-ray film

**KPL, Inc., Gaithersburg, MD**

SureBlue TMB substrate

**New England Biolabs, MA, USA**

Restriction endonucleases

**Pierce, Perbio Science UK Ltd., Tattenhall, Cheshire, UK**

Supersignal West Pico chemiluminescent substrate, EZ-Link Sulfo-NHS-SS Biotin, immobilised streptavidin beads

**Promega UK Ltd., Southampton, UK**

Pfu DNA polymerase, restriction endonucleases, T4 DNA ligase

**Qiagen, Crawley, West Sussex, UK**

QIAfilter maxiprep kit, QIAprep Spin miniprep kit, QIAQuick gel extraction kit, QIAQuick PCR purification kit, RNeasy kit

**Roche Applied Science, Lewes, East Sussex, UK**

DNA molecular weight marker X, shrimp alkaline phosphatase, bovine serum albumin (BSA), fatty acid free (BSA), complete EDTA-free protease inhibitor tablet, deoxyribonucleotide triphosphates (dNTPs), N-Glycosidase-F, DOTAP transfection agent

**Semat International, Hatfield, UK**

GF/C fibreglass filters

**Sigma-Aldrich Company Ltd., Poole, Dorset, UK**

Triton X-100, Na-deoxycholate, magnesium chloride ( $MgCl_2$ ), bromophenol blue, BCA solution A, copper sulphate ( $CuSO_4$ ), rubidium chloride ( $RbCl_2$ ), ampicillin, kanamycin, Tween-20, ascorbic acid, sodium fluoride (NaF), guanosine diphosphate (GDP), deoxycholic acid (sodium salt), sodium azide ( $NaN_3$ ), DL- $\beta$ -hydroxybutric acid sodium crystalline, paraformaldehyde (PFA), dimethyl sulfoxide (DMSO), Hoechst stain, ethylene glycol, sodium acetate ( $CH_3COONa$ ), di-sodium orthophosphate, ethidium bromide, forskolin, phorbol 12-myristate 13-acetate (PMA), nicotinic acid, H 89 dihydrochloride hydrate, RO 31-8220 methanesulfonate salt, guanosine 5'-diphosphate sodium salt, UK 14304

**Stratagene, Amsterdam, The Netherlands**

QuikChange site directed mutagenesis kit

**Tocris Bioscience, Northpoint, Avonmouth, UK**

Acifran

**ThermoElectron, Ulm, Germany**

All oligonucleotides used for PCR reactions

## **2.1.2. Tissue culture plastic ware and reagents**

### **Amaya Biosciences**

MEF nucleofector Kit

### **American Tissue Culture Collection, Rockville, USA**

HEK293T cells

### **BD Bioscience, Cowley, UK**

75 cm<sup>2</sup> and 125 cm<sup>2</sup> Falcon vented tissue culture flasks

### **Costar, Cambridge, MA, USA**

5 ml, 10 ml and 25 ml pipettes, 75 cm<sup>2</sup> and 125 cm<sup>2</sup> vented tissue culture flasks, 6 well plates, and 10 cm dishes

### **Invitrogen, Paisley, UK**

DMEM/F12 (minus L-glutamine), MEM non-essential amino acids, foetal bovine serum, dialysed foetal bovine serum, lipofectamine 2000 transfection agent, opti-mem-1, L-glutamine (200 mM), zeocin, blasticidin, penicillin-streptomycin, geneticin G418, hygromycin B, new born calf serum, 2-mercaptoethanol, CHO K1 cell line, Flp-In CHO KI cell line, TrypLE Select animal origin free, CHO K1 cells, Flp-In CHO-K1 cells

### **Greiner Bio-One, Kremsmünster, Austria**

384-well clear low volume plates

### **GlaxoSmithKline, Harlow, UK**

Acipimox, MPCA and all GSK compounds were synthesised by GSK

**MP Biomedicals, Solon, Ohio**

Phosphate-free DMEM

**Roche Applied Science, Lewes, East Sussex, UK**

Hygromycin B

**Sigma-Aldrich Company Ltd., Poole, Dorset, UK**

DMEM (plus glucose plus L-glutamine minus pyruvate, L-glutamine), DMEM powder, 0.25 % trypsin-EDTA, poly-D-lysine, doxycycline, pertussis toxin, puromycin, poly-D-Lysine coated multiwell plates

**2.1.3. Radiochemicals**

**Perkin-Elmer Life and Analytical Sciences, Beaconsfield, Buckinghamshire, UK**

[<sup>35</sup>S] GTP $\gamma$ S (1250 Ci/mmol)

**Amersham Pharmacia Biotech UK Ltd., Little Chalfont, Buckinghamshire, UK**

[<sup>32</sup>] P orthophosphate

**2.1.4. Antisera**

**Amersham Pharmacia Biotech UK Ltd., Little Chalfont, Buckinghamshire, UK**

Donkey anti mouse IgG-HRP conjugate, donkey anti rabbit IgG-HRP conjugate

**Abcam plc, Cambridge Science Park, Cambridge, UK**

Anti GAPDH, anti phospho-CREB ser 133

## **Cell Signaling Technologies, Danvers, MA, USA**

Anti p42/44 MAP kinase, anti phospho-p42/44 MAP kinase

## **Santa Cruz Biotechnology, INC**

Anti GRK 2 (C-15), anti tubulin

Anti VSV-G and all G protein antibodies were produced in-house.

Refer to Tables 2.2 and 2.3 for details.

### **2.1.5. Molecular Probes, Eugene, Oregon, USA**

Anti-mouse Alexa® 594 IgG conjugate, anti-rabbit Alexa® 594 IgG conjugate

## **2.2. Buffers**

### **2.2.1. General buffers**

#### **Phosphate Buffered Saline (PBS) (10 x)**

137 mM NaCl, 2.7 mM KCl, 1.5 mM KH<sub>2</sub>PO<sub>4</sub>, 8 mM Na<sub>2</sub>HPO<sub>4</sub>, pH 7.4

Diluted 1 in 10 prior to use and stored at 4 °C

#### **Tris Buffered Saline (TBS) (10 x)**

20 mM Tris-base, 150 mM NaCl pH 7.4

Diluted 1 in 10 prior to use and stored at room temperature

#### **Tris-EDTA (TE) Buffer**

10 mM Tris, 0.1 mM EDTA pH 7.4

Stored at 4 °C

**Radioimmune precipitation assay (RIPA) Buffer (2x)**

100 mM HEPES (pH7.4), 300 mM NaCl, 2 % (v/v) Triton X-100, 1 % (w/v) Na-deoxycholate, 0.2 % (w/v) SDS

Stored at 4 °C

Diluted 1:2 prior to use with:

0.5 M NaF, 0.5 M EDTA, 0.2 M Na<sub>4</sub>P<sub>2</sub>O<sub>7</sub>, 10 % (v/v) ethylene glycol, complete EDTA free protease inhibitor tablet

**Physiological Saline Solution pH 7.4**

130 mM NaCl, 5 mM KCl, 1 mM CaCl<sub>2</sub>, 1 mM MgCl<sub>2</sub>, 20 mM HEPES, 10 mM D-glucose

**Laemelli Buffer (2 x)**

0.4 M DTT, 0.17 M SDS, 50 mM Tris, 50 % (v/v) glycerol, 0.01 % (w/v) bromophenol blue

Stored in aliquots at -20 °C

**2.2.2. Molecular biology solutions**

**TAE Buffer (50 x) pH 8.0**

40 mM Tris base, 5 mM EDTA, 5.71 % (v/v) glacial acetic acid

Diluted 1 in 50 prior to use and stored at room temperature

**DNA Gel Loading Buffer (5 x)**

0.25 % (w/v) bromophenol blue, 40 % sucrose (w/v) in distilled H<sub>2</sub>O

**LB Media (Luria-Bertani Medium)**

1 % (w/v) bactotryptone, 0.5 % (w/v) yeast extract, 1 % NaCl (w/v), pH 7.4

Sterilised by autoclaving at 126 °C

**LB Media containing agar (LBA)**

As above, with the addition of bactotryptone at 15 g/L prior to autoclaving

**Competent Bacteria Buffers**

*Competent Bacteria Buffer 1:*

1 M KAc, 1 M RbCl<sub>2</sub>, 1 M CaCl<sub>2</sub>, 1 M MnCl<sub>2</sub>, 80 % glycerol

pH 5.8 with acetic acid

Filter sterilised and stored at 4 °C

*Competent Bacteria Buffer 2:*

100 mM MOPS pH 6.5, 1 M CaCl<sub>2</sub>, 1 M RbCl<sub>2</sub>, 80 % glycerol

pH 6.5 with concentrated HCl

Filter sterilised and stored at 4 °C

## **2.3. Molecular biology protocols**

All reactions were performed using sterile techniques.

### **2.3.1. Preparation of LB agar plates**

LBA medium was prepared as detailed in section 2.2.2. After autoclaving, the medium was allowed to cool to 50 °C prior to the addition of a selective antibiotic; ampicillin (50 µg/ml) and kanamycin (25 µg/ml). Approximately 25 ml of the LBA medium was poured per 10 cm Petri dish. The plates were left to set at room temperature before being stored at 4 °C.

### **2.3.2. Preparation of competent bacterial cells**

DH5α *E.coli* cells were streaked onto an LB agar plate in the absence of selective antibiotics and incubated overnight at 37 °C. A single colony was inoculated into a 5 ml culture of LB broth and grown in a shaking incubator for 16 hours at 37 °C. The culture was used to inoculate 100 ml of LB broth; this was grown with aeration at 37 °C until the optical density at 550 nm reached 0.48. The culture was chilled on ice for 5 minutes then spun at 805 g for 10 minutes at 4 °C. All traces of LB broth were removed and the pellet re-suspended in 20 ml of competent bacteria buffer one. The suspension was chilled on ice for 5 minutes prior to centrifugation at 805 g for 10 minutes at 4 °C. The supernatant was removed and the cell pellet was re-suspended in 2 ml of competent bacteria buffer two. The resulting cell suspension was chilled on ice for 15 minutes before being stored at -80 °C in aliquots until required.

### **2.3.3. Transformation of competent bacterial cells**

Competent bacteria were allowed to thaw on ice for 30 minutes prior to use. 50 µl of competent bacteria was added to a chilled microfuge tube containing 1 – 10 ng of DNA. The reaction was chilled on ice for 15 minutes. The cells were heat shocked at 42 °C for 90 seconds and chilled on ice for 2 minutes. 450 µl of LB broth was added to the cells and incubated at 37 °C for 45 minutes in a shaking incubator. 100 – 250 µl

of the reaction was plated onto a LB plate containing the appropriate selective antibiotic and incubated overnight at 37 °C.

### **2.3.4. Preparation of plasmid DNA**

#### **2.3.4.1. Mini-preps**

A single colony of transformed bacteria was used to inoculate a 5 ml LB culture containing the appropriate selective antibiotic. The culture was grown overnight at 37 °C in a shaking incubator. Miniprep purification was carried out using a Qiagen miniprep kit as per manufacturer's instructions.

#### **2.3.4.2. Maxi-preps**

The Qiagen Qiafilter kit was used for larger scale DNA sample preparations. A single colony of transformed bacteria was used to inoculate a starter culture of LB containing the appropriate selective antibiotic. The culture was grown for 8 hours at 37 °C in a shaking incubator. This culture was then used to inoculate 100 ml of LB media also containing the selective antibiotic. This was grown, in a vessel 4 times the volume of the culture, at 37 °C for 12-16 hours. Purification of DNA was carried out as per manufacturer's instructions.

### **2.3.5. Quantification of DNA**

DNA samples, diluted 1:100, were quantified by measuring the absorbance of light at 260 nm in a spectrophotometer. An A<sub>260</sub> value of 1 unit relates to 50 µg/ml of double stranded DNA. Sample concentration is determined by:

$$\text{Sample concentration} = A_{260} \times \text{dilution factor (100)} \times 50 \mu\text{g/ml}$$

The purity of the DNA sample was determined by measuring the absorbance of light at 280 nm. Samples of adequate purity typically have A<sub>260</sub>:A<sub>280</sub> ratio of between 1.5 and 2.0.

### **2.3.6. Digestion of DNA with restriction endonuclease**

Diagnostic digests were prepared with 1 – 2 units of the appropriate restriction enzyme, buffer as specified by the manufacturer, and 1 µg of DNA, in a final volume of 20 µl. Reactions were incubated at the recommended temperature for 1 hour. For cloning purposes, 3 µg of DNA was digested, with 2 – 3 units of the appropriate restriction enzyme, overnight at the recommended temperature. Where appropriate restriction enzymes were heat inactivated at the recommended temperature.

### **2.3.7. DNA gel electrophoresis**

Digested DNA samples or PCR reactions were analysed using gel electrophoresis. A 1 % agarose gel was prepared in 1 x TAE and 0.5 µg/ml ethidium bromide. The gels were set in a horizontal gel tank (Life technologies, Gibco, Horizon 58 model) and once set immersed in 1 x TAE. Samples were diluted in 5 x DNA loading buffer and loaded along with the DNA molecular marker X. A voltage of between 75 – 120 mA was applied to separate the samples. The DNA fragments were visualised using an UV transilluminator. (BioRad transilluminator).

### **2.3.8. DNA purification from agarose gels**

DNA fragments of interest were excised from the gel and purified using the QiaQuick gel extraction kit as per the manufacturer's instructions. DNA was eluted from the purification column using 30 µl sterile water. It is generally accepted around 20 % of the DNA sample is lost in purification steps.

### **2.3.9. Alkaline phosphatase treatment of plasmid vectors**

Digestion by restriction enzymes result in exposed 5'-monophosphate groups in the nucleic acid strands. The 5'-monophosphate groups of the vector DNA can be hydrolysed by phosphatases to minimise vector re-ligation. Digested vector DNA was incubated with two units of shrimp alkaline phosphatase for 15 minutes (cohesive-end cloning) and 60 minutes (blunt-end cloning) at 37 °C. The enzyme was either heat

inactivated at 65 °C for 15 minutes or isolated by resolving on an agarose gel by electrophoresis and then extracted as previously described in section 2.3.8.

### **2.3.10. Ligation of DNA**

Vector and insert DNA fragments were quantified by ethidium bromide fluorescence quantification. Vector and insert DNA fragments were ligated using T4 DNA ligase in a 1:3 ratio. The reaction was set up in a volume of 10 µl containing 1 unit of ligase and the supplied buffer. Cohesive-end ligations were performed at room temperature for 4 hours. Blunt-end ligations were performed overnight at 4 °C. The ligation reactions were transformed as detailed in section 2.3.3.

### **2.3.11. Polymerase chain reaction**

#### **2.3.11.1. Standard PCR**

PCR reactions were carried out to amplify DNA sequences and introduce sequences, such as new restriction sites and epitope tags. Pfu DNA polymerase was used due to its high fidelity and its ability to withstand higher temperatures.

The PCR reactions contained;

Pfu polymerase buffer (10 x)	5 µl
DMSO (optional)	5 µl
Deoxynucleotide tri-phosphates (dNTPs) (0.2 mM of each dATP, dCTP, dGTP, dTTP)	5 µl
Primer sense: 25 pmol/µl	1 µl
Primers antisense: 25 pmol/µl	1 µl
DNA template: 50 ng/µl	1 µl
Pfu enzyme: 1 unit	1 µl
dH <sub>2</sub> O to a final volume of	50 µl

Reactions were carried out on an Eppendorf gradient Thermocycler. PCR cycles used were as follows and the annealing temperatures were dependent on the melting temperature ( $T_m$ ) of primers used;

1.	Preheating	95 °C	5 min
2.	Denaturation	95 °C	1 min
3.	Annealing	50 - 60 °C	1 min
4.	Extension	72 °C	2.30 min
5.	Repeat from step 2.		29 x
6.	End	72 °C	10 min
7.	Hold	4 °C	

#### **2.3.11.2. QuikChange mutagenesis PCR**

The QuikChange site-directed mutagenesis method was used to make point mutations (either single or multiple residues). Manufacturer's instructions were followed when designing primers and carrying out the PCR reactions.

PCR reactions were compiled with the following components: 50 ng DNA template, 15 pM of both sense and anti-sense primers, 1  $\mu$ l of dNTP mix (0.2  $\mu$ M of each dATP, dCTP, dGTP and dTTP) and 2.5 units Pfu DNA polymerase, total volume of 50  $\mu$ l with reaction buffer. Samples were cycled 30 times in an Eppendorf Thermocycler system under the following conditions:

Cycle 1: 95 °C for 30 seconds

Cycles 2-30: 95 °C for 30 seconds,

50 °C for 1 minute

68 °C for 1 minute per kbp of plasmid length

The product was treated with 10 units DpnI restriction enzyme and incubated for 60 minutes at 37 °C. Control reactions contained 50 ng DNA, 1  $\mu$ l of dNTP mix and 1  $\mu$ l



pre-warmed growth medium and centrifuged at 290 g for 5 minutes. The resulting pellet was re-suspended in 10 mls of fresh medium and plated onto a 75 cm<sup>2</sup> flask for recovery. Media was changed after 24 hours and as required thereafter.

## **2.4.2. Cell maintenance**

### **2.4.2.1. CHO-K1**

Chinese hamster ovary cells (CHO-K1) were grown in F12-HAMS Dulbecco's modified Eagle's medium (DMEM) supplemented with 10 % (v/v) foetal bovine serum (FBS) and 2 mM L-glutamine. Cells were grown in a humidified incubator of 95 % air/5 % CO<sub>2</sub> at 37 °C.

### **2.4.2.2. Flp-In CHO-K1**

Cells were maintained in F12-HAMS DMEM supplemented with 10 % (v/v) FBS, 2 mM L-glutamine, 1 % (v/v) penicillin and streptomycin and 100 µg/ml zeocin. Cells were grown in a humidified incubator of 95 % air/5 % CO<sub>2</sub> at 37 °C.

### **2.4.2.3. CHO-K1 stably expressing receptor**

Cells stably expressing the receptor were maintained in F12-HAMS DMEM supplemented with 10 % (v/v) dialysed FBS, 2 mM L-glutamine and 1 mg/ml G418. Cells were grown in a humidified incubator of 95 % air/5 % CO<sub>2</sub> at 37 °C.

### **2.4.2.4. Flp-In CHO-K1 stably expressing receptor**

Flp-In CHO-K1 cells were grown in F12-HAMS DMEM supplemented with 10 % (v/v) dialysed FBS, 2 mM L-glutamine, 1 % (v/v) penicillin and streptomycin and 200 µg/ml hygromycin. Cells were grown in a humidified incubator of 95 % air/5 % CO<sub>2</sub> at 37 °C.

### **2.4.2.5. HEK293T**

Human embryonic kidney cells stably expressing the SV40 large T-antigen (HEK293T) were grown in DMEM supplemented with 10 % (v/v) newborn calf serum and 2 mM L-glutamine. Cells were grown in a humidified incubator of 95 % air/5 % CO<sub>2</sub> at 37 °C.

#### **2.4.2.6. 3T3 L1**

Cells were maintained in DMEM supplemented with 10 % (v/v) newborn calf serum and 1 % (v/v) penicillin and streptomycin. Cells were grown in a humidified incubator of 95 % air/10 % CO<sub>2</sub> at 37 °C.

### **2.4.3. *Passage of cells***

#### **2.4.3.1. CHO-K1 and HEK293T**

Cells 80 – 90 % confluent were washed once with sterile PBS, and then incubated with 3 mls of sterile 0.25 % trypsin-EDTA for 3 minutes at 37 °C in a humidified incubator. Once detached, 5 ml of fresh media was added and the cells centrifuged at 290 g for 5 minutes. The resulting pellet was re-suspended in fresh media and the cells plated into flasks, dishes, plates or coverslips as required.

#### **2.4.3.2. 3T3 L1**

Cells 50 – 60 % confluent were washed once with sterile PBS and incubated with 7 mls of sterile 0.25 % trypsin-EDTA for 3 minutes at room temperature. Appropriate volume of fresh media was added to the trypsinised cells and they were plated into flasks or dishes as required.

### **2.4.4. *Liquid nitrogen storage***

Cells were trypsinised as described above, transferred to a 15 ml falcon tube and centrifuged at 290 g for 5 minutes. The supernatant was removed carefully and the pellet was re-suspended in 10 % (v/v) DMSO in FBS. Cells were aliquoted into 1 ml cryovials and cooled at a rate of -1 °C/minute. After 24 hours the cells were transferred to liquid nitrogen for long term storage.

### **2.4.5. *Differentiation of 3T3 L1***

Cells were grown to confluency, media was replaced with fresh growth media and left for 2 days. Media was then replaced with DMEM supplemented with 10 % (v/v) Myoclone FBS, 1 µg/ml insulin, 5 µM dexamethasone, 112 µg/ml IBMX. After two days, the media was very carefully aspirated so that the loosely attached cells were

not disturbed. DMEM supplemented with 10 % (v/v) myoclone FBS and 1 µg/ml insulin. Thereafter, every 2 days the cells were fed with DMEM supplemented with 10 % (v/v) myoclone FBS. Following treatment with differentiating medium cells accumulated lipids and acquired adipose cell morphology. Cells were ready for use between day 8 and 12 post differentiation.

#### **2.4.6. *Pertussis toxin treatment***

Cells were treated with 25 ng/ml pertussis toxin for 16 hours at 37 °C.

#### **2.4.7. *Transient transfection***

##### **2.4.7.1. Cationic lipid-based transfection**

Transfection of CHO-K1 and HEK293 cells was performed with Lipofectamine 2000 (Invitrogen) in accordance with the manufacturer's instructions.

##### **2.4.7.2. Nucleofection**

Mouse embryo fibroblast (MEF) cells were nucleofected with Amaxa nucleofection kit in accordance with the manufacturer's instructions (Amaxa nucleofector 1).

#### **2.4.8. *Stable transfection***

##### **2.4.8.1. DOTAP**

Fresh media was replaced on CHO-K1 cells that were 50 % confluent in a 10 cm dish. In a sterile microfuge tube, 5 µg of DNA and 40 µl DOTAP was added to a final volume of 200 µl of sterile HEPES Buffered Saline (20 mM HEPES, pH 7.4 150 mM NaCl) and left at room temperature for 15 minutes. This was then added to the cells in a dropwise manner and the cells were incubated in a humidified incubator of 95 % air/5 % CO<sub>2</sub> at 37 °C for 48 hours. The cells were then plated onto four fresh 10 cm dishes and allowed to attach overnight. The following day the media was changed to DMEM containing 1 mg/ml G418. Controls of untransfected and mock transfected cells containing basal or G418 media were also set up and cell death was compared. Media was changed as required until single colonies appeared. These were then

transferred into 12 well plates and allowed to grow before being tested for receptor expression by immunoblotting and immunocytochemistry

#### **2.4.8.2. Lipofectamine 2000**

Transfection of CHO-K1 cells was performed with Lipofectamine 2000 in accordance with the manufacturer's instructions and cells were put on antibiotic selection as outlined as above.

#### **2.4.9. Generation of stable Flp-In CHO-K1 cell line**

Flp-In CHO-K1 cells were transfected with a mixture containing the desired receptor cDNA in the pcDNA5/FRT/TO vector and the Flp recombinase pOG44 vector in a 1:9 ratio using Lipofectamine 2000 in accordance with the manufacturer's instructions. After 48 hours, the medium was changed to medium supplemented with 200 µg/ml hygromycin to initiate selection of stably transfected cells. Resistant clones were screened by immunoblotting and immunocytochemistry.

#### **2.4.10. siRNAi**

Transfection of CHO-K1 cells with siRNAi was performed with Lipofectamine 2000 in accordance with the manufacturer's instructions.

#### **2.4.11. Cell harvesting**

The media was discarded and cells washed 3 times in ice cold 1 x PBS. Cells were scraped from the dish using a disposable cell scraper and transferred to a 15 ml centrifuge tube. The detached cells were centrifuged for five minutes at 805 g at 4 °C. After discarding the supernatant, the cell pellet was frozen at -80 °C until required.

## **2.5. Biochemical assays and other methods of analysis**

### **2.5.1. *Preparation of cell membranes***

#### **2.5.1.1. Teflon homogeniser**

Harvested pellets were thawed and re-suspended in ice-cold Tris/EDTA (T.E.) buffer containing protease inhibitor tablets. The cells were homogenised by 50 passes of a glass-on-Teflon homogeniser. The resulting suspension was centrifuged at 153 g for 10 minutes to remove unbroken cells and nuclei. The supernatant was subsequently ultracentrifuged at 89,000 g for 30 minutes in a Beckman Optima TLX Ultracentrifuge (Palo Alto, CA). The resulting pellet was re-suspended in T.E. buffer and passed 10 times through a 25 gauge needle. The protein concentration was determined as detailed in section 2.5.3 and the membranes diluted to 1 µg/µl and stored at -80 °C until required.

#### **2.5.1.2. Covaris acoustic cell disrupter**

Harvested pellets were thawed and re-suspended in 3 ml ice-cold T.E. buffer containing protease inhibitor tablets as above. Samples were transferred to Covaris tubes and placed in the Covaris acoustic cell disrupter (Covaris model S2) and pulsed (pulse 1) using the power tracking setting. 7 ml of T.E. was added to the sample and centrifuged at 200 g for 10 minutes at 4 °C to remove unbroken cells and nuclei. The supernatant was subsequently centrifuged at 88,900 g for 35 minutes. The supernatant was discarded and the pellet was re-suspended in 500 µl of T.E. buffer and pulsed again (pulse 2 and pulse 3). Settings for the pulses are summarised in table 2.1. The protein concentration was determined and the membranes diluted to 1 µg/µl and stored at -80 °C until required.

	<b>Pulse 1</b>	<b>Pulse 2</b>	<b>Pulse 3</b>
<b>Duty cycle</b>	<b>20 %</b>	<b>20 %</b>	<b>20 %</b>
<b>Cycles/burst</b>	<b>500</b>	<b>500</b>	<b>500</b>
<b>Cycles</b>	<b>1</b>	<b>2</b>	<b>1</b>
<b>Intensity</b>	<b>6</b>	<b>6</b>	<b>2</b>
<b>Time</b>	<b>30 sec</b>	<b>20 sec</b>	<b>40 sec</b>

**Table 2.1 Covaris acoustic cell disrupter settings**

### **2.5.2. Preparation of cell lysates**

Cells were washed 3 times with ice cold 1 x PBS. An appropriate volume of 1 x RIPA buffer supplemented with an EDTA-free protease inhibitor tablet was added to the cells before scrapping. The lysates were rotated for 1 hour at 4 °C on a rotating wheel. After 1 hour, the samples were centrifuged at 21,000 g for 10 minutes. The supernatant was carefully removed into fresh eppendorf tubes and the protein concentrations of the samples were determined as detailed in section 2.5.3. The protein concentration of the samples was equalised to 1 µg/µl using 1 x RIPA and 2 x Laemmli buffer was added to the samples before storage. Cell lysates were then subjected to SDS-PAGE and Western blotting.

### **2.5.3. BCA protein quantification**

The protein concentration in samples was quantified using the BCA assay. This assay utilises bicinchoninic acid (BCA) and copper sulphate solutions, in which proteins reduce the Cu(II) ions to Cu(I) ions in a concentration dependent manner and the reduced Cu(I) can be bound by BCA. When BCA binds Cu(I) a colour change from green to purple occurs which has an absorption maximum of 562 nm. Using solutions of known protein concentrations (0 – 2 mg/ml) a standard curve was constructed, which allows the concentrations of unknown samples to be established. Solutions used in this assay consisted of: Reagent A – 1 % (w/v) BCA, 2 % (w/c) Na<sub>2</sub>CO<sub>3</sub>, 0.16

% (w/v) sodium tartrate, 0.4 % NaOH, 0.95 % NaHCO<sub>3</sub>, pH 11.25 and Reagent B – 4 % CuSO<sub>4</sub>. One part reagent B was mixed with 49 parts reagent A and 200 µl of this solution added to 10 µl of protein standard or unknown sample in a 96 well ELISA plate. The assay was incubated at 37 °C for 20 minutes before the absorbance was measured at 492 nm.

#### **2.5.4. Sodium dodecyl sulphate polyacrylamide gel electrophoresis**

Protein samples were resolved using sodium dodecyl sulphate polyacrylamide gel electrophoresis (SDS-PAGE). Samples and full range Rainbow molecular weight markers were loaded onto pre-cast NuPage Novex bis-tris gels with 4-12 % acrylamide concentration. NuPage MOPS SDS buffer was used for electrophoresis at 200 V using the XCell Surelock mini-cell gel tank until the dye front reached the foot of the gel.

#### **2.5.5. Western blotting**

Following separation of samples by SDS-PAGE as detailed in section 2.5.4, proteins were electrophoretically transferred onto a nitrocellulose membrane using the XCell II blot module. Proteins were transferred at 30 V for at least 1 hour in transfer buffer (0.2 M glycine, 25 mM Tris and 20 % (v/v) methanol). Efficient transfer was monitored using Ponceau stain (0.1 % (w/v) Ponceau S, 3 % (w/v) trichloroacetic acid). To block non-specific binding sites, the nitrocellulose membrane was incubated in 5 % (w/v) low fat milk in TBS/0.1 % (v/v) Tween 20 at room temperature on a rotating shaker for 2 hours. The membrane was incubated with primary antibody overnight in 5 % (w/v) low fat milk, TBS/0.1 % (v/v) Tween 20 containing the required antibody (Table 2.2) at 4 °C. After overnight incubation, the membrane was washed (four 5 minute washes) in TBS/0.1 % (v/v) Tween 20. The horseradish peroxidase conjugated (HRP) secondary antibody (Table 2.2) in 5 % (w/v) low fat milk, TBS/0.1 % (v/v) Tween 20 was incubated at room temperature for 20 minutes. The membrane was washed as before in TBS/0.1 % (v/v) Tween 20. The nitrocellulose membrane was then incubated for 5 minutes with an enhanced chemiluminescent ECL substrate solution. Exposure and development of blue Kodak

film allowed visualisation of the protein of interest. To determine equal loading of samples, the blot was stripped and re-probed using different antibodies. To strip the antibodies from the nitrocellulose membrane, the membrane was washed for 15 minutes in TBS/0.1 % (v/v) Tween 20 and then incubated for 15 minutes in 10 % (v/v) ReBlot Plus solution. The above process was repeated after blocking with 5 % (w/v) low fat milk in TBS/0.1 % (v/v) Tween 20.

<b>Primary antibody</b>	<b>Dilution factor</b>	<b>Secondary antibody</b>	<b>Dilution factor</b>
Anti VSV-G	1:4000	Anti rabbit	1:5000
Anti GFP	1:10000	Anti goat	1:10000
Anti tubulin	1:10000	Anti mouse	1:5000
Anti p44/42 MAP kinase	1:1000	Anti rabbit	1:5000
Anti phospho p44/42 MAP kinase	1:1000	Anti mouse	1:5000
Anti G $\alpha$ 1,2 1319G	1:5000	Anti rabbit	1:5000
Anti G $\alpha$ q/G11	1:10000	Anti rabbit	1:20000
Anti GRK 2 (C-15)	1:1000	Anti rabbit	1:5000
Anti GAPDH	1:20000	Anti mouse	1:1000
Anti phospho CREB ser 133	1:500	Anti rabbit	1:1000

**Table 2.2 Primary and secondary antibody dilutions for immunoblotting**

### **2.5.6. Endoglycosidase treatment**

Membrane preparations (50  $\mu$ g) were treated with 1.5 units of Roche N-Glycosidase-F overnight at 32 °C.

### **2.5.7. Nicotinic acid preparation**

DMEM solution was prepared from powder form and nicotinic acid stock solution was made up in this media. The pH was altered to pH 7.0 and the solution was filter sterilised, aliquoted and stored at 20 °C.

### **2.5.8. ERK1/2 activation phosphorylation assay**

CHO-K1 cells grown to confluency in six well dishes were washed 2 times with 2 ml/well basal media (CHO-K1 media described before containing no supplements) and serum starved overnight with the same media. The following day the media was changed to fresh basal media and the cells were serum starved for a further 2 hours. Unless specified the cells were stimulated for 5 minutes with the drug at 37 °C in a

humidified incubator of 95 % air/5 % CO<sub>2</sub>. Foetal bovine serum was utilised as a positive control. Cell lysates were prepared and samples were resolved and analysed by SDS-PAGE and immunoblotting.

### **2.5.9. Cell surface biotinylation assay**

CHO-K1 cells, grown to 80 – 90 % confluency in six well dishes, were washed and treated with drug/vehicle for 30 minutes in a humidified incubator of 95 % air/5 % CO<sub>2</sub> at 37 °C. The reaction was terminated by placing cells on ice and washing twice with 2 ml/well of ice-cold borate buffer (10 mM boric acid, 154 mM NaCl, 7.2 mM KCl, 1.8 mM CaCl<sub>2</sub>, pH 9.0). Unless otherwise stated, all subsequent procedures were performed at 4 °C. Cell surface glycoproteins were conjugated with biotin by incubation with freshly prepared one ml of 0.8 mM EZ-Link Sulfo-NHS-SS Biotin in borate buffer for 15 minutes at 0 °C in the dark. Cells were quenched by rinsing twice with 2 ml/well of glycine buffer (0.192 M glycine, 25 mM Tris, pH 8.3). The second wash was left on ice for five minutes before removing. Cells were lysed with 500 µl of 1 x RIPA buffer containing an EDTA-free protease inhibitor tablet. Insoluble material was removed by centrifugation for 30 minutes at 21,000 g and the soluble extracts were equalised for protein content and volume. A sample of the total extract was saved at this point. Cell surface biotinylated proteins were isolated using 100 µl of ImmunoPure immobilized streptavidin beads. To avoid damaging the beads, the tip of a p200 pipette tip was cut and then used to dispense the streptavidin beads. After 1 hour constant rotation, samples were centrifuged at 153 g for 2 minutes and the beads were washed 3 times with 1 x RIPA buffer and the residual supernatant was removed with a fine (30 gauge) needle. The biotinylated proteins were eluted from the beads with 200 µl of 2 x Laemmli buffer containing 5 % beta-mercaptoethanol for 1 hour at 37 °C. To pellet the beads, the samples were then centrifuged at 153 g for 2 minutes. A Hamilton syringe was used to remove the samples into a fresh microfuge tube. Laemmli buffer was added to the total and unbound extracts and the samples were analysed by SDS-PAGE and Western blotting.

### **2.5.10. eYFP fluorescence measurement**

Whole cell lysates prepared from cell lines stably expressing eYFP fusion receptors were equalised for protein concentration. 50 µl of cell lysates were then loaded into black-walled multiwell plates in triplicates and eYFP fluorescence was measured at 490 nm with a Victor<sup>2</sup> plate reader. Host cells not expressing the fusion protein and readings from blank wells served as negative controls.

### **2.5.11. [<sup>32</sup>P] Orthophosphate incorporation into receptors**

CHO-K1 cells grown to confluency in six well dishes were washed twice with 2 ml/well phosphate-free DMEM supplemented with 2 mM L-glutamine, 1 % (v/v) penicillin and streptomycin. Media was then replaced with 0.75 ml/well of the same medium supplemented 0.2 mCi/ml [<sup>32</sup>P] orthophosphate and the cells incubated for 90 minutes at 37 °C in a humidified incubator of 95 % air/5 % CO<sub>2</sub>, in order to label the intracellular ATP pool with [<sup>32</sup>P]. After stimulation for 15 minutes at 37 °C with 0.75 ml/well of 2 x concentrated drug/vehicle, the reaction was stopped by placing the cells on ice and washing the cells twice with 3 ml/well of ice-cold PBS. Unless otherwise stated, all subsequent procedures were performed at 4 °C. Cells were lysed with 500 µl of 1 x RIPA supplemented with an EDTA-free protease inhibitor tablet and 100 µM sodium orthovanadate and the samples were rotated for 1 hour. Insoluble material was removed by centrifugation for 15 minutes at 21,000 g and the soluble extracts were equalised for protein content and volume prior to receptor immunoprecipitation. Using a cut p200 tip, 20 µl of protein G was centrifuged at 130 g for 30 seconds. Residual supernatant was removed with a 1 ml syringe. To this, 1 µl of the appropriate antibody and 100 µl of 2 % (w/v) IgG-free BSA in 1 x RIPA (supplemented with an EDTA-free protease inhibitor tablet and 100 µM sodium orthovanadate) was added and briefly vortexed. This antibody mixture was then added to the protein samples and rotated for 1 hour. The immune complexes were isolated by brief centrifugation (25 seconds at 153 g), and washed 3 times with 1 ml of 1 x RIPA, the residual supernatant was removed with a 1 ml syringe, and the immune complexes eluted from the beads by the addition 30 µl of 2 x Laemmli buffer. The samples were incubated overnight at room temperature. To pellet the beads, the samples were then centrifuged at 153 g for 25 seconds. A Hamilton syringe was used

to remove the samples into a fresh microfuge tube. The samples were resolved by SDS-PAGE and the gel dried overnight using Invitrogen's Gel-Dry. The phosphoproteins were visualised by autoradiography after 72 hours exposure at -80 °C.

### **2.5.12. Cell surface receptor measurement and Enzyme-linked Immunosorbent assay (ELISA)**

50, 000 CHO-K1 cells expressing recombinant receptors (100 µl/well) were plated onto poly-D-lysine treated 96 well plates and allowed to attach overnight. The next day the cells were treated with drug/vehicle for 30 minutes in a humidified incubator of 95 % air/5 % CO<sub>2</sub> at 37 °C. Four replicates per sample were included in each assay.

#### **2.5.12.1. Live cells**

Media was removed and the primary anti VSV-G antibody (1:1000 dilution, made up in growth media) was added 100 µl/well and incubated for 30 minutes at 37 °C. The primary antibody was then removed and the cells were washed once with 100 µl/well of sterile DMEM/20 mM HEPES pH 7.4. In a final volume of 100 µl/well, a mixture of HRP-conjugated secondary antibody (anti-rabbit HRP 1:5000 dilution) and Hoechst nuclear stain (1:1000 dilution), made up in growth media, was added to the cells and incubated for a further 30 minutes at 37 °C. The secondary antibody mixture were removed and the cells were washed twice with pre-warmed 1 x PBS. During the second wash, cell number was determined by measuring Hoechst staining (excitation, 355 nm and emission 460 nm). After the reading, the PBS was completely removed and 100 µl/well of SureBlue TMB substrate was added and the cells incubated in the dark for 5 – 10 minutes before the absorbance was measured at 620 nm. Victor<sup>2</sup> plate reader was used for both readings (PerkinElmer Life Sciences).

#### **2.5.12.2. Fixed and permeabilised cells**

Media was removed and the cells were washed 3 times with 100 µl/well room temperature 1 x PBS. The cells were then fixed with 4 % (w/v) PFA/5 % (w/v) sucrose in 1 x PBS for 10 minutes at room temperature. Cells were then permeabilised with 5 % (w/v) BSA/0.15 % (v/v) Triton X-100/1 x PBS for 10 minutes at room temperature. Cells were then washed 3 times with 100 µl/well room temperature 1 x

PBS and the primary anti VSV-G antibody (1:1000 dilution, made up in 5 % (w/v) BSA/1 x PBS) was added 100 µl/well and incubated for 30 minutes at room temperature. The primary antibody was then removed and the cells were washed once with 100 µl/well 1 x PBS. In a final volume of 100 µl/well, a mixture of HRP-conjugated secondary antibody (anti-rabbit HRP 1:5000 dilution) and Hoechst stain (1:1000 dilution), made up in 5 % (w/v) BSA/1 x PBS, was added to the cells and incubated for a further 30 minutes at room temperature. The secondary antibody mixture was removed and the cells were washed twice with pre-warmed 1 x PBS. During the second wash, Hoechst staining was measured (excitation, 355 nm and emission 460 nm). After the reading, the PBS was completely removed and 100 µl/well of TMB substrate was added and the cells incubated in the dark for 5 – 10 minutes before the absorbance was measured at 620 nm. Victor2 plate reader was used for both readings (PerkinElmer Life Sciences).

## **2.6. Immunocytochemistry**

### **2.6.1. Immunostaining**

CHO-K1 cells expressing recombinant receptors were plated onto sterile poly-D-lysine coated coverslips and allowed to attach overnight. Cells were treated with the primary antibody diluted in sterile DMEM/20 mM HEPES pH 7.4 for 40 minutes in a humidified incubator of 95 % air/5 % CO<sub>2</sub> at 37 °C. Following this drug/vehicle was added to the antibody/DMEM/HEPES mix for a further 30 minutes. The cells were washed three times with 2 mls/coverslip ice cold 1 x PBS (each wash was left on for 5 minutes). The cells were then fixed with 1.5 mls/coverslip of 4 % (w/v) PFA/5 % (w/v) sucrose in 1 x PBS for 10 minutes at room temperature. Cells were washed three times again with 1 x PBS, as before. The cells were then permeabilised with 2 mls/coverslip of 3 % (w/v) low fat milk/0.15 % (v/v) Triton X-100/1 x PBS for 10 minutes at room temperature. The secondary antibody was then diluted in 3 % (w/v) low fat milk/0.15 % (v/v) Triton X-100/1 x PBS. The antibody solution was then centrifuged for 1 minute at 130 g to pellet undissolved antibody aggregates and 200 µl of the supernatant was spotted onto nescofilm. Coverslips were incubated cell side down for 1 hour at room temperature. Coverslips were carefully returned to the six

well dishes and washed 3 times with 3 % (w/v) low fat milk/0.15 % (v/v) Triton X-100/1 x PBS for 5 minutes each time. The cells were then washed with 3 times with 1 x PBS, again for 5 minutes each time. The last wash was not removed and 8  $\mu$ l of 40 % (v/v) glycerol in 1 x PBS was spotted onto microscope slides. The excess PBS was removed from the coverslips by brief drying and the coverslip was placed slowly on the spotted glycerol, cell side down avoiding air bubbles. Cells were analysed by confocal microscopy straight away or covered in foil and stored at 4 °C until required.

Primary antibody	Dilution factor	Secondary antibody	Dilution factor
Anti-c-myc	1:100	Anti-rabbit alexa 594	1:400
Anti-flag M2	1:1000	Anti-mouse alexa 594	1:400
Anti-vsv	1:1000	Anti-rabbit alexa 594	1:400

**Table 2.3 Primary and secondary antibody dilutions for immunocytochemistry**

### **2.6.2. Confocal microscopy: Fixed cells**

Cells expressing recombinant receptors were plated onto sterile poly-D-lysine coated coverslips and allowed to attach overnight. Cells were treated with drug/vehicle for 30 minutes in a humidified incubator of 95 % air/5 % CO<sub>2</sub> at 37 °C. The cells were washed 3 times with 2 mls/coverslip room temperature 1 x PBS and fixed with 1.5 mls/coverslip of 4 % PFA 5 % sucrose in 1 x PBS for 10 minutes at room temperature. Cells were washed 3 times again with 2 mls/well room temperature 1 x PBS. The last wash was not removed and 8  $\mu$ l of 40 % (v/v) glycerol in 1 x PBS was spotted onto microscope slides and the coverslips mounted as described before. Cells were analysed by confocal microscopy straight away or covered in foil and stored at 4 °C until required.

Cells were observed using a laser scanning confocal microscope (Zeiss LSM 5 Pascal, Carl Zeiss Inc., Thornwood, NY) with a 63 x 1.40 numeric aperture oil-immersion Plan Fluor Apochromat objective lens, pinhole setting of 20, and electronic zoom of 1 or 2.5. eYFP was excited using 488 nm argon/krypton laser and detected using a 505 – 530 nm band pass filter. Alexa 594 label was detected using a 543 nm helium/neon laser and detected with a 560 nm long-pass filter. Images acquired using identical capture parameters were processed for presentation, off-line, using MetaMorph

software (Version 6.1.3: Universal Imaging Corporation, Downing, PA, USA). For purposes of clarity, some images are presented at different magnifications.

### **2.6.3. *Epifluorescence (widefield) microscopy: Live cells***

CHO-K1 cells expressing recombinant receptors were plated onto sterile poly-D-lysine coated coverslips and allowed to attach overnight. Coverslip fragments were placed into a microscope chamber containing physiological saline solution. Fluorescent images of the cells were acquired using a Nikon Eclipse TE2000-E fluorescence inverted microscope (Nikon Instruments, Melville, NY) equipped with a x40 (numerical aperture 1.3) oil immersion Plan Fluor lens and a cooled digital CoolSNAPHQ charge-coupled device camera (Photometrics, Tucson, AZ). The filter set used for eYFP (excitation – 500/5 nm; emission – 535/30 nm). Collected images were processed off-line, using MetaMorph and MetaFluor imaging software (Universal Imaging Corporation, Downing, PA, USA). Images were compared with identical image capture parameters. For purposes of clarity, some images are presented at different magnifications.

## **2.7. Pharmacological assays**

### **2.7.1. *[<sup>35</sup>S] GTP $\gamma$ S Binding Assay: Filtration***

[<sup>35</sup>S] GTP $\gamma$ S binding experiments were initiated by the addition 10  $\mu$ g of membranes expressing the receptor of interest to 800  $\mu$ l of assay buffer (20 mM HEPES, 10 mM MgCl<sub>2</sub>, 100 mM NaCl pH 7.4 supplemented with 10 mg/litre saponin and 10  $\mu$ M GDP) containing the given concentration of agonist. All reactions were performed in triplicates. After pre-incubation for 15 minutes at room temperature, 0.1 nM [<sup>35</sup>S] GTP $\gamma$ S was added and assays were incubated for a further 30 minutes at room temperature. The reactions were terminated by filtration of the samples onto GF/C fibre glass filters followed by three 4 ml washes of ice-cold 1 x T.E. buffer by a Brandel cell harvester. Three mls of scintillation fluid was added to the filters, the samples were vortexed and the bound [<sup>35</sup>S] GTP $\gamma$ S was measured by liquid-scintillation spectrometry. Data were analysed using GraphPad Prism software.

### **2.7.2. [<sup>35</sup>S] GTP $\gamma$ S Binding Assay: Scintillation proximity assay**

[<sup>35</sup>S] GTP $\gamma$ S binding assays were conducted at room temperature in a 384 well format. Membranes (1.5  $\mu$ g/point) were diluted to 0.3 mg/ml in assay buffer (20 mM HEPES, 10 mM MgCl<sub>2</sub>, 100 mM NaCl pH 7.4) supplemented with 30  $\mu$ g/ml saponin, GDP (10  $\mu$ M/point) and wheat germ agglutinin SPA beads (90  $\mu$ g/point) and allowed to pre-couple on a roller at room temperature for 30 minutes. The membrane and GDP mixture was then mixed with a 0.3 nM of [<sup>35</sup>S] GTP $\gamma$ S in a 1:1 mix. Then 10  $\mu$ l of the reaction was dispensed into a low volume 384 well plate using a Multidrop dispenser and the plates were sealed and centrifuged for one min at 200 g. Bound [<sup>35</sup>S] GTP $\gamma$ S was measured by scintillation counting on a ViewLux 1430 ultraHTS Microplate Imager (PerkinElmer). Data were analysed using GraphPad Prism (GraphPad Software).

### **2.7.3. Pre-treatment**

Monolayers of cells were treated with drug/vehicle for desired time. The reaction was stopped on ice and cells were then washed 3 times with ice cold 1 x PBS. Cells were harvested and membrane preparations were prepared as normal.

### **2.7.4. Data analysis**

Data were analysed using GraphPad Prism software. Concentration response curves for ligand effects on [<sup>35</sup>S] GTP $\gamma$ S binding were analysed by non-linear regression using a sigmoidal concentration/response relationship with a Hill coefficient of 1 to derive pEC<sub>50</sub> values. Where stated, data from at least 3 independent studies were grouped and the means  $\pm$  SEM was presented as per cent stimulation over basal, where the baseline values were normalised to 100 %. Where appropriate a one-way analysis of variance test followed by a Dunnett post test was completed.

### **3. Generation of tools to study regulation and desensitisation mechanisms of the nicotinic acid receptors**

#### **3.1. Introduction**

The molecular identification of receptors for nicotinic acid has provided the tools to further our knowledge of the mechanism of action of this lipid-modulating molecule. In order to study these GPCRs in various biochemical and pharmacological assays a range of tools were generated and assays were optimised.

##### **3.1.1. *Detection and visualisation of GPCRs***

Detection and visualisation of proteins using fluorescent and epitope tags have greatly facilitated the study of GPCR signalling pathways and localisation. The understanding of fluorescent proteins has come a long way since Shimomura and co-workers purified the green fluorescent protein (GFP) from the jellyfish, *Aequoria victoria* in the 1970s (Morise et al., 1974). Subsequent cloning and sequencing of the GFP gene by Prasher and co-workers (Prasher et al., 1992) and demonstration of its expression in *Escherichia coli* (*E.coli*) by Chalfie and his group (Chalfie et al., 1994) allowed its use in cellular assays including reporter gene assays. However, the use of fluorescent proteins has now become routine across many research disciplines and is no longer a novel technique reserved only for molecular biology laboratories.

Its popularity is mainly due to its fully functional fluorescent state, in a variety of expressions systems, without the need for any substrates or accessory proteins (Chalfie et al., 1994). The development of a wide range of variants of GFP, with distinct spectral properties, has also increased its appeal especially in the study of protein-protein interactions. Due to their relatively small size of 27 kDa, these fluorescent proteins have successfully been fused onto the C-terminus of many GPCRs without disrupting the ligand binding and signal transduction characteristics of the receptors (Milligan, 1999). The fluorescent fusion proteins can then simply be

visualised by confocal laser scanning or an epifluorescence microscope; or detected by immunoblotting with an antibody raised against the fluorescent protein.

Like fluorescent proteins epitope tags also serve as useful tools for studying GPCRs. The addition of short peptide sequences, usually added at the N- or C-terminus of a receptor, makes the protein immunoreactive to a known tag-specific antibody. This facilitates the detection of the protein by immunocytochemistry or immunoblotting without the need for receptor specific antibodies. This not only provides a cost effective and rapid method for protein detection but also avoids cross-reaction of the tag-specific antibody with proteins related to the protein of interest (Jarvik & Telmer, 1998). Again, due to their small size the tags are unlikely to affect the biochemical properties of the receptor of interest.

### **3.1.2. [<sup>35</sup>S] GTP $\gamma$ S binding assay**

The [<sup>35</sup>S] guanosine-5'-O-(3-thio) triphosphate (GTP $\gamma$ S) binding assay measures one of the earliest receptor-mediated events. Determining the binding of the poorly hydrolysable GTP-analogue [<sup>35</sup>S] GTP $\gamma$ S to G protein  $\alpha$  subunits measures the level of G protein activation as a result of agonist occupation of a GPCR. Figure 3.1 is a schematic diagram illustrating the principle of this assay, which was first practised in 1984 with purified  $\beta$ -adrenergic receptors (Asano et al., 1984). Binding of this cell impermeable nucleotide is now commonly performed using cell membranes, as described by (Hilf et al., 1989).

The aim of this chapter was to characterise a series of tagged receptor constructs, first in a transient and then in a stable expression system. In order to fully characterise the recombinant receptors the [<sup>35</sup>S] GTP $\gamma$ S binding assay was optimised to investigate the ability of the tagged receptor constructs to respond to nicotinic acid and display native pharmacology.

### 3.2. Optimisation of [<sup>35</sup>S] GTP $\gamma$ S binding

To allow an optimal signal to background window the [<sup>35</sup>S] GTP $\gamma$ S assay was optimised utilising CHO-K1 cell lines stably expressing the HM74A or HM74 receptor, generated by collaborators at GlaxoSmithKline (GSK), Harlow. The optimisation experiments were based around published conditions by this group (Wise et al., 2003). To allow a fair comparison between the experiments, a large membrane preparation was generated for each of the samples and aliquoted for use. Unless stated, HM74A and HM74 expressing membranes were incubated with 1 and 10 mM nicotinic acid respectively. Nicotinic acid was prepared in stock buffer and the pH was altered to pH 7 with potassium hydroxide. In each experiment a negative control of membranes prepared from parental CHO-K1 cells and a positive control of membranes prepared from HEK293 cells expressing the  $\alpha_{2A}$ -adrenergic receptor was also included. The  $\alpha_{2A}$ -adrenergic receptor was fused to the  $\alpha$  subunit of the pertussis toxin-sensitive G protein  $G\alpha_o$  which contained a mutation ( $C^{351I}$ ) making it insensitive to pertussis toxin.

To determine the optimum incubation time, this assay was set up as described in section 2.7.1 and incubated for 0.5, 1, 2 and 4 hours at room temperature. The assay was terminated by filtration of the samples onto GF/C fibre glass filters followed by 3 x 4 ml washes of ice-cold 1 x T.E buffer.

As expected, no increase in [<sup>35</sup>S] GTP $\gamma$ S binding to parental CHO-K1 membranes was observed in the presence of nicotinic acid. However an increase in [<sup>35</sup>S] GTP $\gamma$ S binding was observed in membranes expressing the  $\alpha_{2A}$ -adrenergic receptor and  $G\alpha_o$  fusion protein ( $\alpha_{2A}$ -adrenergic- $G\alpha_o^{C351I}$ ) in the presence of 1  $\mu$ M UK 14304, a known  $\alpha_2$ -adrenergic receptor agonist (Burt et al., 1998). With respect to membranes expressing the HM74A receptor, Figure 3.2 suggests that although [<sup>35</sup>S] GTP $\gamma$ S binding achieved a maximal level by the first time point assessed and did not vary subsequently in the presence of nicotinic acid, due to an increase in the basal binding of [<sup>35</sup>S] GTP $\gamma$ S in the absence of ligand, the longer incubation times reduced the signal to background window. Although the signal to background ratio for both the 0.5 and 1 hour incubation conditions was sufficient for further analysis, the 0.5 hour

time point was chosen for further experiments as it was also the time point published by Wise and co-workers for this particular cell line (Wise et al., 2003).

Varying concentrations (5, 10, 40 and 100  $\mu\text{M}$ ) of guanosine diphosphate (GDP) were then tested for their effect on [ $^{35}\text{S}$ ] GTP $\gamma$ S binding on HM74A expressing membranes. A reduction in basal [ $^{35}\text{S}$ ] GTP $\gamma$ S binding values in the presence of increasing GDP concentration was observed in Figure 3.3. The largest signal to background window was observed in conditions with 10 and 5  $\mu\text{M}$  GDP. 10  $\mu\text{M}$  GDP was chosen for further experiments as this was also the GDP concentration published by collaborators in GSK (Wise et al., 2003). A  $\text{pEC}_{50}$  value of  $6.2 \pm 0.1$  M for nicotinic acid was calculated from concentration response curves utilising 10  $\mu\text{M}$  GDP (Figure 3.4).

Three amounts of HM74A expressing membranes (5, 10, and 15  $\mu\text{g}$ ) were tested to determine the optimal signal to background window for this assay. Increasing amounts of protein, as expected, resulted in higher levels of [ $^{35}\text{S}$ ] GTP $\gamma$ S binding both in the presence and absence of the ligand. Although a suitable signal to background was seen in all conditions, a significant increase in [ $^{35}\text{S}$ ] GTP $\gamma$ S binding over basal was observed in samples containing 10  $\mu\text{g}$  of membranes (Figure 3.5), and therefore 10  $\mu\text{g}$  of protein was utilised for further [ $^{35}\text{S}$ ] GTP $\gamma$ S binding experiments. This was also the protein amount utilised by collaborators at GSK (Wise et al., 2003).

Utilising the optimised conditions established for HM74A expressing CHO-K1 cells, a nicotinic acid concentration response curve was employed to test the response of nicotinic acid at HM74 (Figure 3.6). Nicotinic acid has been described as a low potency ligand at HM74 (Wise et al., 2003). Due to practical limitations, accurate  $\text{pEC}_{50}$  values can not be calculated in such cases, however  $\text{pEC}_{50}$  values can be estimated from the available data. In this case, a  $\text{pEC}_{50}$  value in excess of  $2.9 \pm 0.2$  M was estimated for nicotinic acid.

### **3.3. Generation of tagged receptor constructs**

To allow detection and visualisation of the nicotinic acid receptors, epitope and fluorescent protein tagged recombinant receptors were generated and cloned into a pcDNA3 plasmid. This plasmid is routinely utilised for expression of recombinant

proteins in mammalian cells. It allows efficient expression of proteins of interest under the control of the human cytomegalovirus (CMV) promoter. Amongst features shared with other plasmids it carries an ampicillin antibiotic resistance gene for selection in *E.coli* bacteria and a neomycin antibiotic resistance gene for selection of stable transfects in mammalian cells (Figure 3.7 A).

Nucleotides encoding the eleven amino acid sequence (YTDIEMNRLGK ) for the epitope VSV-G, from the vesicular stomatitis virus glycoprotein, (Kreis, 1986), were introduced by PCR at the 5' end of cDNA encoding both the HM74 and HM74A receptors. The appropriate human cDNA template was utilised. HM74 and HM74A are highly homologous with only 20 base differences at the cDNA level – mainly at the 3' region (Wise et al., 2003). Therefore the same forward primer sequence was utilised for both receptors. The forward primer was designed to introduce a 6 base pair Kozak sequence to the 5' of the VSV-G tag to enhance translation of the protein (Kozak, 1987). The primer also incorporated a Hind III recognition sequence; this introduced the restriction site at the extreme 5' end of the receptor cDNA sequence to aid cloning of the receptor into expression plasmids. To allow primer recognition, 18 bases of the nicotinic acid receptor cDNA sequence minus the ATG start codon were also incorporated into the primer. To allow efficient binding and digestion by the endonuclease, primers were designed with extra bases before the sequence for the restriction site. The reverse primer was designed to introduce a Kpn I restriction site at the 3' end of the receptor cDNA sequence; again extra bases were added after the restriction site sequence to allow efficient digestion of the receptor. Primer sequence information is summarised in Table 3.1.

The resulting VSV-G tagged receptor cDNA was then sub-cloned into a pcDNA3 plasmid already engineered to contain the sequence for enhanced yellow fluorescent protein (eYFP) as shown in Figure 3.7 B. Enhanced (e) YFP is a red-shifted GFP variant with an excitation maximum of 500 nm and an emission maximum of 535 nm.

### **3.4. Characterisation of receptor constructs**

The receptor constructs were then sequenced and tested to confirm that the addition of the epitope tag and fluorescent protein did not have any adverse effects on the

biochemical properties of the receptors. The receptors were transiently transfected into HEK293 and CHO-K1 cells. Introduction of the receptor constructs into the host cell lines will result in the expression of a fusion protein containing the VSV-G epitope and eYFP tagged nicotinic acid receptor. Therefore expression of this receptor can be detected by determining the fluorescence from the eYFP fusion protein in the cells by direct visualisation by imaging or by immunoblotting techniques. The presence of the VSV-G epitope tag can also be detected by these methods however an immunostaining step would be required to visualise the VSV-G tag by imaging techniques.

### **3.4.1. *Detection of recombinant receptor constructs***

Membrane preparations of the transfected HEK293 and CHO-K1 cells were prepared. The samples were resolved by SDS-PAGE and immunoblotted with anti VSV-G and anti GFP antisera as described in chapter 2.5.5. The anti GFP antiserum is able to detect eYFP as eYFP differs from GFP by only one amino acid. Figure 3.8, is an immunoblot of receptor constructs transiently transfected into HEK293 host cells. A VSV-G antibody positive control employed an N-terminally tagged CXCR2 (VSV-G CXCR2) receptor. A negative control of the untransfected parental cell line was also included. The VSV-G CXCR2 receptor was detected only in the anti VSV-G blot, at the expected approximate size of 36 kDa and at around 70 kDa. This larger protein is approximately the size at which the VSV-G CXCR2 homodimer would be expected. The calculated molecular mass of the VSV-G HM74A eYFP and VSV-G HM74 eYFP receptors was approximately 66 and 68 kDa respectively. Both were detected with anti VSV-G and anti GFP antisera. Compared to the VSV-G HM74A eYFP receptor, a very faint band at the expected size was detected for the VSV-G HM74 eYFP receptor. As equal amounts of protein samples were resolved this suggested this receptor was expressed at a lower level. Subsequently, to confirm published data that HM74 lacks N-linked glycosylation sites near the N-terminus (Nomura et al., 1993), membranes expressing recombinant nicotinic acid receptors were treated with N-Glycosidase-F. Again, VSV-G CXCR2 receptor was utilised as a control for the treatment because this receptor is known to be N-glycosylated (Wilson et al., 2005). In samples treated with N-Glycosidase-F, a single polypeptide was detected instead of a doublet at around 35 kDa. There was no change in the pattern of proteins observed

for the recombinant nicotinic acid receptors. This suggests both nicotinic acid receptors are not N-glycosylated or if so, the glycosylation is not susceptible to cleavage by this enzyme. As expected, no immunoreactive proteins were detected in the parental negative control sample. Similar observations were made when the nicotinic acid receptor constructs were transiently expressed in CHO-K1 cell lines (data not shown).

### **3.4.2. Localisation studies**

Detection of the VSV-G epitope and eYFP tagged forms of the nicotinic acid receptors in the membrane preparations by immunoblot suggest the tags have not interfered with the translation. Characteristically GPCRs are expressed at the plasma membrane with an extracellular N-terminus and intracellular C-terminal domain. This allows the receptors to transduce extracellular signals via intracellular messengers. To explore if the tagged nicotinic acid receptor constructs were delivered to the plasma membrane, a cell surface ELISA assay was adopted to detect cell surface expression of the receptors in intact cells. The N-terminal VSV-G tag was utilised in this assay as it would only be detected by an anti VSV-G antibody if expressed at the extracellular surface. Again, the receptor constructs were transiently transfected into a HEK293 cell line. Parental HEK293 cells were included as a negative control. When compared to the background signal detected from parental HEK293 cells the signal observed from cells expressing VSV-G HM74A eYFP receptors was significantly higher ( $P < 0.01$ ). Although the signal detected from cells expressing VSV-G HM74 eYFP receptors was slightly higher when compared to the signal detected in HEK293 cells, it was not significant in a one-way analysis of variance test (Figure 3.9).

The receptors were initially visualised utilising the eYFP tag by confocal imaging. Figure 3.10 A, is a representative image obtained of the VSV-G HM74A eYFP receptor transiently expressed in HEK293 cells. An expression pattern consistent with cell surface expression was observed. A similar expression pattern was also observed when this experiment was repeated in CHO-K1 cells (Figure 3.10 B). Figure 3.10 B demonstrates the ability of the VSV-G epitope tag to be detected by immunocytochemistry techniques. Although a similar expression pattern was also observed for VSV-G HM74 eYFP, due to the very low expression following transient

expression it was not possible to obtain high quality images. Taken together with the data obtained from the cell surface ELISA assay, it can be summarised that HM74A was expressed at the plasma membrane.

### **3.5. Generation and characterisation of CHO-K1 cell lines stably expressing recombinant nicotinic acid receptors**

Epitope and fluorescent protein tagged versions of the nicotinic acid receptors were transfected into CHO-K1 cells using DOTAP, see section 2.4.8.1. The transfected cells were then exposed to G418 antibiotic selection, as described in chapter 2.4.8.1, resulting in the identification of clones that were resistant to the antibiotic and hence potentially expressing the recombinant receptor. Stable expression should allow consistent expression levels of the recombinant nicotinic acid receptors and therefore also consistency between experiments. CHO-K1 cells were chosen due to their robust nature and also to allow comparison with the existing CHO-K1 cell lines stably expressing the untagged nicotinic acid receptors described in section 3.2. As this method of generating cell lines stably expressing the protein of interest relies upon random integration of the cDNA into the genomic DNA of individual CHO-K1 cells, clonal selection of the cells was necessary to generate a population of cells with the same genetic background.

#### **3.5.1. Screening and localisation studies**

As mentioned above, transfection and therefore random integration takes place at a cellular level. Therefore the expression of a protein in each cell is dependent on the transfection efficiency and site of recombination. It is accepted that all cells treated with a transfection agent will not have been successfully transfected. Also, it is possible that in a successfully transfected cell, the cDNA of the receptor may not be integrated in a transcriptionally active locus.

For this reason, following clonal selection by G418, at least 20 clones per cell line were initially tested by confocal microscopy for expression of eYFP and hence the

recombinant receptor. Clones where no eYFP fluorescence was detected were disregarded. From the remaining clones, although some showed intracellular receptor expression, as seen in Figure 3.11 A, seven clones for VSV-G HM74A eYFP demonstrated expression patterns indicative of substantial cell surface expression, Figure 3.11 B. As mentioned earlier, GPCRs are typically expressed at the cell surface. For this reason from the clones displaying predominantly cell surface expression, three clones displaying similar levels of fluorescence were chosen for further examination (Figure 3.11 C). However, only one clone expressing the VSV-G HM74 eYFP receptor was identified (Figure 3.12). Although this clone displayed both cell surface and intracellular expression, due to a lack of choice, this clone was selected and analysed further.

### **3.5.2. Detection of recombinant receptor constructs**

Cell lysates prepared from the chosen clones were resolved by SDS-PAGE and immunoblotted to detect the VSV-G epitope and eYFP tags as described in section 3.4.1. A protein polypeptide of the expected size representing the recombinant HM74A or HM74 receptor was detected in all three clones expressing the VSV-G HM74A eYFP receptor (Figure 3.13) and the only identified clone expressing the VSV-G HM74 eYFP receptor (Figure 3.14).

### **3.5.3. Functional analysis**

The ability of the modified receptors stably expressed in CHO-K1 cell lines to respond to nicotinic acid was tested in a [<sup>35</sup>S] GTP $\gamma$ S binding assay. Membrane preparations expressing the modified HM74 and HM74A receptors were incubated with 1 and 10 mM nicotinic acid respectively. An increase in [<sup>35</sup>S] GTP $\gamma$ S binding over basal was observed for all cell lines and for both receptors (Figure 3.15 A). In nicotinic acid concentration response curves, pEC<sub>50</sub> values comparable to the native nicotinic acid receptors were calculated for all clones expressing VSV-G HM74A eYFP (Figure 3.15 B). Clone B5:16 was chosen for further studies of the VSV-G HM74A eYFP receptor. Due to a low signal to background window and eventual loss of expression of the VSV-G HM74 eYFP receptor, clone D1:12 was disregarded.

### **3.6. Generation of Flp-In CHO-K1 cell lines stably expressing the recombinant nicotinic acid receptors**

As mentioned above, a loss of expression of the VSV-G HM74 eYFP receptor was observed in the only clone identified with expression of this receptor. Due to an extremely low transfection and recombination efficiency experienced with this receptor it was decided to make use of the Flp-In CHO-K1 cell line marketed by Invitrogen. In this cell line a single stably integrated Flp recombinase target (FRT) site has been engineered into a transcriptionally active genomic locus of the CHO-K1 cell line. Complementary (c) DNA of the protein of interest is delivered via a pcDNA5/FRT/T0 expression vector. When transfected together with a Flp recombinase vector, pOG44, it allows targeted homologous recombination as opposed to random integration relied upon in conventional methods of generating cell lines stably expressing proteins of interest. In theory, this should produce an isogenic cell line without the need for clonal selection. A Flp-In CHO-K1 was generated for each of the modified nicotinic acid receptors as described in the chapter 2.4.9.

#### **3.6.1. Localisation, detection and functional analysis**

Direct visualisation of eYFP fluorescence using a fluorescence microscope confirmed receptor expression and localisation indicative of plasma membrane expression (Figure 3.16 A). As before both the VSV-G epitope and eYFP tags were detected by immunoblotting (Figure 3.16 B). Membranes expressing either the VSV-G HM74A eYFP or the VSV-G HM74 eYFP receptors were tested to confirm their response to nicotinic acid in [<sup>35</sup>S] GTP $\gamma$ S binding assays as described before (Figure 3.17). In nicotinic acid concentration response curves, pEC<sub>50</sub> values obtained were comparable to those obtained with the native nicotinic acid receptors. The Flp-In CHO-K1 cell line stably expressing the VSV-G HM74 eYFP receptor was utilised for further experiments.

### 3.7. Receptor expression

Data presented so far suggests that VSV-G HM74 eYFP is expressed at a lower level compared to VSV-G HM74A eYFP following transient expression. Due to the low affinity of HM74 for nicotinic acid, binding studies to quantitatively study receptor numbers was not feasible. For this reason, to measure and compare the relative receptor levels between the CHO-K1 cell line stably expressing VSV-G HM74A eYFP and the Flp-In CHO-K1 cell line stably expressing VSV-G HM74 eYFP, eYFP fluorescence of lysates prepared from the two cell lines was measured using a Victor<sup>2</sup> plate reader (Figure 3.18). Fluorescence measurements obtained for the VSV-G HM74A eYFP receptor were double that for the VSV-G HM74 eYFP receptor.

To examine receptor expression at the cell surface in these cell lines, cell surface biotinylation experiments were utilised as described in chapter 2.5.9. Both cell lines were treated with EZ-Link Sulfo-NHS-SS biotin to label the  $\epsilon$ -amine of lysine residues of proteins expressed at the cell surface. These cells were then lysed and streptavidin beads, which have a high affinity for biotin, were used to pulldown the biotinylated proteins. Biotinylated samples eluted from the beads were then analysed by immunoblotting with an anti VSV-G antibody to detect receptor specific proteins. As only receptors at the cell surface can be biotinylated this assay allowed comparison of cell surface expression of the recombinant nicotinic acid receptors.

Figure 3.19, is an immunoblot comparing cell surface expression of the modified receptors. For each of the receptors three samples were analysed. The samples in lane 1 are aliquots of cell lysates equalised for protein content and represent the total receptor population. An aliquot of the supernatant was also saved after the pulldown step. This sample containing unbound receptor is represented in lane 2. It is difficult to conclude if this represents the intracellular receptor population or unbound biotinylated receptor. However it is likely to be a combination of both. Samples in lane 3 represent the biotinylated receptors present at the cell surface. Both VSV-G HM74A eYFP and VSV-G HM74 eYFP were detected at the anticipated size in all three samples, confirming cell surface expression of these receptors. However, a more intense signal was detected in samples representing biotinylated VSV-G HM74A eYFP compared to the signal corresponding to the biotinylated VSV-G HM74 eYFP.

As protein content of the samples were equalised, this supports the observation that VSV-G HM74 eYFP receptors are expressed at a lower level at the cell surface.

### **3.8. Generation of Flp-In TREx CHO-K1**

The Flp-In TREx system has been developed by Invitrogen to allow control over the expression of a protein from cDNA stably integrated into a cell line (Figure 3.20). It is based on the Flp-In system and has been described on many occasions to express one protein of interest constitutively while the expression of another protein of interest, delivered to the Flp-In locus, is controlled by the experimenter (Lane et al., 2007; Milasta et al., 2006). This system allows the study of two different proteins in the same cell line with the added benefit of control of expression of the inducible protein.

In a Flp-In TREx cell line a Tet repressor gene is stably cloned into the host cell genome. The gene of interest is introduced into the cell line via a pcDNA5/FRT/T0 expression vector and its expression is controlled by the human CMV promoter. In the absence of tetracycline or doxycycline (a tetracycline derivative) the gene encoding the Tet repressor is translated and the resulting protein binds to the Tet operator inserted into the CMV promoter. This represses the expression of the gene of interest. To express the gene of interest, tetracycline or doxycycline is introduced. This then binds strongly to the Tet repressor causing it to undergo a conformational change and therefore unable to bind to the Tet operator.

Invitrogen have developed this system for a number of cell types including HEK293 cells. However, the Flp-In TREx system is not commercially available in a CHO-K1 cell background. Invitrogen supply the materials claimed to allow the generation of this tetracycline regulated expression system in any cell line. With an aim to allow comparison between all cell lines it was decided to generate this system in CHO-K1 cells so studies could be conducted to analyse any interactions between the highly homologous nicotinic acid receptors.

### **3.8.1. Strategy A**

In order to generate the Flp-In TREx system in the CHO-K1 cell line, a pcDNA6/TR regulatory vector expressing high levels of the tetracycline repressor was introduced into the Flp-In CHO-K1 cells stably expressing the VSV-G HM74 eYFP and VSV-G HM74A eYFP receptors (described in section 3.7). These transfected cells were then placed on 200 µg/ml hygromycin and 5 µg/ml blasticidin antibiotic selection to select for cells expressing both the receptor and repressor respectively. The inducible system was tested by analysing the expression of the receptors (by confocal analysis of eYFP fluorescence) in the presence and absence of 1 µg/ml doxycycline. In the absence, of doxycycline treatment the repressor should be active and therefore no receptor eYFP expression should be visualised. However, after a 24 hour doxycycline induction receptor expression is expected in a successful inducible system.

Five clones expressing the VSV-G HM74A eYFP receptor were tested. However, none of these cell lines displayed the characteristics of an inducible cell line. Receptor expression was observed in non-induced and induced cells at similar levels (Figure 3.21). However, out of the eight clones tested for the VSV-G HM74 eYFP expressing cells no receptor expression was detected in doxycycline treated or non-treated cells (Figure 3.22).

### **3.8.2. Strategy B**

In another attempt to make a Flp-In TREx CHO-K1 cell line, the tetracycline repressor was transfected into parental Flp-In CHO-K1 cells. The transfected cells were then placed on zeocin and blasticidin antibiotic selection in accordance with Invitrogen's guidelines. Twenty clones were then screened to identify those with stable expression of the tetracycline repressor. Recombinant HM74A receptor cDNA was transiently transfected into all the clones and fluorescence of the eYFP was visualised in doxycycline treated and non-treated cells. Although receptor expression was observed in control and induced cells (data not shown), the clone displaying the lowest basal levels and highest inducible levels of VSV-G HM74A eYFP receptor expression was chosen to generate two cell lines stably expressing the tagged HM74

or HM74A receptors. Again, VSV-G HM74A eYFP expression was not inducible (data not shown) and no VSV-G HM74 eYFP expressing clones were identified.

### 3.9. Discussion

The recent identification of the nicotinic acid receptors as molecular targets for nicotinic acid therapy has opened up many opportunities for understanding the mechanisms by which it successfully lowers total plasma levels of cholesterol. This may allow further understanding of the pathways involved in the side effects associated with nicotinic acid use, as well the potential for developing more novel and potent drugs. Generating cell lines and developing assays to facilitate our understanding of the molecular pharmacology of these receptors was a major objective of this study.

In this chapter, the optimisation of the [<sup>35</sup>S] GTP $\gamma$ S binding assay has been described for the HM74 and HM74A nicotinic acid receptors stably expressed in CHO-K1 cells. These cell lines were chosen as they expressed the unmodified, wild type receptor proteins and therefore the data obtained from the optimisation experiments could be compared with published data. As noted earlier, collaborators at GSK (Harlow) generated these cell lines and published the conditions used in a [<sup>35</sup>S] GTP $\gamma$ S scintillation proximity assay (SPA) (Wise et al., 2003). Although the principles of this assay are the same, industry favours this low volume high throughput system to enable high throughput screening. The details of this assay have been described in section 2.7.2. The optimisation experiments were based around published data by Wise and co-workers. The optimised conditions of 10  $\mu$ g membranes, 10  $\mu$ M GDP and an incubation time of 30 minutes time were similar to the published conditions. With respect to the GDP concentration, Lorenzen and co-workers have reported maximum agonist-induced increases in [<sup>35</sup>S] GTP $\gamma$ S were observed at 10  $\mu$ M GDP for assays studying these receptors (Lorenzen et al., 2001). As high concentrations of GDP have been reported to reduce agonist affinity (Lorenzen et al., 2001), the lower GDP concentration of 10  $\mu$ M was especially important for the low affinity HM74 receptor. The pEC<sub>50</sub> value for nicotinic acid at HM74A was in agreement with published data (Lorenzen et al., 2001; Wise et al., 2003; Tunaru et al., 2003). Due to

the low potency of nicotinic acid at HM74, it is not possible to calculate accurate pEC<sub>50</sub> values. However, the estimated pEC<sub>50</sub> values were in the mM range described in published studies (Lorenzen et al., 2001; Wise et al., 2003; Tunaru et al., 2003).

Technical difficulties have to be overcome when studying recently identified receptors where protein specific antibodies are not available. For this reason recombinant receptor constructs expressing the VSV-G epitope and eYFP tags were generated for each of the receptors. However, the introduction of N- and C-terminal modifications to GPCRs can potentially impact receptor function. Although, the N-terminal VSV-G epitope tag is not close to the predicted ligand binding sites of the nicotinic acid receptors, formed by transmembrane helices (TMH) II, III and VII (Tunaru et al., 2005), the C-terminal region of GPCRs are often important in regulating receptor endocytosis and G protein interactions. Therefore the addition of a fluorescent protein to the C-terminal region of HM74 or HM74A can potentially alter its regulation or pharmacology.

To rule out any detrimental effects of the tagging, the recombinant receptors were first characterised in transient then stable expression systems. Plasma membrane expression of the receptor was confirmed by confocal analysis, cell surface ELISA and biotinylation studies. In [<sup>35</sup>S] GTPγS binding studies the pEC<sub>50</sub> values obtained for the tagged receptors were comparable to those for the untagged receptors and also the published data. Data presented in this chapter, suggest that the pharmacological properties of the nicotinic acid receptors are not disrupted by the presence of the N- and C-terminal tags.

From the studies conducted, it has become apparent that the VSV-G HM74 eYFP receptor is difficult to transfect into cells; low transfection efficiency together with very low expression made this receptor difficult to work with. Due to very low expression of VSV-G HM74 eYFP in a transient system it was difficult to collect data about the effects of the tags on this receptor. Even in the presence of antibiotic selection pressure during the generation of a CHO-K1 cell line stably expressing this receptor, only one clone expressing VSV-G HM74 eYFP was identified. Unfortunately this clone lost expression of the receptor at an early stage. More success was experienced when a Flp-In CHO-K1 cell line was utilised for stable

expression. Characterisation experiments in this cell line confirmed cell surface expression and native pharmacology.

Due to the very low affinity of HM74 for nicotinic acid, receptor numbers could not be quantified by binding experiments (Taggart et al., 2005; Wise et al., 2003). However, relative receptor levels between the modified HM74 and HM74A expressing cell lines were compared by measuring the eYFP fluorescence in cell lysates prepared from each of the cell lines. Although VSV-G HM74 eYFP was expressed at a lower level compared to VSV-G HM74A eYFP, there were sufficient expression levels for receptor detection and receptor activation studies. The relative expression levels are consistent with literature reporting lower expression of HM74 than HM74A in human adipocytes (Semple et al., 2006).

In order to study both modified HM74 and HM74A receptors together in the same cell line it was decided to make use of the well documented inducible Flp-In TREx system (Milasta et al., 2006; Lane et al., 2007). As noted, this system was not available in a CHO-K1 cell background. With the aim to keep the cell backgrounds for all the cell lines stably expressing the nicotinic acid receptors constant, two independent attempts were made to generate the Flp-In TREx system in CHO-K1 cells. On both occasions a successful inducible system was not achieved. Researchers in Unilever, Netherlands have also experienced problems with generating a Flp-In TREx CHO-K1 cell line (personal communication, Dr. K. Wieland). As this system is available to purchase in a number of cell lines, it is surprising that Invitrogen do not have a Flp-In TREx system for one of the most routinely used cell lines. It may be this particular cell line poses inherent technical difficulties that make it difficult to generate a successful inducible system.

The data shown in this chapter confirm that the N- and C-terminal modified nicotinic acid receptors stably expressed in a CHO-K1 cell background do not possess different pharmacological properties to the untagged receptors.

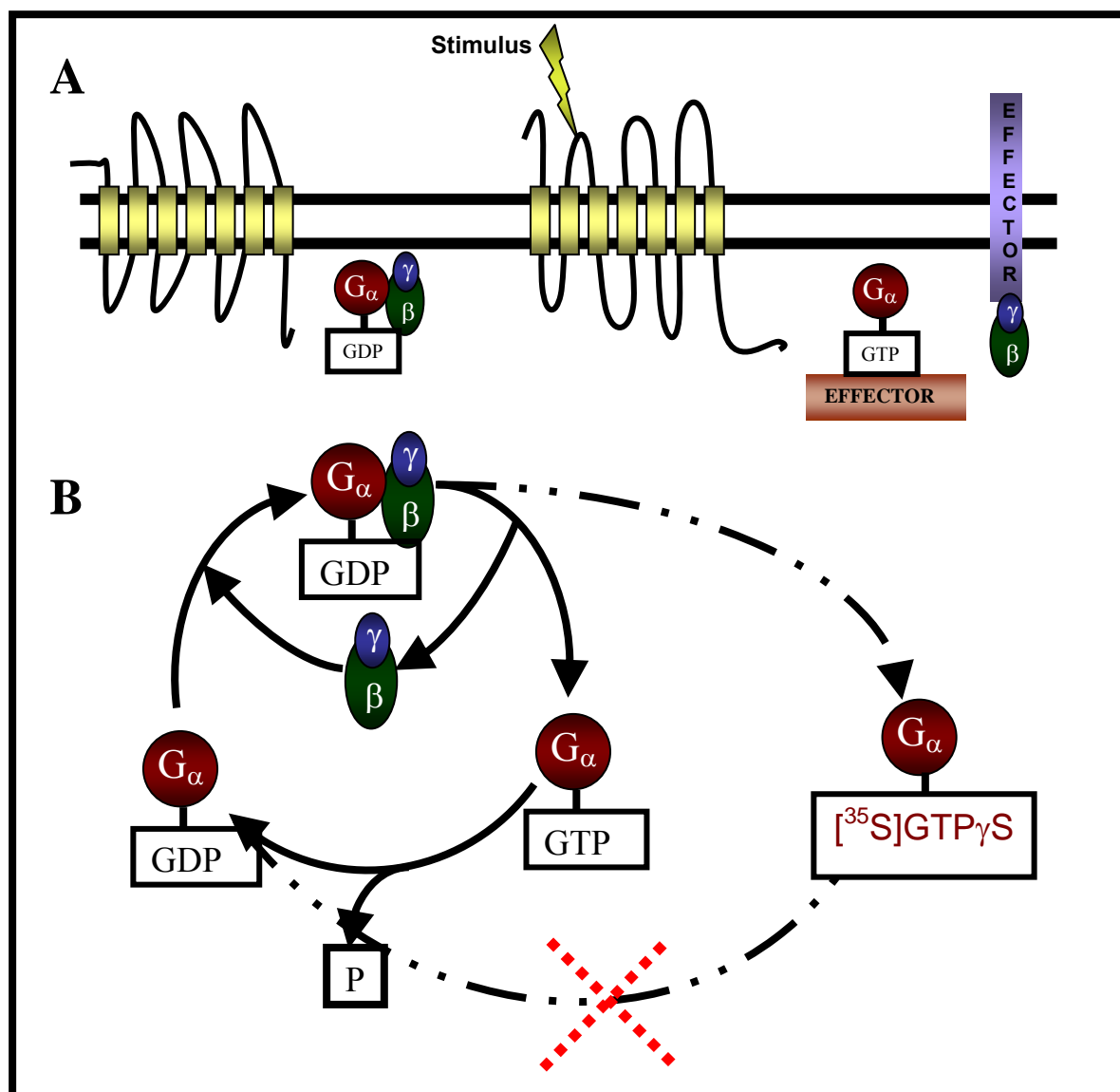


**Figure 3.1 Schematic diagram illustrating the principle of the [<sup>35</sup>S] GTP $\gamma$ S assay**

**A:** In the inactive state the GDP bound G protein  $\alpha$  ( $G\alpha$ ) subunit associates with the  $\beta/\gamma$  complex to form an inactive heterotrimeric G protein. Upon ligand activation the GPCR undergoes a conformational change resulting in increased affinity for the G protein; this results in the exchange of GDP for GTP on the  $G\alpha$  subunit, which reduces the affinity of the  $G\alpha$  subunit for the  $\beta/\gamma$  complex and therefore leads to dissociation of the heterotrimeric G protein. Both the  $G\alpha$  subunit and the  $\beta/\gamma$  complex can then interact with effectors, transducing the signal. **B:** The activated state lasts until the GTP is hydrolysed to GDP by the intrinsic GTPase activity of the  $G\alpha$  subunit. This assay measures the ligand induced activation of the  $G\alpha$  subunit by using a radiolabelled analogue of GTP, [<sup>35</sup>S] GTP $\gamma$ S. The binding of the poorly hydrolysable [<sup>35</sup>S] GTP $\gamma$ S to the  $G\alpha$  subunit can then be measured by liquid-scintillation spectrometry.

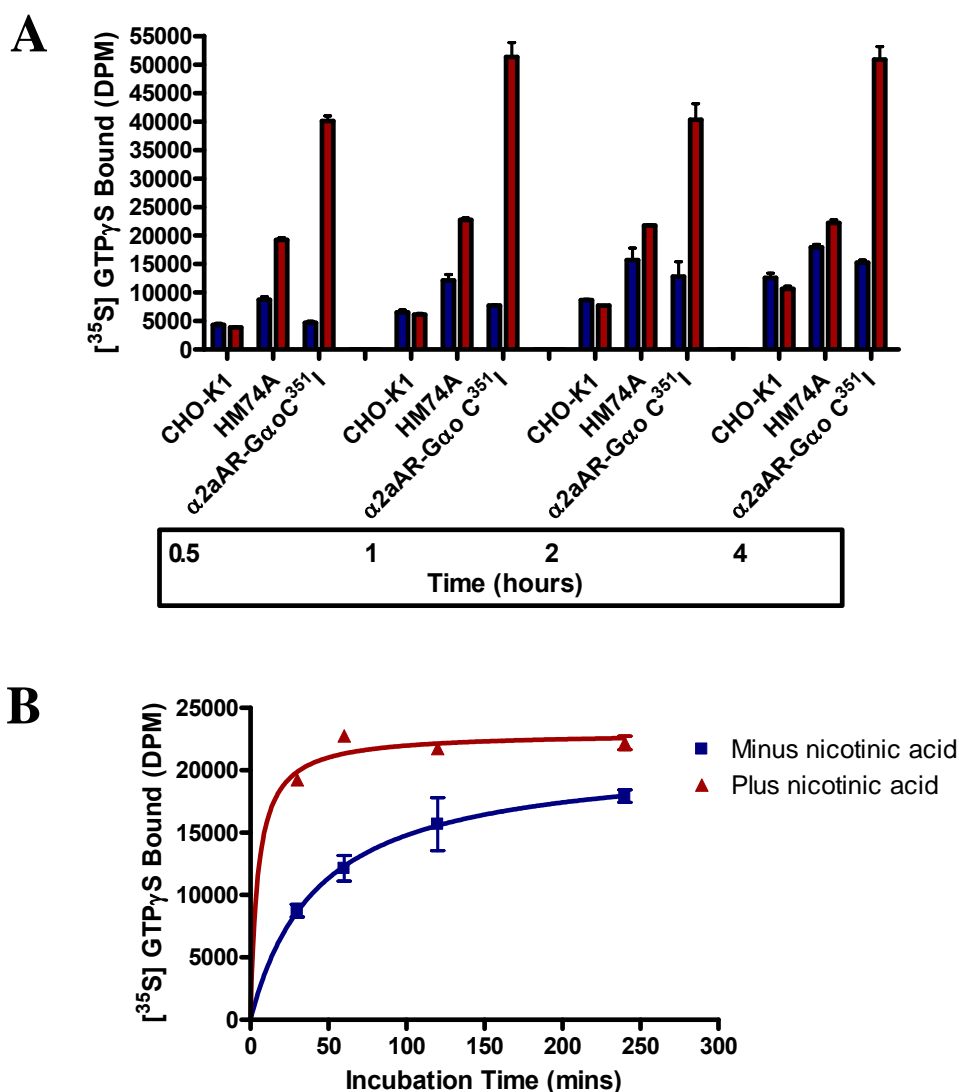
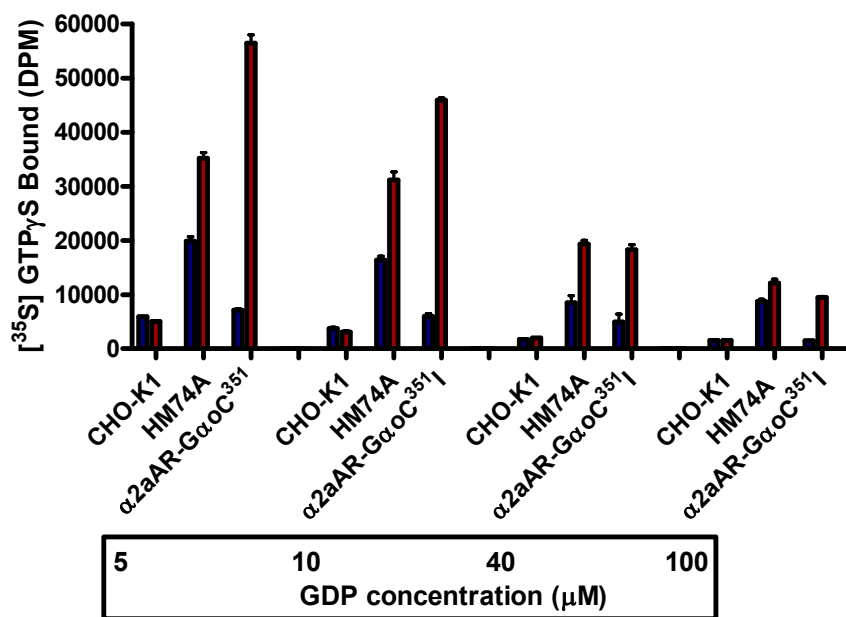


**Figure 3.2** Optimisation of [<sup>35</sup>S] GTP<sub>γ</sub>S assay: Incubation time

10 μg of CHO-K1 membranes stably expressing HM74A were incubated in the presence (red) and absence (blue) of 1 mM nicotinic acid in a [<sup>35</sup>S] GTP<sub>γ</sub>S assay. Assays were incubated for 0.5, 1, 2 and 4 hours at room temperature. Membranes prepared from parental CHO-K1 cells were utilised as a negative control and were incubated with (red) or without (blue) 1 mM nicotinic acid. HEK293 membranes expressing α<sub>2A</sub>-adrenergic-Gα<sub>o</sub><sup>C3511</sup> served as a positive control and were incubated with (red) or without (blue) 1 μM UK 14304. Assays were terminated by filtration of the samples onto GF/C fibre glass filters. Bound [<sup>35</sup>S] GTP<sub>γ</sub>S was measured by liquid-scintillation spectrometry. Assays were performed in triplicate and are representative of three experiments. Data points represent means ± SEM. **A:** Binding of [<sup>35</sup>S] GTP<sub>γ</sub>S. **B:** HM74A expressing membranes.

**A**



**B**

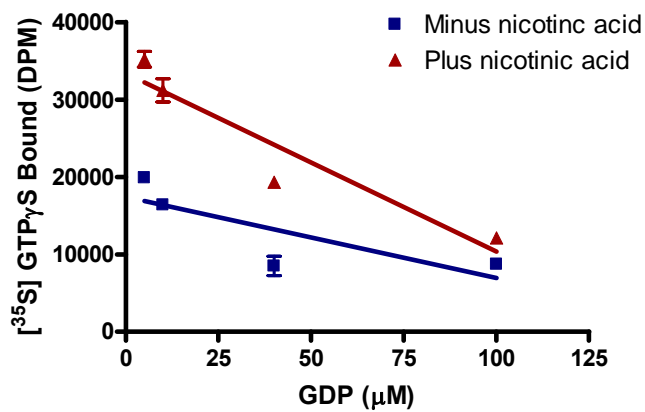


**Figure 3.3 Optimisation of [<sup>35</sup>S] GTP $\gamma$ S assay: GDP concentration**

GDP concentrations of 5, 10, 40 and 100  $\mu$ M were tested using 10  $\mu$ g of HM74A expressing CHO-K1 membranes in a [<sup>35</sup>S] GTP $\gamma$ S assay. Membranes were incubated with (red) or without (blue) 1 mM nicotinic acid for 30 minutes at room temperature. A negative control of membranes generated from parental CHO-K1 cells were incubated with (red) or without (blue) 1 mM nicotinic acid. HEK293 membranes expressing  $\alpha_{2A}$ -adrenergic-G $\alpha_o^{C351}$  were utilised as a positive control and were incubated in the presence (red) and absence (blue) of 1  $\mu$ M UK 14304. Assays were terminated by filtration of the samples onto GF/C fibre glass filters. Bound [<sup>35</sup>S] GTP $\gamma$ S was measured by liquid-scintillation spectrometry. Experiments were performed in triplicate and data points represent means  $\pm$  SEM. Data shown is representative of three experiments. **A:** Binding of [<sup>35</sup>S] GTP $\gamma$ S. **B:** HM74A expressing membranes. A reduction in the binding of [<sup>35</sup>S] GTP $\gamma$ S was observed in the presence of increasing concentrations of GDP.

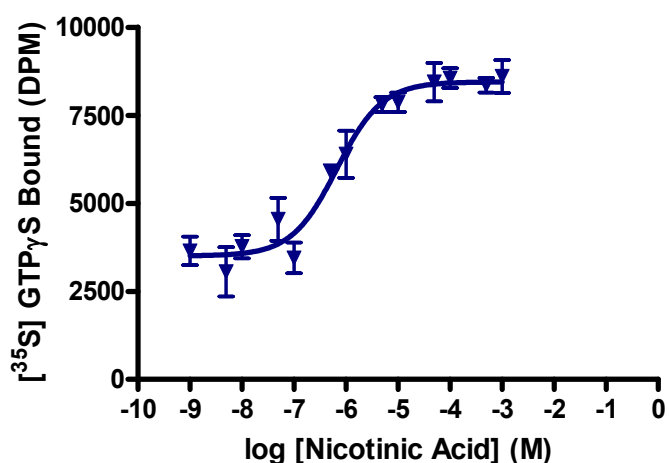
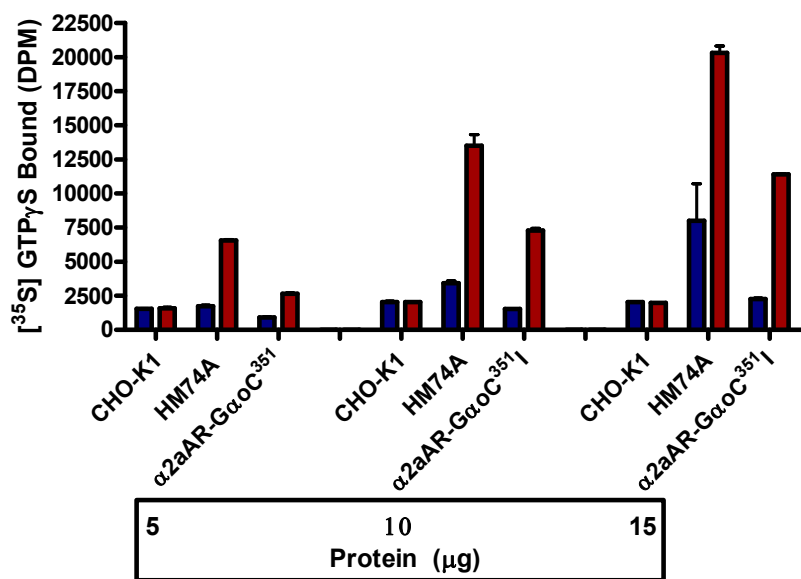


**Figure 3.4 Optimisation of [<sup>35</sup>S] GTP<sub>γ</sub>S assay: Nicotinic acid concentration response curve utilising optimised GDP concentration**

A nicotinic acid concentration response curve was employed using 10  $\mu$ g of HM74A expressing CHO-K1 membranes in a [<sup>35</sup>S] GTP<sub>γ</sub>S assay containing 10  $\mu$ M GDP. Following 30 minutes incubation at room temperature the assay was terminated by filtration of the samples onto GF/C fibre glass filters. Bound [<sup>35</sup>S] GTP<sub>γ</sub>S was measured by liquid-scintillation spectrometry.  $pEC_{50} = 6.2 \pm 0.1$  for nicotinic acid was calculated. Experiments were performed in triplicate and data were analysed using GraphPad Prism software. Data points represent means  $\pm$  SEM from a single experiment, representative of three independent experiments.

**A**



**B**

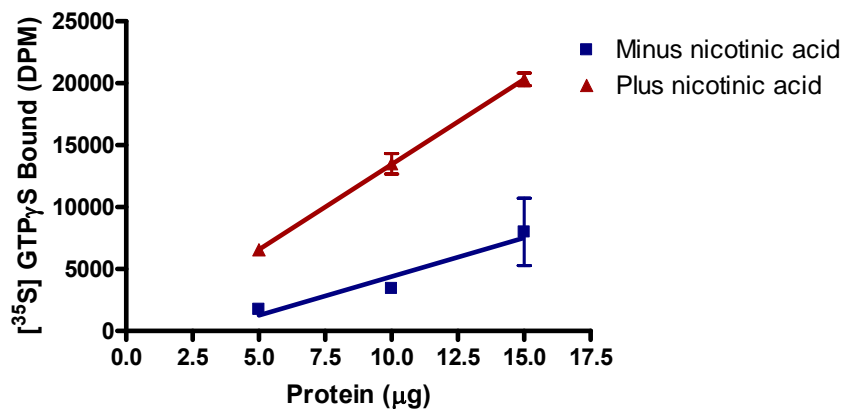


**Figure 3.5 Optimisation of [<sup>35</sup>S] GTP $\gamma$ S assay: Protein amount**

The optimal protein amount was determined by testing 5, 10 and 15  $\mu$ g of HM74A expressing CHO-K1 membranes in a [<sup>35</sup>S] GTP $\gamma$ S assay containing 10  $\mu$ M GDP. The membranes were incubated in the presence (red) or absence (blue) of 1 mM nicotinic acid for 30 minutes at room temperature. Membranes prepared from parental CHO-K1 cells were utilised as a negative control and were incubated as HM74A expressing membranes.  $\alpha_{2A}$ -adrenergic-G $\alpha_o^{C351}$  expressing HEK293 membranes were incubated with (red) or without (blue) 1  $\mu$ M UK 14304 and were utilised as a positive control. Assays were terminated by filtration of the samples onto GF/C fibre glass filters and bound [<sup>35</sup>S] GTP $\gamma$ S was measured by liquid-scintillation spectrometry. Assays were performed in triplicate and data points represent means  $\pm$  SEM, representative of three experiments. **A:** Binding of [<sup>35</sup>S] GTP $\gamma$ S. **B:** HM74A expressing membranes. An increase in the binding of [<sup>35</sup>S] GTP $\gamma$ S was observed in the presence of increasing protein amount.

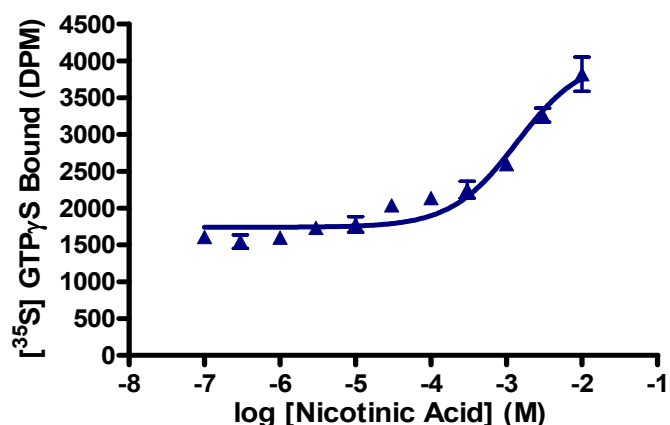
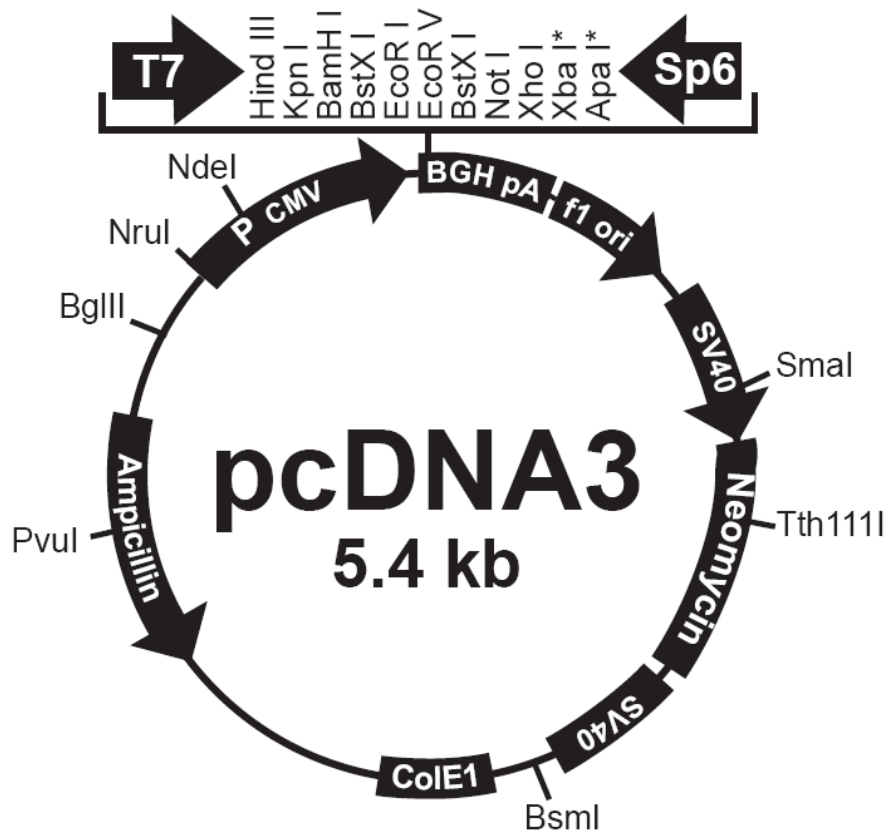


**Figure 3.6 Nicotinic acid concentration response curve: HM74**

A nicotinic acid concentration response curve was set up to test the response of nicotinic acid at HM74 stably expressed in CHO-K1 cells utilising the optimised conditions. Following 30 minutes incubation at room temperature the assay was terminated by filtration of the samples onto GF/C fibre glass filters and bound [<sup>35</sup>S] GTP<sub>γ</sub>S was measured by liquid-scintillation spectrometry.  $pEC_{50} = 2.9 \pm 0.2$  for nicotinic acid was estimated. Experiments were performed in triplicate and data were analysed using GraphPad Prism software. Data points represent means  $\pm$  SEM from a single experiment, representative of three independent experiments.

**A**



**B**



**Figure 3.7 Schematic map of pcDNA3 vector and schematic diagram of the HM74 and HM74A receptor constructs generated**

**A:** pcDNA3 has been engineered to contain a multiple cloning site comprising DNA sequences recognised by the restriction enzymes detailed in the map. This allows introduction of a cDNA sequence of interest which is expressed under the control of the human cytomegalovirus (CMV) promoter. Amongst other features, it carries an ampicillin antibiotic resistance gene for selection in *E.coli* bacteria and a neomycin antibiotic resistance gene for selection of stable transfects in mammalian cells. (pcDNA3 map, Invitrogen) **B:** The VSV-G epitope tag was engineered at the 5' region of the HM74 and HM74A cDNAs by PCR. The Hind III and Kpn I restriction sites also generated by PCR, at the indicated sites, were utilised for sub-cloning the epitope tagged receptors into a pcDNA3 expression vector already possessing eYFP cDNA sequence.

Primer	cDNA template	Introduce	Sequence
Forward	HM74 or HM74A	<i>Hind III</i> restriction site  <i>Kozak sequence</i>  VSV-G epitope tag  At 5' end	5' GTA CGT CCA AGC <b>TTG CCA CCA TGT ACA</b> <b>CCG ATA TCG AAA TGA</b> <b>ACC GCC TTG GTA AGA</b> ATC GGC ACC ATC TGC AG 3'
Reverse	HM74	<i>Kpn I</i> restriction site  At 3' end	5' GTA CGT CCG <b>GTA</b> <b>CCA</b> GGA GAG GTT GGG CCC AG 3'
Reverse	HM74A	<i>Kpn I</i> restriction site  At 3' end	5' GTA CGT CCG <b>GTA</b> <b>CCC</b> TCG ATG CAA CAG CCC AAC TG 3'

**Table 3.1 Primer sequences**

Primer sequences designed to introduce the *Hind III* restriction site and VSV-G epitope at the 5' end and the *Kpn I* restriction site at the 3' end of human HM74 and HM74A receptor cDNA.

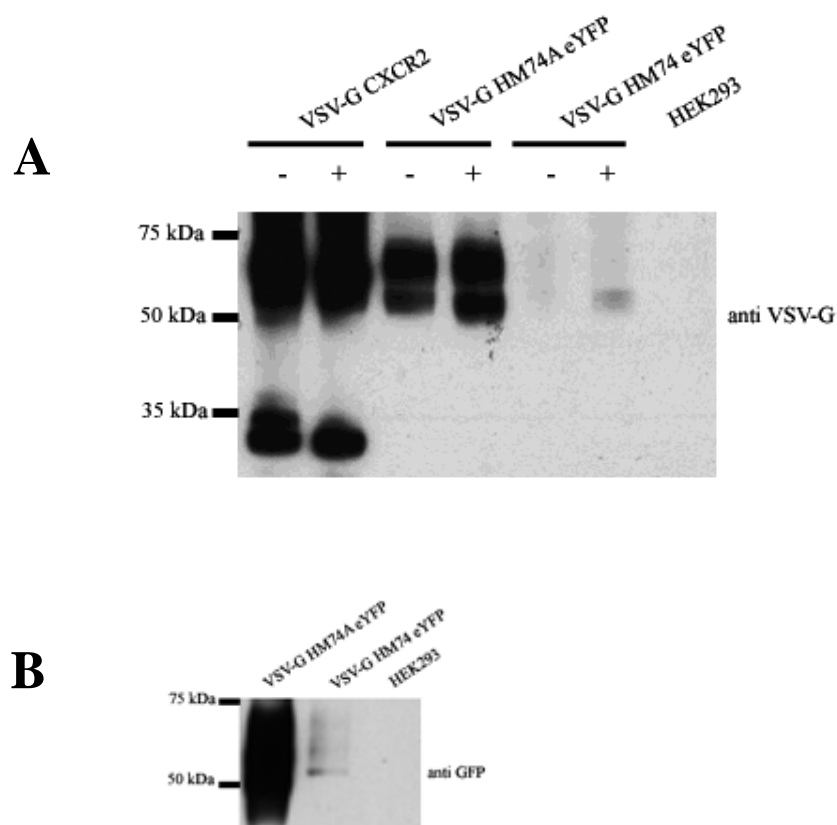


**Figure 3.8 Immunoblot detecting VSV-G epitope and eYFP-tagged forms of the nicotinic acid receptors**

VSV-G HM74A eYFP and VSV-G HM74 eYFP cDNAs were transiently transfected separately into HEK293 cells. 10  $\mu$ g of membrane preparations prepared from each were resolved by SDS-PAGE and immunoblotted to detect the VSV-G (**A**) and eYFP (**B**) tags. A VSV-G antibody positive control used VSV-G CXCR2 receptor expressed in HEK293 cells and detected a band at the expected size of 36 kDa. A negative control of the untransfected parental cell line was also included. VSV-G HM74A eYFP was detected by both anti VSV-G and anti GFP antisera at its anticipated size of 66 kDa. VSV-G HM74 eYFP was also detected by both antisera at around 68 kDa but a weak signal was detected, suggesting lower expression of this receptor. **A**: N-Glycosidase-F treatment (+) of membranes expressing recombinant nicotinic acid receptors did not alter the pattern of proteins detected compared with samples not treated with N-Glycosidase-F (-). VSV-G CXCR2 receptor was utilised as a positive control for N-Glycosidase-F treatment. Results shown are of a single experiment, representative of three individual experiments.

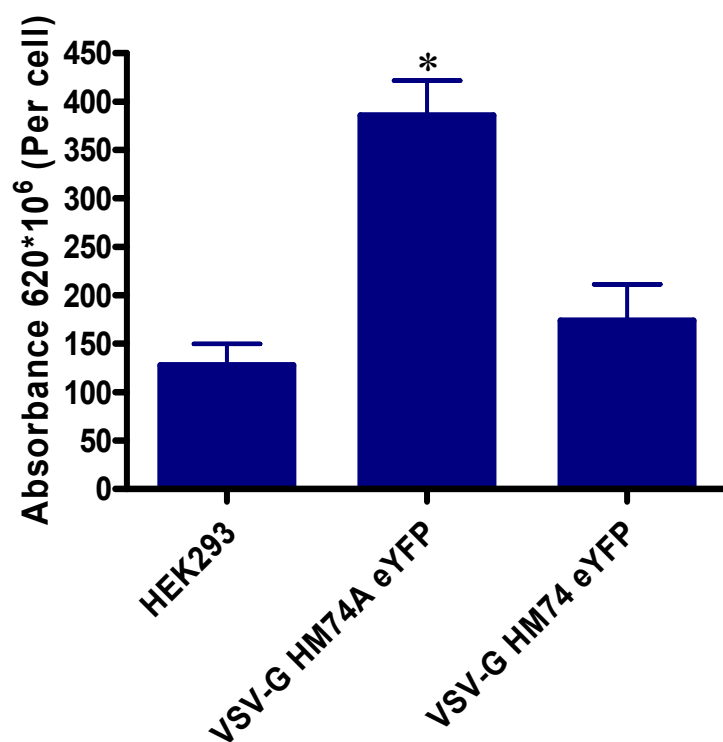
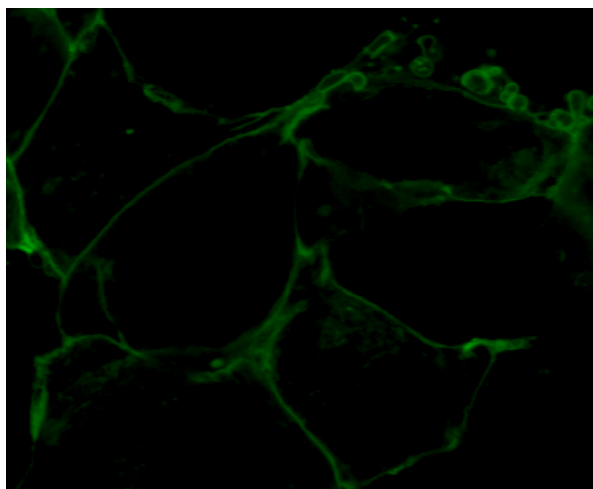


**Figure 3.9 Cell surface receptor measurement by ELISA**

Cell surface expression of the recombinant nicotinic acid receptors was measured in transiently transfected HEK293 cells in a whole cell ELISA assay utilising an anti VSV-G antibody. A negative control of the parental HEK293 cell line was included. When compared to parental HEK293 cells, the signal detected from HEK293 cells expressing VSV-G HM74A eYFP was significantly higher (\* =  $P < 0.01$ ). The signal detected from HEK293 cells expressing VSV-G HM74 eYFP was not significantly different in a one-way analysis of variance test ( $p > 0.05$ ). Data points represent means  $\pm$  SEM. Results are representative of three independent experiments.

**A**



**B**

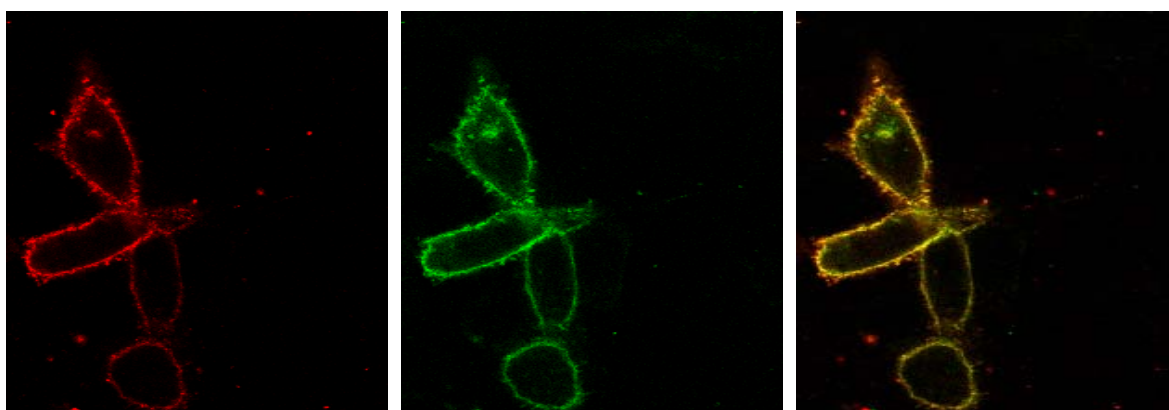


**Figure 3.10 Localisation of VSV-G HM74A eYFP receptors**

VSV-G HM74A eYFP cDNA was transiently transfected into (A) HEK293 and (B) CHO-K1 cells. (A) HEK293 cells expressing VSV-G HM74A eYFP receptor were directly visualised for eYFP fluorescence (green) by confocal imaging. (B) Detection by confocal imaging of the VSV-G tag (red) in permeabilised and immunostained cells, direct visualisation of eYFP fluorescence (green) and a merge of the two images (yellow).

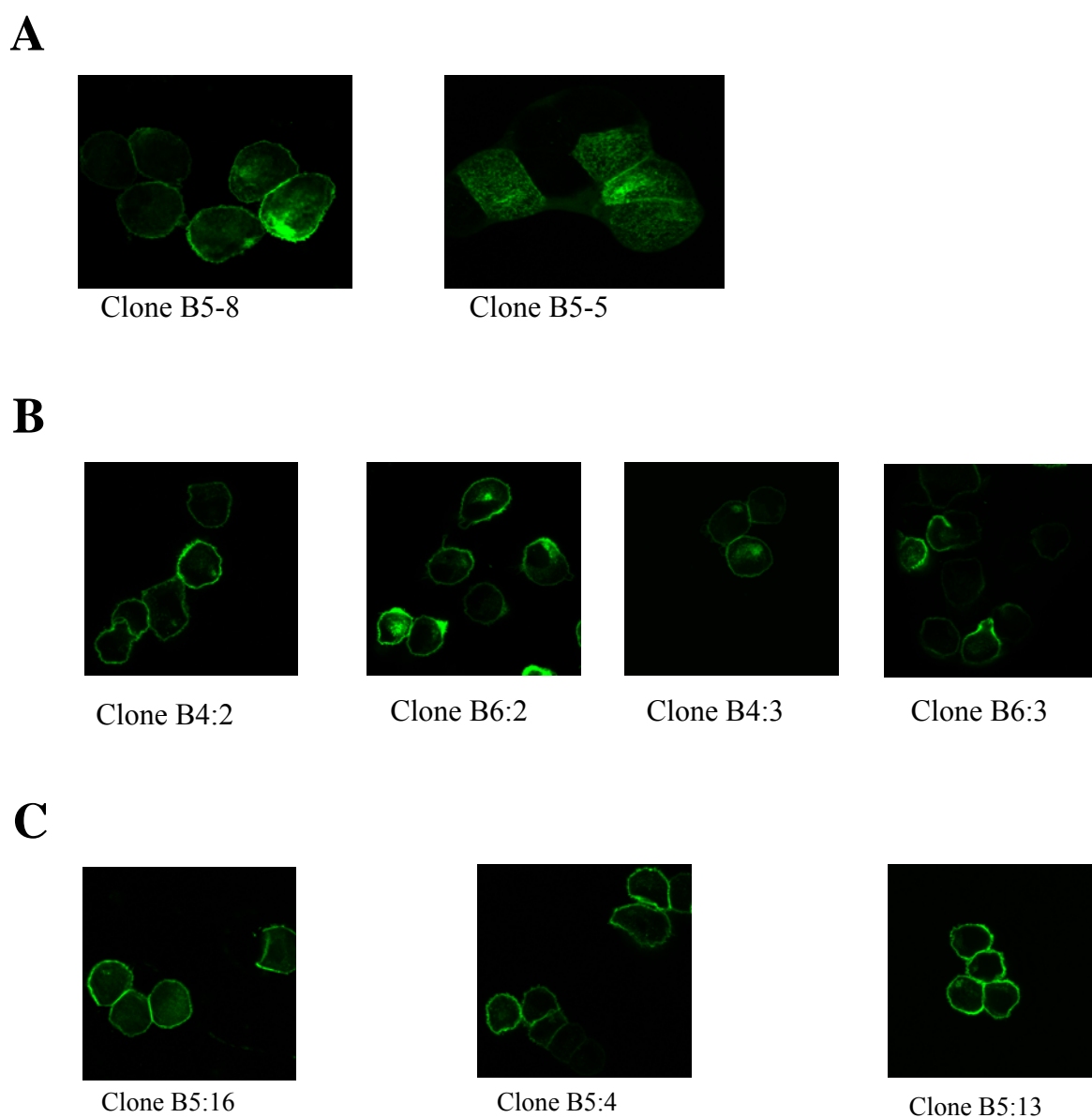
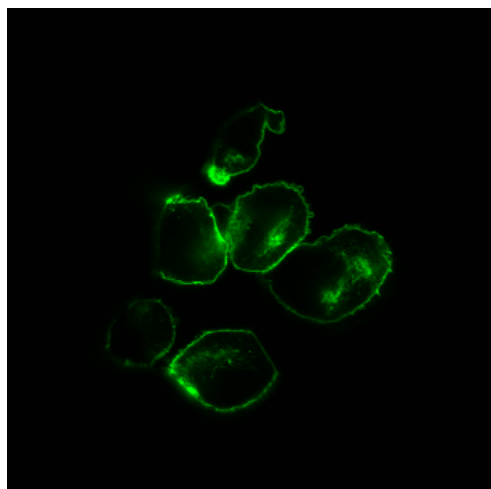


**Figure 3.11 Identification of CHO-K1 cell lines stably expressing the VSV-G HM74A eYFP receptor**

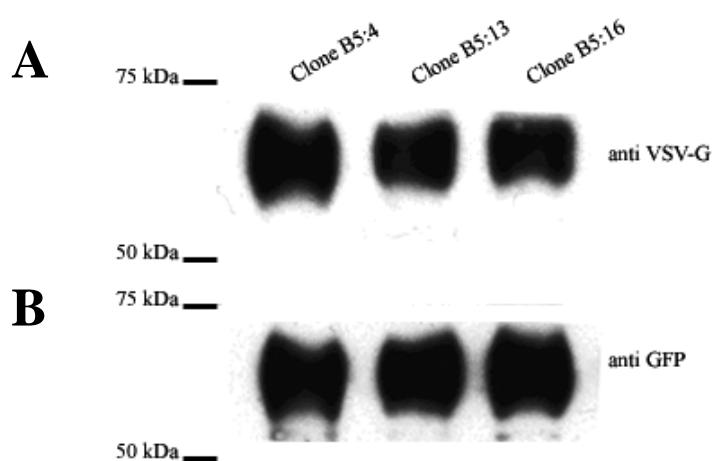
CHO-K1 cells were transfected with VSV-G HM74A eYFP cDNA and subjected to G418 antibiotic selection. Clones resistant to G418 antibiotic selection were screened by direct visualisation by confocal imaging utilising the eYFP tag to identify VSV-G HM74A eYFP expression. **A**: These two images are representative of clones that were disregarded due to intracellular receptor expression. **B** and **C**: Representative of clones with cell surface receptor localisation. **C**: Clones chosen for further analysis.



Clone D1:12

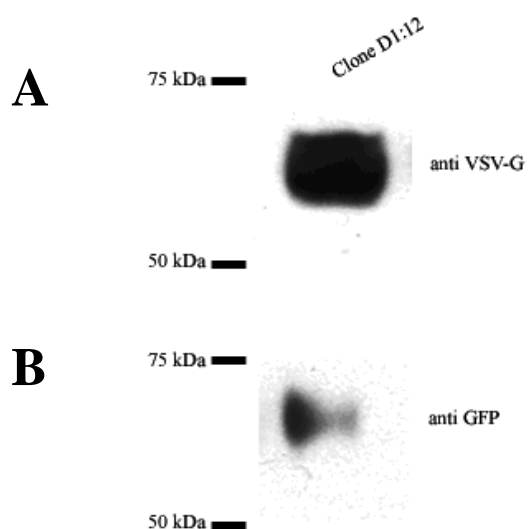
**Figure 3.12 Identification of a CHO-K1 cell line stably expressing the VSV-G HM74 eYFP receptor**

CHO-K1 cells were transfected with VSV-G HM74 eYFP cDNA and placed under G418 antibiotic selection. Clones resistant to G418 antibiotic selection were screened by direct visualisation by confocal imaging utilising the eYFP tag to identify VSV-G HM74 eYFP expression. Only one clone expressing VSV-G HM74 eYFP was identified and therefore analysed further.



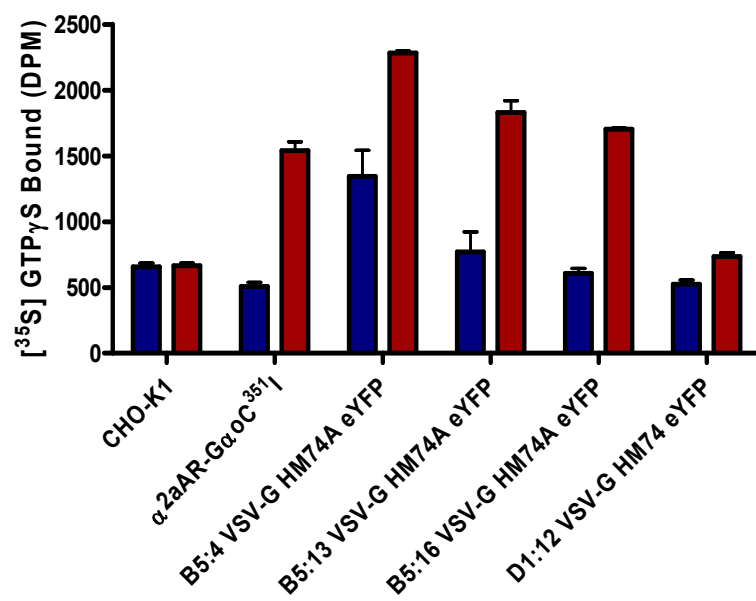
**Figure 3.13 Detection of VSV-G and eYFP tagged forms of the HM74A receptor stably expressed in CHO-K1 cells**

The three clones described in Figure 3.11 stably expressing VSV-G HM74A eYFP were compared to confirm receptor expression and detection of tags. 20  $\mu$ g of cell lysates prepared from these clones were resolved by SDS-PAGE and immunoblotted with anti VSV-G (**A**) and anti GFP (**B**) antibodies. Protein bands representing the tagged receptor were detected at the anticipated size in immunoblots against the VSV-G tag and eYFP protein in each clone.



**Figure 3.14 Detection of VSV-G and eYFP tagged forms of the HM74 receptor stably expressed in CHO-K1 cells**

20  $\mu$ g of cell lysates prepared from cells stably expressing VSV-G HM74 eYFP (described in figure 3.12) were resolved by SDS-PAGE and immunoblotted to detect the VSV-G (**A**) and eYFP (**B**) tags. In each immunoblot, protein bands representing the VSV-G HM74 eYFP receptor were detected at the expected size.

**A****B**

Clone	Nicotinic acid
	pEC <sub>50</sub>
B5:4	6.3 ± 0.1
B5:13	6.6 ± 0.1
B5:16	6.3 ± 0.2

**Figure 3.15 Functional analysis of CHO-K1 cell lines stably expressing modified versions of the nicotinic acid receptors**

[<sup>35</sup>S] GTPγS binding assays were employed to test the response of tagged nicotinic acid receptors to nicotinic acid. The assays were terminated after 30 minutes at room temperature by filtration of the samples onto GF/C fibre glass filters. Bound [<sup>35</sup>S] GTPγS was measured by liquid-scintillation spectrometry. **A:** Modified HM74A and HM74 were incubated in the presence (red) and absence (blue) of 1 and 10 mM nicotinic acid respectively. Membranes prepared from parental CHO-K1 cells were utilised as a negative control and were incubated with (red) or without (blue) 10 mM nicotinic acid. Membranes expressing α<sub>2A</sub>-adrenergic-Gα<sub>o</sub><sup>C351</sup> served as a positive control and were incubated with (red) or without (blue) 1 μM UK 14304. **B:** Nicotinic acid concentration response curves (final concentrations ranging from 1 nM to 1 mM) on the tagged HM74A receptors (summary of pEC<sub>50</sub> values). Results shown are of an individual experiment and are representative of three individual experiments. Data were analysed using GraphPad Prism software. Data points represent means ± SEM.

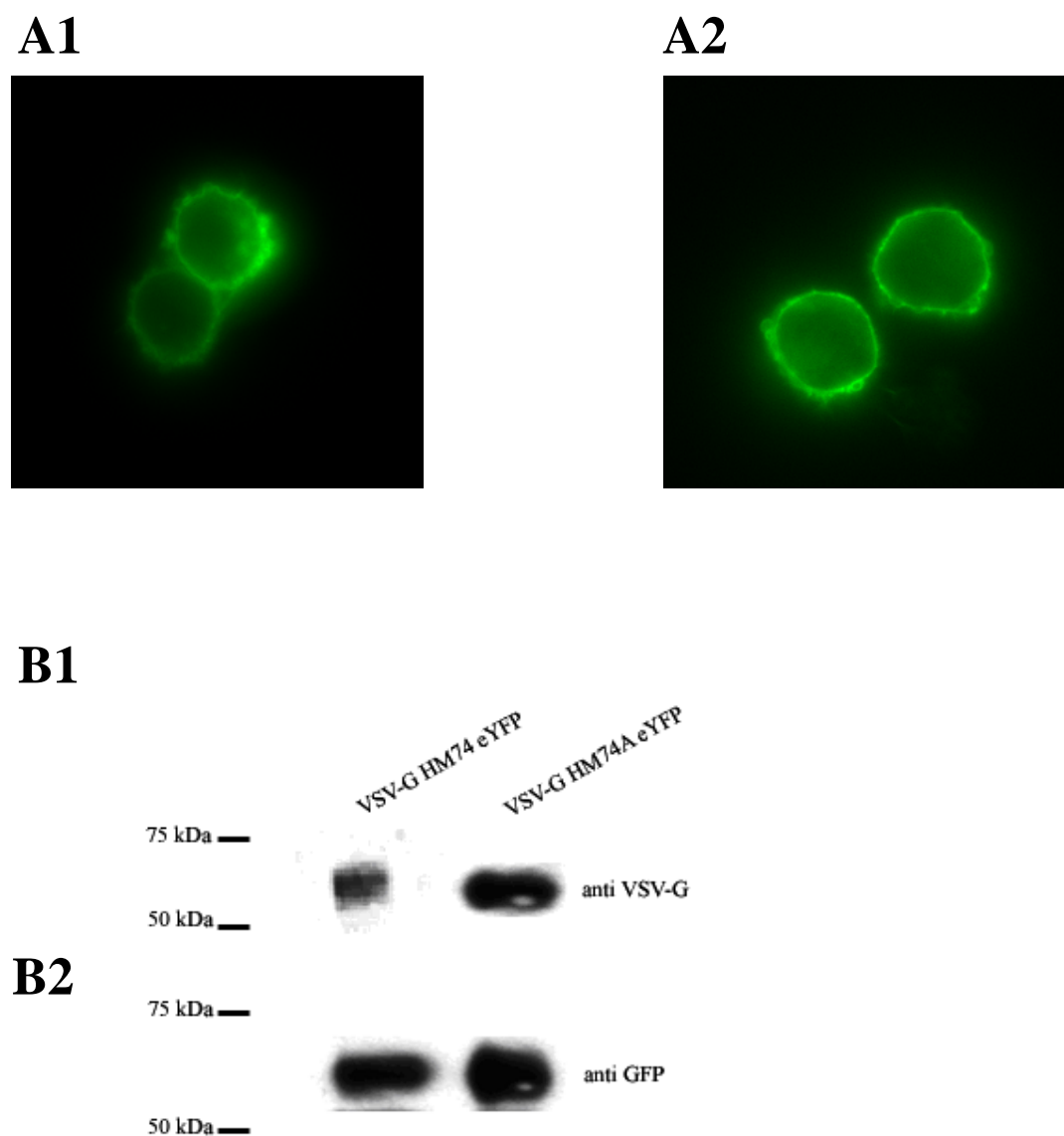
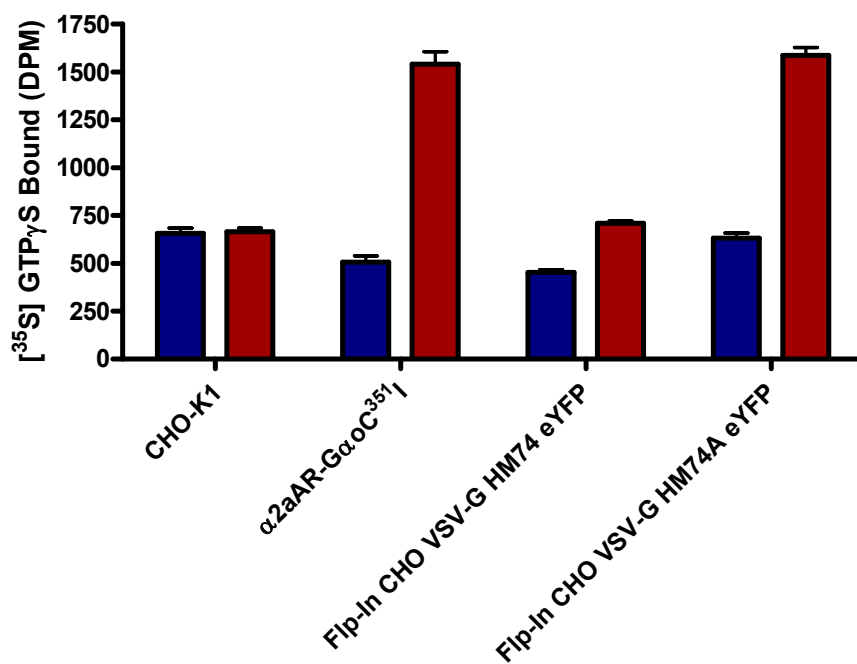


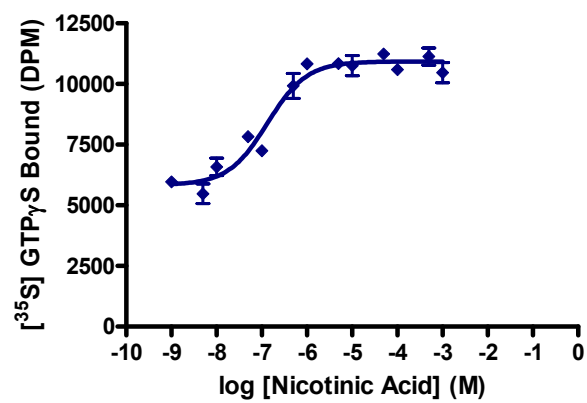
**Figure 3.16 Localisation and detection of modified nicotinic acid receptors stably expressed in Flp-In CHO-K1 cells**

Flp-In CHO-K1 cells were transfected with VSV-G HM74A eYFP or VSV-G HM74 eYFP cDNA and placed under 200  $\mu\text{g/ml}$  hygromycin selection. For each transfected cell line, cells resistant to hygromycin antibiotic selection were pooled and screened by direct visualisation by fluorescence imaging utilising the eYFP tag to identify receptor expression (**A**). VSV-G epitope and eYFP tagged forms of the HM74 (**A1**) and HM74A (**A2**) receptors. **B**: 20  $\mu\text{g}$  of cell lysates prepared from these cells were resolved by SDS-PAGE. Proteins representing the modified receptors were detected at the expected size, in immunoblots against the VSV-G tag (**B1**) and eYFP (**B2**) protein.

**A**



**B1**



**B2**

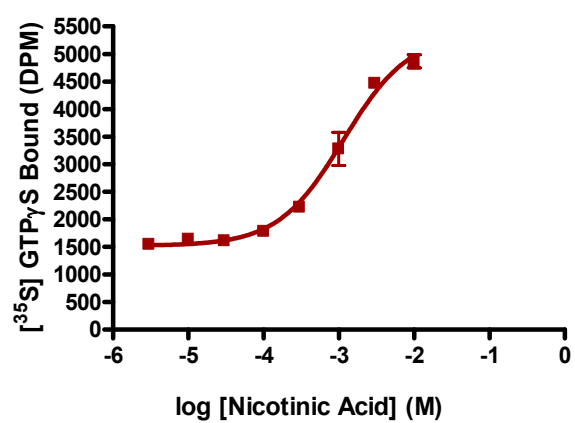


**Figure 3.17 Functional analysis of Flp-In CHO-K1 cell lines stably expressing recombinant nicotinic acid receptors**

**A:** [<sup>35</sup>S] GTPγS binding assays were employed to test the response of the tagged nicotinic acid receptors to nicotinic acid. **A:** Modified HM74A and HM74 were stimulated with 1 and 10 mM nicotinic acid respectively. Membranes prepared from parental CHO-K1 cells were utilised as a negative control and were incubated with (red) or without (blue) 10 mM nicotinic acid. Membranes expressing α<sub>2A</sub>-adrenergic-Gα<sub>o</sub><sup>C351</sup> served as a positive control and were incubated with (red) or without (blue) 1 μM UK 14304. The assays were terminated after 30 minutes incubation at room temperature by filtration of the samples onto GF/C fibre glass filters. Bound [<sup>35</sup>S] GTPγS was measured by liquid-scintillation spectrometry. **B:** Nicotinic acid concentration response curves on the tagged **(B1)** HM74A (pEC<sub>50</sub> = 6.9 ± 0.1) and **(B2)** HM74 (pEC<sub>50</sub> = 2.9 ± 0.1) receptors. Results shown are representative of three individual experiments. Data were analysed using GraphPad Prism software. Data points represent means ± SEM.

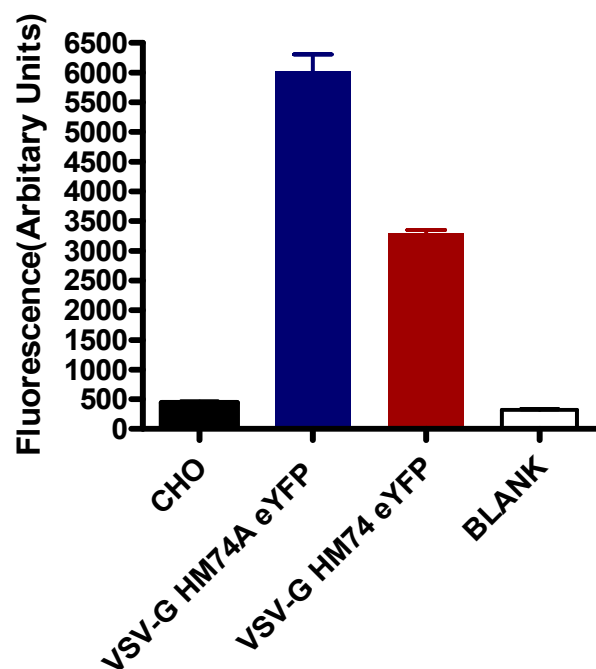


**Figure 3.18 VSV-G HM74A eYFP expression compared to VSV-G HM74 eYFP**

Whole cell lysates prepared from CHO-K1 and Flp-In CHO-K1 cell lines stably expressing either the modified HM74A or HM74 receptor, respectively, were equalised for protein concentration and the eYFP fluorescence was measured with a Victor<sup>2</sup> plate reader. Negative controls of lysates prepared from parental CHO-K1 cells and a reading from an empty well (labelled blank) were also included. VSV-G HM74A eYFP stably expressed in CHO-K1 cells has a higher expression level than VSV-G HM74 eYFP stably expressed in a Flp-In CHO-K1.

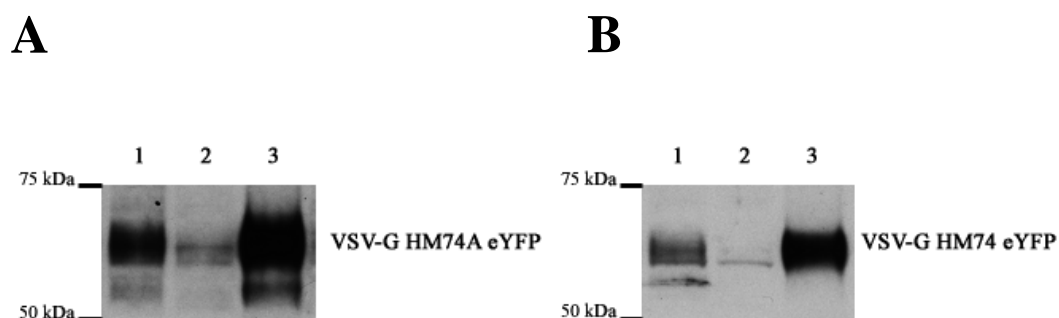


**Figure 3.19 Biotin labelling of cell surface expressed nicotinic acid receptors**

Cell lines stably expressing VSV-G HM74A eYFP (CHO-K1 background) or VSV-G HM74 eYFP (Flp-In CHO-K1 background) were treated with EZ-Link Sulfo-NHS-SS biotin to label proteins expressed at the cell surface. Cells were then lysed and an equal amount of protein was rotated with 100  $\mu$ l of streptavidin beads at 4  $^{\circ}$ C for 1 hour, to pulldown biotinylated proteins. Biotinylated samples were eluted from the beads with 100  $\mu$ l of Laemmli buffer containing 5% beta-mercaptoethanol by incubating at 37  $^{\circ}$ C for 1 hour. 30  $\mu$ l of the samples were resolved by SDS-PAGE and analysed by immunoblotting with an anti VSV-G antibody to detect receptor proteins. The samples in lane 1 are aliquots of cell lysates equalised for protein content. An aliquot of the supernatant was also saved after the pulldown step. This sample containing unbound receptor is represented in lane 2. Samples in lane 3 represent the biotinylated receptors present at the cell surface. VSV-G HM74A eYFP (**A**) and VSV-G HM74 eYFP (**B**) expression detected at the anticipated size, confirming cell surface expression of this receptor. Results shown are of an individual experiment and are representative of three independent experiments.

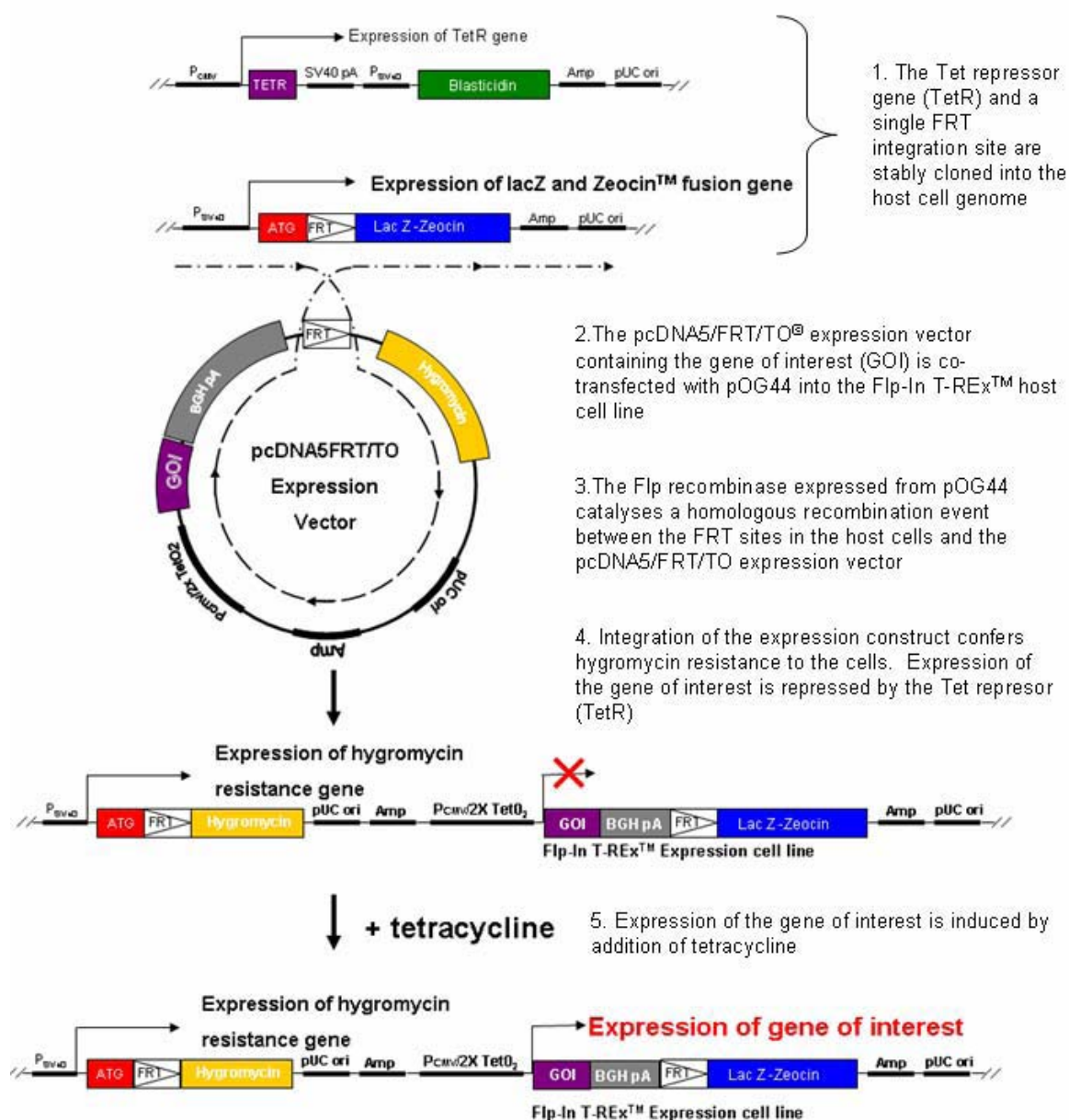
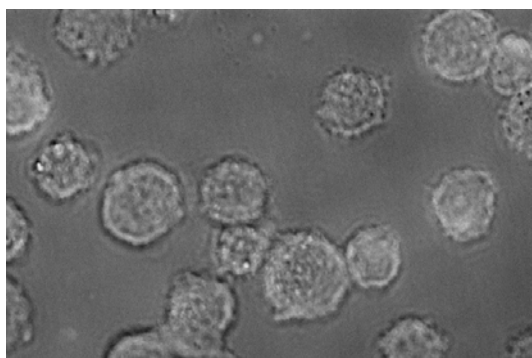


**Figure 3.20 Flp-In TREx system**

Schematic diagram illustrating the principle behind the inducible system (Invitrogen Flp-In. TREx Core Kit manual).

**Minus doxycycline**



**Plus doxycycline**

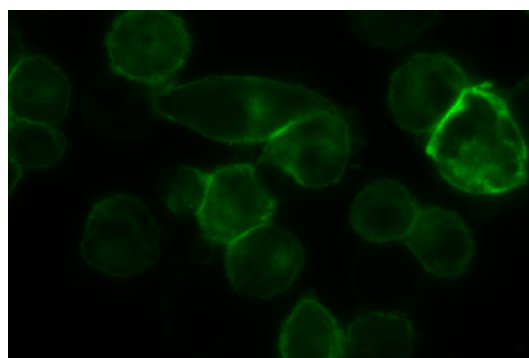
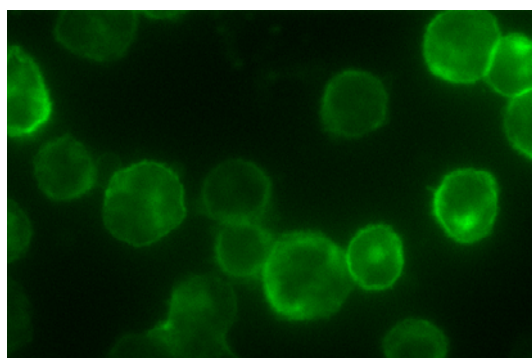
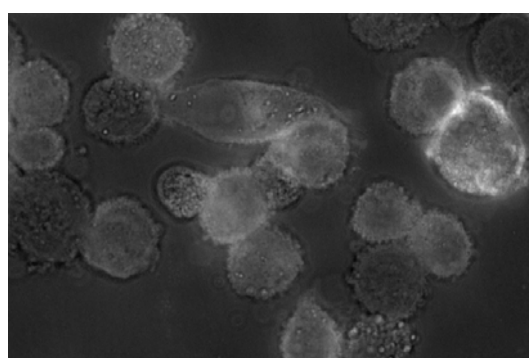
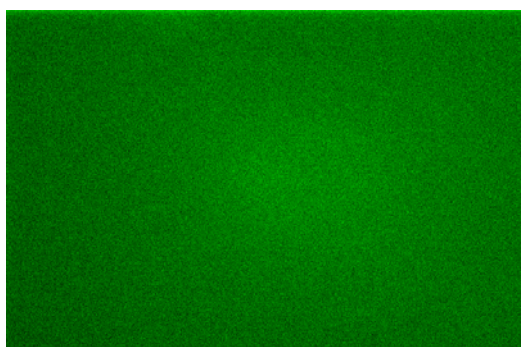
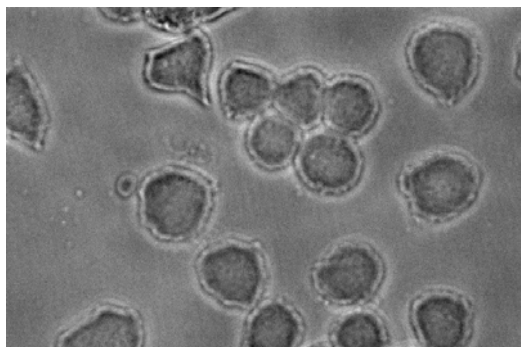


**Figure 3.21 Flp-In TREx CHO-K1 cell line stably expressing VSV-G HM74A eYFP**

Flp-In TREx CHO-K1 cells stably expressing VSV-G HM74A eYFP receptors were transfected with a pcDNA6/TR vector carrying a tetracycline repressor gene. The cells were then placed on hygromycin and blasticidin antibiotic selection to select for cells expressing both the receptor and repressor respectively. Following clonal selection, the inducible function of the clones was tested. Clones were treated with 1  $\mu\text{g/ml}$  of doxycycline overnight and visualised for eYFP fluorescence by confocal imaging using the same settings. Receptor expression was observed in both the control and treated samples. Images are representative of all the clones tested.

**Minus doxycycline**



**Plus doxycycline**

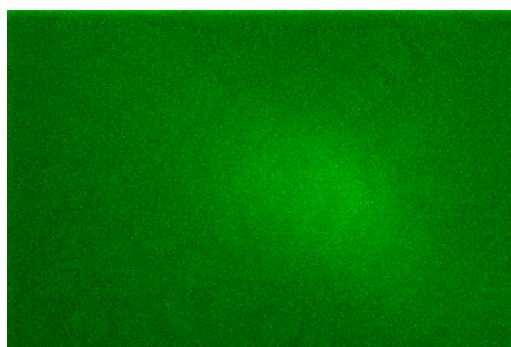
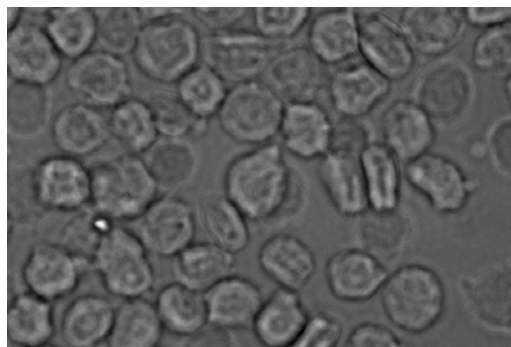


**Figure 3.22 Flp-In TREx CHO-K1 cell line not expressing VSV-G HM74 eYFP**

Flp-In TREx CHO-K1 cells stably expressing VSV-G HM74 eYFP receptors were transfected with a pcDNA6/TR vector carrying a tetracycline repressor gene. The cells were then placed on hygromycin and blasticidin antibiotic selection to select for cells expressing both the receptor and repressor respectively. Following clonal selection, the inducible function of the clones was tested. Clones were treated with 1  $\mu\text{g/ml}$  of doxycycline overnight and visualised for eYFP fluorescence by confocal imaging using the same settings. Receptor expression was not observed in either the control or treated samples. Images are representative of all the clones tested.

## **4. Regulation and desensitisation studies on the nicotinic acid receptors**

### **4.1. Introduction**

Many mechanisms have evolved for regulating GPCR signalling. Mechanisms operate at the receptor level to prevent or block initiation of the signalling cascade in the presence of continuous agonist stimulation. These phenomena, termed desensitisation, prevent over-stimulation of the receptor.

The first stage of this regulatory pathway for many GPCRs involves phosphorylation of serine and threonine residues within the third intracellular loop or C-terminal domain of the receptor. GRK and second messenger-dependent protein kinases, such as PKA or PKC are known to phosphorylate GPCRs. GRK family members selectively phosphorylate agonist-occupied receptors marking them for further desensitisation by arrestin proteins.

$\beta$ -arrestin 1 and 2 are expressed widely and therefore have relatively broad receptor specificity. Following agonist stimulation these cytoplasmic proteins undergo a substantial conformational change into a high-affinity receptor binding state and translocate rapidly to the plasma membrane where they bind to phosphorylated GPCRs (Lohse et al., 1990; Gurevich & Benovic, 1993). By binding to the receptor the arrestin protein prevents G protein coupling by steric hindrance (Kuhn & Wilden, 1987; Krupnick et al., 1997). The arrestin protein can then interact with various other proteins of the endocytotic machinery and internalise the GPCR (Goodman, Jr. et al., 1996).

The aim of this chapter was to study regulation of the nicotinic acid receptors. These highly homologous receptors share 96 % identity at the protein level with the main differences in the C-terminal tail region (Zellner et al., 2005). A five base-pair insertion at the 3' end of the gene encoding the HM74A receptor ultimately results in HM74A possessing a shorter C-terminal tail compared to HM74 (Wise et al., 2003). As the C-terminal tail of GPCRs often plays a key role in the regulation of receptor

signalling, the aim of this study was to identify any potential differences in the regulation of these receptors.

## 4.2. Basic pharmacology

Nicotinic acid receptors have been reported to couple to the  $G_i$  class of G proteins (Wise et al., 2003; Aktories et al., 1983b; Tunaru et al., 2003). The conserved cysteine residue at position 351, in the  $\alpha$ -subunits of the  $G_i$  class of G proteins act as a substrate for ADP-ribosylation catalysed by pertussis toxin (Burns, 1988). ADP-ribosylation prevents effective information transfer between the receptor and G protein by steric hindrance. To confirm published work, CHO-K1 cell lines stably expressing HM74 or HM74A receptors were incubated in the presence and absence of 25 ng/ml pertussis toxin for 16 hours. Membrane preparations were generated and [ $^{35}\text{S}$ ] GTP $\gamma$ S binding assays were utilised to test the response of the nicotinic acid receptors to nicotinic acid (Figure 4.1). When incubated in the presence of nicotinic acid, an increase in [ $^{35}\text{S}$ ] GTP $\gamma$ S binding above basal was observed in non-treated samples. However, nicotinic acid-mediated stimulation of [ $^{35}\text{S}$ ] GTP $\gamma$ S binding was abolished following pertussis toxin treatment supporting previous reports that nicotinic acid receptors couple to the  $G_i$  family of G proteins. A reduction in basal [ $^{35}\text{S}$ ] GTP $\gamma$ S binding was also observed in membranes prepared from pertussis toxin treated CHO-K1 cells stably expressing HM74A. This suggests HM74A displays  $G_i$  mediated constitutive activity.

To confirm basic pharmacology of the nicotinic acid receptors, [ $^{35}\text{S}$ ] GTP $\gamma$ S binding assays were utilised to confirm the potency of agonists at HM74 and HM74A (Tables 4.1 and 4.2). As shown previously, (Wise et al., 2003), acifran was a more potent agonist at HM74 than nicotinic acid. Acifran was also an agonist at HM74A (Wise et al., 2003). Agonist activity of acipimox and 5-methyl pyrazole-3-carboxylic acid (MPCA) at HM74A were also confirmed (Wise et al., 2003), with the rank order of potencies nicotinic acid > MPCA > acifran > acipimox. Two novel compounds, GSK 1 and GSK 2, developed by GSK, displayed similar potencies to nicotinic acid at HM74A (Table 4.2). Published reports have identified  $\beta$ -hydroxybutyrate as the

endogenous ligand for HM74A (Taggart et al., 2005). The observed low potency of  $\beta$ -hydroxybutyrate at HM74A was in agreement with published studies.

### **4.3. Nicotinic acid stimulates ERK1/2 phosphorylation**

The ability of nicotinic acid to activate ERK1/2 phosphorylation via the nicotinic acid receptors was determined by treating CHO-K1 cell lines stably expressing HM74 or HM74A with or without of 10 mM nicotinic acid for 5 minutes (Figure 4.2). In both cases, a significant increase in phosphorylated ERK1/2 was detected in samples treated with nicotinic acid. Such experiments were repeated with CHO-K1 cell lines stably expressing the N- and C-terminally modified forms of the nicotinic acid receptors (Figure 4.2). The addition of the VSV-G epitope tag and fluorescent protein did not interfere with the receptor's ability to transduce this signal. In the case of both HM74 and HM74A, wild type and tagged receptors, the observed signal was abolished by pertussis toxin treatment suggesting nicotinic acid-stimulated ERK1/2 phosphorylation was mediated via a pertussis toxin sensitive G protein. Nicotinic acid-mediated ERK1/2 phosphorylation at HM74A was concentration-dependent with a response detectable at 100 nM nicotinic acid (Figure 4.3). However, 10 mM nicotinic acid was required to induce ERK1/2 phosphorylation via HM74 (Figure 4.3). With respect to HM74A, time courses of nicotinic acid treatment showed rapid and sustained stimulation of nicotinic acid-induced ERK1/2 phosphorylation (Figure 4.3). However, in the case of ERK1/2 phosphorylation via HM74, nicotinic acid-induced ERK1/2 phosphorylation was delayed and more transient (Figure 4.3). Foetal bovine serum has been reported to induce ERK1/2 phosphorylation and therefore served as a positive control in every experiment. It is not known which components of serum activate ERK1/2 phosphorylation and by which mechanism. However, the numerous peptides and growth factors naturally found in serum are likely to act, at least partly, through various endogenously expressed receptors such as sphingosine-1-phosphate or epidermal growth factor receptors. The slight reduction in serum-stimulated ERK1/2 phosphorylation as a result of pertussis toxin treatment suggests one such mechanism is via pertussis toxin sensitive G proteins. Total levels of ERK1/2, detected in parallel studies, served as loading controls.

#### **4.4. Desensitisation studies on the nicotinic acid receptors**

In order to determine if prolonged exposure of HM74 to nicotinic acid caused desensitisation of the receptor, in an initial experiment a CHO-K1 cell line stably expressing HM74 was treated with 10 mM nicotinic for 0 and 15 minutes. A high concentration of nicotinic acid was chosen at approximately ten times the estimated pEC<sub>50</sub> value at this receptor. Membrane preparations generated from these samples were then exposed to increasing concentrations of nicotinic acid in a [<sup>35</sup>S] GTPγS binding assay (Figure 4.4). Although no change in the pEC<sub>50</sub> value was observed in control and nicotinic acid pre-treated samples, a significant reduction ( $p < 0.03$ ) in the maximum binding of [<sup>35</sup>S] GTPγS was observed in the presence of 10 mM nicotinic acid. To examine effects of longer pre-treatments, membrane preparations were generated from cells pre-treated with nicotinic acid for 0, 15, 30, 45 and 60 minutes (Figure 4.4). In a [<sup>35</sup>S] GTPγS binding assay, these membrane preparations were incubated in the presence or absence of 10 mM nicotinic acid. Although when compared to non-treated samples, a trend towards a reduction in [<sup>35</sup>S] GTPγS binding was observed in all pre-treated samples challenged with nicotinic acid, this was only statistically significant ( $p < 0.05$ ) in samples pre-treated for 60 minutes with nicotinic acid.

In a similar study, a CHO-K1 cell line stably expressing HM74A was pre-treated with 10 μM nicotinic acid, a maximally effective concentration at this receptor (based on previous [<sup>35</sup>S] GTPγS binding studies), for 0, 15, 30 and 60 minutes. Membrane preparations generated from these cells were then incubated in the presence or absence of 10 μM nicotinic acid in a [<sup>35</sup>S] GTPγS binding assay (Figure 4.5). When compared to control samples, no statistically significant change in [<sup>35</sup>S] GTPγS binding was observed in pre-treated samples incubated with nicotinic acid.

#### **4.5. Regulation studies on the nicotinic acid receptors**

The studies described above suggest HM74, but not HM74A displays desensitisation characteristics. In order to investigate regulation of the nicotinic acid receptors,

including the mechanism by which HM74 was desensitised following exposure to nicotinic acid the studies detailed below were conducted.

#### **4.5.1. Study of $G\alpha_i$ expression level**

First the potential role of downregulation of  $G\alpha_i$  G proteins in the desensitisation observed in nicotinic acid pre-treated HM74 samples was examined. This was investigated by studying the expression level of  $G\alpha_i$  G protein in control and nicotinic acid pre-treated samples.

No change in  $G\alpha_i$  G protein expression level was detected in membrane preparations generated from CHO-K1 cells stably expressing HM74 and pre-treated with 10 mM nicotinic acid for 0, 15 minutes and 24 hours (Figure 4.6). Nicotinic acid pre-treatment also had no effect on the expression of  $G\alpha_{q/11}$  class of G protein. Equal loading of the control and nicotinic acid pre-treated samples was confirmed by immunoblotting with an anti tubulin antiserum. Membranes prepared from Flp-In HEK293 cells expressing  $G\alpha_{i1}$  G protein as described by (Lane et al., 2007) were included as positive antibody control for the  $G\alpha_{i1}$  and 2 antibody. In a similar manner, membranes prepared from HEK293 cells transiently expressing G protein  $G\alpha_{i1}$  served as an antibody control for the  $G\alpha_{q/11}$  antibody.

#### **4.5.2. Internalisation studies on the nicotinic acid receptor**

A number of assays were used to determine whether HM74 desensitisation was due to nicotinic acid-dependent internalisation of HM74. In parallel studies, internalisation of HM74A as a regulatory mechanism for HM74A signalling was also examined. Mu-opioid receptor, which is known to internalise by a  $\beta$ -arrestin dependent pathway (Milasta et al., 2005), was utilised as a positive control in these studies (data not shown).

##### **4.5.2.1. Mouse embryo fibroblast (MEF) cells**

Wild type and  $\beta$ -arrestin 1 and 2 knock out MEF cells (kindly gifted by Robert J. Lefkowitz) (Kohout et al., 2001) were utilised to study nicotinic acid-induced

internalisation of the nicotinic acid receptors and to determine if  $\beta$ -arrestins 1 and 2 played a role in this.

Receptor cDNA was introduced into wild type and  $\beta$ -arrestin 1 and 2 knock out MEF cells by nucleofection as described in section 2.4.7.2. Nucleofected cells incubated in the presence and absence of 10 mM nicotinic acid were fixed and eYFP fluorescence was visualised by confocal microscopy (Figure 4.7). In the absence of nicotinic acid, a distribution pattern indicative of cell surface expression was observed in both wild type and knock out cells. Following nicotinic acid treatment no change in distribution pattern was observed.

#### **4.5.2.2. CHO-K1 cells**

As nicotinic acid desensitisation studies were conducted in a CHO-K1 cell background, internalisation studies were repeated in these cells to rule out any cell type specific effects. A CHO-K1 cell line stably expressing VSV-G HM74 eYFP was incubated in the presence or absence of 10 mM nicotinic acid. Live cells were then imaged by fluorescence microscopy (Figure 4.8). Again, an expression pattern consistent with plasma membrane expression was visualised in the presence and absence of nicotinic acid.

When similar studies were adopted for HM74A, VSV-G HM74A eYFP did not internalise in response to 10  $\mu$ M or even a higher concentration of 10 mM nicotinic acid treatment (Figures 4.8 and 4.9). To assess if longer nicotinic acid treatments induced internalisation, cells were incubated up to 1 hour, however this also did not result in detectable receptor internalisation (Figure 4.9).

#### **4.5.2.3. Cell surface biotinylation**

To confirm the above observations, a cell surface labelling technique was adopted (as described in sections 2.5.9 and 3.7). Figure 4.10 A is a schematic diagram illustrating the application of the cell surface biotin labelling technique to study receptor internalisation. For each cell line stably expressing either VSV-G HM74 eYFP or VSV-G HM74A eYFP, biotin labelling of cell surface receptors was compared in ligand treated and non-treated cells. Compared to non-treated samples, receptor internalisation as a result of ligand treatment would result in a reduction in the amount

of biotinylated protein detected. However, in the absence of ligand-dependent internalisation similar amounts of biotinylated protein would be detected in both treated and untreated samples. In the case of both receptors, nicotinic acid failed to induce receptor internalisation even at a 10 mM concentration (Figure 4.10). To examine if the lack of internalisation detected was nicotinic acid specific, these studies were repeated with  $\beta$ -hydroxybutyrate (Figure 4.10 C2). Again, internalisation of VSV-G HM74A eYFP was not detected.

#### **4.5.2.4. Cell surface ELISA**

In another attempt to study agonist-induced receptor internalisation, a cell surface ELISA assay, as described in section 3.4.2, was adopted. CHO-K1 cell lines stably expressing either VSV-G HM74 eYFP or VSV-G HM74A eYFP were incubated in the presence or absence of nicotinic acid, as described in chapter 2.5.11 (Figure 4.11). No significant change in cell surface expression of either receptor was observed in the presence of nicotinic acid. Receptor function was confirmed in these cell lines by nicotinic acid-induced phosphorylation of ERK1/2 via VSV-G HM74 eYFP and VSV-G HM74A eYFP (Figure 4.11).

#### **4.5.2.5. $\beta$ -arrestin 2 GFP translocation study**

Although the pharmacology of the tagged receptor constructs were shown, in chapter 3, to be comparable to wild type receptors in both transient and stable expression systems, to rule out any detrimental effects of the N-terminal VSV-G and more importantly the C-terminal eYFP tag on the internalisation characteristics of this receptor,  $\beta$ -arrestin translocations studies, utilising CHO-K1 cell lines stably expressing either the wild type HM74 or HM74A receptor, were performed.  $\beta$ -arrestin is a cytosolic protein; agonist-mediated translocation from the cytoplasm to the plasma membrane would provide evidence of receptor internalisation mechanisms being engaged. If, however translocation of  $\beta$ -arrestin is not detected, in isolation these studies would not provide definitive evidence for a lack internalisation as GPCRs have been reported to internalise by  $\beta$ -arrestin-independent pathways (Claing et al., 2000; Teixeira et al., 1999), however taken together with the other studies presented, it would support previous observations.

A GFP C-terminal tagged  $\beta$ -arrestin 2 fusion protein was utilised for these studies. Bovine  $\beta$ -arrestin 2 GFP cDNA was transiently introduced into CHO-K1 cell lines stably expressing HM74 or HM74A and translocation of the arrestin protein in response to nicotinic acid was examined (Figure 4.12).  $\beta$ -arrestin 2 GFP demonstrated a cytoplasmic distribution pattern which remained unchanged following nicotinic acid treatment.

#### **4.5.3. Nicotinic acid-induced phosphorylation of the nicotinic acid receptors**

Data presented so far suggest nicotinic acid receptor signalling is not regulated by receptor sequestration and  $\beta$ -arrestin involvement has also been ruled out. As receptor phosphorylation by a GRK is considered to be the 'trigger' for  $\beta$ -arrestin recruitment the ability of the nicotinic acid receptors to be phosphorylated in an agonist-dependent manner was investigated.

In [ $^{32}$ P] orthophosphate assays, as described in section 2.5.10, CHO-K1 cells expressing VSV-G HM74A eYFP were incubated with vehicle or 10 mM nicotinic acid for 15 or 30 minutes. An increase in phospho-HM74A was observed in samples treated with nicotinic acid after only 15 minutes of nicotinic acid treatment (Figure 4.13). Phosphorylation of HM74A was concentration dependent with the biggest increase in phosphorylation observed with 10 mM nicotinic acid treatment however 10  $\mu$ M nicotinic acid was sufficient to phosphorylate HM74A to detectable levels (Figure 4.13). HM74 was also phosphorylated in an agonist dependent manner (Figure 4.15 A).

#### **4.5.4. Kinase inhibitor study**

NetPhos phosphorylation prediction software was utilised to identify possible phosphorylation sites. This application predicts serine, threonine and tyrosine phosphorylation sites in eukaryotic proteins. As both receptors are highly homologous and were phosphorylated in an agonist-dependent manner it was not surprising many common sites were identified. However, the longer C-terminal region of HM74

contained a predicted PKC phosphorylation site not present in HM74A (Figure 4.14). To investigate which kinase(s) was responsible for phosphorylating HM74, selective kinase inhibitors were utilised. RO318220 is a known PKC inhibitor shown to block PKC dependent phosphorylation (Beltman et al., 1996). H89 is a known PKA inhibitor documented to block PKA dependent phosphorylation (Chijiwa et al., 1990). When [<sup>32</sup>P] orthophosphate experiments were performed in the presence of either RO318220 or H89, although nicotinic acid-stimulated phosphorylation of VSV-G HM74A eYFP was not abolished a reduction in nicotinic acid-induced phosphorylation was observed (Figure 4.15 A). In the presence of RO318220, a reduction in the basal phosphorylation was also observed. However, when similar experiments were performed with VSV-G HM74A eYFP expressing cells, no reduction in HM74A phosphorylation was observed in samples treated with either inhibitor (Figure 4.15 B).

In parallel studies, cell lines stably expressing VSV-G HM74 eYFP or VSV-G HM74A eYFP were each treated with phorbol 12-myristate 13-acetate (PMA), a known PKC activator (Niedel et al., 1983) or forskolin, known to activate PKA via adenylate cyclase (de Souza et al., 1983) in the presence and absence of the corresponding kinase inhibitor. In each case, controls of vehicle and nicotinic acid treatment were also included. RO318220 and H89 were shown to inhibit ERK 1/2 and CREB phosphorylation, respectively (Figure 4.16).

## 4.6. Discussion

Regulation of GPCR signalling is vital in order to avoid receptor over-stimulation as a result of prolonged exposure to agonist. With respect to this, regulation of the nicotinic acid receptors was examined in this study.

First, published data describing the basic pharmacology of the receptors was confirmed. Nicotinic acid receptors have been reported to couple to the G<sub>i</sub> class of G proteins (Wise et al., 2003; Aktories et al., 1983b; Tunaru et al., 2003). Studies utilised pertussis toxin, which catalyses the ADP-ribosylation of a conserved cysteine residue in the  $\alpha$ -subunits of the G<sub>i</sub> class of G proteins and therefore prevents effective information transfer between receptor and G proteins (Burns, 1988). In the case of

both HM74 and HM74A, nicotinic acid stimulated [<sup>35</sup>S] GTPγS binding was abolished following pertussis toxin treatment. This confirms that these receptors mediate nicotinic acid-induced signal transduction via G<sub>i</sub> G proteins. With respect to HM74A, a reduction in basal [<sup>35</sup>S] GTPγS binding was also observed in pertussis toxin treated samples. This suggests a degree of G<sub>i</sub> mediated constitutive activity at HM74A.

In [<sup>35</sup>S] GTPγS binding assays, in agreement with published data, acifran demonstrated higher potency at HM74 than nicotinic acid (Wise et al., 2003). Agonist activity of acifran, acipimox and MPCA at HM74A was also confirmed however, the rank order of potencies obtained was nicotinic acid > MPCA > acifran > acipimox. Published data suggest MPCA is least potent at HM74A (Wise et al., 2003). β-hydroxybutyrate, which has been described as the endogenous ligand for HM74A, was less potent than nicotinic acid (Taggart et al., 2005). Two novel compounds, GSK 1 and GSK 2, with similar molecular structures to nicotinic acid were developed by GlaxoSmithKline. These compounds were more potent at HM74A than nicotinic acid and are now in trials for their suitability as drug compounds.

The ability of nicotinic acid to stimulate ERK1/2 phosphorylation via the nicotinic acid receptors was examined next. Data published by Mahboubi and co-workers detected nicotinic acid-induced ERK1/2 phosphorylation via HM74A but not HM74 (Mahboubi et al., 2006). However they utilised 1 μM nicotinic acid, which from nicotinic acid concentration response experiments presented in Figure 4.3, is not sufficient for ERK1/2 phosphorylation via HM74. As reported, nicotinic acid-stimulated ERK1/2 phosphorylation was G<sub>i</sub> mediated (Mahboubi et al., 2006; Tunaru et al., 2003) and the addition of N or C-terminal tags did not affect this response. Nicotinic acid-induced ERK1/2 phosphorylation via HM74A was rapid and sustained. However, nicotinic acid-induced ERK1/2 phosphorylation via HM74 was slower and transient. Although sustained ERK1/2 phosphorylation suggests β-arrestin-mediated signalling (Ahn et al., 2004), as pertussis toxin treatment abolished ERK1/2 phosphorylation this suggested G protein involvement. Also, in β-arrestin translocation studies, there was no evidence of β-arrestin 2 GFP translocation to the plasma membrane or interaction with HM74A in response to nicotinic acid.

In nicotinic acid pre-treatment studies of HM74, a reduction in [<sup>35</sup>S] GTPγS binding was observed in samples incubated with nicotinic acid. Although there was no change in the pEC<sub>50</sub> values estimated from nicotinic acid concentration curves, the reduction in the maximum binding of [<sup>35</sup>S] GTPγS was significant in a one way analysis of variance statistical test and therefore suggested desensitisation of HM74 signalling. However, no desensitisation of HM74A as a result of prolonged exposure to nicotinic acid was detected. Studies conducted by Green and co-workers in 1992, before the identification of the nicotinic acid receptors, suggest prolonged incubation of adipocytes with nicotinic acid reduced sensitivity of the cells to nicotinic acid in a subsequent lipolysis assay (Green et al., 1992). Published data also confirmed the observations made in this study, that nicotinic acid does not induce Gα<sub>i</sub> G protein down-regulation (Green et al., 1992).

To investigate this further, nicotinic acid-induced internalisation of the nicotinic acid receptors was examined utilising various tools and techniques. In the case of each receptor, there was no convincing evidence of receptor internalisation in response to nicotinic acid and in the case of HM74A, β-hydroxybutyrate treatment. In β-arrestin translocation studies, no change in the localisation of β-arrestin 2 GFP was detected in cells treated with nicotinic acid. This, taken together with observations from the internalisation studies, suggests nicotinic acid receptors do not recruit β-arrestin or sequester in response to agonist treatment. However, recent findings by Richman and co-workers not only suggest nicotinic acid-induced internalisation of HM74A (Richman et al., 2007) but also co-localisation with β-arrestin 2 (personal communication, Professor G. Milligan). Differences in the findings may be addressed by the tools utilised in the studies. For example, in the studies by Richman and co-workers, COS-7 cells were utilised and both HM74A and β-arrestin were transiently introduced into these cells. It can be argued that CHO-K1 and COS-7 cells inherently possess different 'internalisation machinery' and therefore this can result in the different internalisation characteristics observed. One such example has been described by Barlic and co-workers. In this study, CXCR1 has been described to internalise in rat basophilic leukemia 2H3 (RBL-2H3) cells but not in HEK 293 cells (Barlic et al., 1999). Closer examination revealed that endogenous β-arrestin 2 expression in HEK 293 cells was not sufficient for CXCR1 internalisation. Another

plausible explanation may implicate the addition of the N- or C-terminal tags utilised in the studies outlined in this chapter. Studies conducted by Richman and co-workers utilised an N-terminus epitope tagged HM74A receptor. It could be argued, especially in the case of the C-terminus, that the tags are interfering or preventing effective receptor/ $\beta$ -arrestin binding and therefore receptor internalisation. This issue was addressed in the study by utilising wild type HM74A in the  $\beta$ -arrestin translocation studies. Despite this, no translocation of  $\beta$ -arrestin 2 GFP was visualised in response to nicotinic acid. Human  $\beta$ -arrestin 2 was utilised in the study by Richman and co-workers whereas studies described here utilised bovine  $\beta$ -arrestin 2, therefore it could be argued that a  $\beta$ -arrestin protein from a different species was unable to interact with human HM74A. However, bovine and human  $\beta$ -arrestin 2 share 94.8 % identity at the protein level (Figure 4.17). The region (amino acids 24 – 330) in which the receptor activation recognition and the secondary receptor binding domains fall (Gurevich et al., 1995) are highly conserved between the two species. Taken together with reports of bovine  $\beta$ -arrestin 2 interaction with other human GPCRs, this is unlikely to be an issue (Milasta et al., 2005). Personal communication with Professor Stefan Offermanns has also addressed many of the above concerns. Experimental studies by his group have also failed to detect internalisation of the nicotinic acid receptors in response to nicotinic acid. Studies utilised N-terminal tagged receptors in a variety of cell types including COS-7 and CHO-K1 cell lines.

When phosphorylation of the nicotinic acid receptors was examined, an increase in receptor phosphorylation as a result of nicotinic acid treatment was observed for both HM74 and HM74A. As these receptors are highly homologous and are both phosphorylated in an agonist-dependent manner, it is possible that both HM74 and HM74A share the same phosphorylation sites. Phosphorylation prediction software programmes predict several common phosphorylation sites for the nicotinic acid receptors, however there are two extra predicted phosphorylation sites, serines in both cases, on the C-tail region of HM74, as indicated in Figure 4.14. The serine at position 366 is predicted to be phosphorylated by PKC as it conforms to the determined consensus PKC phosphorylation motif. This motif is comprised of three amino acids where a serine/threonine residue is followed by any amino acid and then either an arginine or lysine (Hocevar et al., 1993). However, this region does not

contain a GRK consensus motif, a diacidic sequence upstream of serine residues (Berrada et al., 2000). GRK, PKA and PKC are expressed in adipocytes and therefore they play a potential role in the nicotinic acid-dependent phosphorylation of the nicotinic acid receptors (Usui et al., 2004; Zhou et al., 2006; Li et al., 2008). Kinase inhibitor studies have implicated both PKC and PKA in the agonist-dependent phosphorylation of HM74. However, other kinases are also likely to play a role as phosphorylation was not completely abolished. An increase in phosphorylation as a result of nicotinic acid treatment was observed despite the presence of these kinase inhibitors. Also, due to the poor immunoprecipitation qualities of this receptor it is important to verify the role of both PKC and PKA through other means. For example, it can be examined if over-expression of PKC or PKA results in an increase in agonist-dependent HM74 phosphorylation. The role of both PKC and PKA in the agonist-dependent phosphorylation of HM74A was ruled out.

The role of GRKs in the phosphorylation of the nicotinic acid receptors could not be investigated due to a lack of suitable tools. GRK2 dominant negative mutants that can be transfected into cell lines are available (Kong et al., 1994), however due to the poor transfection efficiency experienced with cell lines stably expressing the nicotinic acid receptors, this avenue was not explored. As the hamster genome has not been sequenced, gene silencing approaches utilising GRK siRNA to explore the role of GRK in the existing CHO-K1 cell lines, could not be exploited. At present human GRK2 siRNA is available and although in preliminary studies hamster GRK2 expression was knocked down (Figure 4.18), this level of knock down was not consistent from experiment to experiment as with HEK293 cells. Also, with knockdown studies as not all endogenous protein expression is silenced it is possible that remaining expression is sufficient for phosphorylation. Therefore, studies of this sort would not be conclusive on their own but would complement other findings. The role of GRKs can also be studied by over expressing these proteins and then examining if this results in an increase in receptor phosphorylation. Again, results from a study like this would not be compelling on their own but would require further evidence.

In summary, key differences in the signalling and regulation of the nicotinic acid receptors were identified in this study. HM74 and HM74A display differential

kinetics with respect to nicotinic acid-stimulated ERK 1/2 phosphorylation. Also studies in this chapter identified the desensitisation of HM74 but not HM74A as a result of prolonged nicotinic acid exposure. An increase in HM74 and HM74A phosphorylation was detected in samples treated with nicotinic acid. In the case of HM74, both PKC and PKA may play a partial role in this. However, both nicotinic acid receptors failed to internalise in response to nicotinic acid and in the case of HM74A, also in response to  $\beta$ -hydroxybutyrate.

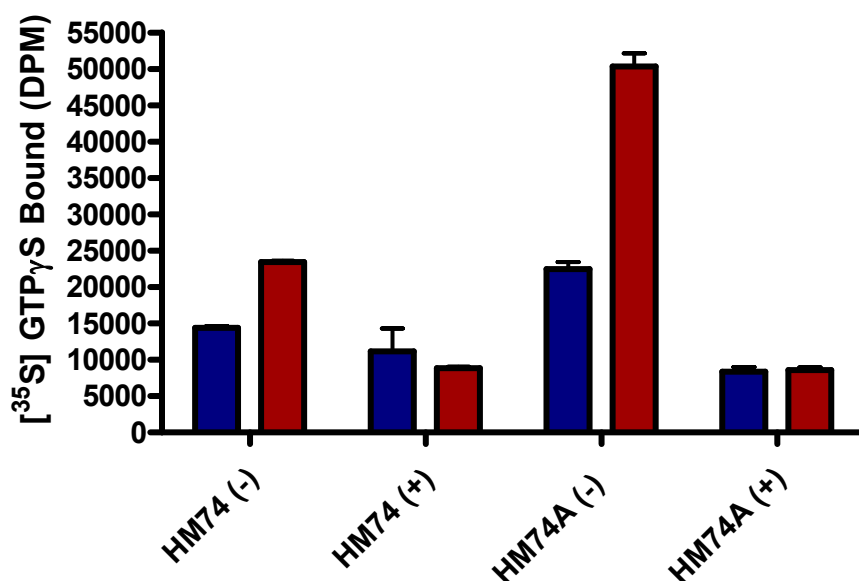


**Figure 4.1 Nicotinic acid stimulated [<sup>35</sup>S] GTP $\gamma$ S binding is abolished by pertussis toxin treatment**

CHO-K1 cell lines stably expressing HM74 or HM74A were treated with 25 ng/ml pertussis toxin for 16 hours at 37 °C and membranes were prepared from treated (+) and untreated cells (-). 10  $\mu$ g of membranes were incubated in the presence (red) and absence (blue) of 1 mM (HM74) or 1  $\mu$ M (HM74A) nicotinic acid in [<sup>35</sup>S] GTP $\gamma$ S binding assays containing 0.3 nM [<sup>35</sup>S] GTP $\gamma$ S. The assay was terminated by filtration of the samples onto GF/C fibre glass filters and bound [<sup>35</sup>S] GTP $\gamma$ S was measured by liquid-scintillation spectrometry. In both cases, nicotinic acid stimulated [<sup>35</sup>S] GTP $\gamma$ S binding was abolished by pertussis toxin treatment. Experiments were performed in triplicate and data points represent means  $\pm$  SEM.

<b>Ligand</b>	<b>pEC<sub>50</sub></b>
<b>Nicotinic acid</b>	<b>3.0 ± 0.2</b>
<b>Acifran</b>	<b>4.1 ± 0.1</b>

**Table 4.1 HM74 basic pharmacology**

[<sup>35</sup>S] GTP $\gamma$ S binding scintillation proximity assays were employed to test the response of HM74 stably expressed in CHO-K1 cells to nicotinic acid (blue) and acifran (red) at final concentrations ranging from 1 nM to 1 mM. Bound [<sup>35</sup>S] GTP $\gamma$ S was measured by scintillation counting. Data were analysed using GraphPad Prism software. pEC<sub>50</sub> values are means  $\pm$  SEM calculated from three independent experiments.

<b>Ligand</b>	<b>pEC<sub>50</sub></b>
<b>Nicotinic acid</b>	<b>5.9 ± 0.3</b>
<b>Acifran</b>	<b>4.4 ± 0.2</b>
<b>Acipimox</b>	<b>3.7 ± 0.1</b>
<b>MPCA</b>	<b>4.6 ± 0.2</b>
<b>GSK 1</b>	<b>6.0 ± 0.2</b>
<b>GSK 2</b>	<b>5.6 ± 0.3</b>
<b>β-hydroxybutyrate</b>	<b>2.9 ± 0.2</b>

**Table 4.2 HM74A basic pharmacology**

[<sup>35</sup>S] GTPγS binding assays were employed to test the response of HM74A stably expressed in CHO-K1 cells to various ligands at final concentrations ranging from 1 nM to 1 mM. Bound [<sup>35</sup>S] GTPγS was measured by scintillation counting. Data were analysed using GraphPad Prism software. pEC<sub>50</sub> values are means ± SEM obtained from three independent experiments.

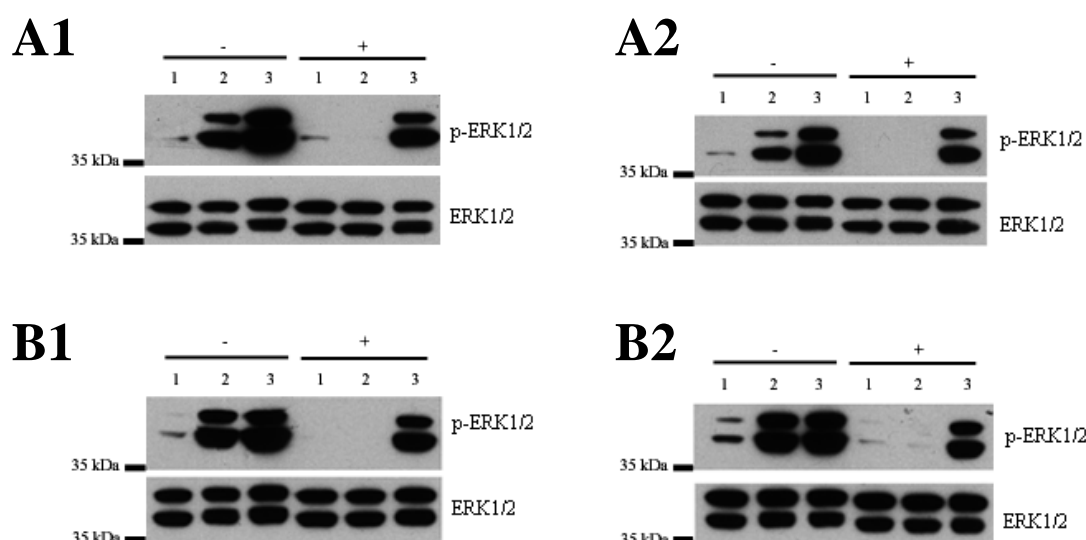


**Figure 4.2 Nicotinic acid stimulates ERK1/2 phosphorylation. ERK1/2 phosphorylation was abolished by pertussis toxin treatment**

CHO-K1 cell lines stably expressing wild type or modified nicotinic acid receptors were serum starved and treated in the presence (+) and absence (-) of 25 ng/ml pertussis toxin for 16 hours at 37 °C. Cells were then incubated with 10 mM nicotinic acid (lane 2) for 5 minutes in an ERK1/2 phosphorylation assay. A negative control of vehicle (lane 1) and positive control of 10 % foetal bovine serum treatment (lane 3) were included in all experiments. Cell lysates prepared from the samples were equalised for protein content, resolved by SDS-PAGE and immunoblotted with anti ERK1/2 antiserum to determine equal loading of samples (42/44 kDa) and anti phospho-ERK1/2 antibody to study ERK1/2 phosphorylation (42/44 kDa). Nicotinic acid stimulated ERK1/2 phosphorylation via HM74 (**A1**), VSV-G HM74 eYFP (**A2**), HM74A (**B1**) and VSV-G HM74A eYFP (**B2**). ERK1/2 phosphorylation by nicotinic acid was abolished by pertussis toxin treatment. Immunoblots shown are representative of at least three independent experiments.

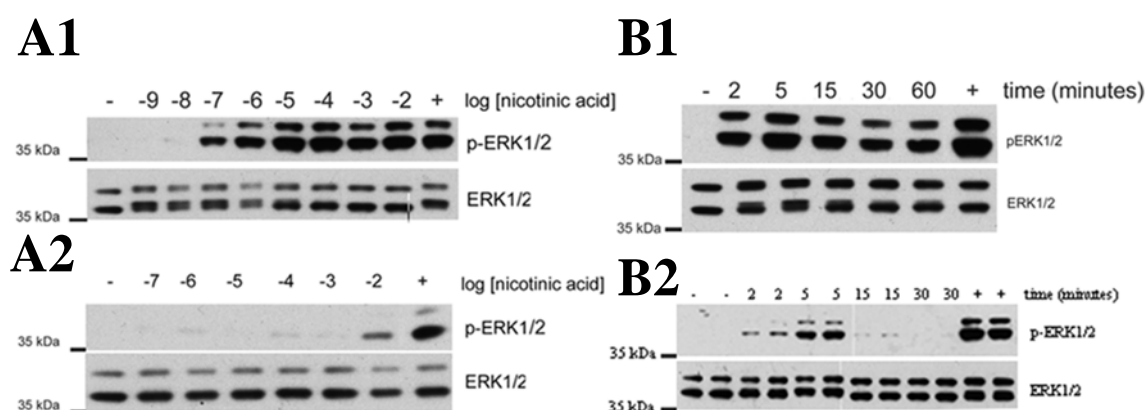


**Figure 4.3 Nicotinic acid induced ERK1/2 activation via HM74A was rapid and sustained. Nicotinic acid induced ERK1/2 activation via HM74 was slower and more transient**

**A:** CHO-K1 cell lines stably expressing HM74A (**A1**) or HM74 (**A2**) were exposed to varying concentrations of nicotinic acid for 5 minutes in an ERK1/2 phosphorylation assay. A negative control of vehicle (-) and positive control of 10 % foetal bovine serum (+) were included in each experiment. **B:** CHO-K1 cell lines stably expressing HM74A (**B1**) or HM74 (**B2**) were incubated with 10 mM nicotinic acid for varying lengths of time in an ERK1/2 phosphorylation assay. Cell lysates prepared from these samples were equalised for protein content, resolved by SDS-PAGE and immunoblotted with anti ERK1/2 antiserum to determine equal loading of samples and anti phospho-ERK1/2 antibody to study ERK1/2 phosphorylation. **A1:** 100 nM nicotinic acid was sufficient to activate ERK1/2 phosphorylation via HM74A. **A2:** 10 mM nicotinic acid activated ERK1/2 phosphorylation via HM74. **B1:** Nicotinic acid induced ERK1/2 phosphorylation via HM74A was rapid and sustained. **B2:** Nicotinic acid induced ERK1/2 phosphorylation via HM74 was slower and transient. Immunoblots shown are representative of at least three independent experiments.

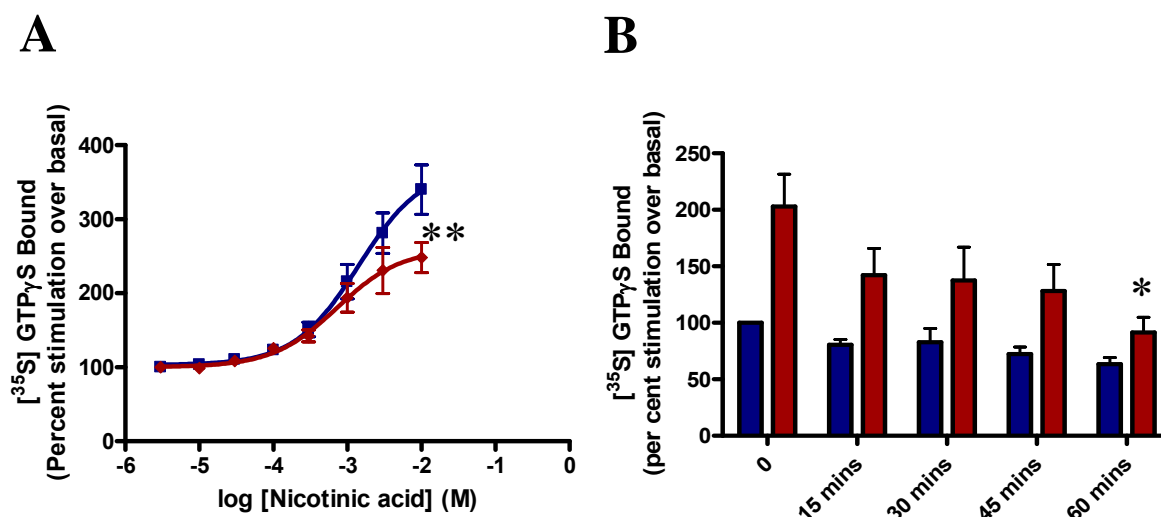


**Figure 4.4 Nicotinic acid pre-treatment causes desensitisation of HM74 mediated activation of  $G\alpha_i$**

CHO-K1 cells stably expressing HM74 were pre-treated with 10 mM nicotinic acid for 0 or 15 minutes and membranes were prepared. **A:** Nicotinic acid concentration curves of control (blue) and 15 minute nicotinic acid pre-treated (red) samples were compared in a [ $^{35}$ S] GTP $\gamma$ S binding assay. Binding of [ $^{35}$ S] GTP $\gamma$ S: Group data of  $n=3$ . The reduction in the nicotinic acid stimulated maximum binding of [ $^{35}$ S] GTP $\gamma$ S observed in pre-treated samples was significant in a one way analysis of variance test (\*\* =  $p < 0.03$ ). **B:** Samples prepared from cells pre-treated with nicotinic acid for 0, 15, 30, 45 and 60 minutes were incubated in the presence (red) and absence (blue) of 10 mM nicotinic acid in a [ $^{35}$ S] GTP $\gamma$ S binding assay. Binding of [ $^{35}$ S] GTP $\gamma$ S: Group data of  $n=4$ . When compared to control samples, the reduction in the binding of [ $^{35}$ S] GTP $\gamma$ S observed in samples pre-treated with nicotinic acid for 60 minutes and then challenged with nicotinic acid was significant in a one way analysis of variance test (\* =  $p < 0.05$ ). Data were analysed using GraphPad Prism software. Data points represent means  $\pm$  SEM.

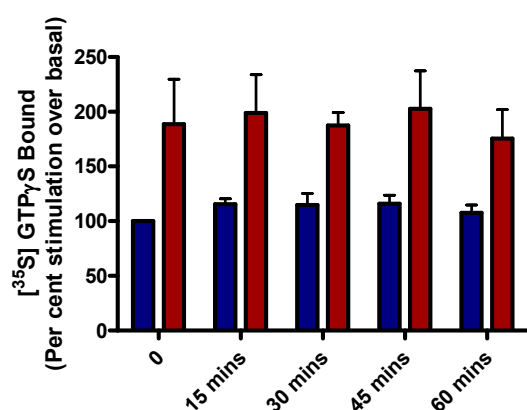


**Figure 4.5 Nicotinic acid pre-treatment does not cause desensitisation of HM74A mediated activation of  $G\alpha_i$**

Membrane preparations were generated from CHO-K1 cells stably expressing HM74A and pre-treated with 10  $\mu$ M nicotinic acid for 0, 15, 30, 45 and 60 minutes. Samples were incubated in the presence (red) and absence (blue) of 10  $\mu$ M nicotinic acid in a [<sup>35</sup>S] GTP $\gamma$ S binding assay. Binding of [<sup>35</sup>S] GTP $\gamma$ S: Group data of n=3. When compared to control samples, no significant reduction ( $p > 0.05$ ) in either basal or nicotinic acid stimulated binding of [<sup>35</sup>S] GTP $\gamma$ S was observed in pre-treated samples in a one way analysis of variance test. Data points represent means  $\pm$  SEM.

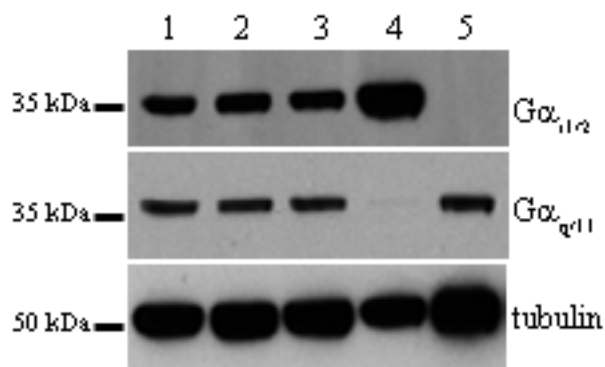
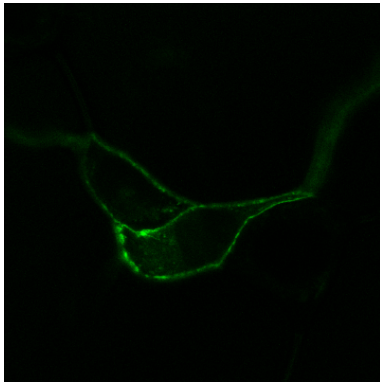


**Figure 4.6 No change in  $G\alpha_{i1 \text{ and } 2}$  G protein expression level in control and nicotinic acid pre-treated HM74 samples**

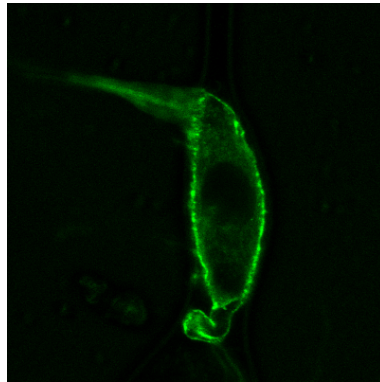
Membrane preparations, generated from CHO-K1 cells stably expressing HM74 and pre-treated with 10 mM nicotinic acid for 0, 15 minutes and 24 hours, were resolved by SDS-PAGE (lanes 1, 2 and 3 respectively). A positive antibody control employed HEK293 membranes expressing  $G\alpha_{i1}$  G protein (lane 4). Membranes prepared from HEK293 cells transiently expressing G protein  $G\alpha_{i1}$  (lane 5) were also included. An anti  $G\alpha_{i1 \text{ and } 2}$  antiserum was utilised to detect  $G\alpha_{i1}$  G proteins (40 kDa), anti  $G\alpha_{q/11}$  antiserum to detect  $G\alpha_{i1}$  G protein (40 kDa) and anti tubulin antiserum to detect tubulin (57 kDa), a loading control for HM74 expressing membranes. No change in  $G\alpha_{i1 \text{ and } 2}$  and  $G\alpha_{q/11}$  G protein expression levels were detected. Results shown are of a single experiment, representative of three independent experiments.

**A1**

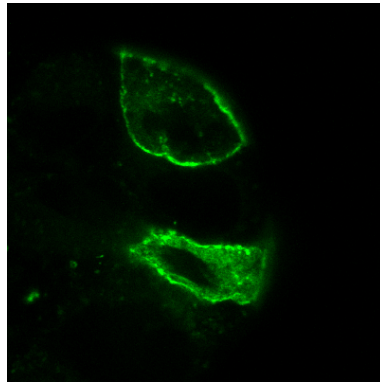
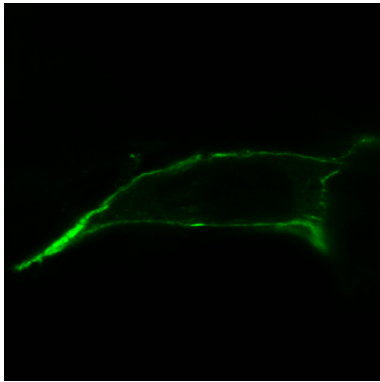
-



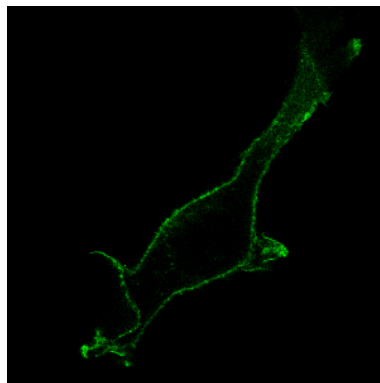
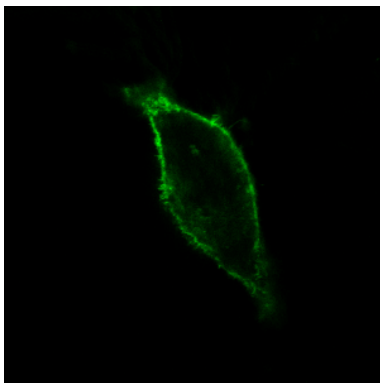
+



**A2**



**B1**



**B2**

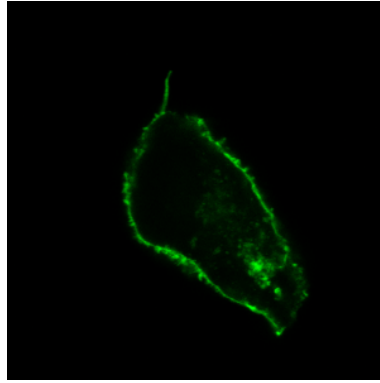
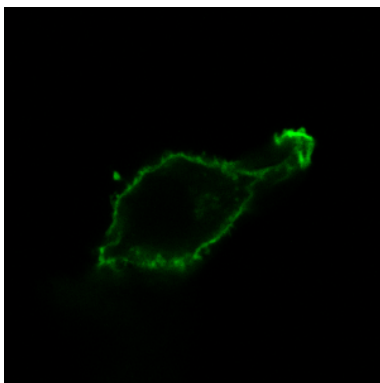
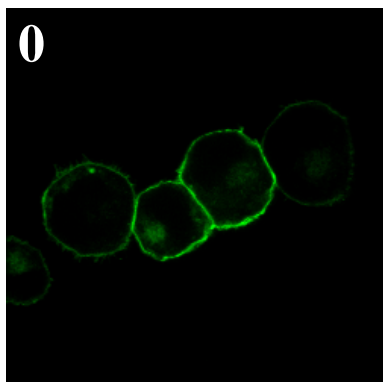


**Figure 4.7 Lack of detectable internalisation of the nicotinic acid receptors transiently expressed in mouse embryonic fibroblasts when challenged with nicotinic acid**

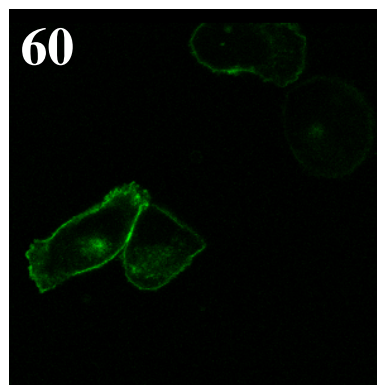
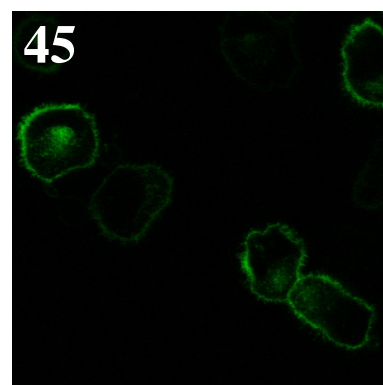
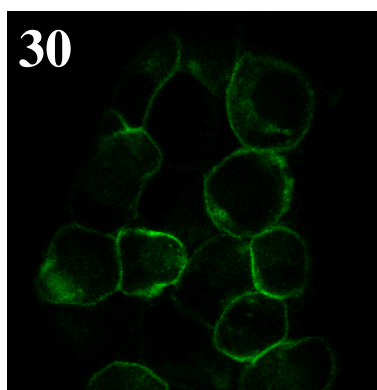
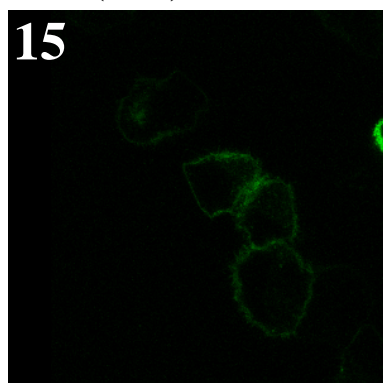
VSV-G HM74 eYFP (**A**) or VSV-G HM74A eYFP (**B**) cDNA was introduced into mouse embryonic fibroblast (MEF) wild type (**1**) and  $\beta$ -arrestin 1 and 2 knock out (**2**) cells by nucleofection. Transfected cells were incubated in the presence (+) or absence (-) of 10 mM or 10  $\mu$ M nicotinic acid, respectively, for 30 minutes. Cells were fixed and eYFP fluorescence visualised by confocal microscopy. In both cases, no substantial change in receptor localisation was observed following nicotinic acid treatment in wild type or  $\beta$ -arrestin 1 and 2 knock out cells. Results are representative of at least three experiments.



**A** time (mins)



**B** time (mins)



**C** time (mins)

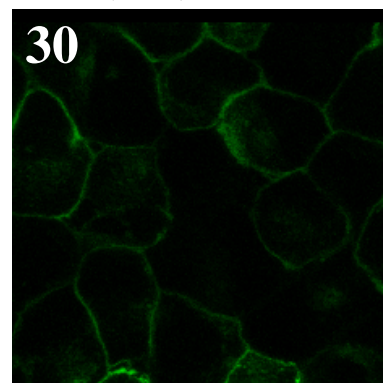
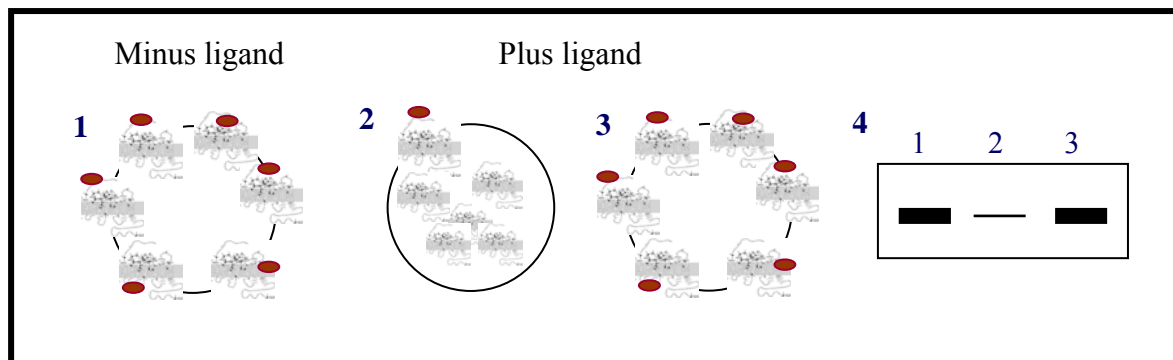


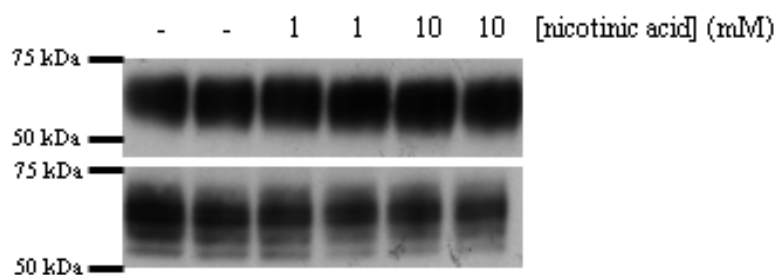
**Figure 4.9 Nicotinic acid does not internalise VSV-G HM74A eYFP**

CHO-K1 cells stably expressing VSV-G HM74A eYFP were incubated with 10  $\mu$ M nicotinic acid for 0 (**A**), 15, 30, 45 and 60 minutes (**B**). CHO-K1 cells stably expressing VSV-G HM74A eYFP were treated with 10 mM nicotinic acid for 0 (**A**) and 30 minutes (**C**). Cells were fixed and imaged by confocal microscopy to visualise the eYFP tag. Receptor localisation was unchanged with nicotinic acid treatment. Results are representative of at least three experiments.

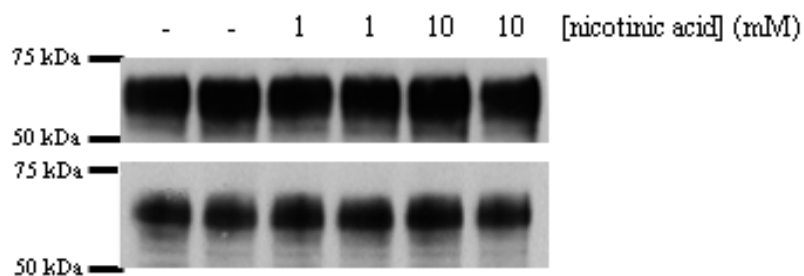
# A



# B



# C1



# C2

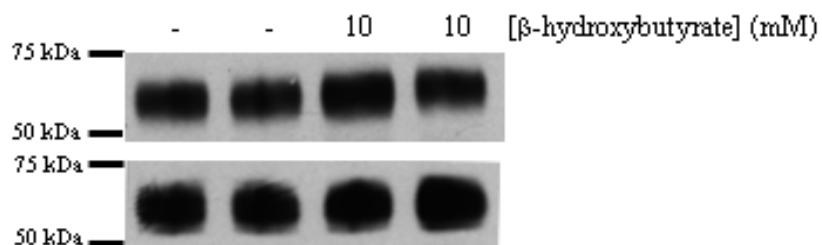
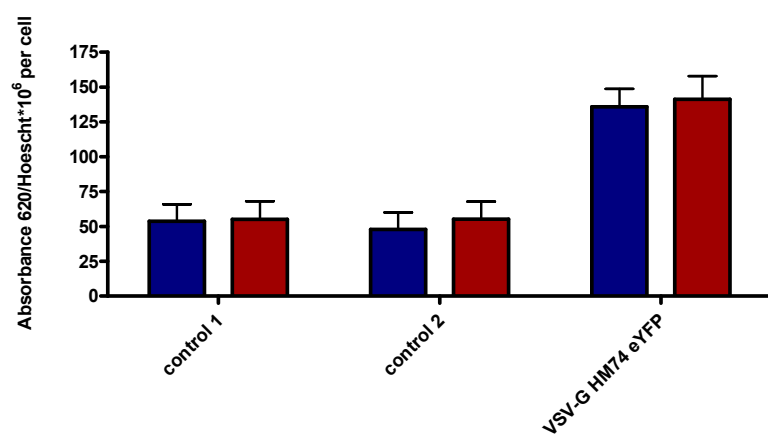


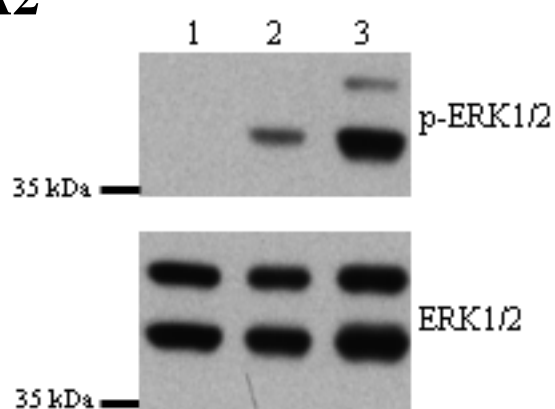
**Figure 4.10 Lack of internalisation of the nicotinic acid receptors**

**A:** Schematic diagram illustrating the application of the cell surface biotinylation assay to study receptor internalisation. In the absence of ligand treatment (1), receptors at the cell surface are labelled with biotin (indicated as red) and can be detected by immunoblotting (4, lane 1). Receptor internalisation as a result of ligand treatment (2) would result in little or no labelling, therefore in an immunoblot, when compared to non-treated samples, a reduced amount of protein would be detected (4, lane 2). No internalisation as a result of ligand exposure (3) would result in equivalent labelling of cell surface expressing receptors as in non-treated samples and therefore detection of protein in an immunoblot (4, lane 3) would be similar to that of non-treated samples. CHO-K1 cells stably expressing either VSV-G HM74 eYFP (**B**) or VSV-G HM74A eYFP (**C**) were incubated in the absence (-) or presence of nicotinic acid (**B**, **C1**) or  $\beta$ -hydroxybutyrate (**C2**) for 30 minutes and treated with EZ-Link Sulfo-NHS-SS biotin. Resulting samples were then resolved by SDS-PAGE and analysed by immunoblotting with an anti VSV-G antibody to detect receptor proteins. Samples in the lower panels are cell lysates equalised for protein content. Samples in the upper panels represent receptors at the cell surface. In all cases, receptor internalisation was not detected. Results shown are representative of at least 3 independent experiments.

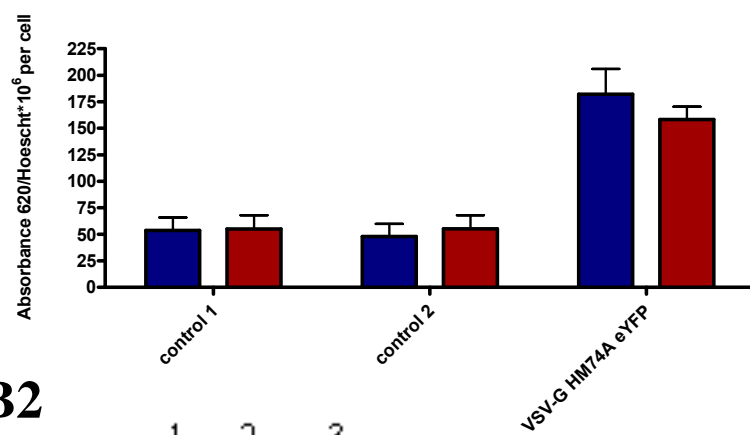
## A1



## A2



## B1



## B2

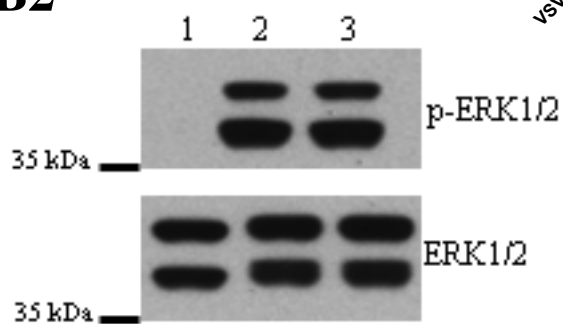
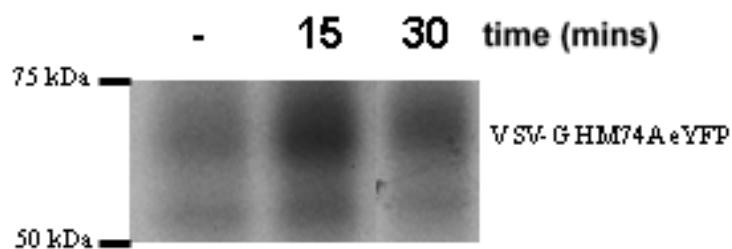


**Figure 4.11 Nicotinic acid does not internalise either VSV-G HM74 eYFP or VSV-G HM74A eYFP**

CHO-K1 cells stably expressing VSV-G HM74 eYFP (**A**) or VSV-G HM74A eYFP (**B**) were incubated in the presence (red) or absence (blue) of 10 mM nicotinic acid for 30 minutes. Cell surface expression of each receptor (**A1**, **B1**) was measured in an intact cell ELISA assay utilising an anti VSV-G antibody. Negative controls of no primary antibody (control 1) and no primary and secondary antibody (control 2) were incubated in the presence (red) or absence (blue) of 10 mM nicotinic acid. In a two-tailed t test, p values of 0.8 (**A1**) and 0.4 (**B1**) were calculated. Nicotinic acid receptors did not internalise in response to nicotinic acid. Grouped data of n=4 shown. Data points represent means  $\pm$  SEM. In an ERK1/2 phosphorylation assay these cells were incubated with 10 mM nicotinic acid (lane 2) for 5 minutes (**A2**, **B2**). A negative control of vehicle (lane 1) and positive control 10 % foetal bovine serum (lane 3) were also included. Cell lysates prepared from the samples were equalised for protein content, resolved by SDS-PAGE and immunoblotted with anti ERK1/2 antiserum, to determine equal loading of samples and an anti phospho-ERK1/2 antibody to study ERK1/2 phosphorylation. Immunoblots shown are representative of at least three independent experiments. Internalisation of VSV-G HM74 eYFP or VSV-G HM74A eYFP in response to nicotinic acid was not detected. Nicotinic acid induced ERK1/2 phosphorylation via VSV-G HM74 eYFP and VSV-G HM74A eYFP.



**A**



**B**

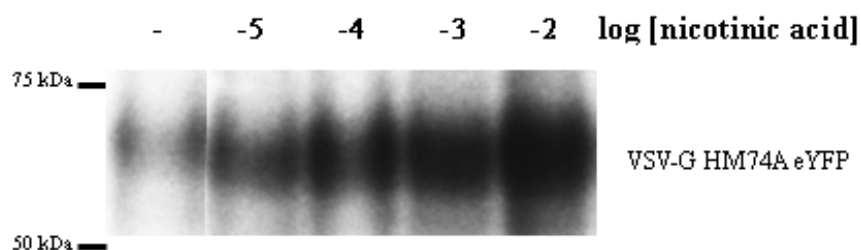


**Figure 4.13 VSV-G HM74A eYFP was phosphorylated in an agonist-dependent manner**

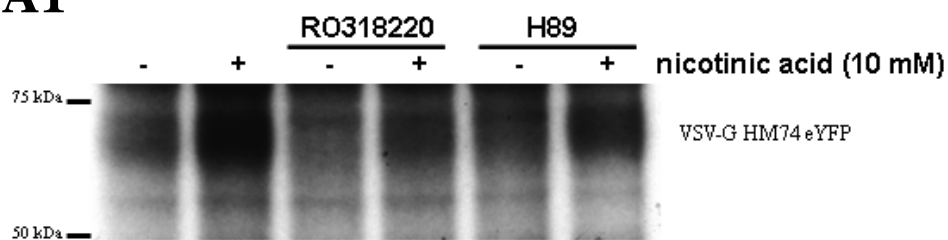
CHO-K1 cells stably expressing VSV-G HM74A eYFP were pre-incubated with 0.2 mCi/ml [<sup>32</sup>P] orthophosphate for 90 minutes. **A:** Cells were incubated in the presence or absence (-) of 10 mM nicotinic acid for 15 and 30 minutes. Cell lysates were prepared and equalised for protein content and volume before immunoprecipitating with an anti VSV-G antiserum to isolate the receptor. Samples were resolved by SDS-PAGE and phospho-proteins visualised by autoradiography. 15 minutes was sufficient for nicotinic acid induced phosphorylation of VSV-G HM74A eYFP. **B:** Cells were incubated for 15 minutes in the presence of increasing concentrations of nicotinic acid. Control of cells treated with vehicle (-) were also included. Nicotinic acid dependent phosphorylation was concentration dependent. Results are representative of three independent experiments.



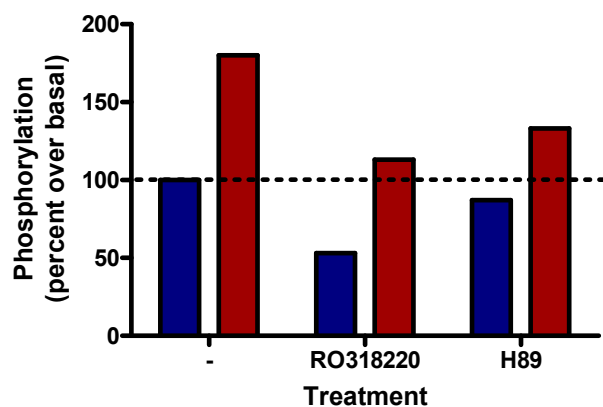
**Figure 4.14 Schematic diagram illustrating predicted phosphorylation sites on the C-terminus of HM74**

HM74A has a 24 amino acid shorter C-terminus than HM74. Common predicted phosphorylation sites in the C-terminal region of the nicotinic acid receptors are in blue. Sites in red are predicted phosphorylation sites exclusive to HM74; SKK is a predicted PKC phosphorylation site. Phosphorylation sites were predicted with NetPhos phosphorylation prediction software.

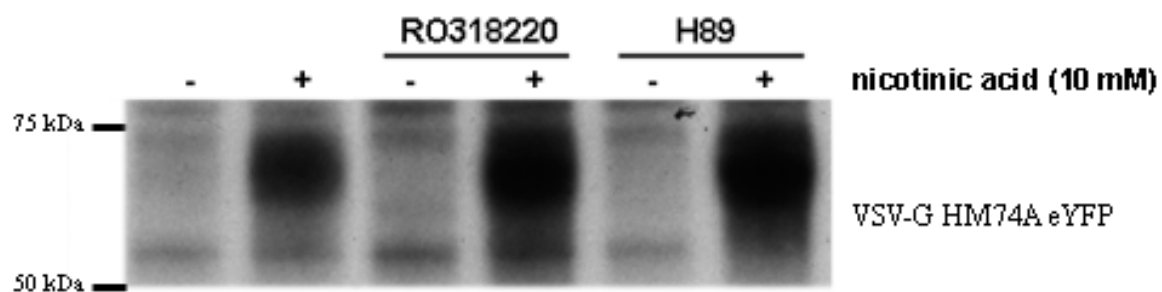
### A1



### A2



### B2



### B1

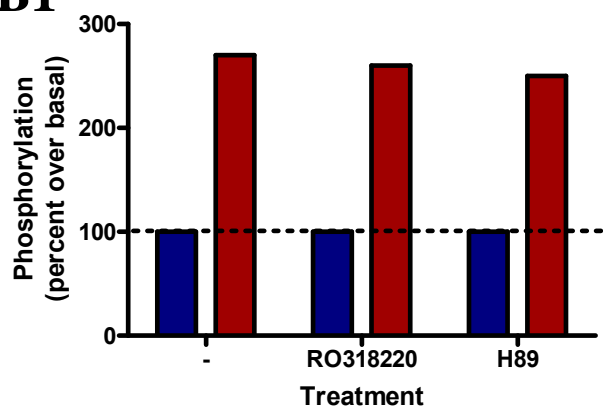
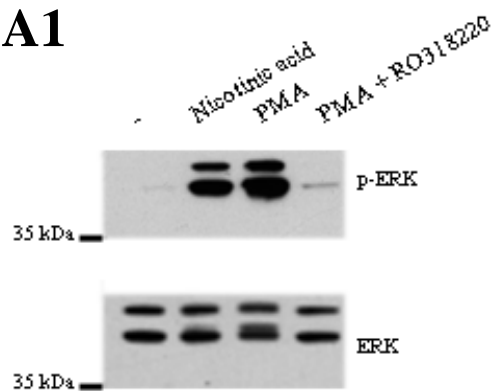


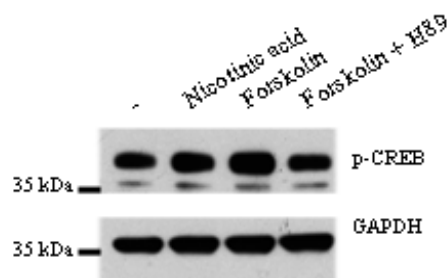
**Figure 4.15 VSV-G HM74 eYFP was phosphorylated in an agonist-dependent manner. PKC and PKA inhibitors did not abolish nicotinic acid induced phosphorylation**

CHO-K1 cells stably expressing VSV-G HM74 eYFP (A) or VSV-G HM74A eYFP (B) were pre-incubated with 0.2 mCi/ml [<sup>32</sup>P] orthophosphate supplemented with vehicle, 1 μM RO318220 or 10 μM H89 for 90 minutes. Cells were then incubated for a further 15 minutes in the presence (+) and absence (-) of 10 mM nicotinic acid and where appropriate, in the presence of the indicated kinase inhibitor. Cell lysates were prepared and equalised for protein content before immunoprecipitating with an anti VSV-G antiserum to isolate the receptor. **1:** Samples were resolved by SDS-PAGE and phospho-proteins visualised by autoradiography. **2:** Quantification of signal intensity represented as per cent phosphorylation over basal. Results shown are representative of three independent experiments.

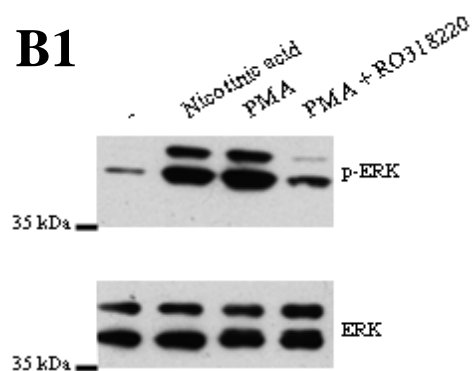
**A1**



**A2**



**B1**



**B2**

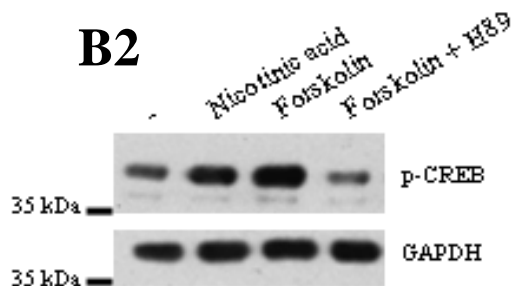


**Figure 4.16 RO318220 inhibits ERK1/2 phosphorylation. H89 inhibits CREB phosphorylation**

In an ERK1/2 phosphorylation assay, Flp-In CHO-K1 and CHO-K1 cells stably expressing VSV-G HM74 eYFP (**A1**) or VSV-G HM74A eYFP (**B1**), respectively, were serum starved overnight. Next day, cells were incubated with vehicle (-), 10 mM nicotinic acid, 1  $\mu$ M PMA or 1  $\mu$ M PMA in the presence of 1  $\mu$ M RO318220 for 15 minutes. Samples treated with RO318220 were pre-incubated with 1  $\mu$ M RO318220 for 30 minutes. Cell lysates were prepared and resolved by SDS-PAGE and immunoblotted with anti ERK1/2 antiserum to determine equal loading of samples and an anti phospho-ERK1/2 antibody to study ERK1/2 phosphorylation. After an overnight serum starvation step, CHO-K1 cells stably expressing VSV-G HM74 eYFP (**A2**) or VSV-G HM74A eYFP (**B2**) were incubated with vehicle (-), 10 mM nicotinic acid, 50  $\mu$ M forskolin or 50  $\mu$ M forskolin in the presence of 10  $\mu$ M H89 for 15 minutes. Samples treated with H89 were pre-incubated with the PKA inhibitor for 30 minutes. Cell lysates were prepared and resolved by SDS-PAGE and immunoblotted with an anti GAPDH antibody to demonstrate equal loading of samples (36 kDa) and an anti phospho-CREB ser133 antibody to study CREB phosphorylation (45 kDa). Both PKC and PKA inhibitors were biologically active.

```

human,      1 MGEKPGTRVFKKSSPNCKLTVYLGKRDFVDHLDKVDVPDGVVLDVDPDYLKDRKVFVTLTC
bovine,     1 MGEKPGTRVFKKSSPNCKLTVYLGKRDFVDHLDKVDVPDGVVLDVDPDYLKDRKVFVTLTC
*****

human,      61 AFRYGRELDVGLSFRKDLFIATYQAFPPVFNPPRPPTLQDRLLRKLQHAHPFFFTI
bovine,     61 AFRYGRELDVGLSFRKDLFIANYQAFPPTPNPPRPPTLQERLLRKLQHAHPFFFTI
*****

human,     121 PQNLPCSVTLQPGPEDTGKACGVDFEIRAFCAKSLEEKSHKRNSVRLVIRKVQFAPEKPG
bovine,    121 PQNLPCSVTLQPGPEDTGKACGVDFEIRAFCAKSLEEKSHKRNSVRLVIRKVQFAPEKPG
*****

human,     181 PQPSAETTRHFLMSDRSLHLEASLDKELYHGEPLNVNVHVTNNSKTVKKIKVSVRQYA
bovine,    181 PQPSAETTRHFLMSDRSLHLEASLDKELYHGEPLNVNVHVTNNSKTVKKIKVSVRQYA
*****

human,     241 DICLFSTAQYKCPVAQLEQDDQVSPSSTFCKVYTITPLLSDNREKRGALDGLKHEDTN
bovine,    241 DICLFSTAQYKCPVAQVEQDDQVSPSSTFCKVYTITPLLSNREKRGALDGLKHEDTN
*****

human,     301 LASSTIVKEGANKEVLGILVSYRVKVKLVVSRGGDVSVELPFVLMHPKPHDHIPLPRPQS
bovine,    301 LASSTIVKEGANKEVLGILVSYRVKVKLVVSRGGDVSVELPFVLMHPKPHDHIPLPRPQS
*****

human,     361 AA-----PETDVPVDTNLIETFNYATDDDIVFEDFARLRLKGMKDDDYDDQLC
bovine,    361 AATHPPTLLPSAVPETDAPVDTNLIETFNYATDDDIVFEDFARLRLKGLKDEDYDDQFC
**          **** ***** ***** ***** ** ***** *

```

**Figure 4.17 Alignment of human and bovine  $\beta$ -arrestin 2 amino acid sequences**

Human and bovine  $\beta$ -arrestin 2 share a 94.8 % identity at the protein level. Protein sequence alignment using SIM alignment software.

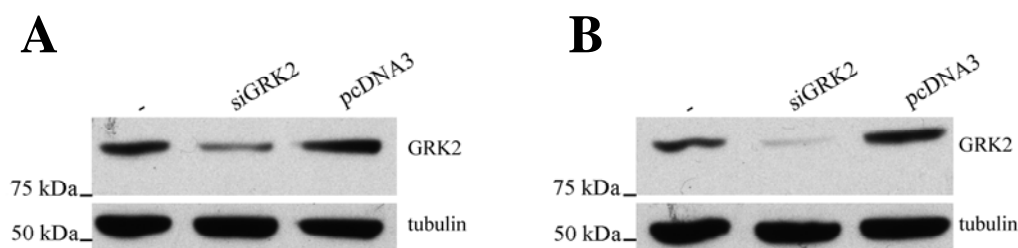


**Figure 4.18 Knockdown of GRK2 in CHO-K1 and HEK293 cells**

CHO-K1 (**A**) and HEK293 (**B**) cells were transiently transfected with either GRK2 siRNA or pcDNA3 cDNA. 48 hours after transfection, cell lysates were prepared from transfected and non-transfected (-) cells. Samples, equalised for protein content, were resolved by SDS-PAGE and immunoblotted with anti GRK2 antiserum to detect reduction in the expression of GRK2 protein (80 kDa). Total levels of tubulin (57 kDa), detected in parallel studies, served as loading controls. Compared to non-transfected cells, a greater reduction in GRK2 expression was observed in HEK293 cells. No change in GRK2 expression was observed in cells transfected with pcDNA3. Immunoblot presented displays the greatest knockdown of GRK2 in CHO-K1 cells observed from three independent experiments.

## 5. Nicotinic acid receptor chimeras as tools to study desensitisation

### 5.1. Introduction

Advances in molecular biology have allowed for creative methods to study protein function. One such method is the use of chimeric proteins. The use of chimeric GPCRs to study G protein-coupling was first reported in 1998 (Kobilka et al., 1988; Kubo et al., 1988). GPCR chimeras have been used to help define domains within receptors critical for roles such as, ligand recognition, receptor activation, downstream signalling and receptor trafficking. For example, C-terminal regions of homologous receptors, such as the  $\alpha_{1A}$ - and  $\alpha_{1B}$ -adrenergic receptors have successfully been exchanged and as a result downstream signalling of the receptors studied. In this study it was shown that by introducing the C-terminal tail of the  $\alpha_{1B}$ -adrenergic receptor, its phosphorylation characteristics were then adopted by the  $\alpha_{1A}$ -adrenergic receptor (Vazquez-Prado et al., 2000).

The nicotinic acid receptors are highly homologous and differ by only 20 base-pairs at the cDNA sequence level corresponding to the open reading frame (Wise et al., 2003). The gene encoding HM74A has a 5 base-pair insertion at the 3' end which results in HM74A possessing a shorter C-terminal tail than HM74 (Wise et al., 2003). Cytoplasmic domains of GPCRs are implicated in G protein interaction and are important for post-translational modifications such as phosphorylation. As the C-terminal region of GPCRs is often important in the regulation of receptor signalling, it was hypothesised that the differences in the desensitisation characteristics of HM74 and HM74A, identified in chapter 4, could be due to the differences in the C-terminal region of the nicotinic acid receptors. To explore this hypothesis, chimeric nicotinic acid receptors were generated. Here the intracellular C-terminal region of HM74 and HM74A were exchanged and the resulting 'nicotinic acid receptor C-terminal tail chimeras' were expressed in a stable expression system. Nicotinic acid pre-treatment studies were then conducted on these cell lines to explore the characteristics of desensitisation.

By exchanging domains of related GPCRs, chimeric receptors have been reported to take on the properties and characteristics of the donor or host receptor (Yin et al., 2004). For example, when the C-terminal regions of the gonadotrophin-releasing hormone (GnRH) receptors type I and type II were exchanged, GnRH type I adopted the desensitisation properties of GnRH type II and exhibited phosphorylation and desensitisation characteristics (McArdle et al., 2002). If the C-terminal region of HM74 is important for nicotinic acid-induced desensitisation, then by truncating this region to resemble the C-terminal region of HM74A, desensitisation may be altered. In a similar fashion, by introducing the HM74 C-terminal tail to HM74A, HM74A may then display the desensitisation characteristics of HM74. This hypothesis was examined in this study.

## **5.2. Generation of nicotinic acid receptor chimera constructs**

Nicotinic acid receptor chimeras, where the C-terminal tails of HM74 and HM74A were exchanged, were engineered by digesting VSV-G HM74 eYFP and VSV-G HM74A eYFP constructs with the restriction enzymes indicated in Figure 5.1. The resulting DNA fragments, representing the N- and C-termini of the receptors, were then swapped in a DNA ligation reaction, as illustrated in Figure 5.1. The chimeric HM74A receptor engineered to possess the longer C-terminal tail of HM74 will be referred to as VSV-G HM74A/HM74 eYFP. In a similar fashion, the chimeric HM74 receptor modified to incorporate the HM74A C-terminal region will be referred to as VSV-G HM74/HM74A eYFP.

## **5.3. Generation of Flp-In CHO-K1 cell lines stably expressing the chimeric nicotinic acid receptors**

Two Flp-In CHO-K1 cell lines each stably expressing one of the chimeric receptors were generated as described in section 2.4.9.

### **5.3.1. Localisation, detection and functional analysis**

There is a possibility chimeric receptors may not function due to misfolding or problems with targeting of the chimeric receptor to the plasma membrane. For this reason, the localisation and pharmacology of the chimeric nicotinic acid receptors was investigated.

Direct visualisation of eYFP fluorescence using a fluorescence microscope confirmed receptor expression and localisation consistent with cell surface expression (Figure 5.2 A). Both VSV-G epitope and eYFP tags were also detected by immunoblotting (Figure 5.2 B). Relative receptor levels were compared by measuring eYFP fluorescence of cell lysates prepared from the two cell lines (Figure 5.2 C). VSV-G HM74A/HM74 eYFP was expressed at a higher level than VSV-G HM74/HM74A eYFP.

Membrane preparations generated from the two cell lines stably expressing the chimeric receptors were incubated in the presence and absence of nicotinic acid and [<sup>35</sup>S] GTP $\gamma$ S binding measured as previously described (Figure 5.3 A1). Both chimeric receptors responded to nicotinic acid and an increase in [<sup>35</sup>S] GTP $\gamma$ S binding was observed in the presence of the drug. As mentioned previously,  $\beta$ -hydroxybutyrate has been described as the endogenous ligand for HM74A but not HM74 (Taggart et al., 2005). To confirm the basic pharmacological properties of the nicotinic acid receptors had not been swapped by introducing the C-terminal region of either HM74A or HM74 to the corresponding receptor, membranes expressing the chimeric receptors were incubated in the presence and absence of  $\beta$ -hydroxybutyrate in a [<sup>35</sup>S] GTP $\gamma$ S binding assay (Figure 5.3 A2). In the presence of  $\beta$ -hydroxybutyrate, an increase in [<sup>35</sup>S] GTP $\gamma$ S binding was only observed in membranes expressing the chimeric VSV-G HM74A/HM74 eYFP receptor. When membranes generated from each cell line were incubated with increasing concentrations of nicotinic acid or acifran (Figure 5.3 B and C), pEC<sub>50</sub> values obtained were comparable to those calculated for the host wild type receptor (Tables 4.1 and 4.2).

### **5.3.2. Internalisation studies**

No agonist-induced internalisation of the nicotinic acid receptors was detected in previous studies detailed in chapter 4. Based on this, neither chimeric receptor was expected to internalise in response to nicotinic acid treatment. This was examined utilising a cell surface ELISA assay, as described in section 4.5.2.4. CHO-K1 cell lines stably expressing VSV-G HM74A/HM74 eYFP or VSV-G HM74/HM74A eYFP were incubated in the presence and absence of nicotinic acid, as described in chapter 2.5.11 (Figure 5.4 A). No significant change in cell surface expression of either chimeric receptor was observed in the presence of nicotinic acid. Samples incubated only with a secondary antibody or in the absence of both primary and secondary antibodies served as negative controls.

To test the above observations did not reflect a lack of biological activity of the nicotinic acid utilised, the ability of nicotinic acid to induce ERK1/2 phosphorylation via the chimeric receptors was tested. Figure 5.4 B confirmed that nicotinic acid was able to induce ERK1/2 phosphorylation via the chimeric receptors and the lack of detectable internalisation of the chimeric receptors was not an artefact due to the use of inactive nicotinic acid. Total levels of ERK1/2, detected in parallel studies, served as loading controls.

## **5.4. Desensitisation studies**

In order to determine if the C-terminal region of the nicotinic acid receptors played a role in the desensitisation characteristics of HM74 and HM74A, nicotinic acid pre-treatment studies similar to those detailed in chapter 4 were conducted with CHO-K1 cell lines stably expressing the chimeric nicotinic acid receptors.

### **5.4.1. VSV-G HM74/HM74A eYFP**

A CHO-K1 cell line stably expressing VSV-G HM74/HM74A eYFP was treated with 10  $\mu$ M (Figure 5.5) or 10 mM (Figure 5.6) nicotinic acid for 0, 30, 60 minutes and 24 hours. The selected concentrations of nicotinic acid were approximately ten times the estimated pEC<sub>50</sub> value at either the host or donor receptors which formed the chimeric

receptor. Membrane preparations generated from these samples were then exposed to increasing concentrations of nicotinic acid, acifran or GSK 1 in [<sup>35</sup>S] GTP $\gamma$ S binding assays (Figures 5.5 A and 5.6 A respectively). For each of the pre-treatments, pEC<sub>50</sub> values for the ligands have been summarised in Figures 5.5 B and 5.6 B. In all cases, no significant change in the pEC<sub>50</sub> value was observed in control and nicotinic acid pre-treated samples and no significant change in the maximum binding of [<sup>35</sup>S] GTP $\gamma$ S was observed. In the same study, a significant reduction in [<sup>35</sup>S] GTP $\gamma$ S binding was observed in nicotinic acid pre-treated membranes prepared from CHO-K1 cells stably expressing wild type HM74 receptor when compared to membranes prepared from non-treated control cells.

#### **5.4.2. VSV-G HM74A/HM74 eYFP**

In a similar study, a CHO-K1 cell line stably expressing VSV-G HM74A/HM74 eYFP was treated with 10 mM nicotinic for 0 and 24 hours. Membrane preparations generated from these samples were then exposed to increasing concentrations of nicotinic acid in [<sup>35</sup>S] GTP $\gamma$ S binding assays (Figure 5.7). Although no significant change in the pEC<sub>50</sub> value was calculated in control and nicotinic acid pre-treated samples, a small reduction in [<sup>35</sup>S] GTP $\gamma$ S binding in samples pre-treated for 24 hours was observed (Figure 5.7). However this was not statistically significant.

## **5.5. Discussion**

Studies conducted in chapter 4 suggest HM74 and HM74A share many characteristics including nicotinic acid-induced receptor phosphorylation, a lack of  $\beta$ -arrestin 2 recruitment and no detectable receptor internalisation. However, desensitisation of G $\alpha_i$  mediated signalling was only observed as a result of prolonged nicotinic acid exposure to HM74 but not HM74A.

HM74 and HM74A are highly homologous, sharing 96 % identity at the protein level. As mentioned previously, the main structural difference between the two receptors is the longer C-terminal tail of HM74. As the C-terminal region of GPCRs is often important for receptor regulation, to test the hypothesis that the C-terminal region of

HM74 may play a role in the desensitisation characteristics of this receptor, 'nicotinic acid receptor C-terminal tail chimeras' were generated.

Due to the highly homologous nature of the receptors, exchanging the C-terminal regions of HM74 and HM74A did not disrupt the protein folding or targeting to the plasma membrane. The chimeras displayed wild type characteristics of cell surface expression. Despite the modification in the C-terminal region of the receptors, the relative expression levels of the receptors did not change; VSV-G HM74A/HM74 eYFP was expressed at a higher level than VSV-G HM74/HM74A eYFP. In cell lines stably expressing the original tagged receptor constructs, VSV-G HM74A eYFP was expressed at a higher level than VSV-G HM74 eYFP. This suggests that the protein domains upstream of the C-terminal region may be implicated in regulating receptor expression level.

The C-terminal chimeras were generated without disturbing the predicted ligand binding site formed by transmembrane helices II, III and VII (Tunaru et al., 2005). Therefore the exchange of the C-terminal region did not change the pharmacology of the host receptors. Furthermore, both chimeric receptors retained their ability to mediate ERK1/2 phosphorylation and did not internalise in response to nicotinic acid treatment.

To investigate the role of the C-terminal region of the nicotinic acid receptors in the regulation of these receptors, nicotinic acid pre-treatment studies were repeated with the CHO-K1 cell lines stably expressing the chimeric receptors. Membrane preparations generated from these samples were exposed to increasing concentrations of nicotinic acid, acifran and GSK 1 in [<sup>35</sup>S] GTP $\gamma$ S binding assays. In nicotinic acid pre-treatment studies of VSV-G HM74/HM74A eYFP, the desensitisation of HM74 observed in chapter 4 was abolished. This suggests the C-terminal tail of HM74 may be implicated in the regulation of this receptor. However, when these studies were repeated with the VSV-G HM74A/HM74 eYFP receptor chimera the reduction in [<sup>35</sup>S] GTP $\gamma$ S binding in samples pre-treated with nicotinic acid was not significant in a one way analysis of variance test.

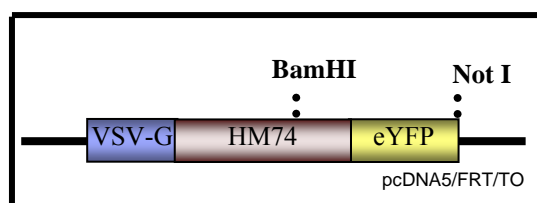
From the data presented for the VSV-G HM74A/HM74 eYFP receptor chimera, although a trend indicative of desensitisation is observed, the errors are large. In an ideal situation, these studies should have been repeated until satisfactory and reliable results were obtained. Due to time constraints this was not possible. Since the reduction in the maximum binding of [<sup>35</sup>S] GTPγS observed in nicotinic pre-treated samples was not significant, firm conclusions cannot be drawn from such data.

Thus it can only conclude that although the C-terminal region may play a role in the desensitisation of HM74 it is not clear at this present time if this region is sufficient or crucial for desensitisation of the HM74 receptor.

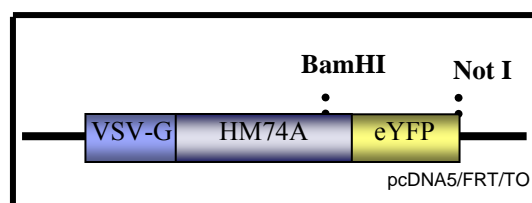
**A**

HM74	T S N N H S K K G H C H Q E P A S L E K Q L G C C I E
HM74A	T S P

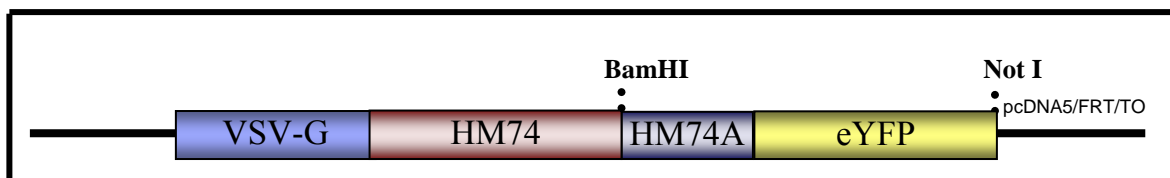
**B1**



**B2**



**B3**



**B4**

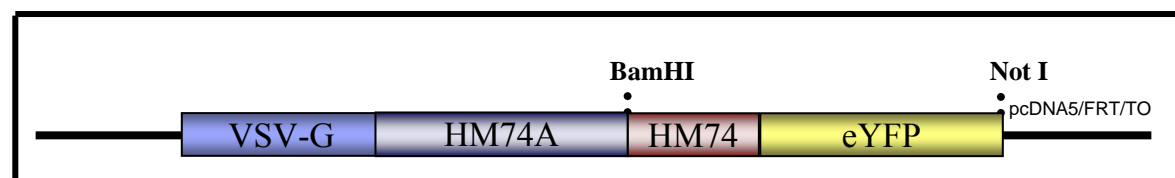
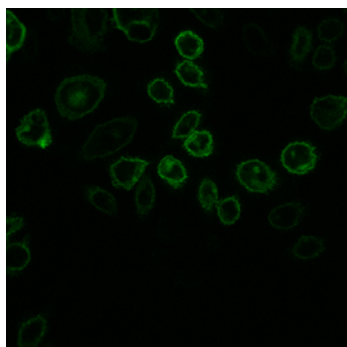


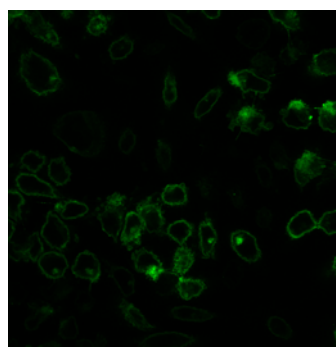
**Figure 5.1 Schematic diagram of C-terminal tail nicotinic acid receptor chimeras generated**

**A:** Alignment of HM74 and HM74A C-terminal sequences illustrating the longer C-terminal tail of HM74. **B:** Schematic figure illustrating the strategy designed to generate ‘C-tail’ chimeras of the nicotinic acid receptors. VSV-G HM74 eYFP (**B1**) and VSV-G HM74A eYFP (**B2**) receptor constructs were digested with the restriction enzymes indicated in **B1** and **B2**. The resulting receptor fragments were ligated to generate chimeric receptor constructs, VSV-G HM74/HM74A eYFP (**B3**) and VSV-G HM74A/HM74 eYFP (**B4**).

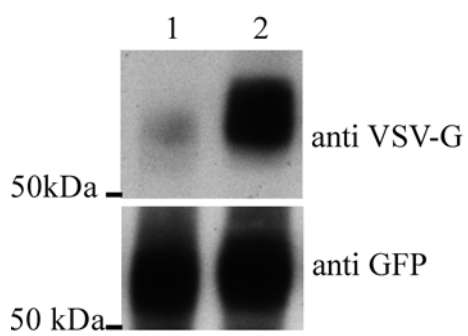
**A1**



**A2**



**B**



**C**

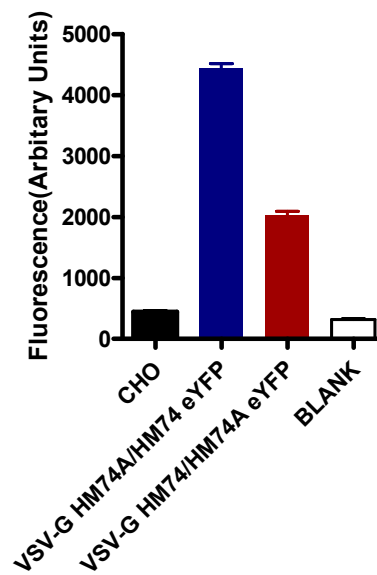
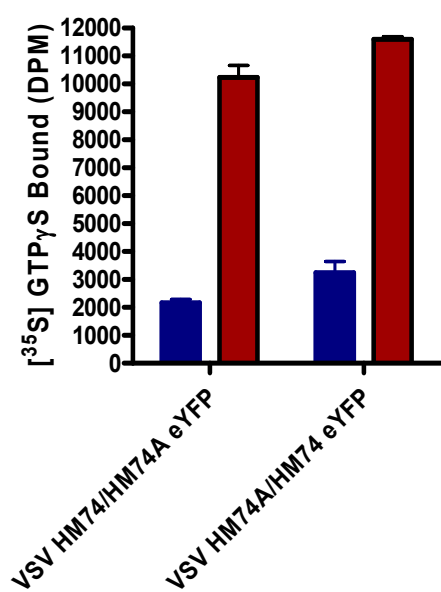


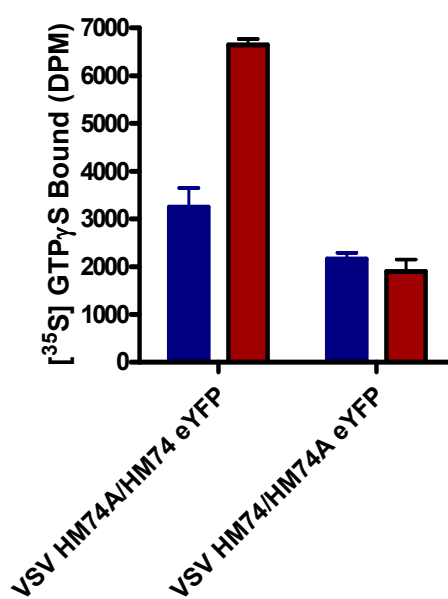
**Figure 5.2 Localisation and detection of chimeric nicotinic acid receptors stably expressed in Flp-In CHO-K1 cells**

Flp-In CHO-K1 cells were transfected with VSV-G HM74/HM74A eYFP or VSV-G HM74A/HM74 eYFP cDNA and subjected to 200 µg/ml hygromycin selection. For each transfected cell line, cells resistant to hygromycin antibiotic selection were pooled and screened by fluorescence imaging utilising the eYFP tag to identify receptor expression (**A**). VSV-G epitope and eYFP tagged forms of the HM74/HM74A (**A1**) and HM74A/HM74 (**A2**) receptors. **B**: 20 µg of cell lysates prepared from these cells were resolved by SDS-PAGE. Proteins representing the chimeric receptors were detected at the expected size (66 kDa); VSV-G HM74/HM74A eYFP (lane 1) and VSV-G HM74A/HM74 eYFP (lane 2). **C**: Whole cell lysates prepared from these cell lines were equalised for protein concentration and the eYFP fluorescence was measured with a Victor<sup>2</sup> plate reader. Negative controls of lysates prepared from parental CHO-K1 cells and a reading from an empty well (labelled blank) were also included. VSV-G HM74A/HM74 eYFP has a higher expression level than VSV-G HM74/HM74A eYFP.

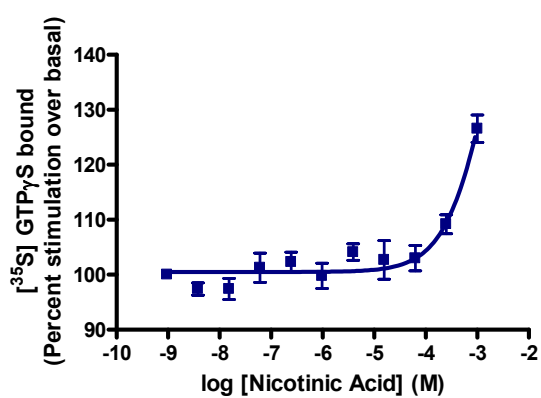
**A1**



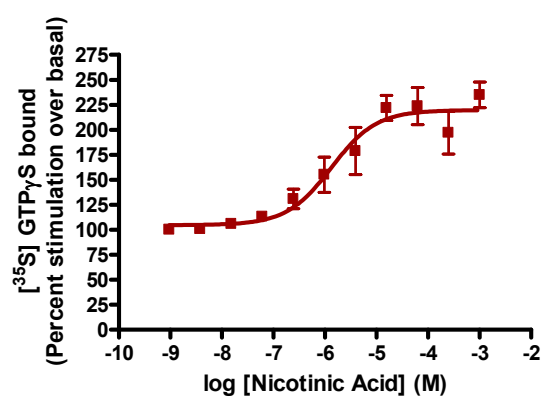
**A2**



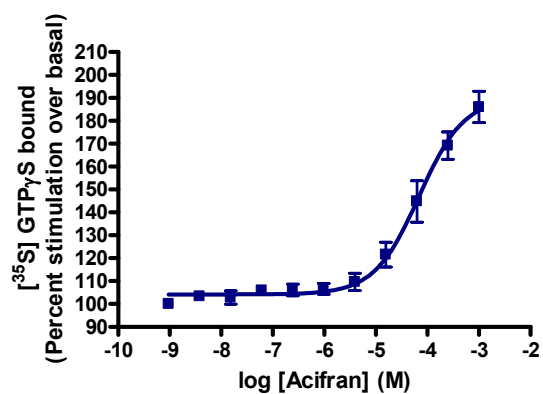
**B1**



**B2**



**C1**



**C2**

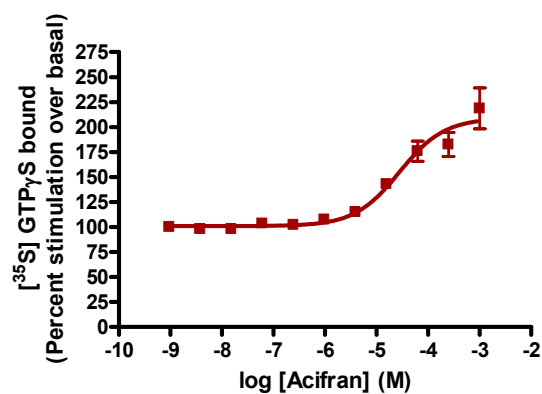


**Figure 5.3 Functional analysis of Flp-In CHO-K1 cell lines stably expressing chimeric nicotinic acid receptors**

**A:** A [ $^{35}\text{S}$ ] GTP $\gamma$ S binding assay was employed to test the response of the chimeric nicotinic acid receptors. The assays were terminated after 30 minutes incubation at room temperature by filtration of the samples onto GF/C fibre glass filters. Bound [ $^{35}\text{S}$ ] GTP $\gamma$ S was measured by liquid-scintillation spectrometry. Membrane preparations generated from cell lines expressing either the chimeric HM74A or chimeric HM74 receptor were incubated in the presence (red) and absence (blue) of **(A1)** 1 and 10 mM nicotinic acid respectively or **(A2)** 10 mM  $\beta$ -hydroxybutyrate. **B:** [ $^{35}\text{S}$ ] GTP $\gamma$ S binding scintillation proximity assays were employed to investigate native receptor pharmacology. Bound [ $^{35}\text{S}$ ] GTP $\gamma$ S was measured by scintillation counting. Nicotinic acid concentration response curves on membranes expressing **(B1)** VSV-G HM74/HM74A eYFP (estimated  $\text{pEC}_{50} = 2.8 \pm 0.5$ ) and **(B2)** VSV-G HM74A/HM74 eYFP ( $\text{pEC}_{50} = 5.9 \pm 0.2$ ) receptors. **C:** Acifran concentration response curves on membranes expressing **(C1)** VSV-G HM74/HM74A eYFP ( $\text{pEC}_{50} = 4.2 \pm 0.1$ ) and **(C2)** VSV-G HM74A/HM74 eYFP ( $\text{pEC}_{50} = 4.6 \pm 0.1$ ) receptors. Data were analysed using GraphPad Prism software. Grouped data of  $n=3$  shown. Data points represent means  $\pm$  SEM.

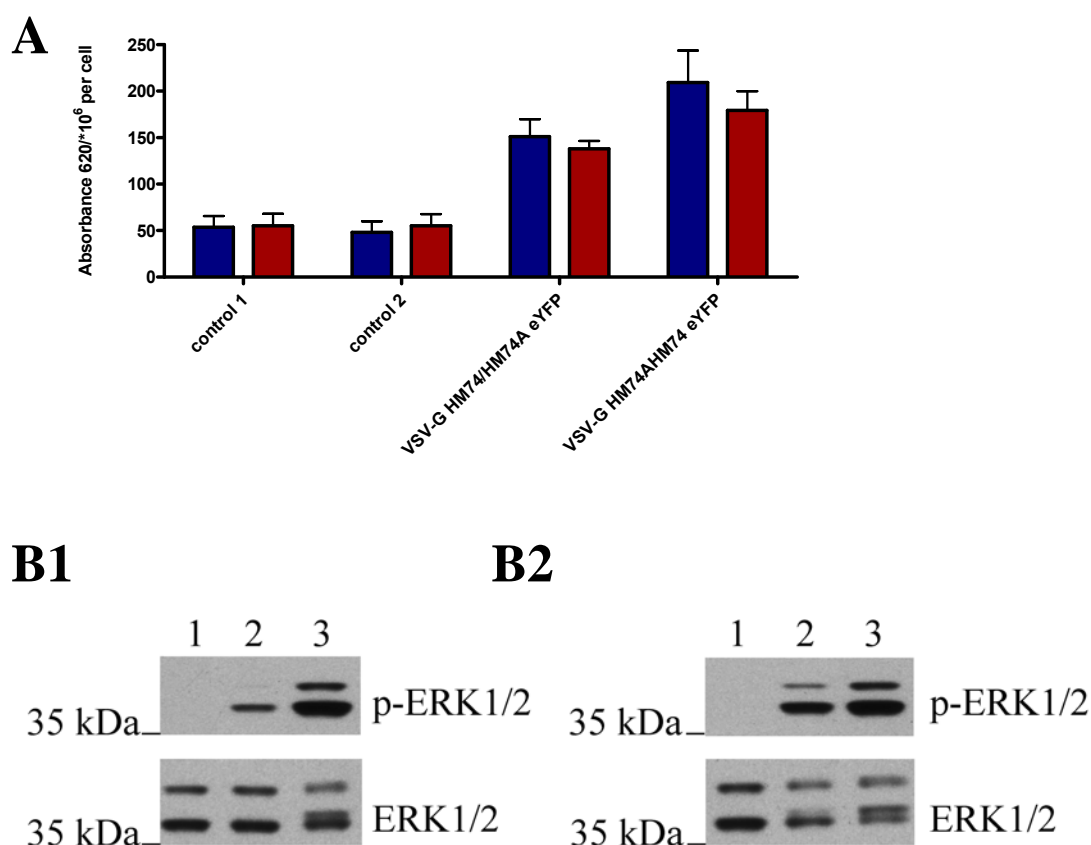
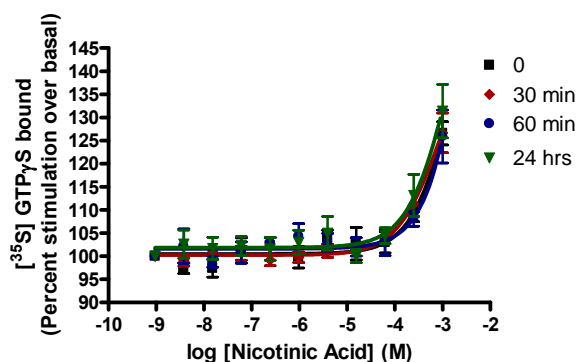


**Figure 5.4 Nicotinic acid does not internalise the chimeric receptors**

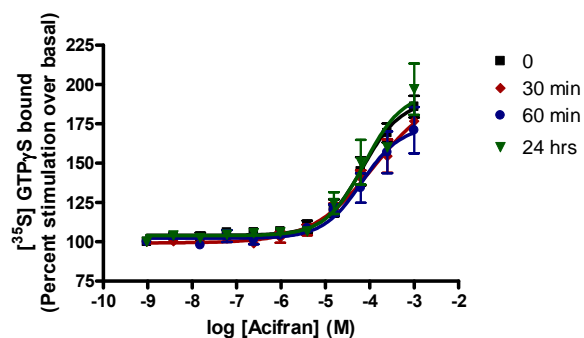
**A:** CHO-K1 cells stably expressing VSV-G HM74/HM74A eYFP or VSV-G HM74A/HM74 eYFP were incubated in the presence (red) and absence (blue) of 10 mM nicotinic acid for 30 minutes. Cell surface expression of the chimeric receptors was measured in an intact cell ELISA assay utilising an anti VSV-G antibody. Negative controls of no primary antibody (control 1) and no primary and secondary antibody (control 2) were incubated in the presence (red) and absence (blue) of 10 mM nicotinic acid. In a two-tailed t test, a p value of 0.5 was calculated in both cases; no significant change in cell surface expression was detected. Grouped data of  $n=4$  shown. Data points represent means  $\pm$  SEM. **B:** CHO-K1 cell line stably expressing VSV-G HM74/HM74A eYFP (**B1**) or VSV-G HM74A/HM74 eYFP (**B2**) were incubated with 10 mM nicotinic acid (lane 2) for 5 minutes in an ERK1/2 phosphorylation assay. A negative control of vehicle (lane 1) and positive control of 10 % foetal bovine serum treatment (lane 3) was included. Cell lysates prepared from the samples were equalised for protein content, resolved by SDS-PAGE and immunoblotted with anti ERK1/2 antiserum, to determine equal loading of samples and an anti phospho-ERK1/2 antibody to study ERK1/2 phosphorylation.

Immunoblots shown are representative of at least three independent experiments.  
Nicotinic acid induced ERK1/2 phosphorylation via the chimeric receptors.

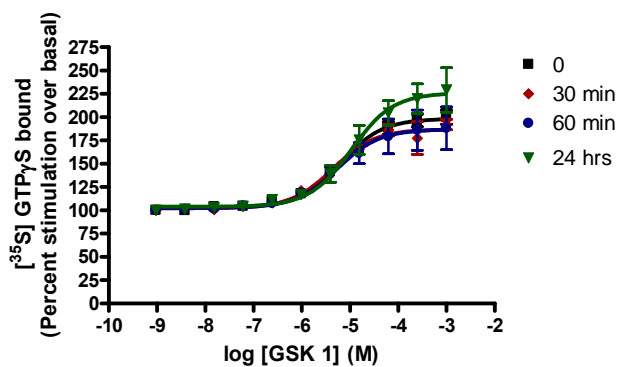
### A1



### A2



### A3



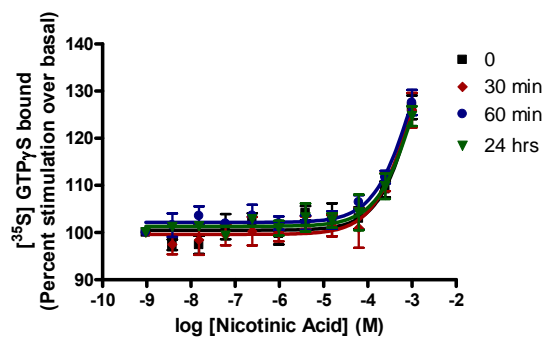
### B

10 $\mu$ M nicotinic acid pre-treatment (time)	Nicotinic acid pEC <sub>50</sub>	Acifran pEC <sub>50</sub>	GSK 1 pEC <sub>50</sub>
0	2.8 $\pm$ 0.5	4.2 $\pm$ 0.1	5.2 $\pm$ 0.1
30 mins	2.2 $\pm$ 2.8	3.9 $\pm$ 0.3	5.3 $\pm$ 0.1
60 mins	2.2 $\pm$ 1.8	4.2 $\pm$ 0.2	5.3 $\pm$ 0.2
24 hours	2.9 $\pm$ 0.4	4.1 $\pm$ 0.2	5.0 $\pm$ 0.1

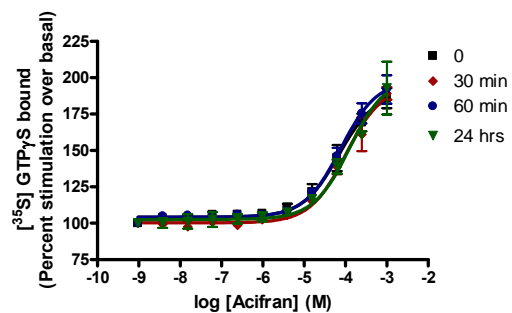
**Figure 5.5 Nicotinic acid pre-treatment does not cause desensitisation of VSV-G HM74/HM74A eYFP mediated activity of  $G\alpha_i$**

CHO-K1 cells stably expressing VSV-G HM74/HM74A eYFP receptor were incubated for 24 hours, 10  $\mu$ M nicotinic acid was present for 0, 30, 60 minutes and 24 hours. Membrane preparations generated were incubated in the presence of increasing concentrations of nicotinic acid (**A1**), acifran (**A2**) and GSK 1 (**A3**) in [ $^{35}$ S] GTP $\gamma$ S binding assays. Bound [ $^{35}$ S] GTP $\gamma$ S was measured by scintillation counting. When compared to control samples, no significant change in the maximum binding of [ $^{35}$ S] GTP $\gamma$ S was observed in pre-treated samples in a one way analysis of variance test. (**B**) Summary of pEC<sub>50</sub> values. Data were analysed using GraphPad Prism software. Grouped data of n=3 shown. Data points represent means  $\pm$  SEM.

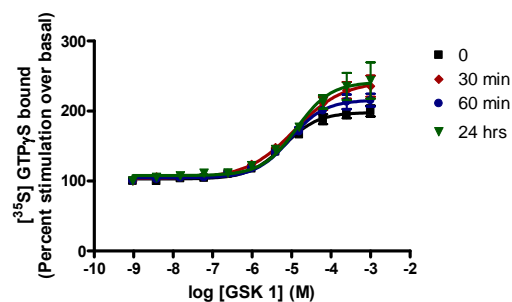
### A1



### A2



### A3

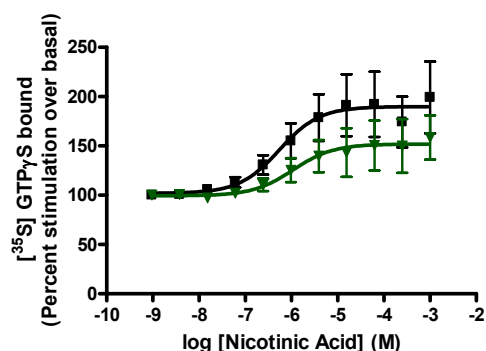


### B

10 mM nicotinic acid pre-treatment (time)	Nicotinic acid pEC <sub>50</sub>	Acifran pEC <sub>50</sub>	GSK 1 pEC <sub>50</sub>
0	2.8 ± 0.5	4.2 ± 0.1	5.2 ± 0.1
30 mins	3.4 ± 0.3	3.7 ± 0.3	4.9 ± 0.1
60 mins	3.0 ± 0.2	4.1 ± 0.1	5.0 ± 0.1
24 hours	2.9 ± 0.3	3.9 ± 0.1	4.9 ± 0.1

**Figure 5.6 Nicotinic acid pre-treatment does not cause desensitisation of VSV-G HM74/HM74A eYFP mediated activity of G $\alpha_i$**

CHO-K1 cells stably expressing VSV-G HM74/HM74A eYFP receptor were pre-treated with 10 mM nicotinic acid for 0, 30, 60 minutes and 24 hours. Membrane preparations generated were incubated in the presence of increasing concentrations of nicotinic acid (**A1**), acifran (**A2**) and GSK 1 (**A3**) in [ $^{35}$ S] GTP $\gamma$ S binding assays. Bound [ $^{35}$ S] GTP $\gamma$ S was measured by scintillation counting. When compared to control samples, no significant change in the maximum binding of [ $^{35}$ S] GTP $\gamma$ S was observed in pre-treated samples in a one way analysis of variance test. (**B**) Summary of pEC $_{50}$  values. Data were analysed using GraphPad Prism software. Grouped data of n=3 shown. Data points represent means  $\pm$  SEM.

**A****B**

10 mM nicotinic acid pre-treatment (time)	Nicotinic acid pEC <sub>50</sub>
0	6.2 ± 0.3
24 hours	6.0 ± 0.4

**Figure 5.7 No significant reduction in the maximum binding of [<sup>35</sup>S] GTP<sub>γ</sub>S observed in nicotinic acid pre-treated samples**

CHO-K1 cells stably expressing the VSV-G HM74A/HM74 eYFP chimeric receptor were pre-treated with 10 mM nicotinic acid for 0 (black) and 24 hours (green). Membrane preparations generated were incubated in the presence of increasing concentrations of nicotinic acid in [<sup>35</sup>S] GTP<sub>γ</sub>S binding assays (**A**). Bound [<sup>35</sup>S] GTP<sub>γ</sub>S was measured by scintillation counting. When compared to control samples, no significant change in nicotinic acid stimulated binding of [<sup>35</sup>S] GTP<sub>γ</sub>S was observed in pre-treated samples ( $p > 0.7$ ) in a one way analysis of variance test. (**B**). Data were analysed using GraphPad Prism software. Grouped data of  $n=3$  shown. Data points represent means  $\pm$  SEM.

## 6. Discussion

For nearly 50 years nicotinic acid has been successfully prescribed by clinicians to prevent cardiovascular disease and its associated mortality (Altschul et al., 1955). A greater understanding of the roles of different lipids, especially high levels of LDL cholesterol and low levels of HDL cholesterol as a risk factor for cardiovascular disease, has fostered a new enthusiasm for nicotinic acid therapy. To date, nicotinic acid is the only drug on the market proven to successfully raise HDL cholesterol levels to higher, protective concentrations. Nicotinic acid's molecular mechanism of action, however, still remains elusive. In order to address issues such as the gram quantities required to observe its lipid-modulating qualities and the main side effect, the so called 'niacin flush' it is critical to understand the basis by which nicotinic acid is able to lower total plasma levels of cholesterol and raise levels of protective lipids (Altschul et al., 1955; Morrow et al., 1989; Sakai et al., 2001). The recent identification of the nicotinic acid receptors as molecular targets for nicotinic acid has allowed these issues to be explored (Soga et al., 2003; Tunaru et al., 2003; Wise et al., 2003).

The gene encoding the high affinity nicotinic acid receptor, HM74A, is located in close proximity on chromosome 12 to the gene encoding its low affinity counterpart HM74 and to a more distantly related receptor, GPR81 (Zellner et al., 2005). Comparison of these homologues revealed a high degree of similarity, with HM74 and HM74A sharing the highest homology (Zellner et al., 2005). The main structural difference between these receptors is the extended C-terminal tail of HM74 (Wise et al., 2003). As the C-terminal tail of GPCRs is often implicated in receptor regulation it was hypothesised that the differences in this region may result in the differential regulation of HM74 and HM74A. This hypothesis was tested by examining the regulation and desensitisation characteristics of each receptor in a heterologous expression system and then, based on any differences identified, the importance of the C-terminal region was further analysed by the use of chimeric nicotinic acid receptors, where the C-terminal tail of HM74 and HM74A were exchanged.

The tools required for this study were generated; N- and C-terminus tagged HM74 and HM74A receptor constructs were engineered. The introduction of N- and C-terminal tags can potentially impact receptor localisation or function, for example, by disrupting protein folding. In the case of the  $\beta_2$ -adrenergic receptor, a single amino acid change in the C-terminal tail is sufficient to disrupt interactions with intracellular endocytic machinery and influence GPCR trafficking (Cao et al., 1999; Hall et al., 1998). The possibility of generating a non-functional or 'faulty' protein by introducing both N- and C-terminal tags should not be overlooked and for this reason the recombinant receptors were thoroughly characterised in transient and stable expression systems.

Localisation studies confirmed expression of the tagged nicotinic acid receptor constructs at the plasma membrane, however some intracellular expression was also observed. The cell surface expression pattern suggested that the N- and C-terminus tags did not interfere with trafficking of the receptor to the plasma membrane. The intracellular expression observed may be due to over-expression of the recombinant receptors, which is not unusual in heterologous expression systems where there is limited control over protein expression levels. Another possibility is that the long half-life of the fluorescent proteins contributed to the maintained presence of the GFP tagged receptors within the intracellular vesicles (McLean & Milligan, 2000). Published studies have reported plasma membrane expression of the nicotinic acid receptors, however additional intracellular expression has also been observed (Tunaru et al., 2005; Zhang et al., 2005). Again, these studies were also utilising receptors tagged with fluorescent proteins in a heterologous expression system.

The ligand binding sites of the nicotinic acid receptors is predicted to be formed by TM II, III and VII (Tunaru et al., 2005). Although, the N-terminal VSV-G epitope tag is not close to this predicted ligand binding site and studies have reported that the addition of N-terminal epitope tags has no effect on ligand binding, the ability of the modified receptors to respond to nicotinic acid was examined (Terrillon et al., 2004). As the C-terminal region of GPCRs are important for G protein interactions, G protein coupling was also assessed in this study. It was shown that the presence of the N- and C-terminal tags did not disrupt the pharmacological properties of the nicotinic acid receptors by altering the ligand binding site or preventing G protein coupling. The

pEC<sub>50</sub> values determined in this study were consistent with values obtained from both endogenously expressed receptors and recombinant expression systems (Lorenzen et al., 2001; Tunaru et al., 2003; Wise et al., 2003). Recombinant nicotinic acid receptors displayed native pharmacology and therefore were shown to be useful and reliable tools to study the regulation of the nicotinic acid receptors.

In desensitisation studies, HM74 but not HM74A displayed desensitisation as a result of prolonged exposure to nicotinic acid. Although, in nicotinic acid concentration response curves there was no change in pEC<sub>50</sub> values estimated for membranes prepared from control and pre-treated cells expressing HM74, there was a significant reduction in the maximum binding of [<sup>35</sup>S] GTPγS. This suggested desensitisation of HM74 signalling. This observation was in agreement with studies conducted by Green and co-workers in 1992, which reported that prolonged incubation of adipocytes with nicotinic acid reduced sensitivity of the cells to nicotinic acid in lipolysis assays (Green et al., 1992). However, as these studies were published before the identification of the nicotinic acid receptors the mechanism behind the desensitisation could not be explored. Green and co-workers also confirmed the observations made in this study, that nicotinic acid does not induce Gα<sub>i</sub> G protein downregulation (Green et al., 1992). Therefore studies presented in this thesis build upon the work by Green and co-workers and suggests a potential role for HM74 in the reduced sensitivity observed.

To examine the potential role of the C-terminal tail of HM74 in the desensitisation characteristics of this receptor, nicotinic acid C-terminal tail chimeras were generated; the C-terminal region of HM74 and HM74A receptor were exchanged. With respect to basic pharmacology, these receptor chimeras were shown to behave as their wild type counterparts. As the ligand binding site was not modified in the generation of the chimeric receptors a change in the basic pharmacological properties was not expected. With the use of a HM74A selective agonist, β-hydroxybutyrate, results obtained from [<sup>35</sup>S] GTPγS binding assays confirmed this. β-hydroxybutyrate was only active at the chimera with the HM74A N-terminal region. When nicotinic acid pre-treatment studies were conducted on cell lines stably expressing the HM74 receptor modified to possess the HM74A C-terminal region, the desensitisation of HM74 observed in previous studies was abolished. This suggests the C-terminal region of HM74 may be

implicated in the desensitisation of HM74. As no firm conclusions could be drawn from studies of the HM74A chimera possessing the HM74 C-terminal region, it is not possible to conclude whether the C-terminal region of HM74 alone is crucial for desensitisation or required in combination with other regions. If however, HM74A/HM74 C-terminal chimera was shown to desensitise a more conclusive observation could have been drawn. For this reason, to understand the role of the C-terminal region in the regulation of the nicotinic acid receptors, nicotinic acid pre-treatment studies should be repeated with this cell line.

If the presence of the C-terminal region of HM74, results in desensitisation of HM74A, then in future experiments HM74A chimeras possessing truncated forms of the HM74 C-terminal region should be engineered and the nicotinic acid pre-treatments studies repeated. These studies should highlight the important regions of the C-terminal tail. Once the crucial region has been identified, the key amino acid(s) can then be determined by site directed mutagenesis studies.

The ability of nicotinic acid to stimulate ERK1/2 phosphorylation via the nicotinic acid receptors was examined and differential kinetics were identified. Nicotinic acid was able to stimulate ERK1/2 phosphorylation rapidly via HM74A and signalling was sustained at least until 60 minutes. However, signalling via HM74 was slower and more transient. The mechanisms behind these kinetic differences can be investigated by utilising the C-terminal chimeras. It is possible the C-terminal region of the nicotinic acid receptors play a role and if the characteristics of ERK1/2 phosphorylation are switched in the chimeras then this would provide strong evidence for this. Key players at the amino acid level could then be identified by site-directed mutagenesis studies similar to those described above.

Alternatively, if the kinetics of ERK1/2 phosphorylation remain unchanged in the studies utilising the chimeric receptors, then it is possible that the difference observed is due to the different ligand (nicotinic acid) on/off rate at each receptor. The ligand on/off rate at each receptor can be calculated by performing association and dissociation binding assays. However, due to the relatively low potency of nicotinic acid at both HM74 and HM74A, these experiments would require huge amounts of radiolabelled ligand and therefore were not considered viable. However, it can be

hypothesised that nicotinic acid has a slower on rate at HM74 than HM74A and therefore this translates as slower ERK1/2 phosphorylation via HM74. It would be interesting to perform ERK1/2 phosphorylation assays with acifran, which has a similar potency at both HM74 and HM74A. Acifran, which has been shown to stimulate ERK1/2 phosphorylation (Mahboubi et al., 2006), may have a similar on/off rate at both receptors, and therefore it can be further hypothesised similar ERK1/2 phosphorylation kinetics.

With the increasing interest in examining GPCR signalling at different levels of the downstream pathway, if time had permitted, the nicotinic acid pre-treatment studies described in this thesis to study receptor desensitisation would have been investigated with respect to ERK1/2 phosphorylation. These findings could then be compared to those obtained from [<sup>35</sup>S] GTPγS binding assays. It would not be inconceivable that prolonged nicotinic acid exposure results in desensitisation of receptor signalling in one pathway but not in another. Should this be the case, it would add to the many published reports of biased agonism or ‘agonist-directed trafficking’ (Kenakin, 1995; Berg et al., 1998; Backstrom et al., 1999; Richman et al., 2007). As nicotinic acid-stimulated ERK1/2 phosphorylation was demonstrated to be G protein mediated any agonist bias with respect to ERK1/2 phosphorylation is likely to be post G protein activation.

The regulation of the nicotinic acid receptors was investigated further by examining nicotinic acid-induced internalisation of both HM74 and HM74A. However, there was no convincing evidence of receptor internalisation or β-arrestin 2 interactions in response to nicotinic acid treatment.

These findings were not consistent with published work which demonstrated nicotinic acid-induced internalisation of HM74A in a β-arrestin dependent fashion (Richman et al., 2007). Potentially these opposing findings may be related to differences in the experimental set up, such as cell background or species of β-arrestin utilised, or the possible detrimental effects of N- or C-terminal tagging of the receptors, as detailed in section 4.6. However, as discussed previously, these issues are unlikely to explain the differences. For example, by utilising wild type nicotinic acid receptors in the β-arrestin translocation studies any detrimental effect of the C-terminal eYFP tagging on

the receptor/ $\beta$ -arrestin binding was avoided. However,  $\beta$ -arrestin 2 GFP did not translocate to the cell surface in response to nicotinic acid in cells expressing the unmodified receptors. Although, this observation on its own is not sufficient to conclude that the nicotinic acid receptors do not internalise in response to nicotinic acid, a lack of  $\beta$ -arrestin translocation is supportive of the observations made in various internalisation studies.

To add value to the observations made from the  $\beta$ -arrestin translocation experiments,  $\beta$ -arrestin trapping experiments can also be performed.  $\beta$ -arrestin internalises GPCRs via a clathrin-dependent pathway (von Zastrow & Kobilka, 1994; Ferguson et al., 1996). Sucrose inhibits clathrin recruitment and interferes with coated-pit formation and therefore endocytosis (Ashworth et al., 1995; Hansen et al., 1993). Therefore hypertonic concentrations of sucrose would prevent  $\beta$ -arrestin from internalising the receptor. It could be argued that the lack of translocation observed actually is a lack of detectable translocation and does not necessarily equate to no translocation. In the case that the nicotinic acid receptors only interact with  $\beta$ -arrestin in a rapid and transient fashion, experiments where high concentrations of sucrose are included would 'trap'  $\beta$ -arrestin at the cell surface. The use of high affinity  $\beta$ -arrestin mutants would complement this study. By introducing two mutations (R404E, R406E) into the amino acid sequence of  $\beta$ -arrestin 2, it has been shown that  $\beta$ -arrestin 2 gains higher affinity for GPCRs (Heding, 2004). If the nicotinic acid receptors interact with  $\beta$ -arrestin 2 then by using the mutant protein this interaction would be more stable and therefore more likely to be detected.

As mentioned previously, unpublished studies by Offermanns and co-workers have also failed to detect internalisation of HM74A in response to nicotinic acid. These studies utilised N-terminal tagged receptors in a variety of cell types including COS-7 and CHO-K1 cell lines (personal communication, Professor S. Offermanns). This further supports the observations made in this thesis.

As receptor phosphorylation can play a role in the regulation of receptor signalling, the ability of the nicotinic acid receptors to be phosphorylated in an agonist-dependent manner was examined. In both cases, an increase in receptor phosphorylation was

observed following nicotinic acid treatment. As agonist-dependent phosphorylation is often considered to be one of the first stages of  $\beta$ -arrestin interaction and receptor sequestration, at this moment the function or the downstream implication of receptor phosphorylation is unclear. In any case, it is possible that the nicotinic acid receptors can undergo dephosphorylation and therefore resensitisation at the plasma membrane, much like the thyrotropin-releasing hormone receptor which has been reported to dephosphorylate at the cell surface without the need to be internalised (Jones & Hinkle, 2005).

GRK, PKA and PKC are expressed in adipocytes and therefore it was hypothesised they may play a role in the agonist-dependent phosphorylation of the nicotinic acid receptors. Through kinase inhibitor studies both PKC and PKA were implicated, to some degree, in HM74 but not HM74A phosphorylation. However, as PKC and PKA selective inhibitors failed to completely abolish nicotinic acid-induced phosphorylation of HM74, other kinases are anticipated to be involved. It would be interesting to repeat these studies with the C-tail chimeras to examine if PKC and PKA inhibitors have an effect on the phosphorylation of the HM74A chimera with the HM74 C-tail and vice versa. A note of caution should be highlighted here with respect to studying receptor regulation in recombinant systems (as used in this study) as receptors may be differentially regulated from those that are endogenously expressed. For example, the M<sub>3</sub> muscarinic receptor can be differentially phosphorylated depending on whether it is heterologously expressed in CHO cells or endogenously expressed in cerebellar granule neurons (Torrecilla et al., 2007). This highlights the importance of studying receptor function/regulation in native cell types where possible.

Due to the lack of robust tools, the role of GRKs in the phosphorylation of the nicotinic acid could not be investigated. Although a gene silencing approach was attempted, due to an inconsistency with the level of knockdown achieved from experiment to experiment, this approach could not be pursued.

Although existing evidence supports the role of HM74A as the mediator of nicotinic acid's lipid-modulating effects, the potential importance of HM74 can not be ignored (Tunaru et al., 2003; Zhang et al., 2005; Taggart et al., 2005). As mentioned in section

1.6, the high doses of nicotinic acid required to produce a pharmacological response suggest HM74 may mediate some of the anti-lipolytic effects. It has, however, been reported that 90 % of nicotinic acid administered is eliminated from the body as unchanged nicotinic acid or nicotinuric acid (Gille et al., 2008). The remaining 10 % has a half-life of only 20 – 45 minutes in the plasma, so there is a possibility that the vitamin may not be able to maintain the concentrations required to activate HM74.

Based on current evidence, a role for HM74 in nicotinic acid-mediated lipolysis inhibition can not be fully ruled out. For example of the three studies reporting HM74A as the clinical target for nicotinic acid, two have been conducted in mouse model systems where there is no HM74 orthologue (Taggart et al., 2005; Tunaru et al., 2003). Therefore the role of HM74 could not be investigated. In studies by Zhang and colleagues, although it was demonstrated that nicotinic acid was unable to inhibit lipolysis in 3T3 L1 cells expressing human HM74 cDNA, this conclusion was drawn from data obtained from a heterologous expression system examining HM74 in isolation (Zhang et al., 2005).

In humans, due to the presence of both HM74A and HM74, deduction of the clinical target is more complicated and therefore only studies conducted in native cell lines in a physiologically relevant context can be conclusive. For example, there is the possibility that an individual's response to nicotinic acid may be dependent on which HM74 and HM74A haplotype they carry. At least two non-synonymous nucleotide changes that fall within the coding regions of HM74 have been identified (Zellner et al., 2005). These changes in amino acid sequence may impact receptor function. Studies examining receptors in isolation do not allow for these types of issues to be addressed. It may also be possible that HM74 requires the expression of HM74A to mediate anti-lipolytic effects. Given the high homology between these receptors it would not be surprising if they form heterodimers. It would be interesting to examine this by utilising co-immunoprecipitation and various biophysical techniques such as resonance energy transfer (RET) based methods, including fluorescence resonance energy transfer (FRET) and bioluminescence resonance energy transfer (BRET). RET based techniques are highly sensitive and enable protein-protein interactions to be analysed in real time, in living cells. Briefly, RET is the energy transfer from a donor molecule to an acceptor molecule as a result of dipole-dipole coupling in a non-

radiative manner. In the case where the donor molecule is a fluorescent molecule, exposure to light of a characteristic wavelength will result in excitation and subsequent energy transfer is then referred to as a FRET signal. Where the donor is the enzyme *Renilla luciferase* (Rluc), oxidation of a suitable substrate releases energy and the resultant energy transfer to a fluorescent acceptor molecule is referred to as BRET signal. These RET based techniques have been summarised in Figure 6.1 (Pfleger & Eidne, 2005).

The physiological relevance of the desensitisation of HM74 has yet to be determined. At this moment it is not known if this level of desensitisation could be translated into a significant response in a physiological system. Although, studies by Green and co-workers suggested reduced sensitivity of nicotinic acid pre-treated adipocytes to nicotinic acid, this was a measurement of lipolysis by quantification of glycerol release (Green et al., 1992). An examination of HDL and LDL cholesterol levels would be more informative and these studies would have to be conducted with the knowledge that HM74A does not desensitise and therefore could compensate for HM74. Keeping in mind the importance of endogenously expressed receptors, further studies, if possible, should be conducted in cells which endogenously express the nicotinic acid receptors, such as adipocytes or human epidermoid A431 cells (Zhou et al., 2007). The identification of selective agonists for HM74A and HM74 should help clarify the roles of each receptor in lipolysis and lipid-modulation.

Currently, there are limited published studies highlighting GPCRs which do not desensitise in response to prolonged agonist exposure. However, the  $\alpha_2$ -adrenergic subtype  $\alpha_2C10$ ,  $\beta_3$ -adrenergic and GnRH type I receptors are examples of such GPCRs (Kurose & Lefkowitz, 1994; Jewell-Motz & Liggett, 1996; Liggett et al., 1993; McArdle et al., 2002). As it is generally accepted that HM74A is likely to be the clinical target for nicotinic acid it will be of great interest to pharmaceutical companies that this receptor did not display any desensitisation characteristics (Tunaru et al., 2003; Zhang et al., 2005). Patients on nicotinic acid therapy develop tolerance to the nicotinic acid-induced flushing response, however do not develop tolerance to the lipid-modifying effects of this drug (Stern et al., 1991; Offermanns, 2006). In this context, a lack of desensitisation of HM74A could begin to explain the lasting effects of nicotinic acid treatment. Once the mechanism(s) by which nicotinic

acid acts is fully understood, novel, more potent drugs which do not cause desensitisation or the uncomfortable flushing response may be designed.

As expected, many pharmaceutical companies are already in the process of developing such compounds. Arena and Merck, for example, have reported compounds which have anti-lipolytic qualities but apparently do not cause the flushing normally associated with the use of nicotinic acid (Richman et al., 2007; Shen et al., 2007a; Shen et al., 2007b). Published studies by Richman and co-workers show these non-flushing compounds do not internalise HM74A or induce ERK1/2 phosphorylation via this receptor (Richman et al., 2007). Recent communication suggests the beneficial effects of these compounds did not translate in their entirety in human trials (personal communication, Prof. G. Milligan). It seems the beneficial rise in HDL levels was not observed in humans, therefore nicotinic acid remains the only drug in the market capable of this.

GlaxoSmithKline have developed similar compounds that also do not cause flushing (unpublished data). One such compound, a xanthine derivative (GSK 3), is a selective agonist at HM74A (SmithKline Beecham Corporation., 2005). GSK 3 is more potent than nicotinic acid in [<sup>35</sup>S] GTP $\gamma$ S assays of HM74A activation (Figure 6.2). Unlike the compounds described by Richman and co-workers, this ligand does induce ERK1/2 phosphorylation in a pertussis toxin-sensitive manner (Figure 6.3). GSK 3-induced ERK1/2 phosphorylation was not as sustained as that observed with nicotinic acid (Figure 4.3) but could be detected at a lower level for up to 60 minutes (Figure 6.3). Preliminary [<sup>32</sup>P] orthophosphate experiments suggest 10  $\mu$ M GSK 3 is required to stimulate HM74A phosphorylation (Figure 6.4). However, the ability of GSK 3 to induce internalisation of HM74A has not been examined thus far.

Studies by Benyo and co-workers have implicated HM74A receptors, expressed on Langerhans cells, as the mediators of nicotinic acid-induced flushing (Benyo et al., 2005; Benyo et al., 2006). It is currently thought that HM74A mediates this flushing response via the prostanoids, especially prostaglandin D<sub>2</sub> (PGD<sub>2</sub>), which are produced after nicotinic acid administration (Morrow et al., 1989; Stern et al., 1991). Merck's attempt to capitalise on this knowledge and introduce Cordaptive, the brand name for a novel drug combining extended-release nicotinic acid and a selective prostaglandin

antagonist, laropiprant, has recently been rejected by the FDA. Although the reasons behind the rejection are not clear, it can be speculated that the use of selective inhibitors of prostaglandin function may result in other unknown or unwanted biological effects.

Although, a lack of available tools and the low affinity of the nicotinic acid receptors has made the characterisation of both HM74 and HM74A difficult, the identification of selective agonists at either HM74 (Skinner et al., 2007a; Semple et al., 2006) or HM74A (Taggart et al., 2005; Skinner et al., 2007b; Shen et al., 2007a; Shen et al., 2007b) will be beneficial for future studies. The studies described in this thesis have generated many tools and identified differences between HM74 and HM74A which can be exploited to further investigate the mechanisms by which the nicotinic acid receptors are regulated.

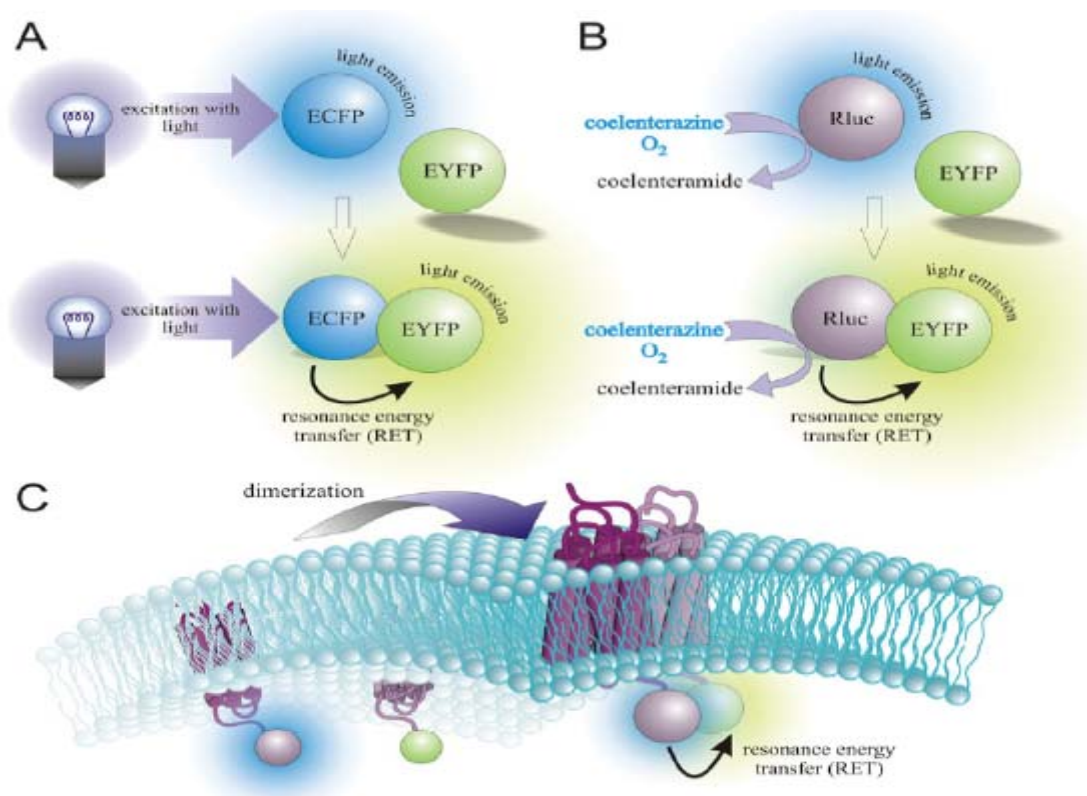


**Figure 6.1** Diagram illustrating principles of RET based techniques

**A:** FRET is the result of the energy transfer from a donor fluorophore excited with light at specific wavelength. **B:** Oxidation of coelenterazine to coelenteramide by the donor Rluc results in an energy transfer to a fluorescent molecule, resulting in a BRET signal. **C:** Example illustrating how the RET based techniques can be adopted to study dimerisation of receptors. Figure from (Pfleger & Eidne, 2005).

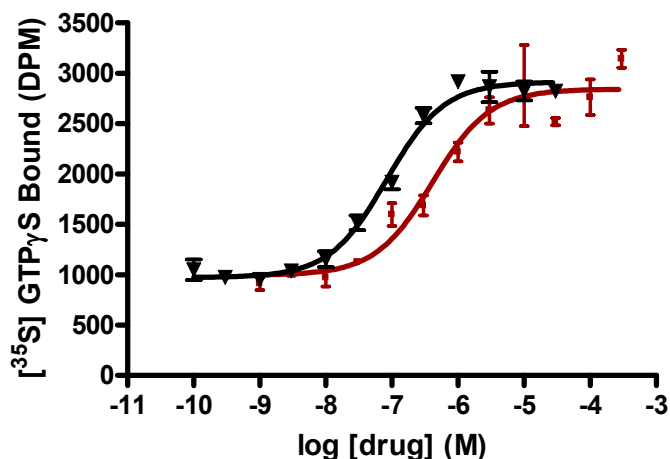
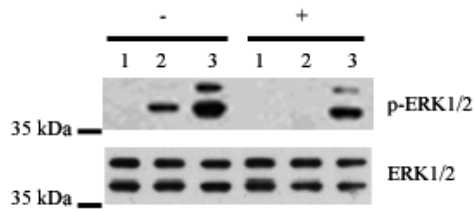


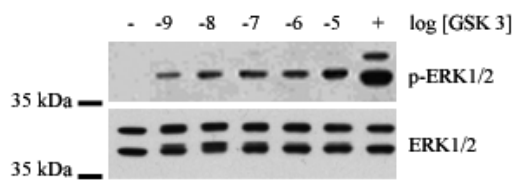
**Figure 6.2 GSK 3: A novel and potent HM74A agonist that does not induce flushing**

A [<sup>35</sup>S] GTP<sub>γ</sub>S binding assay was employed to compare the response of HM74A expressing CHO-K1 membranes to increasing concentrations of GSK 3 (black: pEC<sub>50</sub> = 7.1 ± 0.1) and nicotinic acid (red: pEC<sub>50</sub> = 6.4 ± 0.2). Bound [<sup>35</sup>S] GTP<sub>γ</sub>S was measured by liquid-scintillation spectrometry. Results are representative of three independent experiments. Data points represent means ± SEM. Data were analysed using GraphPad Prism software.

**A**



**B**



**C**

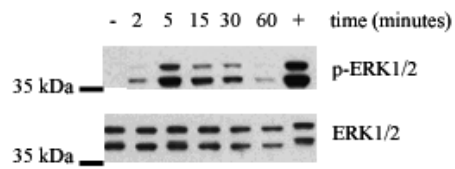


**Figure 6.3 GSK 3 stimulated ERK1/2 phosphorylation. ERK1/2 phosphorylation was abolished by pertussis toxin treatment**

**A:** CHO-K1 cells stably expressing HM74A were serum starved and treated in the presence (+) and absence (-) of 25 ng/ml pertussis toxin for 16 hours at 37 °C. Cells were then incubated with 100 nM GSK 3 (lane 2) for 5 minutes in an ERK1/2 phosphorylation assay. A negative control of vehicle (lane 1) and positive control of 10 % foetal bovine serum treatment (lane 3) were included. In similar assays, cells were exposed to increasing concentrations of GSK 3 for 5 minutes (**B**) or 100 nM GSK 3 for varying lengths of time (minutes) (**C**). A negative control of vehicle (-) and positive control of 10 % foetal bovine serum treatment (+) was included in every experiment. Cell lysates prepared from the samples were equalised for protein content, resolved by SDS-PAGE and immunoblotted with anti ERK1/2 antiserum to determine equal loading of samples (42/44 kDa) and anti phospho-ERK1/2 antibody to study ERK1/2 phosphorylation (42/44 kDa). GSK 3 induced ERK1/2 phosphorylation via HM74A was detected at low levels up until 60 minutes and was abolished by pertussis toxin treatment. 1 nM GSK 3 was sufficient to stimulate ERK1/2 phosphorylation. Results shown are representative of three independent experiments.

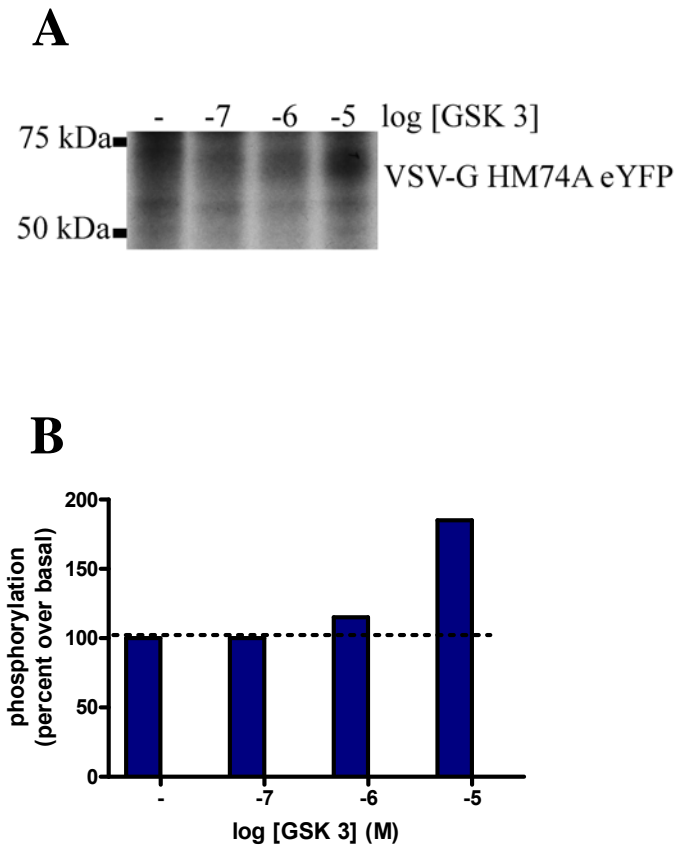


**Figure 6.4 GSK 3-induced phosphorylation of VSV-G HM74A eYFP**

CHO-K1 cells stably expressing VSV-G HM74A eYFP were pre-incubated with 0.2 mCi/ml [ $^{32}$ P] orthophosphate for 90 minutes. Cells were incubated for 15 minutes in the presence of increasing concentrations of GSK 3. Control of cells treated with vehicle (-) were also included. Cell lysates were prepared and equalised for protein content and volume before immunoprecipitating with an anti VSV-G antiserum to isolate the receptor. **A:** Samples were resolved by SDS-PAGE and phospho-proteins visualised by autoradiography. **B:** Quantification of signal intensity represented as percent phosphorylation over basal. VSV-G HM74A eYFP was phosphorylated by 10  $\mu$ M GSK 3. Results are representative of three independent experiments.

## 7. Reference List

Ahn, S., Shenoy, S. K., Wei, H., & Lefkowitz, R. J. (2004). Differential kinetic and spatial patterns of  $\beta$ -arrestin and G protein-mediated ERK activation by the angiotensin II receptor. *Journal of Biological Chemistry* **279**, 35518-35525.

Aktories, K., Schultz, G., & Jakobs, K. H. (1983a). Inhibition of adenylate cyclase and stimulation of a high affinity GTPase by the antilipolytic agents, nicotinic acid, acipimox and various related compounds. *Arzneimittelforschung*. **33**, 1525-1527.

Aktories, K., Schultz, G., & Jakobs, K. H. (1983b). Islet-activating protein prevents nicotinic acid-induced GTPase stimulation and GTP but not GTP $\gamma$ S-induced adenylate cyclase inhibition in rat adipocytes. *FEBS Lett.* **156**, 88-92.

Altschul, R., Hoffer, A., & Stephen, J. D. (1955). Influence of nicotinic acid on serum cholesterol in man. *Arch.Biochem.* **54**, 558-559.

Anderson, H. A., Chen, Y., & Norkin, L. C. (1996). Bound simian virus 40 translocates to caveolin-enriched membrane domains, and its entry is inhibited by drugs that selectively disrupt caveolae. *Mol.Biol.Cell* **7**, 1825-1834.

Anderson, R. G. (1993). Caveolae: where incoming and outgoing messengers meet. *Proc.Natl.Acad.Sci.U.S.A* **90**, 10909-10913.

Anderson, R. G., Kamen, B. A., Rothberg, K. G., & Lacey, S. W. (1992). Potocytosis: sequestration and transport of small molecules by caveolae. *Science* **255**, 410-411.

Arena Pharmaceuticals.Inc. Human G protein-coupled receptors and modulators thereof for the treatment of metabolic-related disorders. [US2004/0142377A1]. 2008. Ref Type: Patent

Asano, T., Pedersen, S. E., Scott, C. W., & Ross, E. M. (1984). Reconstitution of catecholamine-stimulated binding of guanosine 5'-O-(3-thiotriphosphate) to the stimulatory GTP-binding protein of adenylate cyclase. *Biochemistry* **23**, 5460-5467.

Ashworth, R., Yu, R., Nelson, E. J., Dermer, S., Gershengorn, M. C., & Hinkle, P. M. (1995). Visualization of the thyrotropin-releasing hormone receptor and its ligand during endocytosis and recycling. *Proc.Natl.Acad.Sci.U.S.A* **92**, 512-516.

Attramadal, H., Arriza, J. L., Aoki, C., Dawson, T. M., Codina, J., Kwatra, M. M., Snyder, S. H., Caron, M. G., & Lefkowitz, R. J. (1992).  $\beta$ -arrestin2, a novel member

of the arrestin/ $\beta$ -arrestin gene family. *Journal of Biological Chemistry* **267**, 17882-17890.

Backstrom, J. R., Chang, M. S., Chu, H., Niswender, C. M., & Sanders-Bush, E. (1999). Agonist-directed signaling of serotonin 5-HT<sub>2C</sub> receptors: differences between serotonin and lysergic acid diethylamide (LSD). *Neuropsychopharmacology* **21**, 77S-81S.

Ballesteros, J. A., Jensen, A. D., Liapakis, G., Rasmussen, S. G., Shi, L., Gether, U., & Javitch, J. A. (2001). Activation of the  $\beta_2$ -adrenergic receptor involves disruption of an ionic lock between the cytoplasmic ends of transmembrane segments 3 and 6. *Journal of Biological Chemistry* **276**, 29171-29177.

Barak, L. S., Ferguson, S. S., Zhang, J., & Caron, M. G. (1997). A  $\beta$ -arrestin/green fluorescent protein biosensor for detecting G protein-coupled receptor activation. *Journal of Biological Chemistry* **272**, 27497-27500.

Barlic, J., Khandaker, M. H., Mahon, E., Andrews, J., DeVries, M. E., Mitchell, G. B., Rahimpour, R., Tan, C. M., Ferguson, S. S., & Kelvin, D. J. (1999).  $\beta$ -arrestins regulate interleukin-8-induced CXCR1 internalization. *Journal of Biological Chemistry* **274**, 16287-16294.

Beltman, J., McCormick, F., & Cook, S. J. (1996). The selective protein kinase C inhibitor, Ro-31-8220, inhibits mitogen-activated protein kinase phosphatase-1 (MKP-1) expression, induces c-Jun expression, and activates Jun N-terminal kinase. *Journal of Biological Chemistry* **271**, 27018-27024.

Benovic, J. L., Kuhn, H., Weyand, I., Codina, J., Caron, M. G., & Lefkowitz, R. J. (1987). Functional desensitization of the isolated  $\beta$ -adrenergic receptor by the  $\beta$ -adrenergic receptor kinase: potential role of an analog of the retinal protein arrestin (48-kDa protein). *Proc.Natl.Acad.Sci.U.S.A* **84**, 8879-8882.

Benovic, J. L., Pike, L. J., Cerione, R. A., Staniszewski, C., Yoshimasa, T., Codina, J., Caron, M. G., & Lefkowitz, R. J. (1985). Phosphorylation of the mammalian beta-adrenergic receptor by cyclic AMP-dependent protein kinase. Regulation of the rate of receptor phosphorylation and dephosphorylation by agonist occupancy and effects on coupling of the receptor to the stimulatory guanine nucleotide regulatory protein. *Journal of Biological Chemistry* **260**, 7094-7101.

Benovic, J. L., Strasser, R. H., Caron, M. G., & Lefkowitz, R. J. (1986).  $\beta$ -adrenergic receptor kinase: identification of a novel protein kinase that phosphorylates the agonist-occupied form of the receptor. *Proc.Natl.Acad.Sci.U.S.A* **83**, 2797-2801.

- Benyo, Z., Gille, A., Bennett, C. L., Clausen, B. E., & Offermanns, S. (2006). Nicotinic acid-induced flushing is mediated by activation of epidermal langerhans cells. *Mol.Pharmacol.* **70**, 1844-1849.
- Benyo, Z., Gille, A., Kero, J., Csiky, M., Suchankova, M. C., Nusing, R. M., Moers, A., Pfeffer, K., & Offermanns, S. (2005). GPR109A (PUMA-G/HM74A) mediates nicotinic acid-induced flushing. *J.Clin.Invest* **115**, 3634-3640.
- Berg, K. A., Maayani, S., Goldfarb, J., Scaramellini, C., Leff, P., & Clarke, W. P. (1998). Effector pathway-dependent relative efficacy at serotonin type 2<sub>A</sub> and 2<sub>C</sub> receptors: evidence for agonist-directed trafficking of receptor stimulus. *Mol.Pharmacol.* **54**, 94-104.
- Berman, D. M., Wilkie, T. M., & Gilman, A. G. (1996). GAIP and RGS4 are GTPase-activating proteins for the Gi subfamily of G protein  $\alpha$  subunits. *Cell* **86**, 445-452.
- Berrada, K., Plesnicher, C. L., Luo, X., & Thibonnier, M. (2000). Dynamic interaction of human vasopressin/oxytocin receptor subtypes with G protein-coupled receptor kinases and protein kinase C after agonist stimulation. *Journal of Biological Chemistry* **275**, 27229-27237.
- Bodor, E. T. & Offermanns, S. (2008). Nicotinic acid: an old drug with a promising future. *Br.J.Pharmacol.* **153 Suppl 1**, S68-S75.
- Bouvier, M., Hausdorff, W. P., De Blasi, A., O'Dowd, B. F., Kobilka, B. K., Caron, M. G., & Lefkowitz, R. J. (1988). Removal of phosphorylation sites from the  $\beta_2$ -adrenergic receptor delays onset of agonist-promoted desensitization. *Nature* **333**, 370-373.
- Brink, C. B., Harvey, B. H., Bodenstein, J., Venter, D. P., & Oliver, D. W. (2004). Recent advances in drug action and therapeutics: relevance of novel concepts in G-protein-coupled receptor and signal transduction pharmacology. *Br.J.Clin.Pharmacol.* **57**, 373-387.
- Brown, B. G., Zhao, X. Q., Chait, A., Fisher, L. D., Cheung, M. C., Morse, J. S., Dowdy, A. A., Marino, E. K., Bolson, E. L., Alaupovic, P., Frohlich, J., & Albers, J. J. (2001). Simvastatin and niacin, antioxidant vitamins, or the combination for the prevention of coronary disease. *N.Engl.J.Med.* **345**, 1583-1592.
- Buck, L. & Axel, R. (1991). A novel multigene family may encode odorant receptors: a molecular basis for odor recognition. *Cell* **65**, 175-187.

- Bunemann, M., Frank, M., & Lohse, M. J. (2003). G<sub>i</sub> protein activation in intact cells involves subunit rearrangement rather than dissociation. *Proc.Natl.Acad.Sci.U.S.A* **100**, 16077-16082.
- Bunzow, J. R., Van Tol, H. H., Grandy, D. K., Albert, P., Salon, J., Christie, M., Machida, C. A., Neve, K. A., & Civelli, O. (1988). Cloning and expression of a rat D<sub>2</sub> dopamine receptor cDNA. *Nature* **336**, 783-787.
- Burns, D. L. (1988). Subunit structure and enzymic activity of pertussis toxin. *Microbiol.Sci.* **5**, 285-287.
- Burt, A. R., Sautel, M., Wilson, M. A., Rees, S., Wise, A., & Milligan, G. (1998). Agonist occupation of an  $\alpha$ 2A-adrenoreceptor-G<sub>i1</sub>alpha fusion protein results in activation of both receptor-linked and endogenous G<sub>i</sub> proteins. Comparisons of their contributions to GTPase activity and signal transduction and analysis of receptor-G protein activation stoichiometry. *Journal of Biological Chemistry* **273**, 10367-10375.
- Canner, P. L., Berge, K. G., Wenger, N. K., Stamler, J., Friedman, L., Prineas, R. J., & Friedewald, W. (1986). Fifteen year mortality in Coronary Drug Project patients: long-term benefit with niacin. *J.Am.Coll.Cardiol.* **8**, 1245-1255.
- Cao, T. T., Deacon, H. W., Reczek, D., Bretscher, A., & von Zastrow, M. (1999). A kinase-regulated PDZ-domain interaction controls endocytic sorting of the  $\beta$ <sub>2</sub>-adrenergic receptor. *Nature* **401**, 286-290.
- Carlson, L. A. (1963). Studies on the effect of nicotinic acid on catecholamine stimulated lipolysis in adipose tissue in vitro. *Acta Med.Scand.* **173**, 719-722.
- Carlson, L. A. (2005). Nicotinic acid: the broad-spectrum lipid drug. A 50th anniversary review. *J.Intern.Med.* **258**, 94-114.
- Carlson, L. A. & Hanngren, A. (1964). Initial distribution in mice of <sup>3</sup>H-labelled nicotinic acid studied with autoradiography. *Life Sci.* **3**, 867-871.
- Carlson, L. A. & ORO, L. (1962). The effect of nicotinic acid on the plasma free fatty acid; demonstration of a metabolic type of sympathicolysis. *Acta Med.Scand.* **172**, 641-645.
- Cerione, R. A., Strulovici, B., Benovic, J. L., Lefkowitz, R. J., & Caron, M. G. (1983). Pure  $\beta$ -adrenergic receptor: the single polypeptide confers catecholamine responsiveness to adenylate cyclase. *Nature* **306**, 562-566.

Chabre, M., Cone, R., & Saibil, H. (2003). Biophysics: is rhodopsin dimeric in native retinal rods? *Nature* **426**, 30-31.

Chalfie, M., Tu, Y., Euskirchen, G., Ward, W. W., & Prasher, D. C. (1994). Green fluorescent protein as a marker for gene expression. *Science* **263**, 802-805.

Cheng, K., Wu, T. J., Wu, K. K., Sturino, C., Metters, K., Gottesdiener, K., Wright, S. D., Wang, Z., O'Neill, G., Lai, E., & Waters, M. G. (2006). Antagonism of the prostaglandin D<sub>2</sub> receptor 1 suppresses nicotinic acid-induced vasodilation in mice and humans. *Proc.Natl.Acad.Sci.U.S.A* **103**, 6682-6687.

Cherezov, V., Rosenbaum, D. M., Hanson, M. A., Rasmussen, S. G., Thian, F. S., Kobilka, T. S., Choi, H. J., Kuhn, P., Weis, W. I., Kobilka, B. K., & Stevens, R. C. (2007). High-resolution crystal structure of an engineered human  $\beta_2$ -adrenergic G protein-coupled receptor. *Science* **318**, 1258-1265.

Chijiwa, T., Mishima, A., Hagiwara, M., Sano, M., Hayashi, K., Inoue, T., Naito, K., Toshioka, T., & Hidaka, H. (1990). Inhibition of forskolin-induced neurite outgrowth and protein phosphorylation by a newly synthesized selective inhibitor of cyclic AMP-dependent protein kinase, N-[2-(p-bromocinnamylamino)ethyl]-5-isoquinolinesulfonamide (H-89), of PC12D pheochromocytoma cells. *Journal of Biological Chemistry* **265**, 5267-5272.

Cho, E. Y., Cho, D. I., Park, J. H., Kurose, H., Caron, M. G., & Kim, K. M. (2007). Roles of protein kinase C and actin-binding protein 280 in the regulation of intracellular trafficking of dopamine D<sub>3</sub> receptor. *Mol.Endocrinol.* **21**, 2242-2254.

Chun, M., Liyanage, U. K., Lisanti, M. P., & Lodish, H. F. (1994). Signal transduction of a G protein-coupled receptor in caveolae: colocalization of endothelin and its receptor with caveolin. *Proc.Natl.Acad.Sci.U.S.A* **91**, 11728-11732.

Claing, A., Laporte, S. A., Caron, M. G., & Lefkowitz, R. J. (2002). Endocytosis of G protein-coupled receptors: roles of G protein-coupled receptor kinases and  $\beta$ -arrestin proteins. *Prog.Neurobiol.* **66**, 61-79.

Claing, A., Perry, S. J., Achiriloaie, M., Walker, J. K., Albanesi, J. P., Lefkowitz, R. J., & Premont, R. T. (2000). Multiple endocytic pathways of G protein-coupled receptors delineated by GIT1 sensitivity. *Proc.Natl.Acad.Sci.U.S.A* **97**, 1119-1124.

Coronary Drug Project Research Group (1975). Clofibrate and niacin in coronary heart disease. *JAMA* **231**, 360-381.

Costa, T. & Herz, A. (1989). Antagonists with negative intrinsic activity at  $\delta$  opioid receptors coupled to GTP-binding proteins. *Proc.Natl.Acad.Sci.U.S.A* **86**, 7321-7325.

Craft, C. M., Whitmore, D. H., & Wiechmann, A. F. (1994). Cone arrestin identified by targeting expression of a functional family. *Journal of Biological Chemistry* **269**, 4613-4619.

Daaka, Y., Luttrell, L. M., Ahn, S., Della Rocca, G. J., Ferguson, S. S., Caron, M. G., & Lefkowitz, R. J. (1998). Essential role for G protein-coupled receptor endocytosis in the activation of mitogen-activated protein kinase. *Journal of Biological Chemistry* **273**, 685-688.

Daaka, Y., Luttrell, L. M., & Lefkowitz, R. J. (1997a). Switching of the coupling of the  $\beta_2$ -adrenergic receptor to different G proteins by protein kinase A. *Nature* **390**, 88-91.

Daaka, Y., Pitcher, J. A., Richardson, M., Stoffel, R. H., Robishaw, J. D., & Lefkowitz, R. J. (1997b). Receptor and G $\beta\gamma$  isoform-specific interactions with G protein-coupled receptor kinases. *Proc.Natl.Acad.Sci.U.S.A* **94**, 2180-2185.

Davidson, J. S., Flanagan, C. A., Zhou, W., Becker, I. I., Elario, R., Emeran, W., Sealton, S. C., & Millar, R. P. (1995). Identification of N-glycosylation sites in the gonadotropin-releasing hormone receptor: role in receptor expression but not ligand binding. *Mol.Cell Endocrinol.* **107**, 241-245.

de Souza, N. J., Dohadwalla, A. N., & Reden, J. (1983). Forskolin: a labdane diterpenoid with antihypertensive, positive inotropic, platelet aggregation inhibitory, and adenylate cyclase activating properties. *Med.Res.Rev.* **3**, 201-219.

DeFea, K. A., Zalevsky, J., Thoma, M. S., Dery, O., Mullins, R. D., & Bunnett, N. W. (2000).  $\beta$ -arrestin-dependent endocytosis of proteinase-activated receptor 2 is required for intracellular targeting of activated ERK1/2. *J.Cell Biol.* **148**, 1267-1281.

Dixon, R. A., Kobilka, B. K., Strader, D. J., Benovic, J. L., Dohlman, H. G., Frielle, T., Bolanowski, M. A., Bennett, C. D., Rands, E., Diehl, R. E., Mumford, R. A., Slater, E. E., Sigal, I. S., Caron, M. G., Lefkowitz, R. J., & Strader, C. D. (1986). Cloning of the gene and cDNA for mammalian  $\beta$ -adrenergic receptor and homology with rhodopsin. *Nature* **321**, 75-79.

Dupre, D. J., Robitaille, M., Ethier, N., Villeneuve, L. R., Mamarbachi, A. M., & Hebert, T. E. (2006). Seven transmembrane receptor core signaling complexes are assembled prior to plasma membrane trafficking. *Journal of Biological Chemistry* **281**, 34561-34573.

- Dupree, P., Parton, R. G., Raposo, G., Kurzchalia, T. V., & Simons, K. (1993). Caveolae and sorting in the trans-Golgi network of epithelial cells. *EMBO J.* **12**, 1597-1605.
- Ebisuya, M., Kondoh, K., & Nishida, E. (2005). The duration, magnitude and compartmentalization of ERK MAP kinase activity: mechanisms for providing signaling specificity. *J. Cell Sci.* **118**, 2997-3002.
- Eklund, B., Kaijser, L., Nowak, J., & Wennmalm, A. (1979). Prostaglandins contribute to the vasodilation induced by nicotinic acid. *Prostaglandins* **17**, 821-830.
- Elam, M. B., Hunninghake, D. B., Davis, K. B., Garg, R., Johnson, C., Egan, D., Kostis, J. B., Sheps, D. S., & Brinton, E. A. (2000). Effect of niacin on lipid and lipoprotein levels and glycemic control in patients with diabetes and peripheral arterial disease: the ADMIT study: A randomized trial. Arterial Disease Multiple Intervention Trial. *JAMA* **284**, 1263-1270.
- Fargin, A., Raymond, J. R., Lohse, M. J., Kobilka, B. K., Caron, M. G., & Lefkowitz, R. J. (1988). The genomic clone G-21 which resembles a  $\beta$ -adrenergic receptor sequence encodes the 5-HT<sub>1A</sub> receptor. *Nature* **335**, 358-360.
- Ferguson, S. S. (2001). Evolving concepts in G protein-coupled receptor endocytosis: the role in receptor desensitization and signaling. *Pharmacol.Rev.* **53**, 1-24.
- Ferguson, S. S. (2007). Phosphorylation-independent attenuation of GPCR signalling. *Trends Pharmacol.Sci.* **28**, 173-179.
- Ferguson, S. S., Downey, W. E., III, Colapietro, A. M., Barak, L. S., Menard, L., & Caron, M. G. (1996). Role of  $\beta$ -arrestin in mediating agonist-promoted G protein-coupled receptor internalization. *Science* **271**, 363-366.
- Feron, O., Smith, T. W., Michel, T., & Kelly, R. A. (1997). Dynamic targeting of the agonist-stimulated m2 muscarinic acetylcholine receptor to caveolae in cardiac myocytes. *Journal of Biological Chemistry* **272**, 17744-17748.
- Fotiadis, D., Liang, Y., Filipek, S., Saperstein, D. A., Engel, A., & Palczewski, K. (2003). Atomic-force microscopy: Rhodopsin dimers in native disc membranes. *Nature* **421**, 127-128.
- Garg, A. & Grundy, S. M. (1990). Nicotinic acid as therapy for dyslipidemia in non-insulin-dependent diabetes mellitus. *JAMA* **264**, 723-726.

Gharbaoui, T., Skinner, P. J., Shin, Y. J., Averbuj, C., Jung, J. K., Johnson, B. R., Duong, T., Decaire, M., Uy, J., Cherrier, M. C., Webb, P. J., Tamura, S. Y., Zou, N., Rodriguez, N., Boatman, P. D., Sage, C. R., Lindstrom, A., Xu, J., Schrader, T. O., Smith, B. M., Chen, R., Richman, J. G., Connolly, D. T., Colletti, S. L., Tata, J. R., & Semple, G. (2007). Agonist lead identification for the high affinity niacin receptor GPR109a. *Bioorg.Med.Chem.Lett.* **17**, 4914-4919.

Gilbert, T. L., Bennett, T. A., Maestas, D. C., Cimino, D. F., & Prossnitz, E. R. (2001). Internalization of the human N-formyl peptide and C5a chemoattractant receptors occurs via clathrin-independent mechanisms. *Biochemistry* **40**, 3467-3475.

Gille, A., Bodor, E. T., Ahmed, K., & Offermanns, S. (2008). Nicotinic acid: pharmacological effects and mechanisms of action. *Annu.Rev.Pharmacol.Toxicol.* **48**, 79-106.

Goodman, O. B., Jr., Krupnick, J. G., Santini, F., Gurevich, V. V., Penn, R. B., Gagnon, A. W., Keen, J. H., & Benovic, J. L. (1996).  $\beta$ -arrestin acts as a clathrin adaptor in endocytosis of the  $\beta_2$ -adrenergic receptor. *Nature* **383**, 447-450.

Green, A., Milligan, G., & Dobias, S. B. (1992).  $G_i$  down-regulation as a mechanism for heterologous desensitization in adipocytes. *Journal of Biological Chemistry* **267**, 3223-3229.

Grundy, S. M., Vega, G. L., McGovern, M. E., Tulloch, B. R., Kendall, D. M., Fitz-Patrick, D., Ganda, O. P., Rosenson, R. S., Buse, J. B., Robertson, D. D., & Sheehan, J. P. (2002). Efficacy, safety, and tolerability of once-daily niacin for the treatment of dyslipidemia associated with type 2 diabetes: results of the assessment of diabetes control and evaluation of the efficacy of niaspan trial. *Arch.Intern.Med.* **162**, 1568-1576.

Gurevich, V. V. & Benovic, J. L. (1993). Visual arrestin interaction with rhodopsin. Sequential multisite binding ensures strict selectivity toward light-activated phosphorylated rhodopsin. *Journal of Biological Chemistry* **268**, 11628-11638.

Gurevich, V. V., Dion, S. B., Onorato, J. J., Ptasienski, J., Kim, C. M., Sterne-Marr, R., Hosey, M. M., & Benovic, J. L. (1995). Arrestin interactions with G protein-coupled receptors. Direct binding studies of wild type and mutant arrestins with rhodopsin,  $\beta_2$ -adrenergic, and  $M_2$  muscarinic cholinergic receptors. *Journal of Biological Chemistry* **270**, 720-731.

Gurevich, V. V. & Gurevich, E. V. (2006). The structural basis of arrestin-mediated regulation of G-protein-coupled receptors. *Pharmacol.Ther.* **110**, 465-502.

- Guzzi, F., Zanchetta, D., Cassoni, P., Guzzi, V., Francolini, M., Parenti, M., & Chini, B. (2002). Localization of the human oxytocin receptor in caveolin-1 enriched domains turns the receptor-mediated inhibition of cell growth into a proliferative response. *Oncogene* **21**, 1658-1667.
- Hall, R. A., Ostedgaard, L. S., Premont, R. T., Blitzer, J. T., Rahman, N., Welsh, M. J., & Lefkowitz, R. J. (1998). A C-terminal motif found in the  $\beta_2$ -adrenergic receptor, P2Y1 receptor and cystic fibrosis transmembrane conductance regulator determines binding to the Na<sup>+</sup>/H<sup>+</sup> exchanger regulatory factor family of PDZ proteins. *Proc.Natl.Acad.Sci.U.S.A* **95**, 8496-8501.
- Hansen, S. H., Sandvig, K., & van Deurs, B. (1993). Clathrin and HA2 adaptors: effects of potassium depletion, hypertonic medium, and cytosol acidification. *J.Cell Biol.* **121**, 61-72.
- Heding, A. (2004). Use of the BRET 7TM receptor/ $\beta$ -arrestin assay in drug discovery and screening. *Expert.Rev.Mol.Diagn.* **4**, 403-411.
- Hein, L., Ishii, K., Coughlin, S. R., & Kobilka, B. K. (1994). Intracellular targeting and trafficking of thrombin receptors. A novel mechanism for resensitization of a G protein-coupled receptor. *Journal of Biological Chemistry* **269**, 27719-27726.
- Hermans, E. (2003). Biochemical and pharmacological control of the multiplicity of coupling at G-protein-coupled receptors. *Pharmacol.Ther.* **99**, 25-44.
- Hilf, G., Gierschik, P., & Jakobs, K. H. (1989). Muscarinic acetylcholine receptor-stimulated binding of guanosine 5'-O-(3-thiotriphosphate) to guanine-nucleotide-binding proteins in cardiac membranes. *Eur.J.Biochem.* **186**, 725-731.
- Hirsch, J. A., Schubert, C., Gurevich, V. V., & Sigler, P. B. (1999). The 2.8 Å crystal structure of visual arrestin: a model for arrestin's regulation. *Cell* **97**, 257-269.
- Hocevar, B. A., Burns, D. J., & Fields, A. P. (1993). Identification of protein kinase C (PKC) phosphorylation sites on human lamin B. Potential role of PKC in nuclear lamina structural dynamics. *Journal of Biological Chemistry* **268**, 7545-7552.
- Hollinger, S. & Hepler, J. R. (2002). Cellular regulation of RGS proteins: modulators and integrators of G protein signaling. *Pharmacol.Rev.* **54**, 527-559.
- Inglese, J., Freedman, N. J., Koch, W. J., & Lefkowitz, R. J. (1993). Structure and mechanism of the G protein-coupled receptor kinases. *Journal of Biological Chemistry* **268**, 23735-23738.

Innamorati, G., Le Gouill, C., Balamotis, M., & Birnbaumer, M. (2001). The long and the short cycle. Alternative intracellular routes for trafficking of G-protein-coupled receptors. *Journal of Biological Chemistry* **276**, 13096-13103.

Jacoby, E., Bouhelal, R., Gerspacher, M., & Seuwen, K. (2006). The 7 TM G-protein-coupled receptor target family. *ChemMedChem*. **1**, 761-782.

Jala, V. R., Shao, W. H., & Haribabu, B. (2005). Phosphorylation-independent  $\beta$ -arrestin translocation and internalization of leukotriene B4 receptors. *Journal of Biological Chemistry* **280**, 4880-4887.

Jarvik, J. W. & Telmer, C. A. (1998). Epitope tagging. *Annu.Rev.Genet.* **32**, 601-618.

Javitch, J. A., Fu, D., Liapakis, G., & Chen, J. (1997). Constitutive activation of the  $\beta_2$  adrenergic receptor alters the orientation of its sixth membrane-spanning segment. *Journal of Biological Chemistry* **272**, 18546-18549.

Jewell-Motz, E. A. & Liggett, S. B. (1996). G protein-coupled receptor kinase specificity for phosphorylation and desensitization of  $\alpha_2$ -adrenergic receptor subtypes. *Journal of Biological Chemistry* **271**, 18082-18087.

Jones, B. W. & Hinkle, P. M. (2005).  $\beta$ -arrestin mediates desensitization and internalization but does not affect dephosphorylation of the thyrotropin-releasing hormone receptor. *Journal of Biological Chemistry* **280**, 38346-38354.

Jones, K. A., Borowsky, B., Tamm, J. A., Craig, D. A., Durkin, M. M., Dai, M., Yao, W. J., Johnson, M., Gunwaldsen, C., Huang, L. Y., Tang, C., Shen, Q., Salon, J. A., Morse, K., Laz, T., Smith, K. E., Nagarathnam, D., Noble, S. A., Branchek, T. A., & Gerald, C. (1998). GABA(B) receptors function as a heteromeric assembly of the subunits GABA(B)R1 and GABA(B)R2. *Nature* **396**, 674-679.

Jung, J. K., Johnson, B. R., Duong, T., Decaire, M., Uy, J., Gharbaoui, T., Boatman, P. D., Sage, C. R., Chen, R., Richman, J. G., Connolly, D. T., & Semple, G. (2007). Analogues of acifran: agonists of the high and low affinity niacin receptors, GPR109a and GPR109b. *J.Med.Chem.* **50**, 1445-1448.

Kahn, S. E., Beard, J. C., Schwartz, M. W., Ward, W. K., Ding, H. L., Bergman, R. N., Taborsky, G. J., Jr., & Porte, D., Jr. (1989). Increased  $\beta$ -cell secretory capacity as mechanism for islet adaptation to nicotinic acid-induced insulin resistance. *Diabetes* **38**, 562-568.

Kaijser, L., Eklund, B., Olsson, A. G., & Carlson, L. A. (1979). Dissociation of the effects of nicotinic acid on vasodilatation and lipolysis by a prostaglandin synthesis inhibitor, indomethacin, in man. *Med.Biol.* **57**, 114-117.

Kang, J., Shi, Y., Xiang, B., Qu, B., Su, W., Zhu, M., Zhang, M., Bao, G., Wang, F., Zhang, X., Yang, R., Fan, F., Chen, X., Pei, G., & Ma, L. (2005). A nuclear function of  $\beta$ -arrestin1 in GPCR signaling: regulation of histone acetylation and gene transcription. *Cell* **123**, 833-847.

Kaupmann, K., Malitschek, B., Schuler, V., Heid, J., Froestl, W., Beck, P., Mosbacher, J., Bischoff, S., Kulik, A., Shigemoto, R., Karschin, A., & Bettler, B. (1998). GABA(B)-receptor subtypes assemble into functional heteromeric complexes. *Nature* **396**, 683-687.

Kenakin, T. (1995). Agonist-receptor efficacy. II. Agonist trafficking of receptor signals. *Trends Pharmacol.Sci.* **16**, 232-238.

Kirchhausen, T. (1999). Adaptors for clathrin-mediated traffic. *Annu.Rev.Cell Dev.Biol.* **15**, 705-732.

Kiss, A. L. & Geuze, H. J. (1997). Caveolae can be alternative endocytotic structures in elicited macrophages. *Eur.J.Cell Biol.* **73**, 19-27.

Knowles, H. J., te Poele, R. H., Workman, P., & Harris, A. L. (2006). Niacin induces PPARgamma expression and transcriptional activation in macrophages via HM74 and HM74a-mediated induction of prostaglandin synthesis pathways. *Biochem.Pharmacol.* **71**, 646-656.

Kobilka, B. K., Frielle, T., Collins, S., Yang-Feng, T., Kobilka, T. S., Francke, U., Lefkowitz, R. J., & Caron, M. G. (1987). An intronless gene encoding a potential member of the family of receptors coupled to guanine nucleotide regulatory proteins. *Nature* **329**, 75-79.

Kobilka, B. K., Kobilka, T. S., Daniel, K., Regan, J. W., Caron, M. G., & Lefkowitz, R. J. (1988). Chimeric  $\alpha_2$ - $\beta_2$ -adrenergic receptors: delineation of domains involved in effector coupling and ligand binding specificity. *Science* **240**, 1310-1316.

Kohout, T. A., Lin, F. S., Perry, S. J., Conner, D. A., & Lefkowitz, R. J. (2001).  $\beta$ -Arrestin 1 and 2 differentially regulate heptahelical receptor signaling and trafficking. *Proc.Natl.Acad.Sci.U.S.A* **98**, 1601-1606.

Kong, G., Penn, R., & Benovic, J. L. (1994). A  $\beta$ -adrenergic receptor kinase dominant negative mutant attenuates desensitization of the  $\beta_2$ -adrenergic receptor. *Journal of Biological Chemistry* **269**, 13084-13087.

Kozak, M. (1987). At least six nucleotides preceding the AUG initiator codon enhance translation in mammalian cells. *J.Mol.Biol.* **196**, 947-950.

Krasel, C., Bunemann, M., Lorenz, K., & Lohse, M. J. (2005).  $\beta$ -arrestin binding to the  $\beta_2$ -adrenergic receptor requires both receptor phosphorylation and receptor activation. *Journal of Biological Chemistry* **280**, 9528-9535.

Kreis, T. E. (1986). Microinjected antibodies against the cytoplasmic domain of vesicular stomatitis virus glycoprotein block its transport to the cell surface. *EMBO J.* **5**, 931-941.

Kristiansen, K. (2004). Molecular mechanisms of ligand binding, signaling, and regulation within the superfamily of G-protein-coupled receptors: molecular modeling and mutagenesis approaches to receptor structure and function. *Pharmacol.Ther.* **103**, 21-80.

Krueger, K. M., Daaka, Y., Pitcher, J. A., & Lefkowitz, R. J. (1997). The role of sequestration in G protein-coupled receptor resensitization. Regulation of  $\beta_2$ -adrenergic receptor dephosphorylation by vesicular acidification. *Journal of Biological Chemistry* **272**, 5-8.

Krupnick, J. G. & Benovic, J. L. (1998). The role of receptor kinases and arrestins in G protein-coupled receptor regulation. *Annu.Rev.Pharmacol.Toxicol.* **38**, 289-319.

Krupnick, J. G., Gurevich, V. V., & Benovic, J. L. (1997). Mechanism of quenching of phototransduction. Binding competition between arrestin and transducin for phosphorhodopsin. *Journal of Biological Chemistry* **272**, 18125-18131.

Kubo, T., Bujo, H., Akiba, I., Nakai, J., Mishina, M., & Numa, S. (1988). Location of a region of the muscarinic acetylcholine receptor involved in selective effector coupling. *FEBS Lett.* **241**, 119-125.

Kuhn, H. & Wilden, U. (1987). Deactivation of photoactivated rhodopsin by rhodopsin-kinase and arrestin. *J.Recept.Res.* **7**, 283-298.

Kunapuli, P., Gurevich, V. V., & Benovic, J. L. (1994). Phospholipid-stimulated autophosphorylation activates the G protein-coupled receptor kinase GRK5. *Journal of Biological Chemistry* **269**, 10209-10212.

Kurose, H. & Lefkowitz, R. J. (1994). Differential desensitization and phosphorylation of three cloned and transfected  $\alpha_2$ -adrenergic receptor subtypes. *Journal of Biological Chemistry* **269**, 10093-10099.

Lagerstrom, M. C. & Schioth, H. B. (2008). Structural diversity of G protein-coupled receptors and significance for drug discovery. *Nat.Rev.Drug Discov.* **7**, 339-357.

Lamb, M. E., De Weerd, W. F., & Leeb-Lundberg, L. M. (2001). Agonist-promoted trafficking of human bradykinin receptors: arrestin- and dynamin-independent sequestration of the B<sub>2</sub> receptor and bradykinin in HEK293 cells. *Biochem.J.* **355**, 741-750.

Lane, J. R., Powney, B., Wise, A., Rees, S., & Milligan, G. (2007). Protean agonism at the dopamine D<sub>2</sub> receptor: (S)-3-(3-hydroxyphenyl)-N-propylpiperidine is an agonist for activation of Go1 but an antagonist/inverse agonist for G<sub>i1</sub>, Gi2, and G<sub>i3</sub>. *Mol.Pharmacol.* **71**, 1349-1359.

Laporte, S. A., Oakley, R. H., Zhang, J., Holt, J. A., Ferguson, S. S., Caron, M. G., & Barak, L. S. (1999). The  $\beta_2$ -adrenergic receptor/ $\beta$ arrestin complex recruits the clathrin adaptor AP-2 during endocytosis. *Proc.Natl.Acad.Sci.U.S.A* **96**, 3712-3717.

Lewis, G. F. & Rader, D. J. (2005). New insights into the regulation of HDL metabolism and reverse cholesterol transport. *Circ.Res.* **96**, 1221-1232.

Li, F., Wang, D., Zhou, Y., Zhou, B., Yang, Y., Chen, H., & Song, J. (2008). Protein kinase A suppresses the differentiation of 3T3-L1 preadipocytes. *Cell Res.* **18**, 311-323.

Liang, Y., Fotiadis, D., Filipek, S., Saperstein, D. A., Palczewski, K., & Engel, A. (2003). Organization of the G protein-coupled receptors rhodopsin and opsin in native membranes. *J.Biol.Chem.* **278**, 21655-21662.

Libert, F., Parmentier, M., Lefort, A., Dinsart, C., Van Sande, J., Maenhaut, C., Simons, M. J., Dumont, J. E., & Vassart, G. (1989). Selective amplification and cloning of four new members of the G protein-coupled receptor family. *Science* **244**, 569-572.

Liggett, S. B., Freedman, N. J., Schwinn, D. A., & Lefkowitz, R. J. (1993). Structural basis for receptor subtype-specific regulation revealed by a chimeric  $\beta_3/\beta_2$ -adrenergic receptor. *Proc.Natl.Acad.Sci.U.S.A* **90**, 3665-3669.

- Lin, F. T., Chen, W., Shenoy, S., Cong, M., Exum, S. T., & Lefkowitz, R. J. (2002). Phosphorylation of  $\beta$ -arrestin2 regulates its function in internalization of  $\beta_{(2)}$ -adrenergic receptors. *Biochemistry* **41**, 10692-10699.
- Lin, F. T., Krueger, K. M., Kendall, H. E., Daaka, Y., Fredericks, Z. L., Pitcher, J. A., & Lefkowitz, R. J. (1997). Clathrin-mediated endocytosis of the  $\beta$ -adrenergic receptor is regulated by phosphorylation/dephosphorylation of  $\beta$ -arrestin1. *Journal of Biological Chemistry* **272**, 31051-31057.
- Lin, F. T., Miller, W. E., Luttrell, L. M., & Lefkowitz, R. J. (1999). Feedback regulation of  $\beta$ -arrestin1 function by extracellular signal-regulated kinases. *Journal of Biological Chemistry* **274**, 15971-15974.
- Lisanti, M. P., Scherer, P. E., Vidugiriene, J., Tang, Z., Hermanowski-Vosatka, A., Tu, Y. H., Cook, R. F., & Sargiacomo, M. (1994). Characterization of caveolin-rich membrane domains isolated from an endothelial-rich source: implications for human disease. *J. Cell Biol.* **126**, 111-126.
- Lohse, M. J., Andexinger, S., Pitcher, J., Trukawinski, S., Codina, J., Faure, J. P., Caron, M. G., & Lefkowitz, R. J. (1992). Receptor-specific desensitization with purified proteins. Kinase dependence and receptor specificity of  $\beta$ -arrestin and arrestin in the  $\beta_2$ -adrenergic receptor and rhodopsin systems. *Journal of Biological Chemistry* **267**, 8558-8564.
- Lohse, M. J., Benovic, J. L., Codina, J., Caron, M. G., & Lefkowitz, R. J. (1990).  $\beta$ -Arrestin: a protein that regulates  $\beta$ -adrenergic receptor function. *Science* **248**, 1547-1550.
- Lorenzen, A., Stannek, C., Lang, H., Andrianov, V., Kalvinsh, I., & Schwabe, U. (2001). Characterization of a G protein-coupled receptor for nicotinic acid. *Mol. Pharmacol.* **59**, 349-357.
- Lundstrom, K. (2006). Latest development in drug discovery on G protein-coupled receptors. *Curr. Protein Pept. Sci.* **7**, 465-470.
- Luttrell, L. M., Ferguson, S. S., Daaka, Y., Miller, W. E., Maudsley, S., Della Rocca, G. J., Lin, F., Kawakatsu, H., Owada, K., Luttrell, D. K., Caron, M. G., & Lefkowitz, R. J. (1999).  $\beta$ -arrestin-dependent formation of  $\beta_2$  adrenergic receptor-Src protein kinase complexes. *Science* **283**, 655-661.
- Luttrell, L. M. & Lefkowitz, R. J. (2002). The role of  $\beta$ -arrestins in the termination and transduction of G-protein-coupled receptor signals. *J. Cell Sci.* **115**, 455-465.

Ma, L. & Pei, G. (2007).  $\beta$ -arrestin signaling and regulation of transcription. *J.Cell Sci.* **120**, 213-218.

Maciejewski-Lenoir, D., Richman, J. G., Hakak, Y., Gaidarov, I., Behan, D. P., & Connolly, D. T. (2006). Langerhans cells release prostaglandin D<sub>2</sub> in response to nicotinic acid. *J.Invest Dermatol.* **126**, 2637-2646.

Madabushi, S., Gross, A. K., Philippi, A., Meng, E. C., Wensel, T. G., & Lichtarge, O. (2004). Evolutionary trace of G protein-coupled receptors reveals clusters of residues that determine global and class-specific functions. *Journal of Biological Chemistry* **279**, 8126-8132.

Maggio, R., Vogel, Z., & Wess, J. (1993). Coexpression studies with mutant muscarinic/adrenergic receptors provide evidence for intermolecular "cross-talk" between G-protein-linked receptors. *Proc.Natl.Acad.Sci.U.S.A* **90**, 3103-3107.

Mahboubi, K., Witman-Jones, T., Adamus, J. E., Letsinger, J. T., Whitehouse, D., Moorman, A. R., Sawicki, D., Bergenhem, N., & Ross, S. A. (2006). Triglyceride modulation by acifran analogs: activity towards the niacin high and low affinity G protein-coupled receptors HM74A and HM74. *Biochem.Biophys.Res.Comm.* **340**, 482-490.

Malik, S. & Kashyap, M. L. (2003). Niacin, lipids, and heart disease. *Curr.Cardiol.Rep.* **5**, 470-476.

Margeta-Mitrovic, M., Jan, Y. N., & Jan, L. Y. (2000). A trafficking checkpoint controls GABA(B) receptor heterodimerization. *Neuron* **27**, 97-106.

McArdle, C. A., Franklin, J., Green, L., & Hislop, J. N. (2002). Signalling, cycling and desensitisation of gonadotrophin-releasing hormone receptors. *J.Endocrinol.* **173**, 1-11.

McDonald, P. H., Chow, C. W., Miller, W. E., Laporte, S. A., Field, M. E., Lin, F. T., Davis, R. J., & Lefkowitz, R. J. (2000).  $\beta$ -arrestin 2: a receptor-regulated MAPK scaffold for the activation of JNK3. *Science* **290**, 1574-1577.

McDonald, P. H. & Lefkowitz, R. J. (2001).  $\beta$ -Arrestins: new roles in regulating heptahelical receptors' functions. *Cell Signal.* **13**, 683-689.

McKenney, J. (2004). New perspectives on the use of niacin in the treatment of lipid disorders. *Arch.Intern.Med.* **164**, 697-705.

McLean, A. J. & Milligan, G. (2000). Ligand regulation of green fluorescent protein-tagged forms of the human  $\beta_{(1)}$ - and  $\beta_{(2)}$ -adrenoceptors; comparisons with the unmodified receptors. *Br.J.Pharmacol.* **130**, 1825-1832.

Michal, P., El Fakahany, E. E., & Dolezal, V. (2007). Muscarinic  $M_2$  receptors directly activate  $G_{q/11}$  and  $G_s$  G-proteins. *J.Pharmacol.Exp.Ther.* **320**, 607-614.

Milano, S. K., Kim, Y. M., Stefano, F. P., Benovic, J. L., & Brenner, C. (2006). Nonvisual arrestin oligomerization and cellular localization are regulated by inositol hexakisphosphate binding. *Journal of Biological Chemistry* **281**, 9812-9823.

Milasta, S., Evans, N. A., Ormiston, L., Wilson, S., Lefkowitz, R. J., & Milligan, G. (2005). The sustainability of interactions between the orexin-1 receptor and  $\beta$ -arrestin-2 is defined by a single C-terminal cluster of hydroxy amino acids and modulates the kinetics of ERK MAPK regulation. *Biochem.J.* **387**, 573-584.

Milasta, S., Padiani, J., Appelbe, S., Trim, S., Wyatt, M., Cox, P., Fidock, M., & Milligan, G. (2006). Interactions between the Mas-related receptors MrgD and MrgE alter signalling and trafficking of MrgD. *Mol.Pharmacol.* **69**, 479-491.

Miller, W. E. & Lefkowitz, R. J. (2001). Expanding roles for  $\beta$ -arrestins as scaffolds and adapters in GPCR signaling and trafficking. *Curr.Opin.Cell Biol.* **13**, 139-145.

Miller, W. E., Maudsley, S., Ahn, S., Khan, K. D., Luttrell, L. M., & Lefkowitz, R. J. (2000).  $\beta$ -arrestin1 interacts with the catalytic domain of the tyrosine kinase c-SRC. Role of  $\beta$ -arrestin1-dependent targeting of c-SRC in receptor endocytosis. *Journal of Biological Chemistry* **275**, 11312-11319.

Milligan, G. (1999). Exploring the dynamics of regulation of G protein-coupled receptors using green fluorescent protein. *Br.J.Pharmacol.* **128**, 501-510.

Mills, E., Prousky, J., Raskin, G., Gagnier, J., Rachlis, B., Montori, V. M., & Juurlink, D. (2003). The safety of over-the-counter niacin. A randomized placebo-controlled trial [ISRCTN18054903]. *BMC.Clin.Pharmacol.* **3**, 4.

Morise, H., Shimomura, O., Johnson, F. H., & Winant, J. (1974). Intermolecular energy transfer in the bioluminescent system of *Aequorea*. *Biochemistry* **13**, 2656-2662.

Morrow, J. D., Parsons, W. G., III, & Roberts, L. J. (1989). Release of markedly increased quantities of prostaglandin  $D_2$  in vivo in humans following the administration of nicotinic acid. *Prostaglandins* **38**, 263-274.

- Murakami, A., Yajima, T., Sakuma, H., McLaren, M. J., & Inana, G. (1993). X-arrestin: a new retinal arrestin mapping to the X chromosome. *FEBS Lett.* **334**, 203-209.
- Neuhaus, E. M., Mashukova, A., Barbour, J., Wolters, D., & Hatt, H. (2006). Novel function of  $\beta$ -arrestin2 in the nucleus of mature spermatozoa. *J.Cell Sci.* **119**, 3047-3056.
- Niedel, J. E., Kuhn, L. J., & Vandenberg, G. R. (1983). Phorbol diester receptor copurifies with protein kinase C. *Proc.Natl.Acad.Sci.U.S.A* **80**, 36-40.
- Nomura, H., Nielsen, B. W., & Matsushima, K. (1993). Molecular cloning of cDNAs encoding a LD78 receptor and putative leukocyte chemotactic peptide receptors. *Int.Immunol.* **5**, 1239-1249.
- Oakley, R. H., Laporte, S. A., Holt, J. A., Barak, L. S., & Caron, M. G. (1999). Association of  $\beta$ -arrestin with G protein-coupled receptors during clathrin-mediated endocytosis dictates the profile of receptor resensitization. *J.Biol.Chem.* **274**, 32248-32257.
- Oakley, R. H., Laporte, S. A., Holt, J. A., Caron, M. G., & Barak, L. S. (2000). Differential affinities of visual arrestin,  $\beta$  arrestin1, and  $\beta$  arrestin2 for G protein-coupled receptors delineate two major classes of receptors. *Journal of Biological Chemistry* **275**, 17201-17210.
- Offermanns, S. (2006). The nicotinic acid receptor GPR109A (HM74A or PUMA-G) as a new therapeutic target. *Trends Pharmacol.Sci.* **27**, 384-390.
- Oh, P. & Schnitzer, J. E. (2001). Segregation of heterotrimeric G proteins in cell surface microdomains.  $G(q)$  binds caveolin to concentrate in caveolae, whereas  $G(i)$  and  $G(s)$  target lipid rafts by default. *Mol.Biol.Cell* **12**, 685-698.
- Ostrowski, J., Kjelsberg, M. A., Caron, M. G., & Lefkowitz, R. J. (1992). Mutagenesis of the  $\beta_2$ -adrenergic receptor: how structure elucidates function. *Annu.Rev.Pharmacol.Toxicol.* **32**, 167-183.
- Pagano, A., Rovelli, G., Mosbacher, J., Lohmann, T., Duthey, B., Stauffer, D., Ristig, D., Schuler, V., Meigel, I., Lampert, C., Stein, T., Prezeau, L., Blahos, J., Pin, J., Froestl, W., Kuhn, R., Heid, J., Kaupmann, K., & Bettler, B. (2001). C-terminal interaction is essential for surface trafficking but not for heteromeric assembly of GABA(b) receptors. *J.Neurosci.* **21**, 1189-1202.

Palczewski, K. (2006). G protein-coupled receptor rhodopsin. *Annu.Rev.Biochem.* **75**, 743-767.

Palczewski, K., Kumasaka, T., Hori, T., Behnke, C. A., Motoshima, H., Fox, B. A., Le, T., I, Teller, D. C., Okada, T., Stenkamp, R. E., Yamamoto, M., & Miyano, M. (2000). Crystal structure of rhodopsin: A G protein-coupled receptor. *Science* **289**, 739-745.

Parsons, W. B., Jr. & Flinn, J. H. (1959). Reduction of serum cholesterol levels and  $\beta$ -lipoprotein cholesterol levels by nicotinic acid. *AMA.Arch.Intern.Med.* **103**, 783-790.

Paton, W. D. & Rang, H. P. (1965). The uptake of atropine and related drugs by intestinal smooth muscle of the guinea-pig in relation to acetylcholine receptors. *Proc.R.Soc.Lond B Biol.Sci.* **163**, 1-44.

Pfister, C., Chabre, M., Plouet, J., Tuyen, V. V., De Kozak, Y., Faure, J. P., & Kuhn, H. (1985). Retinal S antigen identified as the 48K protein regulating light-dependent phosphodiesterase in rods. *Science* **228**, 891-893.

Pfleger, K. D. & Eidne, K. A. (2005). Monitoring the formation of dynamic G-protein-coupled receptor-protein complexes in living cells. *Biochem.J.* **385**, 625-637.

Pierce, K. L. & Lefkowitz, R. J. (2001). Classical and new roles of  $\beta$ -arrestins in the regulation of G-protein-coupled receptors. *Nat.Rev.Neurosci.* **2**, 727-733.

Pike, N. B. (2005). Flushing out the role of GPR109A (HM74A) in the clinical efficacy of nicotinic acid. *J.Clin.Invest* **115**, 3400-3403.

Pike, N. B. & Wise, A. (2004). Identification of a nicotinic acid receptor: is this the molecular target for the oldest lipid-lowering drug? *Curr.Opin.Investig.Drugs* **5**, 271-275.

Pitcher, J., Lohse, M. J., Codina, J., Caron, M. G., & Lefkowitz, R. J. (1992). Desensitization of the isolated  $\beta_2$ -adrenergic receptor by  $\beta$ -adrenergic receptor kinase, cAMP-dependent protein kinase, and protein kinase C occurs via distinct molecular mechanisms. *Biochemistry* **31**, 3193-3197.

Pitcher, J. A., Freedman, N. J., & Lefkowitz, R. J. (1998). G protein-coupled receptor kinases. *Annu.Rev.Biochem.* **67**, 653-692.

Prasher, D. C., Eckenrode, V. K., Ward, W. W., Prendergast, F. G., & Cormier, M. J. (1992). Primary structure of the *Aequorea victoria* green-fluorescent protein. *Gene* **111**, 229-233.

Premont, R. T., Koch, W. J., Inglese, J., & Lefkowitz, R. J. (1994). Identification, purification, and characterization of GRK5, a member of the family of G protein-coupled receptor kinases. *Journal of Biological Chemistry* **269**, 6832-6841.

Rasmussen, S. G., Choi, H. J., Rosenbaum, D. M., Kobilka, T. S., Thian, F. S., Edwards, P. C., Burghammer, M., Ratnala, V. R., Sanishvili, R., Fischetti, R. F., Schertler, G. F., Weis, W. I., & Kobilka, B. K. (2007). Crystal structure of the human  $\beta_2$  adrenergic G-protein-coupled receptor. *Nature* **450**, 383-387.

Ray, K., Clapp, P., Goldsmith, P. K., & Spiegel, A. M. (1998). Identification of the sites of N-linked glycosylation on the human calcium receptor and assessment of their role in cell surface expression and signal transduction. *Journal of Biological Chemistry* **273**, 34558-34567.

Rebois, R. V., Robitaille, M., Gales, C., Dupre, D. J., Baragli, A., Trieu, P., Ethier, N., Bouvier, M., & Hebert, T. E. (2006). Heterotrimeric G proteins form stable complexes with adenylyl cyclase and Kir3.1 channels in living cells. *J. Cell Sci.* **119**, 2807-2818.

Revankar, C. M., Cimino, D. F., Sklar, L. A., Arterburn, J. B., & Prossnitz, E. R. (2005). A transmembrane intracellular estrogen receptor mediates rapid cell signaling. *Science* **307**, 1625-1630.

Richman, J. G., Kanemitsu-Parks, M., Gaidarov, I., Cameron, J. S., Griffin, P., Zheng, H., Guerra, N. C., Cham, L., Maciejewski-Lenoir, D., Behan, D. P., Boatman, D., Chen, R., Skinner, P., Ornelas, P., Waters, M. G., Wright, S. D., Semple, G., & Connolly, D. T. (2007). Nicotinic acid receptor agonists differentially activate downstream effectors. *Journal of Biological Chemistry* **282**, 18028-18036.

Roettger, B. F., Rentsch, R. U., Pinon, D., Holicky, E., Hadac, E., Larkin, J. M., & Miller, L. J. (1995). Dual pathways of internalization of the cholecystokinin receptor. *J. Cell Biol.* **128**, 1029-1041.

Rosenbaum, D. M., Cherezov, V., Hanson, M. A., Rasmussen, S. G., Thian, F. S., Kobilka, T. S., Choi, H. J., Yao, X. J., Weis, W. I., Stevens, R. C., & Kobilka, B. K. (2007). GPCR engineering yields high-resolution structural insights into  $\beta_2$ -adrenergic receptor function. *Science* **318**, 1266-1273.

Roth, N. S., Campbell, P. T., Caron, M. G., Lefkowitz, R. J., & Lohse, M. J. (1991). Comparative rates of desensitization of  $\beta$ -adrenergic receptors by the  $\beta$ -adrenergic

receptor kinase and the cyclic AMP-dependent protein kinase.  
*Proc.Natl.Acad.Sci.U.S.A* **88**, 6201-6204.

Rubic, T., Trottmann, M., & Lorenz, R. L. (2004). Stimulation of CD36 and the key effector of reverse cholesterol transport ATP-binding cassette A1 in monocyte cells by niacin. *Biochem.Pharmacol.* **67**, 411-419.

Sakai, T., Kamanna, V. S., & Kashyap, M. L. (2001). Niacin, but not gemfibrozil, selectively increases LP-AI, a cardioprotective subfraction of HDL, in patients with low HDL cholesterol. *Arterioscler.Thromb.Vasc.Biol.* **21**, 1783-1789.

Sakmar, T. P. (2002). Structure of rhodopsin and the superfamily of seven-helical receptors: the same and not the same. *Curr.Opin.Cell Biol.* **14**, 189-195.

Salahpour, A., Angers, S., & Bouvier, M. (2000). Functional significance of oligomerization of G-protein-coupled receptors. *Trends Endocrinol.Metab* **11**, 163-168.

Salim, K., Fenton, T., Bacha, J., Urien-Rodriguez, H., Bonnert, T., Skynner, H. A., Watts, E., Kerby, J., Heald, A., Beer, M., McAllister, G., & Guest, P. C. (2002). Oligomerization of G-protein-coupled receptors shown by selective co-immunoprecipitation. *J.Biol.Chem.* **277**, 15482-15485.

Sallese, M., Lombardi, M. S., & De Blasi, A. (1994). Two isoforms of G protein-coupled receptor kinase 4 identified by molecular cloning. *Biochem.Biophys.Res.Comm.* **199**, 848-854.

Schaub, A., Futterer, A., & Pfeffer, K. (2001). PUMA-G, an IFN- $\gamma$ -inducible gene in macrophages is a novel member of the seven transmembrane spanning receptor superfamily. *Eur.J.Immunol.* **31**, 3714-3725.

Schleicher, A., Kuhn, H., & Hofmann, K. P. (1989). Kinetics, binding constant, and activation energy of the 48-kDa protein-rhodopsin complex by extra-metarhodopsin II. *Biochemistry* **28**, 1770-1775.

Schnitzer, J. E., Oh, P., Pinney, E., & Allard, J. (1994). Filipin-sensitive caveolae-mediated transport in endothelium: reduced transcytosis, scavenger endocytosis, and capillary permeability of select macromolecules. *J.Cell Biol.* **127**, 1217-1232.

Semple, G., Skinner, P. J., Cherrier, M. C., Webb, P. J., Sage, C. R., Tamura, S. Y., Chen, R., Richman, J. G., & Connolly, D. T. (2006). 1-Alkyl-benzotriazole-5-carboxylic acids are highly selective agonists of the human orphan G-protein-coupled receptor GPR109b. *J.Med.Chem.* **49**, 1227-1230.

Shen, H. C., Ding, F. X., Luell, S., Forrest, M. J., Carballo-Jane, E., Wu, K. K., Wu, T. J., Cheng, K., Wilsie, L. C., Krsmanovic, M. L., Taggart, A. K., Ren, N., Cai, T. Q., Deng, Q., Chen, Q., Wang, J., Wolff, M. S., Tong, X., Holt, T. G., Waters, M. G., Hammond, M. L., Tata, J. R., & Colletti, S. L. (2007a). Discovery of biaryl anthranilides as full agonists for the high affinity niacin receptor. *J.Med.Chem.* **50**, 6303-6306.

Shen, H. C., Szymonifka, M. J., Kharbanda, D., Deng, Q., Carballo-Jane, E., Wu, K. K., Wu, T. J., Cheng, K., Ren, N., Cai, T. Q., Taggart, A. K., Wang, J., Tong, X., Waters, M. G., Hammond, M. L., Tata, J. R., & Colletti, S. L. (2007b). Discovery of orally bioavailable and novel urea agonists of the high affinity niacin receptor GPR109A. *Bioorg.Med.Chem.Lett.* **17**, 6723-6728.

Shenoy, S. K., McDonald, P. H., Kohout, T. A., & Lefkowitz, R. J. (2001). Regulation of receptor fate by ubiquitination of activated  $\beta_2$ -adrenergic receptor and  $\beta$ -arrestin. *Science* **294**, 1307-1313.

Shepherd, J., Packard, C. J., Patsch, J. R., Gotto, A. M., Jr., & Taunton, O. D. (1979). Effects of nicotinic acid therapy on plasma high density lipoprotein subfraction distribution and composition and on apolipoprotein A metabolism. *J.Clin.Invest* **63**, 858-867.

Siehler, S. & Manning, D. R. (2002). Pathways of transduction engaged by sphingosine 1-phosphate through G protein-coupled receptors. *Biochim.Biophys.Acta* **1582**, 94-99.

Skinner, P. J., Cherrier, M. C., Webb, P. J., Sage, C. R., Dang, H. T., Pride, C. C., Chen, R., Tamura, S. Y., Richman, J. G., Connolly, D. T., & Semple, G. (2007a). 3-Nitro-4-amino benzoic acids and 6-amino nicotinic acids are highly selective agonists of GPR109b. *Bioorg.Med.Chem.Lett.* **17**, 6619-6622.

Skinner, P. J., Cherrier, M. C., Webb, P. J., Shin, Y. J., Gharbaoui, T., Lindstrom, A., Hong, V., Tamura, S. Y., Dang, H. T., Pride, C. C., Chen, R., Richman, J. G., Connolly, D. T., & Semple, G. (2007b). Fluorinated pyrazole acids are agonists of the high affinity niacin receptor GPR109a. *Bioorg.Med.Chem.Lett.* **17**, 5620-5623.

Skinner, P. J., Cherrier, M. C., Webb, P. J., Shin, Y. J., Gharbaoui, T., Lindstrom, A., Hong, V., Tamura, S. Y., Dang, H. T., Pride, C. C., Chen, R., Richman, J. G., Connolly, D. T., & Semple, G. (2007c). Fluorinated pyrazole acids are agonists of the high affinity niacin receptor GPR109a. *Bioorg.Med.Chem.Lett.* **17**, 5620-5623.

Smith, W. C., Milam, A. H., Dugger, D., Arendt, A., Hargrave, P. A., & Palczewski, K. (1994). A splice variant of arrestin. Molecular cloning and localization in bovine retina. *Journal of Biological Chemistry* **269**, 15407-15410.

SmithKline Beecham Corporation. Preparation of xanthine derivatives as HM74A agonists. [WO 2005077950]. 2005. Ref Type: Patent

Soga, T., Kamohara, M., Takasaki, J., Matsumoto, S., Saito, T., Ohishi, T., Hiyama, H., Matsuo, A., Matsushime, H., & Furuichi, K. (2003). Molecular identification of nicotinic acid receptor. *Biochem.Biophys.Res.Commun.* **303**, 364-369.

Soudijn, W., van, W., I, & Ijzerman, A. P. (2007). Nicotinic acid receptor subtypes and their ligands. *Med.Res.Rev.* **27**, 417-433.

Stern, R. H., Spence, J. D., Freeman, D. J., & Parbtani, A. (1991). Tolerance to nicotinic acid flushing. *Clin.Pharmacol.Ther.* **50**, 66-70.

Sterne-Marr, R., Gurevich, V. V., Goldsmith, P., Bodine, R. C., Sanders, C., Donoso, L. A., & Benovic, J. L. (1993). Polypeptide variants of  $\beta$ -arrestin and arrestin3. *Journal of Biological Chemistry* **268**, 15640-15648.

Stoffel, R. H., Randall, R. R., Premont, R. T., Lefkowitz, R. J., & Inglesse, J. (1994). Palmitoylation of G protein-coupled receptor kinase, GRK6. Lipid modification diversity in the GRK family. *Journal of Biological Chemistry* **269**, 27791-27794.

Storez, H., Scott, M. G., Issafras, H., Burtey, A., Benmerah, A., Muntaner, O., Piolot, T., Tramier, M., Coppey-Moisan, M., Bouvier, M., Labbe-Jullie, C., & Marullo, S. (2005). Homo- and hetero-oligomerization of  $\beta$ -arrestins in living cells. *Journal of Biological Chemistry* **280**, 40210-40215.

Strasser, R. H., Sibley, D. R., & Lefkowitz, R. J. (1986). A novel catecholamine-activated adenosine cyclic 3',5'-phosphate independent pathway for  $\beta$ -adrenergic receptor phosphorylation in wild-type and mutant S49 lymphoma cells: mechanism of homologous desensitization of adenylate cyclase. *Biochemistry* **25**, 1371-1377.

Taggart, A. K., Kero, J., Gan, X., Cai, T. Q., Cheng, K., Ippolito, M., Ren, N., Kaplan, R., Wu, K., Wu, T. J., Jin, L., Liaw, C., Chen, R., Richman, J., Connolly, D., Offermanns, S., Wright, S. D., & Waters, M. G. (2005). (D)-  $\beta$ -Hydroxybutyrate inhibits adipocyte lipolysis via the nicotinic acid receptor PUMA-G. *Journal of Biological Chemistry* **280**, 26649-26652.

Tang, Y., Zhou, L., Gunnet, J. W., Wines, P. G., Cryan, E. V., & Demarest, K. T. (2006). Enhancement of arachidonic acid signaling pathway by nicotinic acid receptor HM74A. *Biochem.Biophys.Res.Commun.* **345**, 29-37.

Teixeira, A., Chaverot, N., Schroder, C., Strosberg, A. D., Couraud, P. O., & Cazaubon, S. (1999). Requirement of caveolae microdomains in extracellular signal-regulated kinase and focal adhesion kinase activation induced by endothelin-1 in primary astrocytes. *J.Neurochem.* **72**, 120-128.

Terrillon, S., Barberis, C., & Bouvier, M. (2004). Heterodimerization of V1a and V2 vasopressin receptors determines the interaction with beta-arrestin and their trafficking patterns. *Proc.Natl.Acad.Sci.U.S.A* **101**, 1548-1553.

Tobin, A. B. (1997). Phosphorylation of phospholipase C-coupled receptors. *Pharmacol.Ther.* **75**, 135-151.

Torhan, A. S., Cheewatrakoolpong, B., Kwee, L., & Greenfeder, S. (2007). Cloning and characterization of the hamster and guinea pig nicotinic acid receptors. *J.Lipid Res.* **48**, 2065-2071.

Torrecilla, I., Spragg, E. J., Poulin, B., McWilliams, P. J., Mistry, S. C., Blaukat, A., & Tobin, A. B. (2007). Phosphorylation and regulation of a G protein-coupled receptor by protein kinase CK2. *J.Cell Biol.* **177**, 127-137.

Tunaru, S., Kero, J., Schaub, A., Wufka, C., Blaukat, A., Pfeffer, K., & Offermanns, S. (2003). PUMA-G and HM74 are receptors for nicotinic acid and mediate its anti-lipolytic effect. *Nat.Med.* **9**, 352-355.

Tunaru, S., Lattig, J., Kero, J., Krause, G., & Offermanns, S. (2005). Characterization of determinants of ligand binding to the nicotinic acid receptor GPR109A (HM74A/PUMA-G). *Mol.Pharmacol.* **68**, 1271-1280.

Urrutia, R., Henley, J. R., Cook, T., & McNiven, M. A. (1997). The dynamins: redundant or distinct functions for an expanding family of related GTPases? *Proc.Natl.Acad.Sci.U.S.A* **94**, 377-384.

Usui, I., Imamura, T., Satoh, H., Huang, J., Babendure, J. L., Hupfeld, C. J., & Olefsky, J. M. (2004). GRK2 is an endogenous protein inhibitor of the insulin signaling pathway for glucose transport stimulation. *EMBO J.* **23**, 2821-2829.

van Herk, T., Brussee, J., van den Nieuwendijk, A. M., van der Klein, P. A., Ijzerman, A. P., Stannek, C., Burmeister, A., & Lorenzen, A. (2003). Pyrazole derivatives as partial agonists for the nicotinic acid receptor. *J.Med.Chem.* **46**, 3945-3951.

Vazquez-Prado, J., Medina, L. C., Romero-Avila, M. T., Gonzalez-Espinosa, C., & Garcia-Sainz, J. A. (2000). Norepinephrine- and phorbol ester-induced

phosphorylation of  $\alpha_{(1a)}$ -adrenergic receptors. Functional aspects. *Journal of Biological Chemistry* **275**, 6553-6559.

von Zastrow, M. & Kobilka, B. K. (1994). Antagonist-dependent and -independent steps in the mechanism of adrenergic receptor internalization. *Journal of Biological Chemistry* **269**, 18448-18452.

Whistler, J. L., Enquist, J., Marley, A., Fong, J., Gladher, F., Tsuruda, P., Murray, S. R., & von Zastrow, M. (2002). Modulation of postendocytic sorting of G protein-coupled receptors. *Science* **297**, 615-620.

White, J. H., Wise, A., Main, M. J., Green, A., Fraser, N. J., Disney, G. H., Barnes, A. A., Emson, P., Foord, S. M., & Marshall, F. H. (1998). Heterodimerization is required for the formation of a functional GABA(B) receptor. *Nature* **396**, 679-682.

Wilson, S., Wilkinson, G., & Milligan, G. (2005). The CXCR1 and CXCR2 receptors form constitutive homo- and heterodimers selectively and with equal apparent affinities. *Journal of Biological Chemistry* **280**, 28663-28674.

Wise, A., Foord, S. M., Fraser, N. J., Barnes, A. A., Elshourbagy, N., Eilert, M., Ignar, D. M., Murdock, P. R., Steplewski, K., Green, A., Brown, A. J., Dowell, S. J., Szekeres, P. G., Hassall, D. G., Marshall, F. H., Wilson, S., & Pike, N. B. (2003). Molecular identification of high and low affinity receptors for nicotinic acid. *Journal of Biological Chemistry* **278**, 9869-9874.

Wise, A., Jupe, S. C., & Rees, S. (2004). The identification of ligands at orphan G-protein coupled receptors. *Annu.Rev.Pharmacol.Toxicol.* **44**, 43-66.

Yin, D., Gavi, S., Wang, H. Y., & Malbon, C. C. (2004). Probing receptor structure/function with chimeric G-protein-coupled receptors. *Mol.Pharmacol.* **65**, 1323-1332.

Zellner, C., Pullinger, C. R., Aouizerat, B. E., Frost, P. H., Kwok, P. Y., Malloy, M. J., & Kane, J. P. (2005). Variations in human HM74 (GPR109B) and HM74A (GPR109A) niacin receptors. *Hum.Mutat.* **25**, 18-21.

Zhang, J., Barak, L. S., Winkler, K. E., Caron, M. G., & Ferguson, S. S. (1997). A central role for  $\beta$ -arrestins and clathrin-coated vesicle-mediated endocytosis in  $\beta$ 2-adrenergic receptor resensitization. Differential regulation of receptor resensitization in two distinct cell types. *Journal of Biological Chemistry* **272**, 27005-27014.

Zhang, J., Ferguson, S. S., Barak, L. S., Menard, L., & Caron, M. G. (1996). Dynamin and  $\beta$ -arrestin reveal distinct mechanisms for G protein-coupled receptor internalization. *Journal of Biological Chemistry* **271**, 18302-18305.

Zhang, Y., Schmidt, R. J., Foxworthy, P., Emkey, R., Oler, J. K., Large, T. H., Wang, H., Su, E. W., Mosior, M. K., Eacho, P. I., & Cao, G. (2005). Niacin mediates lipolysis in adipose tissue through its G-protein coupled receptor HM74A. *Biochem.Biophys.Res.Commun.* **334**, 729-732.

Zhou, L., Tang, Y., Cryan, E. V., & Demarest, K. T. (2007). Human epidermoid A431 cells express functional nicotinic acid receptor HM74a. *Mol.Cell Biochem.* **294**, 243-248.

Zhou, Y., Wang, D., Li, F., Shi, J., & Song, J. (2006). Different roles of protein kinase C- $\beta$ I and - $\delta$  in the regulation of adipocyte differentiation. *Int.J.Biochem.Cell Biol.* **38**, 2151-2163.